Theoretical studies on the direct determination of density matrix and the ionization spectra of molecules

Maho NAKATA

2003

PREFACE

Quantitative description of the electronic structure and property of atoms and molecules is one of the most important tasks in quantum chemistry. There are two purposes of this thesis: (i) development of the density matrix theory without using wavefunction, which may lead to an economical and reliable quantum chemical method; and (ii) achievement of precise theoretical studies of the molecules, where two electronic processes are important, albeit it is still difficult to assign such peaks without sophisticated theory.

Parts I and II of this thesis summarize theoretical studies on direct determination of the density matrix. As has often been pointed out, the wavefunction involves more information than we need to know. Since all the operators appearing in quantum mechanics are of the one- and two-body ones, all the elemental physical quantities can be determined from second-order reduced density matrices (2-RDMs). Hence, it may be desirable to use the 2-RDM as a basic variable of quantum mechanics instead of the wave function. However, a difficulty in this approach is that the N-representability condition, which the Pauli principle requires for RDMs, is still not fully understood.

However, very accurate theoretical spectroscopy has been established by the sophisticated wavefunction approach, namely the SAC-CI method. In part III of this thesis, we studied the valence ionization spectra of some molecules such as azines (pyrazine, pyridazine, pyrimidine, and *s*-triazine), methylenecyclopropane and trans-acrolein. Azines are parent molecules of systems such as nicotinic acid and the nucleotides cytosine, uracil and thymine. The other molecules are theoretically interesting since electron correlations play an important role in ionization spectra.

Chapter 1 describes the direct determination of 2-RDM using the density equation. As the density equation involves higher order (> 2) RDMs, higher RDMs must be reconstructed from those of lower orders to complement solving the equation. Therefore, the quality of the solution depends on the reconstruction method. In this approach, N-representability condition is *not* explicitly treated. In this study, we extended the theory to determine not only closed-shell systems but also open-

shell and excited states. We successfully calculated the open-shell systems including Be(^{3}S), Be$^-$(^{2}S), B$^+$(^{3}S), B(^{2}S), C^{2+}(^{3}S) and N^{3+}(^{3}S), and the closed-shell systems involving Be, Be^{2-}, B$^+$, B$^-$, C^{2+}, N^{3+}, H_2O and HF. New properties, such as the transition energies and the spin densities at the nuclei, which were impractical to calculate via spin-free formulation were also calculated.

Chapter 2 describes the application of the density equation method to the potential energy curves of HF, CH_4, BH_3, NH_3 and H_2O. The equilibrium geometries the vibrational force constants of these molecules were determined by the density equation method without using wavefunction. The calculated values were in close agreement with results of the symmetry-adapted cluster (SAC) and full-CI methods. We encountered convergence problems at the elongated nuclear distance, where second-order approximation of higher order RDM may fail for strongly correlated systems.

In chapter 3, we explicitly treated the N-representability condition for direct determination of the density matrix. We employed semidefinite conditions for 2-RDM; viz., P, Q and G conditions that are defined in terms of the 2-RDM. The ground-state 2-RDM per se was then variationally determined as a basic variable (density matrix variational theory; DMVT). The variational calculations were performed using the recently developed semidefinite programming algorithm (SDPA). Although these are *necessary* conditions of N-representability for 2-RDM, we showed that they are quite restrictive and the results reproducibly yielded the full-CI results. We obtained 2-RDM directly for various closed- and open-shell atoms and molecules and the method was very numerically stable; there was not a single case where convergence was not achieved. This approach shows excellent prospects; viz., (i) there is always a mathematical and numerical solution, (ii) all the N-representability conditions are linear to the 2-RDM, where we can incorporate for conditional variations, and (iii) P, Q and G conditions are good restrictive conditions for electronic Hamiltonian.

In chapter 4, we examined the effectiveness of P, Q and G conditions. We extensively investigated systems which are recognized to be challenging in quantum chemistry: the potential energy curves of H_4, CO, N_2, C_2 and Be_2, and double-

and triple- bond dissociations of H_2O, NH_3, BH_3. The DMVT(PQG), using the P, Q and G conditions as subsidiary conditions, reproduced the full-CI curves very accurately even up to the dissociation limit. However, the DMVT(PQ) was not satisfactory, especially in the dissociation limit, and the potential curves were always repulsive. The size-consistency of the method was discussed and the G-condition was found to be essential for the correct behavior of the potential curve.

Chapter 5 describes the extension of the DMVT employing other N-representability conditions. Strictly speaking, P, Q and G conditions are not enough for restrictiveness in some cases. We employed the linear inequalities proposed by Weinhold and Wilson (Weinhold-Wilson inequality) for the new subsidiary conditions. These conditions are easily introduced in the DMVT method, since they are essentially linear constraints on 2-RDMs. These conditions have some adverse effects, however; we could not achieve a drastic improvement of the total energy, which was in the order of 10^{-4} au at best.

Chapter 6 describes the accurate theoretical spectroscopy of the ionization spectra of azines. We applied the SAC-CI SD-R method to the outer-valence ionization spectra of pyrazine, pyridazine, pyrimidine and s-triazine. Since these molecules have n orbitals of nitrogen, correlation peaks were expected in the low-energy region, accompanied by $\pi \rightarrow \pi^*$ or $n \rightarrow \pi^*$ excitation. In this study, we assigned many correlation peaks which have not been assigned in the region of 18$\sim$24eV. It was also found that the position of the correlation peaks at 24$\sim$30eV are mainly governed by the position and the number of nitrogen atoms. Finally, we discussed a remarkable breakdown of the Koopmans' theorem; i.e., the order of ionization from the n and π orbitals is inverted. On analysis of the electron correlation, we found that this is mainly due to dynamic correlation.

In chapter 7, the outer-valence ionization spectra of methylenecyclopropane and trans-acrolein were studied by the SAC-CI general-R method. Methylenecyclopropane is a structurely constrained molecule, and trans-acrolein has two lone pairs, and therefore many shake-up states are expected in the lower energy region. For methylenecyclopropane, three correlation peaks were calculated at around 17eV and the breakdown of one-particle picture was found in the energy region. For trans-

acrolein, the CI state was experimentally observed at 15.47eV, although it has not been theoretically assigned. Many correlation peaks were also calculated in the higher energy region.

ACKNOWLEDGMENTS

The present thesis is a summary of the author's studies carried out at the Department of Synthetic Chemistry and Biological Chemistry, Graduate School of Engineering at Kyoto University from 1996 to 2003. The author would like to express his heartfelt gratitude to Professor Hiroshi Nakatsuji for his guidance and warm encouragement.

The author is deeply grateful to Dr. Koji Yasuda for his continuous advice, constructive discussions, and kind encouragement during the course of this work.

The author wishes to thank Professor Masahiko Hada, Dr. Masahiro Ehara, and Dr. Jun-ya Hasegawa for their critical suggestions and useful advice.

The author would also like to thank Dr. Mitsuhiro Fukuda, Dr. Kazuhide Nakata, Dr. Katsuki Fujisawa, and Professor Masakazu Kojima for their helpful and valuable suggestions on the work of Part II, and Drs. Kazuo Toyota, Yasushi Honda, and Messers. Kazuya Ishimura, Tomonori Takatsu, Mitsunori Kato, Hiroyuki Nakashima, Kei Kuramoto, Houu Kou, Junji Nakatani, Arihiro Yoshida, Jun Yasui and Kazufumi Ohkawa for their helpful discussions. Thanks are also due to the other members of the Quantum Chemistry Group in his Department.

The author also expresses thanks to his friends, Dr. Naoki Shibata, Mr. Nobuyuki Yamasaki, Ms. Yurie Yamaoka, Dr. Norihiro Maeda, Mr. Rikuro Yoshii, Ms. Chisato Koga and all his other friends for their hearty support and patience.

The author is grateful to Dr. Anthony FW Foong and Mr. Henry Foster for reading the English consult of the manuscript.

Finally, the author expresses his sincere gratitude to his parents and brother, Mr. Toshitake Nakata, Ms. Yoneko Nakata, Mr. Toyoakira Nakata for their continuous understanding, financial support and affectionate encouragement.

2002 December

Maho NAKATA

LIST OF PUBLICATIONS

1. Maho Nakata, Masahiro Ehara, Koji Yasuda, and Hiroshi Nakatsuji, "Direct determination of second-order density matrix using density equation: Open-shell system and excited state", Journal of Chemical Physics, **112**, 8772 (2000).

2. Masahiro Ehara, Maho Nakata, Houu Kou, Koji Yasuda and Hiroshi Nakatsuji, Direct determination of the density matrix using the density equation: potential energy curves of HF, CH_4, BH_3, NH_3, and H_2O, Chemical Physics Letters, **305**, 483 (1999).

3. Maho Nakata, Hiroshi Nakatsuji, Masahiro Ehara, Mitsuhiro Fukuda, Kazuhide Nakata and Katsuki Fujisawa "Variational calculations of fermion second-order reduced density matrices by semidefinite programming algorithm", Journal of Chemical Physics, **114**, 8282 (2001).

4. Maho Nakata, Masahiro Ehara, Hiroshi Nakatsuji, "Density matrix variational theory: application to the potential energy surfaces and strongly correlated systems", Journal of Chemical Physics, **116**, 5432 (2002).

5. Maho Nakata, Masahiro Ehara, Hiroshi Nakatsuji, "Density Matrix variational theory: Strength of Weinhold-Wilson inequalities", in *Fundamental Perspectives in Quantum Chemistry: A tribute to the Memory of Per-Olev Loewdin*, Eds. by Erkki Brandas and Eugene Kryachko(Kluwer Academic Publishers, Dordrecht, 2002)

6. Maho Nakata, Masahiro Ehara, Hiroshi Nakatsuji, "Outer-valence ionization spectra of azines: pyrazine, pyridazine, pyrimidine, and *s*-triazine studied by the SAC-CI SD-R method", to be submitted.

7. Maho Nakata, Masahiro Ehara, Hiroshi Nakatsuji, "Outer-valence ionization spectra of methylenecyclopropane and trans-acrolein studied by the SAC-CI general-R method", to be submitted.

CONTENTS

Part I.

Direct determination of second-order density matrix using density equation

Chapter 1.

Direct determination of second-order density matrix using density equation : Open-shell system and excited state

Abstract

We formulated the density equation (DE) method using spin-dependent density matrix (SDM) as basic variable and calculated the density matrices of the open-shell systems and excited states, as well as those of the closed-shell systems, *without* any use of the wave function. We calculated the open-shell systems, Be(^{3}S), Be^-(^{2}S), B^+(^{3}S), B(^{2}S), C^{2+}(^{3}S) and N^{3+}(^{3}S), and the closed-shell systems Be, Be^{2-}, B^+, B^-, C^{2+}, N^{3+}, H_2O, and HF. The new properties we calculated are the transition energies and the spin densities at the nuclei. Generally speaking, the accuracy of the present results is slightly worse than that of the previous one using spin-independent density matrix.

1.1 Introduction

Since all the operators appearing in quantum mechanics are one- and two-body ones, all the elemental physical quantities can be determined from the second-order density matrices (2-DMs). Many-electron wave functions involve more information than we need to know. Hence, it may be desirable to use the 2-DM as a basic variable of quantum mechanics instead of the wave function. However, a difficulty in this approach is that the N-representability condition, which is the condition the Pauli principle enforces on the DMs, is still not completely known.

One of the authors proposed a non-variational method for a direct determination of DM in time-independent [1] and time-dependent [2] cases. He showed that the density equation (DE) he derived is *equivalent* to the Schrödinger equation in the domain of N-representable DMs. However, the DE contains, second, third and fourth order DMs, so that the number of unknown variables exceeds the number of conditions. When the relations between these DMs are given by the N-representability condition, or by some approximate concept, we can directly determine the DM by solving the DE.

Valdemoro and co-workers[3] proposed approximate relations for 2-, 3-, and 4-DMs based on the fermion's anti-commutation relation. We derived more accurate relations via Green's function method[4, 5], and successfully determined the 2-DMs of molecules for the first time without any use of the wave function. Mazziotti gave a reformulation of our approach[6]. Recently, we calculated the potential energy curves, equilibrium geometries, and vibrational frequencies of molecules by the DE method [7]. Here, we formulate the DE method using spin-dependent DMs (SDMs) as basic variables, instead of the spin-independent ones. With this method, we directly calculate the DMs of open-shell and excited states as well as those of the closed-shell systems.

1.2 Theorical outline

The systems which we are interested in are composed of N non-relativistic fermions, whose Hamiltonian involves up to two body interaction terms,

$$\hat{H} = \sum_i v(i) + \sum_{i>j} w(i,j). \tag{1.1}$$

The matrix form of the Hamiltonian given by

$$H^{i_1 i_2}_{j_1 j_2} = w^{i_1 i_2}_{j_1 j_2} + \frac{1}{N-1}(v^{i_1}_{j_1}\delta^{i_2}_{j_2} + v^{i_1}_{j_2}\delta^{i_2}_{j_1}) \tag{1.2}$$

is convenient for the present study. Ensemble density matrix ρ is defined by

$$\rho = \sum_m \alpha_m \Psi_m \Psi^*_m \tag{1.3}$$

where

$$0 \leq \alpha_m \leq 1 \tag{1.4}$$

$$\sum_m \alpha_m = 1 \tag{1.5}$$

and Ψ_m is an antisymmetric N-particle function. ρ describes a pure state when the sum consists of only a single term, i.e.,

$$\rho = \Psi\Psi^*. \tag{1.6}$$

The n-th order density matrices ${}^{(n)}\Gamma$ are defined by

$${}^{(n)}\Gamma(x'_1 \cdots x'_n | x_1 \cdots x_N) = {}_N C_n \int \rho(x'_1 \cdots x'_n x_{n+1} \cdots x_N | x_1 \cdots x_N) dx_{n+1} \cdots dx_N. \tag{1.7}$$

where x_i stands for space-spin coordinate of i-th electron and ${}_N C_n$ the binomial coefficient. Note that we do not integrate the spin variables of the first n particles, so that we are able to deal with *open-shell* system. We refer to ${}^{(2)}\Gamma$ as n-SDM or simply as n-DM. Second-quantized definition equivalent to Eq. (1.7) is

$${}^{(n)}\Gamma^{i_1 i_2 \cdots i_n}_{j_1 j_2 \cdots j_n} = \sum_m \frac{\alpha_m}{n!} \langle \Psi_m | a^\dagger_{i_1} a^\dagger_{i_2} \cdots a^\dagger_{i_n} a_{j_n} \cdots a_{j_2} a_{j_1} | \Psi_m \rangle, \tag{1.8}$$

where $a^\dagger$ and a denote creation and annihilation operators, respectively. The n-particle Green's function[8] is defined as

$$G^{(n)}(x'_1t'_1\cdots x'_nt'_n|x_1t_1\cdots x_nt_n) = (-i)^n\langle T[\phi(x'_1t'_1)\cdots\phi(x'_nt'_n)\phi(x_nt_n)^\dagger\cdots\phi(x_1t_1)^\dagger)]\rangle \tag{1.9}$$

where T denotes time-ordering operator and $\phi^\dagger$ and ϕ denote creation and annihilation field operators, respectively. The DMs are related to the Green's function by

$${}^{(n)}\Gamma(x'_1\cdots x'_n|x_1\cdots x_n) = \frac{(-i)^n}{n!}G^{(n)}(x'_10^-\cdots x'_n0^-|x_10^+\cdots x_n0^+), \tag{1.10}$$

where 0^+ and 0^- denote positive and negative infinitesimals, respectively.

The n-th order density equation (DE) [1] is given by

$$\begin{aligned} E^{(n)}\Gamma &= \{\sum_i^n v(i) + \sum_{i>j}^n w(i,j)\}^{(n)}\Gamma \\ &+ (n+1)\int\{v(n+1) + \sum_i^n w(i,n+1)\}^{(n+1)}\Gamma dx_{n+1} \\ &+ \frac{1}{2}(n+1)(n+2)\int w(n+1,n+2)^{(n+2)}\Gamma dx_{n+1}dx_{n+2}. \end{aligned} \tag{1.11}$$

In matrix form, it it given by

$$E\langle\Psi|a^\dagger_{i_1}a^\dagger_{i_2}\cdots a^\dagger_{i_n}a_{j_n}\cdots a_{j_2}a_{j_1}|\Psi\rangle = \langle\Psi|\hat{H}a^\dagger_{i_1}a^\dagger_{i_2}\cdots a^\dagger_{i_n}a_{j_n}\cdots a_{j_2}a_{j_1}|\Psi\rangle. \tag{1.12}$$

The right hand side of these two equations are the *energy density matrix*, $R^{(n)}$ multiplied by ${}_NC_n$. One of the authors proved in 1976 that *each* DE with n lager than or equal to 2 is equivalent, in necessary and sufficient sense, to the Schrödinger equation if the density matrices involved are N-representable. The matrix form of the second-order DE is written as,

$$\begin{aligned} E\Gamma^{i_1i_2}_{j_1j_2} &= \sum_{j_3j_4i_3i_4} H^{i_3i_4}_{j_3j_4}\langle\Psi|a^\dagger_{i_1}a^\dagger_{i_2}a_{j_2}a_{j_1}a^\dagger_{i_3}a^\dagger_{i_4}a_{j_4}a_{j_3}|\Psi\rangle \\ &= \sum_{j_3j_4} H^{j_1j_2}_{j_3j_4}\Gamma^{j_3j_4}_{i_1i_2} + 3\sum_{j_3j_4i_4} H^{j_2i_4}_{j_3j_4}\Gamma^{j_1j_3j_4}_{i_1i_2i_4} \\ &\quad + 3\sum_{j_3j_4i_3} H^{i_3j_1}_{j_3j_4}\Gamma^{j_2j_3j_4}_{i_1i_2i_3} + 6\sum_{j_3j_4i_3i_4} H^{i_3i_4}_{j_3j_4}\Gamma^{j_1j_2j_3j_4}_{i_1i_2i_3i_4}. \end{aligned} \tag{1.13}$$

Our purpose in this paper is to solve this DE. For this purpose, we have to represent approximately the 3,4-DMs included in the DE in terms of the 1,2-DMs.

We use the Green's function method for this purpose just in the same way as in the previous paper[4, 5], but here the DMs explicity involve the spin variables. The resultant decoupling formula of the 3,4-DMs are written using the wedge product form[6] as

$$
\begin{aligned}
{}^{(3)}\Gamma \;=\; & {}^{(1)}\Gamma^3 + 3({}^{(2)}\Gamma - {}^{(1)}\Gamma^2) \wedge {}^{(1)}\Gamma \\
& - \sum_k P_k (U^{ki_1}_{j_1j_2} U^{i_2i_3}_{kj_3} + U^{ki_2}_{j_1j_2} U^{i_3i_1}_{kj_3} + U^{ki_3}_{j_1j_2} U^{i_1i_2}_{kj_3} + U^{j_1j_2}_{ki_1} U^{kj_3}_{i_2i_3} + U^{j_1j_2}_{ki_2} U^{kj_3}_{i_3i_1} \\
& + U^{j_1j_2}_{ki_3} U^{kj_3}_{i_1i_2} + U^{ki_2}_{j_2j_3} U^{i_3i_1}_{kj_1} + U^{ki_3}_{j_2j_3} U^{i_1i_2}_{kj_1} + U^{ki_1}_{j_2j_3} U^{i_2i_3}_{kj_1} + U^{j_2j_3}_{ki_2} U^{kj_1}_{i_3i_1} \\
& + U^{j_2j_3}_{ki_3} U^{kj_1}_{i_1i_2} + U^{j_2j_3}_{ki_1} U^{kj_1}_{i_2i_3} + U^{ki_3}_{j_3j_1} U^{i_1i_2}_{kj_2} + U^{ki_1}_{j_3j_1} U^{i_2i_3}_{kj_2} + U^{ki_2}_{j_3j_1} U^{i_3i_1}_{kj_2} \\
& + U^{j_3j_1}_{ki_3} U^{kj_2}_{i_1i_2} + U^{j_3j_1}_{ki_1} U^{kj_2}_{i_2i_3} + U^{j_3j_1}_{ki_2} U^{kj_2}_{i_3i_1}) \qquad (1.14)
\end{aligned}
$$

$$
{}^{(4)}\Gamma = {}^{(1)}\Gamma^4 + 4({}^{(3)}\Gamma - {}^{(1)}\Gamma^3) \wedge {}^{(1)}\Gamma - 6({}^{(2)}\Gamma - {}^{(1)}\Gamma^2) \wedge {}^{(1)}\Gamma^2 + \frac{3}{4} U \wedge U \qquad (1.15)
$$

where

$$
\Gamma^n = \underbrace{\Gamma \wedge \Gamma \cdots \wedge \Gamma}_{n \text{ times}}. \qquad (1.16)
$$

U is called collision term and defined by

$$
U = 2{}^{(2)}\Gamma - 2({}^{(1)}\Gamma \wedge {}^{(1)}\Gamma) \qquad (1.17)
$$

P_k is zero or unity for k being unoccupied and occupied, respectively. This decoupling approximation is essentially of the second-order in the correlation-correction perturbation. Note for the 3-DMs, this is *not* an exact second-order correction, and we examined previously some correction terms[5].

1.3 Calculational method

Our basic variable is the spin dependent 2-SDM, which has about 256 times lager freedom than the spin-independent 2-RDM. It is hermitian and antisymmetric. The 3,4-SDMs are represented in terms of the 1,2-DMs by Eqs. (1.14) and (1.15), and the solution of the DE corresponds to finding the vanishing value of the function, $\boldsymbol{f}$.

$$
\boldsymbol{f}({}^{(2)}\Gamma) = {}_N C_2 R({}^{(2)}\Gamma) - E^{(2)}\Gamma. \qquad (1.18)
$$

This function is linearized and solved by using the Newton-Raphson method. The algorithm is essentially the same as the previous one [4, 5] and is summarized as follows.

1. Guess initial 2-SDM, which is ordinally Hartree-Fock ${}^{(2)}\Gamma$.
2. Calculate $E = \mathrm{Tr}({}^{(2)}\Gamma H)$.
3. Construct 3,4-SDM ${}^{(3)}\Gamma$ and ${}^{(4)}\Gamma$ with ${}^{(2)}\Gamma$ and ${}^{(1)}\Gamma$ by Eqs. (1.14) and (1.15)
4. Calculate the error function $\boldsymbol{f}$ by Eq. (1.18).
5. Update 2-SDM by using by the Newton-Raphson method.
6. Repeat the procedure $2 \sim 5$ until convergence.
7. Check the N-representability of the resultant ${}^{(2)}\Gamma$.

In applying the Newton-Raphson method[9], we need to calculate the coefficient matrix $A_{ij} = \frac{\partial f_i}{\partial x_j}$, where x denote the variable ${}^{(2)}\Gamma$ itself and i, j denote the four indices of ${}^{(2)}\Gamma$.

As an initial guess of the 2-SDM, we used the Hartree-Fock estimate,

$$ {}^{(2)}\Gamma^{i_1 i_2}_{j_1 j_2} = \frac{1}{2}(\delta^{i_1}_{j_1}\delta^{i_2}_{j_2} - \delta^{i_1}_{j_2}\delta^{i_2}_{j_1}). \tag{1.19} $$

where δ^i_j is Kronecker's delta, but when the convergency was not good, we used the full CI 2-SDM.

The above procedure was applied to the open-shell atoms, Be(^{3}S), Be$^-$(^{2}S), B$^+$(^{3}S), B(^{2}S), C^{2+}(^{3}S), C$^+$(^{2}S), N^{3+}(^{3}S), N^{2+}(^{2}S) and the closed-shell atoms and molecules, Be, Be^{2-}, B$^+$, B$^-$, C^{2+}, N^{3+}, H_2O and HF. The basis set of Be is double-ζ STO [10] expanded by six GTOs [12]. For B, C and N, double-ζ s-type GTOs by Huzinaga[13] and Dunning[14] were used. For H_2O and HF, STO-6G basis was used. The geometries of H_2O and HF are the experimental ones[15].

1.4 Results

First, we examine the energy and ${}^{(2)}\Gamma$ calculated by the present DE method. In tables I, II, and III the total energy, the correlation energy error, and the root mean square deviation of the SDMs calculated by the DE method from the full CI ones are shown for the open-shell triplet, doublet, and the closed-shell singlet states, respectively.

Since only s-type basis sets are used, the doublet states of the five-electron atoms are not the ground ^{2}P state but actually the excited ^{2}S states and the triplet states of the four-electron atoms are also not the ^{3}P state but the ^{3}S state. Computationally, such S states are easier to calculate than the P states. For the triplet states summarized in table I, the errors in the correlation energy are less than 0.3 % and the total energies of the DE method slightly overshoot those of the full CI. Since the DE method is not variational, this overshooting happened, though the violation of the variational principle is negligibly small. The RMS (root-mean-square) deviation of the SDM is in the order of 10^{-3}, and is much smaller than the Hartree-Fock ones. For the doublet states shown in table II, the DE method also reproduces well the full CI results almost in the same accuracy as for to those of the triplet states. For the closed-shell singlet states given in table III, the energy and ${}^{(2)}\Gamma$ of the DE method show much better agreement with the full CI ones in comparison with the triplet and doublet states. It should be noted that the ${}^{(2)}\Gamma$ by the DE method is more accurate than those of the SDCI, since the DE method determines the DM directly.

The transition energy, ionization energy, and electron affinity are summarized in table IV for Be, B, C, and N atoms. These quantities are calculated for the first time by the DE method. Since the states involved are not the normal ground and excited states, the values themselves may look strange, but in comparison with the full CI results, the DE results are very close. The deviations of the DE values from the full CI ones are less than 2.83×10^{-4} au, while those of the Hartree-Fock and SDCI methods are 4.42×10^{-3} and 1.80×10^{-5}, respectively.

The expectation values of the numbers of α and β spin electrons, $\langle N_\alpha \rangle$ and

TABLE I: Results for the triplet states: total energy (in au), correlation energy error(in %), and RMS deviation of the ${}^{(2)}\Gamma$ calculated by the DE method and the wave function method. Active space denotes number of occupied MOs × virtural MOs and electrons denotes number of α electrons + β electrons, respectively.

			DE method	Wave function method		
				total energy (correlation energy error in %)		
System	Active space			${}^{(2)}\Gamma$ error [a]		
	Electrons	State	DE	Hartree-Fock	SDCI	full CI
Be	4×4	^{3}S	-13.31466 (-0.2)	-13.30361 (100)	-13.31464 (0.0)	-13.31464
	$3 + 1$		1.43×10^{-3}	2.67×10^{-2}	0	0
B^+	4×4	^{3}S	-23.60534 (-0.2)	-23.59233 (100)	-23.60532 (0.0)	-23.60532
	$3 + 1$		5.21×10^{-3}	2.66×10^{-2}	0	0
C^{2+}	4×4	^{3}S	-35.30435 (-0.3)	-35.29153 (100)	-35.304310 (0.0)	-35.30431
	$3 + 1$		6.10×10^{-3}	2.14×10^{-2}	0	0
N^{3+}	4×4	^{3}S	-49.36284 (-0.2)	-49.34852 (100)	-49.362813 (0.0)	-49.36281
	$3 + 1$		4.54×10^{-3}	2.32×10^{-2}	0	0

[a]Square norm of the difference between the calculated 2-SDM and full CI one.

TABLE II: Results for the doublet states: total energy (in au), correlation energy error(in %), and RMS deviation of the ${}^{(2)}\Gamma$ calculated by the DE method and the wave function method. Active space denotes number of occupied MOs × virtural MOs and electrons denotes number of α electrons + β electrons, respectively.

			DE method	Wave function method		
				total energy (correlation energy error in %)		
System	Active space			${}^{(2)}\Gamma$ error[a]		
	Electrons	State	DE	Hartree-Fock	SDCI	full CI
Be^-	5×3	^{2}S	-13.24020 (-)	-	-	-13.24016
	$3 + 2$		2.20×10^{-3}	-	-	0
B	5×3	^{2}S	-24.11436 (-0.3)	-24.09747 (100)	-24.11431 (0.0)	-24.11431
	$3 + 2$		6.03×10^{-3}	2.28×10^{-1}	3.55×10^{-5}	0
C^+	5×3	^{2}S	-36.55658 (-0.2)	-36.54203 (100)	-36.55655 (0.0)	-36.55655
	$3 + 2$		3.77×10^{-3}	1.24×10^{-1}	1.56×10^{-5}	0
N^{2+}	5×3	^{2}S	-51.61476 (-0.2)	-51.60238 (100)	-51.61474 (0.0)	-51.61474
	$3 + 2$		2.47×10^{-3}	1.73×10^{-2}	7.71×10^{-6}	0

[a]Square norm of the difference between the calculated 2-SDMand full CI one.

TABLE III: Results for the closed-shell atoms and molecules: total energy (in au), correlation energy error(in %), and RMS deviation of the ${}^{(2)}\Gamma$ calculated by the DE method and the wave function method. Active space denotes number of occupied MOs × virtural MOs and electrons denotes number of α electrons + β electrons, respectively.

			DE method	Wave function method		
				total energy (correlation energy error in %)		
System	Active space			${}^{(2)}\Gamma$ error [a]		
	Electrons	State	DE	Hartree-Fock	SDCI	full CI
Be	4×4	^{1}S	-14.58270 (-0.1)	-14.56853 (100)	-14.58269 (0.0)	-14.58269
	$2 + 2$		4.25×10^{-5}	4.58×10^{-2}	1.06×10^{-4}	0
Be^{2-}	6×2	^{1}S	-11.26839 (0.0)	-11.25896 (100)	-11.26839 (0.0)	-11.26839
	$3 + 3$		1.32×10^{-5}	2.00×10^{-2}	0	0
B^+	4×4	^{1}S	-24.24908 (1.5)	-24.23434 (100)	-24.24929 (0.1)	-24.24931
	$2 + 2$		5.19×10^{-5}	6.03×10^{-2}	5.17×10^{-4}	0
B^-	6×2	^{1}S	-23.66908 (-0.2)	-23.65664 (100)	-23.66905 (0.0)	-23.66905
	$2 + 2$		5.83×10^{-6}	2.46×10^{-2}	0	0
C^{2+}	4×4	^{1}S	-36.41774 (0.1)	-36.40382 (100)	-36.41775 (0.1)	-36.41776
	$2 + 2$		1.47×10^{-4}	3.92×10^{-2}	1.84×10^{-4}	0
N^{3+}	4×4	^{1}S	-51.08762 (-0.1)	-51.07423 (100)	-51.08760 (0.1)	-51.08761
	$2 + 2$		7.39×10^{-5}	8.25×10^{-2}	7.96×10^{-5}	0
H_2O	8×4	^{1}S	-75.72550 (6.9)	-75.67885 (100)	-75.72821 (1.5)	-75.72894
	$4 + 4$		9.22×10^{-3}	2.59×10^{-1}	7.83×10^{-3}	0
HF	8×2	^{1}S	-99.52361 (8.4)	-99.49984(100)	-99.52577 (0.0)	-99.52577
	$4 + 4$		1.32×10^{-5}	2.00×10^{-2}	0	0

[a] Square norm of the difference between the calculated 2-SDM and full CI one.

TABLE IV: Transition energy, ionization energy and electron affinity (in au.)calculated by the DE method and the wave function method.

System	Transition	DE	Hartree-Fock	SDCI	Full CI
Be	$^1\mathrm{S} \rightarrow {}^3\mathrm{S}$	1.26804	1.26492	1.26805	1.26805
	$^1\mathrm{S} + \mathrm{e}^- \rightarrow {}^2\mathrm{S}$	1.34249	–	–	1.34253
B	$^2\mathrm{S} + \mathrm{e}^- \rightarrow {}^1\mathrm{S}$	0.44528	0.44083	0.44526	0.44526
	$^2\mathrm{S} - \mathrm{e}^- \rightarrow {}^1\mathrm{S}$	-0.13472	-0.13687	-0.13498	-0.13500
B^+	$^1\mathrm{S} \rightarrow {}^3\mathrm{S}$	0.64374	0.64201	0.64397	0.64399
C^{2+}	$^1\mathrm{S} \rightarrow {}^3\mathrm{S}$	1.11339	1.11229	1.11344	1.11345
	$^1\mathrm{S} + \mathrm{e}^- \rightarrow {}^2\mathrm{S}$	-0.13884	-0.13821	-0.13880	-0.13879
N^{3+}	$^1\mathrm{S} \rightarrow {}^3\mathrm{S}$	1.72478	1.72571	1.72479	1.72480
	$^1\mathrm{S} + \mathrm{e}^- \rightarrow {}^2\mathrm{S}$	-0.52714	-0.52815	-0.52714	-0.52713

$\langle N_\beta \rangle$, and those of the operators S_z and S^2, $\langle S_z \rangle$ and $\langle S^2 \rangle$, are calculated and summarized in table V for the triplet, doublet, and singlet states. For the closed-shell singlet state, we obtain almost correct expectation values for atoms, but the deviations are somewhat large for molecules, especially for $\langle S^2 \rangle$. For the open-shell triplet and doublet states, the expectation values $\langle N_\alpha \rangle$, $\langle N_\beta \rangle$, $\langle S_z \rangle$ and $\langle S^2 \rangle$ slightly deviate from the exact values. This is because the present approximate decoupling technique does not include any restrictive conditions for the numbers of the electrons and spins. When we enforce the "normalization" condition, the present calculations did not converge or no refinement of the results obtained.

Next, we examine the N-representability conditions for the 1-SDM and 2-SDM. Table VI gives the occupation numbers of the natural orbital of the 1-SDM, and the lowest eigen values of the P, Q and G matrices [11]. For the closed-shell systems, the N-representability condition of the 1-SDM is completely satisfied, i.e., the occupation numbers are all positive and less than unity. This was also so in the previous spin-free calculations[4, 5]. However, violations of the N-representability of the 1-SDM occur for the open-shell systems. The P, Q and G are necessary conditions for the N-representability of the 2-SDM: the eigenvalues of the P, Q and

TABLE V: $\langle N_\alpha \rangle$, $\langle N_\beta \rangle$, $\langle S_z \rangle$ and $\langle S^2 \rangle$ calculated for the 2-SDM by the DE method.

System	State	$\langle N_\alpha \rangle$	$\langle N_\beta \rangle$	$\langle S_z \rangle$	$\langle S^2 \rangle$
Be	^{3}S	3.00072	0.99928	1.00072	2.00003
B^+	^{3}S	2.99741	1.00259	0.99741	2.00237
C^{2+}	^{3}S	3.00305	0.99694	1.00306	2.00006
N^{3+}	^{3}S	3.00220	0.99780	1.00220	2.00005
Be^-	^{2}S	2.99922	2.00078	0.49922	0.75001
B	^{2}S	3.00161	1.99839	0.50161	0.75000
C^+	^{2}S	3.00113	1.99887	0.50113	0.75000
Be	^{1}S	2.00000	2.00000	0.00000	8.90×10^{-6}
Be^{2-}	^{1}S	3.00000	3.00000	0.00000	4.63×10^{-7}
B^+	^{1}S	2.00004	2.00004	0.00000	4.13×10^{-4}
B^-	^{1}S	3.00000	3.00000	0.00000	-1.94×10^{-6}
C^{2+}	^{1}S	2.00000	2.00000	0.00000	3.87×10^{-5}
N^{3+}	^{1}S	2.00000	2.00000	0.00000	4.74×10^{-6}
H_2O	^{1}S	5.00002	5.00002	0.00000	1.28×10^{-2}
HF	^{1}S	5.00002	5.00002	0.00000	1.03×10^{-2}

TABLE VI: Minimum eigenvalues of the P, Q and G-matrices, numbers of the eigenvalues smaller than 1.0×10^{-6} in the parenthesis, and the range of eigen values of 1-SDM calculated by the DE method.

System	Active electrons	P-matrix	Q-matrix	G-matrix	1-SDM
Be(^{3}S)	4	-6.545×10^{-4}(7)	-6.688×10^{-4}(7)	-7.047×10^{-4}(17)	-3.536×10^{-4} $\sim$ 1.0004
B^+ (^{3}S)	4	-1.815×10^{-4}(4)	-1.896×10^{-4}(3)	-1.937×10^{-4}(11)	3.067×10^{-4} $\sim$ 0.9997
C^{2+} (^{3}S)	4	-3.009×10^{-3}(8)	-3.015×10^{-3}(9)	-3.132×10^{-3}(24)	-1.548×10^{-3} $\sim$ 1.0016
N^{3+} (^{3}S)	4	-2.237×10^{-3}(7)	-2.242×10^{-3}(7)	-2.235×10^{-5}(23)	1.154×10^{-3} $\sim$ 1.0012
Be^- (^{2}S)	5	-4.952×10^{-6}(1)	-6.809×10^{-6}(8)	-7.965×10^{-6}(6)	2.659×10^{-4} $\sim$ 1.0000
B (^{2}S)	5	-2.123×10^{-3}(6)	-2.121×10^{-4}(10)	-4.233×10^{-4}(23)	-2.102×10^{-4} $\sim$ 1.0021
C^+ (^{2}S)	5	-1.331×10^{-3}(5)	-3.015×10^{-3}(7)	-3.132×10^{-3}(18)	-1.316×10^{-3} $\sim$ 1.0000
N^{2+} (^{2}S)	5	-1.555×10^{-5}(2)	-1.396×10^{-4}(10)	-2.928×10^{-4}(14)	-1.154×10^{-3} $\sim$ 1.0012
Be(^{1}S)	4	-6.246×10^{-6}(1)	-3.938×10^{-6}(2)	-4.781×10^{-6}(4)	1.119×10^{-4} $\sim$ 0.9997
Be^{2-} (^{1}S)	6	ok	-3.045×10^{-6}(5)	-4.576×10^{-6}(6)	1.996×10^{-4} $\sim$ 1.00000
B^+ (^{1}S)	4	-6.963×10^{-6}(4)	-1.563×10^{-5}(5)	-4.576×10^{-6}(12)	1.996×10^{-4} $\sim$ 1.0000
B^- (^{1}S)	6	ok	-1.417×10^{-4}(4)	-1.986×10^{-4}(6)	3.009×10^{-4} $\sim$ 1.0000
C^{2+} (^{1}S)	4	-3.818×10^{-5}(5)	-2.019×10^{-6}(1)	-1.998×10^{-5}(7)	5.863×10^{-4} $\sim$ 0.9998
N^{3+} (^{1}S)	4	-1.922×10^{-5}(2)	ok	-1.111×10^{-5}(7)	1.168×10^{-1} $\sim$ 0.9999
H_2O(^{1}S)	8	-6.793×10^{-4}(2)	-4.830×10^{-4}(18)	-6.606×10^{-4}(5)	1.427×10^{-2} $\sim$ 0.9987
HF(^{1}S)	8	-8.303×10^{-4}(1)	-7.688×10^{-4}(14)	-1.221×10^{-3}(5)	1.696×10^{-2} $\sim$ 0.9994

TABLE VII: Second moment ($\langle r^2 \rangle$) of atoms calculated by the DE method and the wave function method.

System	state	DE	Hartree Fock	SDCI	full CI
Be	^{3}S	-4.85006	-4.85021	-4.85006	-4.85006
B^+	^{3}S	-4.95063	-4.95074	-4.95070	-4.95070
C^{2+}	^{3}S	-3.27401	-3.27404	-3.27402	-3.27402
N^{3+}	^{3}S	-2.33906	-2.33908	-2.33906	-2.33906
Be^-	^{2}S	-7.33125	–	-7.33128	-7.33128
B	^{2}S	-6.45884	-6.45765	-6.45889	-6.45892
C^+	^{2}S	-4.08158	-4.08119	-4.08159	-4.08160
N^{2+}	^{2}S	-2.84906	-2.84892	-2.84907	-2.84907
Be	^{1}S	-5.77125	-5.77782	-5.77136	-5.77127
Be^{2-}	^{1}S	-9.56353	-9.56389	–	-9.56355
B^+	^{1}S	-2.71924	-2.69894	-2.71849	-2.71887
B^-	^{1}S	-9.81236	-9.81253	–	-9.81237
C^{2+}	^{1}S	-1.56149	-1.55544	-1.56144	-1.56152
N^{3+}	^{1}S	-1.02144	-1.01932	-1.02143	-1.02145

G matrices should be non-negative. However, some of the eigenvalues are slightly negative, though the numbers of the negative eigenvalues are very small among the total numbers of the eigenvalues. The violations of the N-representability of the 2-SDM seems to be small. This violation becomes large as the number of the electron increases, and seems to be larger for the open-shell systems compared with the closed-shell systems.

Table VII shows the second moment of electron distribution, $\langle r^2 \rangle$. Again, the DE results for the closed-shell systems are better than those for the open-shell systems. Some of them are better than the SDCI results, because the DE method directly determines the SDM. For the open-shell systems, the SDCI results are superior to

the DE ones, because the violation of the N-representability condition tends to accumulate electrons near the nucleus. Some of the SDCI results are identical to the full CI results: for the active space is small, the single and double excitations span the complete space.

Finally, the spin density and the electron density at nucleus are calculated. In table VIII, IX and X, the results are shown for the triplet, doublet, and singlet states, respectively. The spin density at the nucleus is a very important observable in ESR and other magnetic chemistry and calculated for the first time by the DE method. The DE method well reproduces the spin density at the nucleus of the full CI method. The results are almost in the same accuracy as the SDCI ones and much better than the Hartree-Fock ones, since the DE method includes both electron and spin correlations up to second-order in the perturbation. For the closed-shell singlet states, the spin density is exactly zero, therefore, only the total density of the electrons at nucleus is given. The accuracy of the DE method is almost the same as that of SDCI.

TABLE VIII: Electron density and spin density at the nucleus of the triplet state. ρ denotes the total electron density, and ρ_α and ρ_β are the α and β electron densities, respectively, and $\Delta\rho = \rho_\alpha - \rho_\beta$ is spin density at the nucleus.

System(State)	2-DE	Hartree Fock	SDCI	full CI
Be (^{3}S)				
ρ	32.530	32.401	32.530	32.530
ρ_α	18.069	17.593	18.068	18.068
ρ_β	14.461	14.808	14.462	14.462
$\Delta\rho$	3.608	2.785	3.605	3.605
B^+(^{3}S)				
ρ	68.741	68.680	68.742	68.742
ρ_α	36.216	35.947	36.225	36.225
ρ_β	32.525	32.733	32.517	32.517
$\Delta\rho$	3.691	3.215	3.708	3.708
C^{2+}(^{3}S)				
ρ	122.143	122.064	122.143	122.143
ρ_α	64.502	64.083	64.489	64.489
ρ_β	57.641	57.981	57.654	57.654
$\Delta\rho$	6.860	6.103	6.836	6.836
N^{3+}(^{3}S)				
ρ	197.798	197.705	197.798	197.798
ρ_α	104.557	103.989	104.543	104.543
ρ_β	93.241	93.716	93.255	93.255
$\Delta\rho$	11.316	10.273	11.287	11.287

TABLE IX: Electron density and spin density at the nucleus of the doublet state. ρ is the total electron density, and ρ_α and ρ_β are the α and β electron densities, respectively, and $\Delta\rho = \rho_\alpha - \rho_\beta$ is the spin density at the nucleus.

System(State)	DE	Hartree Fock	SDCI	full CI
$Be^-(^2S)$				
ρ	33.568	–	33.568	33.568
ρ_α	17.909	–	17.911	17.911
ρ_β	15.659	–	15.658	15.658
$\Delta\rho$	2.249	–	2.253	2.253
$B(^2S)$				
ρ	70.058	69.998	70.058	70.058
ρ_α	35.980	35.796	35.977	35.977
ρ_β	34.078	34.202	34.081	34.081
$\Delta\rho$	1.902	1.594	1.896	1.896
$C^+(^2S)$				
ρ	125.313	125.238	125.313	125.313
ρ_α	64.033	63.809	64.030	64.030
ρ_β	61.280	61.429	61.284	61.283
$\Delta\rho$	2.753	2.380	2.746	2.746
$N^{2+}(^2S)$				
ρ	203.820	203.732	203.820	203.820
ρ_α	103.832	103.564	103.828	103.828
ρ_β	99.989	100.168	99.992	99.992
$\Delta\rho$	3.843	3.396	3.836	3.836

TABLE X: Electron density at the nucleus of the singlet state.

System(State)	DE	Hartree Fock	SDCI	full CI
Be(^{1}S)	31.489	31.352	31.489	31.489
Be^{2-}(^{1}S)	34.316	34.209	34.316	34.316
B^+(^{1}S)	69.030	68.983	69.031	69.031
B^-(^{1}S)	71.456	71.399	71.457	71.457
C^{2+}(^{1}S)	123.532	123.470	123.532	123.532
N^{3+}(^{1}S)	201.055	200.978	201.055	201.055

1.5 Conclusion

We successfully calculated the SDMs of some open-shell and excited states for the first time by the spin-explicit DE method without *any use* of the wave function. The same method is also applied to the closed-shell systems, though the solution is easier with the spin-free formulation. Generally speaking, the quality of solutions were better for the closed-shell systems than for the open-shell systems. A reason is a lager number of valuables to be solved for open-shell systems. Another one may be a symmetry which may hide some N-representability condition; all the electrons are in pair. As seen from the results, the present method and the solution algorithm are not complete and needs some future refinement. Nonetheless, the present results constitutes a mile stone in the DE approach in theoretical chemistry as its first application to open-shell and excited states.

1.6 Acknowledgments

This study has been supported by the Grand-in-Aid for Scientific Research from the Japanese Ministry of Education, Science, Culture, and Sports.

BIBLIOGRAPHY

[1] H. Nakatsuji, Phys. Rev. A **14**, 41(1976).

[2] H. Nakatsuji, Theor. Chem. Acc. **102**, 97(1999).

[3] C. Valdemoro, Phys.Rev.A **45**,4462(1992); A**47**, 971, 979(1993).

[4] H. Nakatsuji and K. Yasuda, Phys. Rev. Lett. **76**, 1039(1996).

[5] K. Yasuda and H. Nakatsuji, Phys. Rev. A **56**, 2648(1997).

[6] D. A. Mazziotti, Phys, Rev. A **57**, 4219(1998); Chem. Phys. Lett. **289**, 419(1998).

[7] M. Ehara, M. Nakata, H. Kou, K. Yasuda, H. Nakatsuji, Chem. Phys. Lett. **305**, 483(1999).

[8] A. L. Fetter and J.D. Walecka, *Quantum theory of many particle systems*,McGraw Hill, NewYork, (1971); A. A. Abrikosov, L. P. Gorkov, and E. Dzyloshinskii, *Method of Quantum Field Theory in Statistical Physics*, Prentice-Hall, Englewood, Cliffs, NJ,(1963).

[9] W. H. Press, S. A. Teukolsky, W. T. Vetterling and B. Flannery, *Numerical recipes in C*, Cambridge University Press.

[10] E. Clementi and C. Roetti, Atom Data Nucl. Data Tab. **14**, 428(1974); the exponents were reoptimized by T. Koga and S. Watanabe(private communication).

[11] C. Garrod, M. V. Mihailovic, and M. Rosina, J. Math. Phys. **16**, 868 (1975); A. J. Coleman, Rev. Mod. Phys. **35**, 668 (1963); C. Garrod and J. Percus, J. Math. Phys. **5**, 1756 (1964); H. Kummer, J. Math. Phys. **8**, 2063 (1967). ; T. L. Gilbert, Phys. Rev. B **12**, 2111 (1975).

[12] W.J. Hehre, R.F. Stweart, and J.A. Pople, J. Chem. Phys. **51**, 2657(1969).

[13] S. Huzinaga, J. Chem. Phys. **42**, 1293 (1965).

[14] T.H. Dunning, JR., J. Chem. Phys. **53**, 2823 (1970).
T.H. Dunning, JR. and P.J. Hay, In method of electronic structure theory, vol. 2, H.F. Schaefer III, ed., Plenum press (1977).
Actually, basis sets are taken from EMSL Gaussian Basis Set Order Form, `http://www.emsl.pnl.gov:2080/forms/basisform.html`.

[15] L. E. Sutton, D. G. Jenkin, and A. D. Mitchell, *Tables of interatomic distances and configuration in molecules and ions I.*, (The Chemical Society, London, 1958).

Chapter 2.

Direct determination of the density matrix using the density equation: Potential energy curves of HF, CH_4, BH_3, NH_3, and H_2O

Abstract

The density equation (DE) method was utilized for calculations of the potential energy curves of molecules HF, CH_4, BH_3, NH_3, and H_2O. The equilibrium geometries and the vibrational force constants of these molecules were determined for the first time by the DE method without any use of the wave function. The calculated values are in close agreement with the results of the symmetry-adapted cluster (SAC) and full-CI methods.

2.1 Introduction

Recently, a revival of interest has been invoked on the direct determination of the density matrix (DM) without any use of the wave function [1-12]. The density matrix approach is straightforward in comparison with the wave function approach since all the elemental physical quantities can be calculated using sec ond-order density matrices (2-DMs). The basic equation for the DMs exists in an explicit form [1], in contrast to the Hohenberg-Kohn's existing theorem [13] in the density functional approach [14]. Nakatsuji derived in 1976 a basic equation, called density equation (DE), for a direct determination of the DM[1]. Recently, time-dependent DE and the perturbation theory for both time-independent and time-dependent DE were published [2]. He showed that the DE is *equivalent* with the Schröinger equation (by the *necessary and sufficient* condition)in the domain of the N-representable DM's. Unfortunately, the N-representability condit ion on the DM is still not completely known [15], and under such situation, the nth-order DE, containing nth, $(n+1)$th, and $(n+2)$th-order DM's is formally insoluble, for the number of the unknown variables exceeds the number of the conditions. Valdemoro and co-workers reported an interesting approach for solving the density equation [6-12]. (They called the DE contracted Schröinger equation, but this naming does well represent the *sufficiency* nature of the DE, which is a primary feature of the DE.) They suggested a decoupling approximation of higher-order reduced density matrices (RDM's) in terms of the lower-order ones based on the fermion's anticommutation relation. We call this approximation the IPH approximation (the approximation identifying independently the particle and hole parts separately). Nakatsuji and Yasuda proposed a more accurate decoupling approximation on the basis of the Green's-function method [3, 4]. It was called DE2 method since the approximation is correct essentially to the second-order in the correlation perturbation. The method was applied to the calculations of the second-order RDMs of Be, Ne, H_2O, NH_3, H_3O^+, CH_4, BH_4^-, NH_4^+, CH_3F, HF, N_2, CO, C_2H_2, CH_3OH, CH_3NH_2, and C_2H_6 [3, 4].

The RDMs of molecules were determined directly, for the first time, without any use of wave functions. Recently, the method has been reformulated for spin-

dependent DMs and has been applied to some open-shell systems [5]. Mazziotti [11, 12] reported recently a fresh reformulation of the DE method and applied it to the Lipkin model.

In this paper, the DE2 method is applied to the calculations of the potential energy curves of some small molecules. We want to calculate their equilibrium geometries and force constants for the first time by the DE method.

2.2 Computational method

The DE2 method proposed in previous papers [3,4] is applied to the calculations of the potential curves of HF, CH_4, BH_3, NH_3, and H_2O. The calculational procedure was discussed in detail elsewhere [4]. We did not include the term given by Eq. (2.24) of Ref. [4]. The multidimensional nonlinear equation was solved by Newton's method. The Hermiticity and the symmetry properties of the 2-RDM were imposed in solving the DE.

The valence double zeta basis, [3s2p/2s] set [16,17], was used for HF and the minimal STO-6G basis [18] was used for CH_4, BH_3, NH_3, and H_2O. The potential energy curves of HF, CH_4, BH_3, and NH_3 were calculated for the totally-symmetric stretching mode. The potential energy surface of H_2O was calculated along the three normal modes around the equilibrium geometry. The spectroscopic constants of the potential curves were calculated numerically. The full-CI and symmetry-adapted-cluster (SAC) [19] methods were performed, at the same time, to examine the accuracy of the present DE2 results. The HONDO8 program [20] was used for the Hartree-Fock and full-CI calculations and the SAC-CI96 program [21] for SAC calculations.

In all calculations, the 1s orbitals of the first-row atoms were frozen as cores. This was effective to get a good convergence in the present algorithm of solving the DE. When these 1s orbitals were included, the breakdown of the N-representability of the 1-RDM occurred even at the geometries relatively close to the equilibrium geometry. The origin of this non-convergence is not clear, but we have observed that the occupation number of the 1s orbitals slightly exceeds two, when the molecular

geometry is apart from the equilibrium geometry. By adopting the 1s orbitals as a frozen core, the present DE2 calculations have converged in wide regions around the equilibrium geometry.

2.3 Stretching potential for HF, CH_4, BH_3, and NH_3

Fig. 1a shows a comparison of the ground-state potential energy curves of HF molecule calculated by the Hartree-Fock, DE2, SAC, and full-CI methods in the nuclear distance of 0.8 - 1.2 Å. The DE2 method well reproduces the full-CI curve, showing that the DE2 method includes electron correlations very accurately: the errors range from 4.1% to 9.2% in these internuclear distances. The deviations from the full-CI are larger in the large internuclear distance, while a weight of the Hartree-Fock configuration is almost constant, 0.96 - 0.95, in the distance of 0.8 - 1.2 Å. The SAC almost reproduces the full-CI curve: the deviations are within 1.8 mhartree.

The potential curves for the totally-symmetric stretching mode of CH_4 are shown in Fig. 1b. Again, the DE2 method simulates well the full-CI curve: for CH_4, the errors in the correlation energy are 3.3% to 13.1% in the range of $R_{\mathrm{C-H}} = 0.95$ - 1.40Å, where the weight of the Hartree-Fock configuration changes from 0.97 to 0.88, the last figure being very small. Since the present DE2 method is based on the perturbation expansion by the Green function method [3,4], a better agreement is obtained at a shorter internuclear distance where the Hartree-Fock approximation becomes better. The SAC curve is almost superposed with the full-CI one. The DE2 method is correct to the second-order in the correlation perturbation, but still is a subject of improvement and at this moment, it is more expensive than the wavefunction approach like SAC.

The potential curves of BH_3 and NH_3 are depicted in Fig. 2 for the totally-symmetric stretching mode. The stretching potential of BH_3 was obtained by restricting the planer structure of D_{3h}, while for NH_3 the geometry was optimized along the mode by each method. The weight of the Hartree-Fock configuration is 0.98 - 0.93 for $R_{\mathrm{B-H}} = 1.0$ - 1.45Å of BH_3 and 0.97 - 0.93 for $R_{\mathrm{N-H}} = 0.948$ - 1.185Å

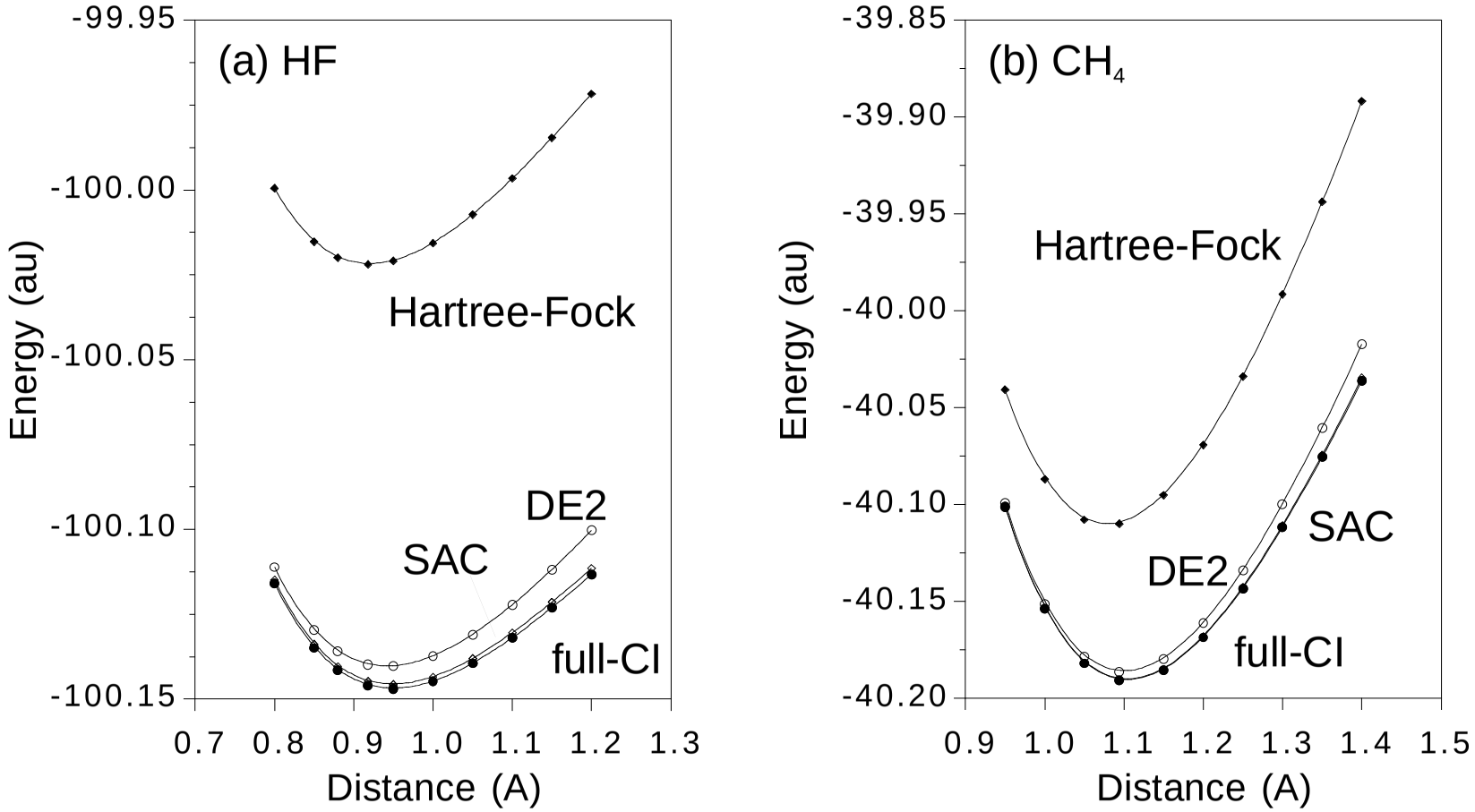

Fig. 1. Potential energy curves of (a) HF and (b) CH_4 calculated by the Hartree-Fock, DE2, SAC, and full-CI methods.

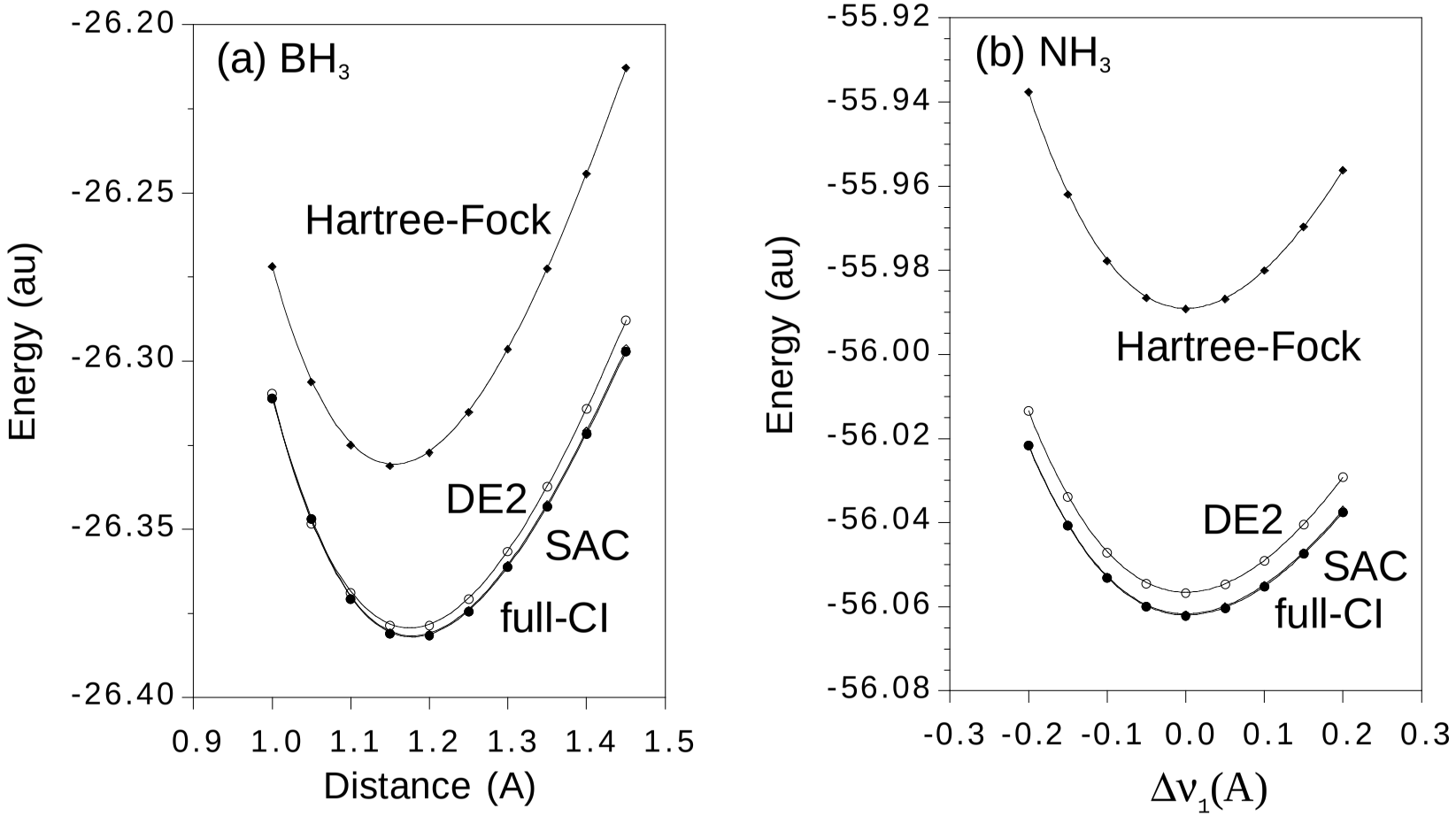

Fig. 2. Potential energy curves for the totally symmetric stretching modes of (a) BH_3 and (b) NH_3 calculated by the Hartree-Fock, DE2, SAC, and full-CI methods.

TABLE I: The equiliburium length R_e and totally-symmetric harmonic vibrational frequency ω_e caluclated for HF, CH_4, and BH_3

		R_e(Å)	ω_e(cm^{-1})
HF[a]			
	Hartree-Fock	0.9195	4233
	DE2	0.9416	3969
	SAC	0.9487	3826
	Full-CI	0.9495	3808
CH_4			
	Hartree-Fock	1.0783	3535
	DE2	1.0998	3306
	SAC	1.1035	3245
	Full-CI	1.1038	3240
BH_3			
	Hartree-Fock	1.1539	3114
	DE2	1.1743	2929
	SAC	1.1774	2879
	Full-CI	1.1778	3884

[a] Experimental values are $R_e = 0.9168$Å and $\omega_e = 4138$[22].

[b] Experimental values are $R_e = 1.0936$Å[23] and $\omega_e = 2915$[24].

of NH_3. The DE2 method describes 96.7 - 89.0% of the electron correlations of BH_3 and 92.6 - 89.8% for NH_3, though the geometry of NH_3 is different for each method.

The spectroscopic constants were numerically evaluated from the potential energy curves of the Hartree-Fock, DE2, SAC, and full-CI methods is shown in table I. The equilibrium distance R_e and the harmonic vibrational frequency armonic vibrational frequency of the DE2 method is much closer to the full-CI result than to the Hartree-Fock result. The SAC and full-CI results are almost the same.

It is important to examine not only the energy but also the details of the density. Fig. 3 shows the dipole moment of HF along the internulcear distance calculated by the Hartree-Fock, DE2, and full-CI methods. The DE2 method reproduces well the full-CI result, which is reasonable since the DE2 method directly calculates the

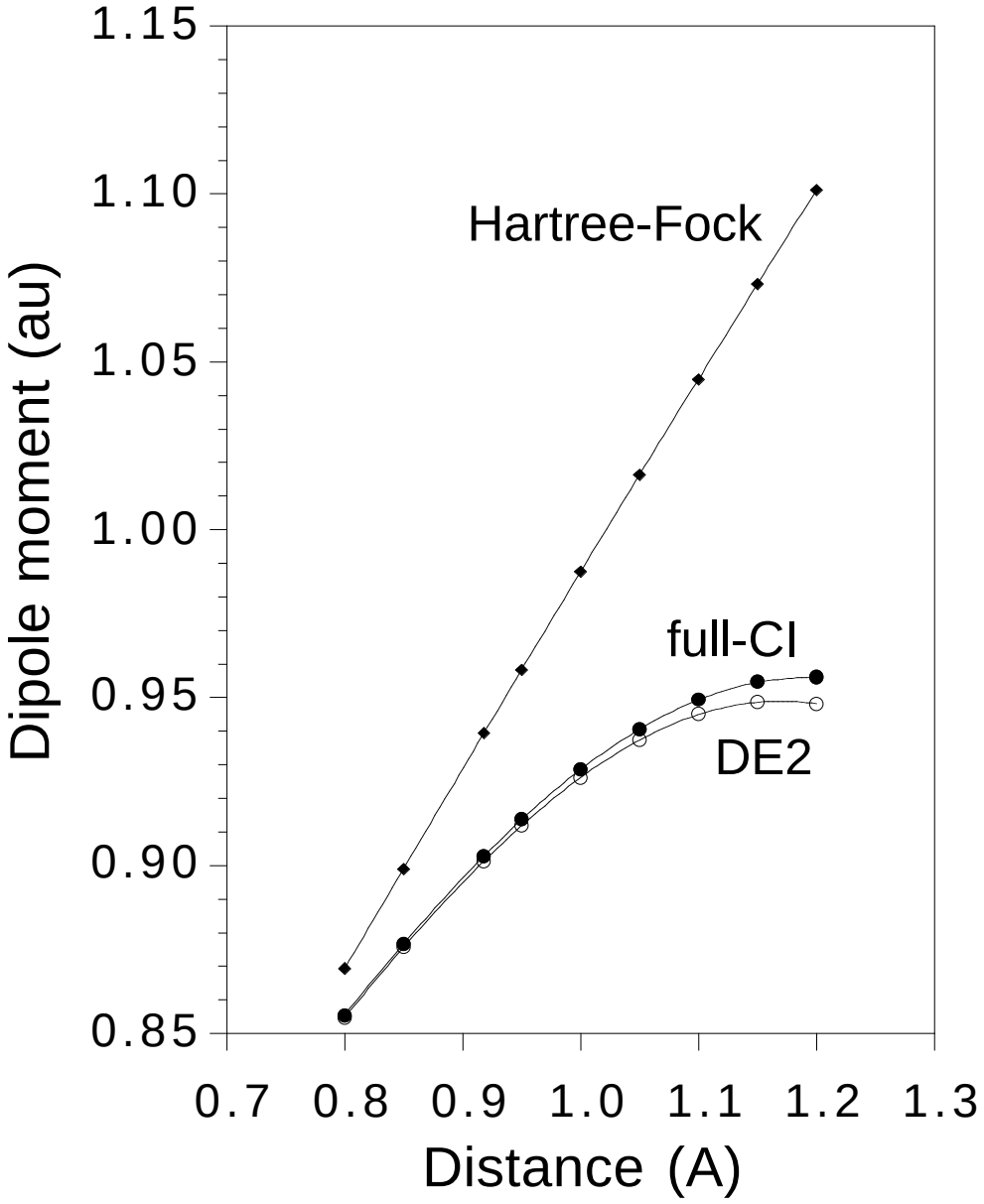

Fig. 3. Dipole moment vs. internulcear distance of HF calculated by the Hartree-Fock, DE2, and full-CI methods.

TABLE II: Optimized geometry and vibrational frequency of the totally symmetric stretching mode of NH_3

	Hartree-Fock	DE2	SAC	Full-CI
Optimized geometry[a]				
r_{NH}(Å)	1.0281	1.0580	1.0662	1.0664
θ_{HNH}	104.46	101.07	100.28	100.29
Vibrational frequency[b]				
$\nu_1(a_1)(\mathrm{cm}^{-1})$	3832	3496	3358	3350

[a] Experimental values are $r_{\mathrm{NH}} = 1.0116$Å and $\theta_{\mathrm{HNH}} = 106.68$[23]

[b] Experimental value is $\nu_1(a_1) = 3336\mathrm{cm}^{-1}$[24].

density matrix.

In the present DE2 calculation, the N-representability condition for the 1-RDM was satisfied for all the calculated geometries shown here: the eigenvalues of the 1-RDM, i.e., the occupation numbers, were all positive and less than two. As for the 2-RDM, the P, Q, and G conditions [3,4] for the N-representability were examined. Fig. 4 shows the lowest value and the sums of the negative eigenvalues of the P, Q, and G matrix of CH_4 along the internulcear distances shown in Fig. 1b. These values should be non-negative for the N-representative 2-RDM, but the lowest values are slightly negative from -1×10^{-4} at $R = 0.95$Å to -6×10^{-3} at $R = 1.4$Å. It should be noted that only 3 to 7 eigenvalues are negative out of the 336 independent variables and the sums of the negative values range from -3×10^{-4} to -1.6×10^{-2}. The calculated 2-RDM are not completely N-representable, but the deviation seems to be small. These conditions are satisfied better in shorter internulcear distances, as expected from the weight of the Hartree-Fock configuration.

We note here that in larger internuclear distances than those shown in this paper, where the Hartree-Fock approximation becomes worse, the DE2 equation was rather unstable and sometimes failed to converge. When we examine the occupation

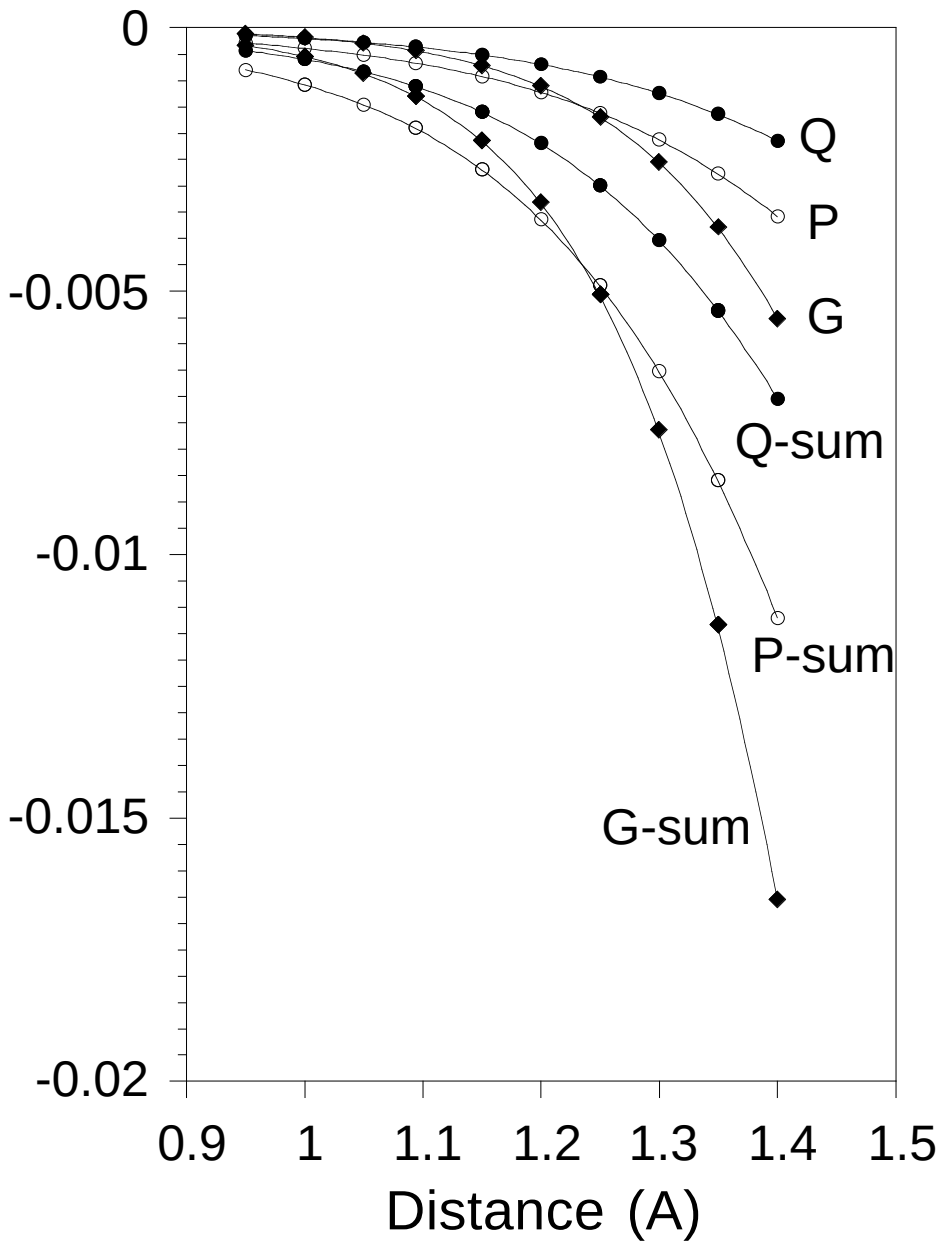

Fig. 4. Lowest values and the sums of the negative eigenvalues of the P, Q, and G matrices along the totally symmetric vibrational mode of CH_4.

TABLE III: Optimized geometry and vibrational frequencies cm^{-1} for the $\nu_1(a_1)$, $\nu_2(a_1)$, $\nu_3(b_2)$ modes of H_2O

	Hartree-Fock	DE2	SAC	Full-CI
Optimized geometry[a]				
r_{OH} (Å)	0.9862	1.0146	1.0262	1.0264
θ_{HOH}	100.01	97.47	96.68	96.68
Vibrational frequency[b]				
$\nu_1(a_1)$	4102	3761	3515	3512
$\nu_2(a_1)$	2162	2078	2031	2027
$\nu_3(a_2)$	4352	4001	3758	3756

[a] Experimental values are $r_{OH} = 0.9575$Å and $\theta_{HOH} = 104.51$[23]

[b] Experimental value is $\nu_1(a_1) = 3657cm^{-1}$, $\nu_2(a_1) = 1595cm^{-1}$, $\nu_3(b_2) = 3756cm^{-1}$ [24].

numbers of the 1-RDM at such a geometry, some of them were negative showing that the N-representability condition was broken. This behavior of the DE implies that it is stable only for the N-representable or almost N-representable DMs.

2.4 Full vibrational potential of H_2O

Finally, the DE2 method was used to calculate the potential energy surface of the ground state of H_2O along the normal modes, $v1(a1)$, $v2(a1)$, and $v3(b1)$, totally-symmetric stretching, bending, and anti-symmetric stretching modes, respectively. Fig. 5 compares the potential energy curves along these three modes around the equilibrium geometry determined by each method. The error in the electron correlation energy is relatively large for H_2O in comparison with other molecules. The errors were from 10.0 to 15.9% in the geometries examined here, although the weight of the Hartree-Fock configuration was as large as $0.95 - 0.97$. The vibrational analysis was performed for these three modes and the results are given in Table III

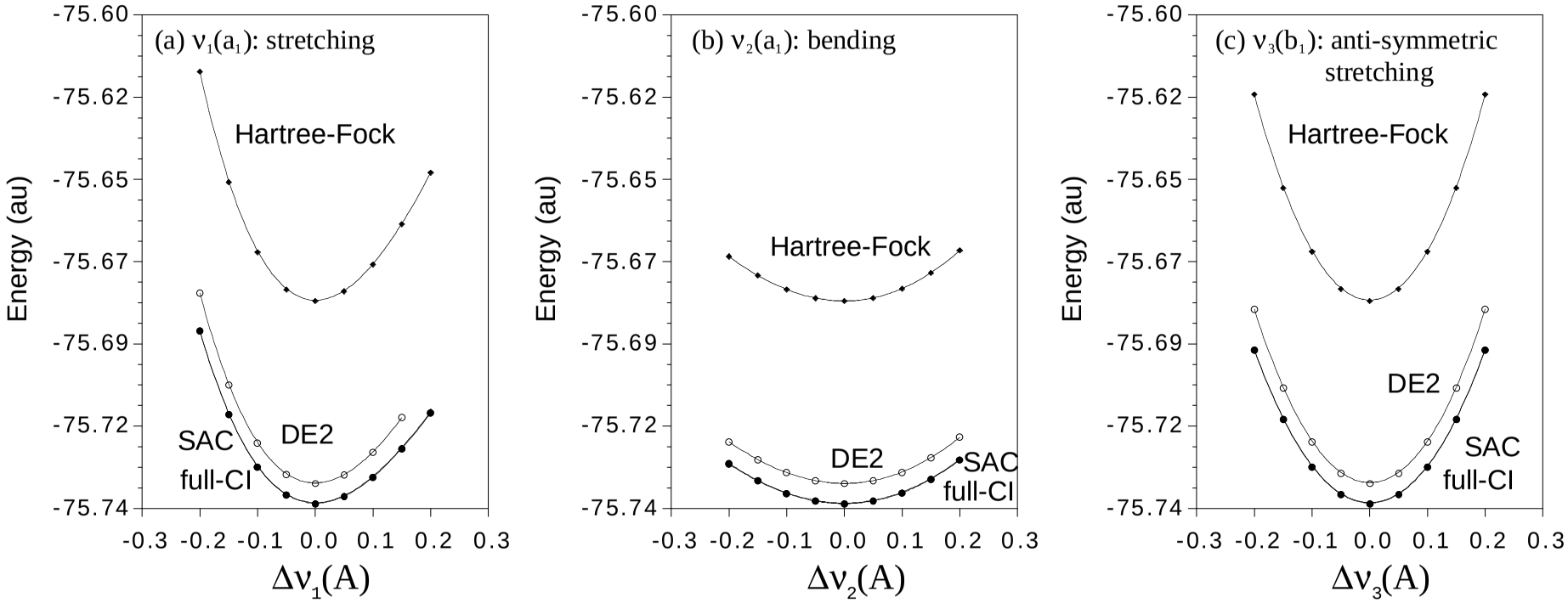

Fig. 5. Potential energy curves of H_2O for (a) $\nu_1(a_1)$, (b) $\nu_2(a_1)$, and (c) $\nu_3(b_1)$ modes calculated by the Hartree-Fock, DE2, SAC, and full-CI methods. Each curve is around the equilibrium geometry determined by each method.

together with the optimized geometry. The DE2 method well reproduces the equilibrium geometry. The vibrational frequencies calculated by the DE2 method are closer to the full-CI values than to the Hartree-Fock ones.

2.5 Conclusion

The density equation method has been applied sucessfully, for the first time, to the calculations of the potential energy curves, equilibrium geometries, and vibrational force constants of molecules without using the wave functions. The results for HF, CH_4, BH_3, NH_3, and H_2O reproduced well the SAC and full-CI results. It was effective in the present algorithm to adopt the 1s orbital of the first-row atoms as frozen core. The resultant density matrices were almost N-representable, in the region reported in this paper.

A note may be necessary about the Hartree-Fock method. When we introduce independent particle approximation, we can derive Hartree-Fock equation from the density equation as shown in Ref. [1]. In other words, the Hartree-Fock equation is a kind of the density equation. We used the Hartree-Fock orbital which is obtained by diagonalizing the first-order density matrix, as reference functions in the second-quantized formulation. So, we never used any wave function.

BIBLIOGRAPHY

[1] H. Nakatsuji, Phys. Rev. A **14** (1976) 41.

[2] H. Nakatsuji, Theor. Chem. Acc. 102(1-6), (1999) 97.

[3] H. Nakatsuji and K. Yasuda, Phys. Rev. Lett. **76** (1996) 1039.

[4] K. Yasuda and H. Nakatsuji, Phys. Rev. A **56** (1997) 2648.

[5] M. Nakata, M. Ehara, K. Yasuda and H. Nakatsuji, J. Chem. Phys., **112**, (2000) 8772.

[6] C. Valdemoro, Phys. Rev. A **45** (1992) 4462.

[7] F. Colmenero, C. Perez del Valle, and C. Valdemoro, Phys. Rev. A **47**(1993) 971.

[8] F. Colmenero, and C. Valdemoro, Phys. Rev. A **47** (1993) 979.

[9] F. Colmenero, and C. Valdemoro, Int. J. Quantum Chem. **51** (1997) 369.

[10] C. Valdemoro, L.M. Tel, and E. Perez-Romero, Adv. Quantum Chem. **28** (1997) 33.

[11] D.A. Mazziotti, Phys. Rev. A **57** (1998) 4219.

[12] D.A. Mazziotti, Chem. Phys. Lett. **289** (1998) 419.

[13] P. Hohenberg and W. Kohn, Phys. Rev. B **864** (1965) 136.

[14] R.G. Parr and W. Yang, Density-Functional Theory of Atoms and Molecules Oxford Univ. Press, New York, 1989.

[15] A.J. Coleman, Rev. Mod. Phys. **35** (1963) 668.

[16] S. Huzinaga, J. Chem. Phys. **42** (1965) 1293.

[17] T.H. Dunning Jr., J. Chem. Phys. **53** (1970) 2823.

[18] W.J. Hehre, R.F. Stewart and J.A. Pople, J. Chem. Phys. **51** (1969) 2657.

[19] H. Nakatsuji and K. Hirao, J. Chem. Phys. **68** (1978) 2053.

[20] M. Dupuis, J.D. Watts, H.O. Viller and G.J.B. Hurst,Program System HONDO8.

[21] H. Nakatsuji, M. Hada, M. Ehara, J. Hasegawa, T. Nakajima, H. Nakai, O. Kitao and K. Toyota, SAC/SAC-CI program system (SAC-CI96) for calculating ground, excited, ionized, and electron-attached states having singlet to septet spin multiplicities, 1996.

[22] K.P. Huber and G. Herzberg, Molecular Spectra and Molecular Structure IV. Constants of Diatomic Molecules, Van Nostrand Reinhold, New York, 1979.

[23] J.H. Callomon, E. Hirota, K. Kuchitsu, W.J. Lafferty, A.G. Maki and C.S. Pote, Landolt-Brönstein, Springer-Verlag, Berlin, 1976.

[24] G. Herzberg, Molecular Spectra and Molecular Structure III., Electronic Spectra and Electronic Structure of Polyatomic Molecules, Krieger, Florida, 1991.

Part II.

Density matrix variational theory

Chapter 3.

Variational calculations of fermion second-order reduced density matrices by semidefinite programming algorithm

Abstract

The ground-state fermion second-order reduced density matrix (2-RDM) is determined variationally using itself as a basic variable. As necessary conditions of the N-representability, we used the positive semidefiniteness conditions, P, Q and G conditions that are described in terms of the 2-RDM. The variational calculations are performed by using recently developed semidefinite programming algorithm (SDPA). The calculated energies of various closed- and open-shell atoms and molecules are excellent, overshooting only slightly the full-CI energies. There was no case where convergence was not achieved. The calculated properties also reproduce well the full-CI results.

3.1 Introduction

The ground state of N-body fermion system is completely described by the second-order reduced density matrix (2-RDM) $\Gamma^{(2)}$ because any observable properties of the system can be calculated from the 2-RDM [1, 2]. This fact led us to desire to use 2-RDM as a basic variable of quantum mechanics instead of the wave function Ψ: if we can determine $\Gamma^{(2)}$ without using Ψ, we have a closed form of quantum mechanics where the basic variable is 2-RDM. We refer to such formalism of quantum mechanics as density matrix theory (DMT)[3].

In non-relativistic case, the determinative equation for Ψ is the Schrödinger equation (SE). Therefore, to establish DMT, we have to formulate the equation for the RDM that is equivalent to the SE in the necessary and sufficient sense[3]. As such a equation, one of the author derived density equation (DE)[4, 5] that has recently been used successfully to calculate the 2-RDMs of atoms and molecules directly without any use of the wavefunction[6, 7, 8, 9]. This approach is called density equation theory (DET) and a review on the DET in chemical physics has recently been summarized together with some later developments[3].

Another equation that is equivalent to the SE but includes 2-RDM alone as a variable is the variational equation of the form

$$E_g \leq E[\Gamma^{(2)}] \tag{3.1}$$

where E_g is the exact ground-state energy. This method called density matrix variational theory (DMVT) is a straightforward consequence of the Ritz variational principle combined with the fact that the Hamiltonian involves only one- and two-body operators. The problem here is how well we can restrict our variable $\Gamma^{(2)}$ to be N-representable[10]. The N-representability condition that is enforced by the Pauli principle is not completely known for $\Gamma^{(2)}$ and this is an obstacle of the DMT in general.

The P, Q[10] and G[11] conditions are the well-known necessary conditions of the N-representability. They are the semidefiniteness conditions of the matrices derived from $\Gamma^{(2)}$. Though these three conditions are not complete, they seem to be quite strong to characterize the N-representability of the ground-state 2-RDM.

First calculations along this line were performed in a beautiful way by Garrod *et al.* [12, 13] for the ground state of Be, and Mihailović *et al.* [14] for the nuclear ground state of ^{15}O,^{16} O,^{17} O,^{18} O,^{20} Ne,^{24} Mg and ^{28}Si. At that time their method was very heuristic and hardly be applied to general systems. We found that this method can be elegantly realized using the semidefinite programming algorithm (SDPA)[15], recently developed in the field of mathematical programming. We calculated the ground-state energies of atoms and molecules using these three necessary conditions and employing SDPA as our problem solver.

3.2 Theorical outline

First and second order reduced density matrices (1-, 2-RDMs), γ and Γ, respectively, are defined by

$$\gamma^i_j = \langle\Psi|a^\dagger_i a_j|\Psi\rangle, \tag{3.2}$$

and

$$\Gamma^{i_1 i_2}_{j_1 j_2} = \frac{1}{2}\langle\Psi|a^\dagger_{i_1} a^\dagger_{i_2} a_{j_2} a_{j_1}|\Psi\rangle, \tag{3.3}$$

where $a^\dagger$ and a denote creation and annihilation operators, respectively. Note we have simplified $\Gamma^{(2)}$ as Γ. Throughout this paper, we assume the elements of 1-RDM and 2-RDM to be real. Complete N-representability condition is known for γ[10], but for Γ, we know only necessary conditions (the known complete condition is not practical). Some trivial conditions for 2-RDM are:

1. Antisymmetric condition

$$\Gamma^{i_1 i_2}_{j_1 j_2} = -\Gamma^{i_2 i_1}_{j_1 j_2} = -\Gamma^{i_1 i_2}_{j_2 j_1} \tag{3.4}$$

2. Hermiticity

$$\Gamma^{i_1 i_2}_{j_1 j_2} = \Gamma^{j_1 j_2}_{i_1 i_2} \tag{3.5}$$

3. trace condition

$$\sum_k \Gamma^{ik}_{jk} = \frac{2}{N-1}\gamma^i_j \tag{3.6}$$

4. number of electrons

$$N = \sum_k \gamma_k^k \tag{3.7}$$

5. eigenstate of the number of α (or β) electrons

$$\mathrm{tr} N_\alpha \Gamma = N_\alpha \quad \text{and} \quad \mathrm{tr} N_\alpha^2 \Gamma = N_\alpha^2 \tag{3.8}$$

where the operators of N_α and N_α^2 are written as:

$$\begin{aligned} N_\alpha &= \sum_i a_{i\alpha}^\dagger a_{i\alpha} \\ N_\alpha^2 &= \sum_{ij} a_{i\alpha}^\dagger a_{i\alpha} a_{j\alpha}^\dagger a_{j\alpha} \end{aligned} \tag{3.9}$$

6. spin symmetry

$$\Gamma_{j_1\sigma_1' j_2\sigma_2'}^{i_1\sigma_1 i_2\sigma_2} = 0 \tag{3.10}$$

when $\sigma_1 \neq \sigma_1'$ or $\sigma_2 \neq \sigma_2'$ and $\sigma_1 \neq \sigma_2'$ or $\sigma_2 \neq \sigma_1'$, where σ denotes spin variable.

7. expectation value of S^2

$$\mathrm{tr} S^2 \Gamma = S(S+1) \tag{3.11}$$

where the spin-squared operator S^2 is given by

$$\begin{aligned} S^2 &= S_z + S_z^2 + S_- S_+ \\ &= \frac{1}{2}\sum_i \left(a_{i\alpha}^\dagger a_{i\alpha} - a_{i\beta}^\dagger a_{i\beta} \right) + \frac{1}{4}\left(\sum_i a_{i\alpha}^\dagger a_{i\alpha} - a_{i\beta}^\dagger a_{i\beta} \right)^2 \\ &\quad + \sum_{ij} a_{i\beta}^\dagger a_{i\alpha} a_{j\alpha}^\dagger a_{j\beta} \end{aligned} \tag{3.12}$$

8. positive semidefiniteness of P matrix, which is just 2-RDM

$$\sum x_{i_1 i_2} \Gamma_{j_1 j_2}^{i_1 i_2} x_{j_1 j_2} \geq 0 \tag{3.13}$$

where $x_{i_1 i_2}$ is an arbitrary geminal.

Note that except for the condition 8, all of these conditions are linear to 2-RDM.

The Q and G matrices are defined by

$$Q_{j_1 j_2}^{i_1 i_2} = \langle \Psi | a_{i_1} a_{i_2} a_{j_2}^\dagger a_{j_1}^\dagger | \Psi \rangle \tag{3.14}$$

and

$$G^{i_1 i_2}_{j_1 j_2} = \langle \Psi | a^\dagger_{i_1} a_{i_2} a^\dagger_{j_2} a_{j_1} | \Psi \rangle. \tag{3.15}$$

These matrices are semidefinite[11] and linear to Γ as

$$Q^{i_1 i_2}_{j_1 j_2} = (\delta^{i_1}_{j_1}\delta^{i_2}_{j_2} - \delta^{i_1}_{j_2}\delta^{i_2}_{j_1}) - (\delta^{i_1}_{j_1}\gamma^{i_2}_{j_2} + \delta^{i_2}_{j_2}\gamma^{i_1}_{j_1}) + (\delta^{i_1}_{j_2}\gamma^{i_2}_{j_1} + \delta^{i_2}_{j_1}\gamma^{i_1}_{j_2}) - 2\Gamma^{i_1 i_2}_{j_1 j_2} \tag{3.16}$$

and

$$G^{i_1 i_2}_{j_1 j_2} = \delta^{i_2}_{j_2}\gamma^{i_1}_{j_1} - 2\Gamma^{i_1 j_2}_{j_1 i_2}. \tag{3.17}$$

We note that originally the G matrix was written in an equivalent nonlinear form[16].

The Hamiltonian of the system can be written as,

$$H^{i_1 i_2}_{j_1 j_2} = w^{i_1 i_2}_{j_1 j_2} + \frac{1}{N-1}(v^{i_1}_{j_1}\delta^{i_2}_{j_2} + v^{i_1}_{j_2}\delta^{i_2}_{j_1}). \tag{3.18}$$

where v and w are 1- and 2-body operators, respectively. Then, the basic equation of DMVT given by Eq.(3.1) is written as the variational minimization of the energy within our constraints,

$$E_{\min} = \underset{\Gamma \in {}^{(2)}\mathcal{P}}{\mathrm{Min}} \ \mathrm{Tr} H\Gamma \tag{3.19}$$

where ${}^{(2)}\mathcal{P}$ is the set of 2-RDMs which satisfies the above necessary N-representability conditions, namely,

$${}^{(2)}\mathcal{P} = \{\Gamma | P,\, Q,\, G \text{ matrices are non-negative and the conditions } 1 \sim 7 \text{ are satisfied}\}. \tag{3.20}$$

Either of the P, Q and G conditions forms compact convex set with trace topology[17], and a finite combination of compact convex sets is also compact convex set, therefore this method should find a minimum in energy. This method can be applied to the ground state of any space and spin symmetry.

3.3 Calculation method

The minimization problem with some linear constraints can be achieved by using semidefinite programming algorithm(SDPA)[15] as a problem solver. The SDPA has recently been developed in the field of mathematical programming. In this section,

we explain how to apply SDPA to our problem of solving $\Gamma^{(2)}$ in the constrained variational method given by Eq.(3.19). The dimensions of the matrices are $n \times n$, if they are not explicitly defined.

3.3.1 Simplified problem

First, we introduce a simplified problem which contains all the essentials, that is

> Problem(a): Minimize the total energy of the 2-RDM Γ subject to the fixed number of electrons and the positive semidefiniteness of Γ.

The positive semidefiniteness of Γ is the P condition. Note that this problem gives the exact solution for $N = 2$. Problem (a) is written as,

$$\text{Problem(a}'\text{):} \begin{cases} \text{Minimize} & \mathrm{Tr}H\Gamma \\ \text{subject to} & \mathrm{Tr}N\Gamma = N \\ & \text{and } \Gamma \text{ is positive semidefinite.} \end{cases} \tag{3.21}$$

Formal expression of the problem[15] is,

$$\text{Problem(a}''\text{):} \begin{cases} \text{Minimize} & \boldsymbol{F}_0 \bullet \boldsymbol{Y} \\ \text{subject to} & \boldsymbol{F}_1 \bullet \boldsymbol{Y} = c_1 \\ & \text{and } \boldsymbol{Y} \text{ is positive semidefinite} \end{cases} \tag{3.22}$$

where $\boldsymbol{F}_0$ and $\boldsymbol{F}_1$ are constant $n \times n$ symmetric matrices, and $\boldsymbol{Y}$ is $n \times n$ symmetric variable matrix, c_1 is real constant, and $\bullet$ is an operator such that

$$\boldsymbol{F} \bullet \boldsymbol{Y} = \sum_{i,j} (\boldsymbol{F})_{ij} (\boldsymbol{Y})_{ij}. \tag{3.23}$$

One can easily confirm that problem (a$'$) and problem (a$''$) are the same when we take $\boldsymbol{Y}$ as Γ, $\boldsymbol{F}_0$ as Hamiltonian, and $\boldsymbol{F}_1$ as number of operator. A generalization of the problem (a$''$) is called semidefinite programming(SDP).

3.3.2 Semidefinite programming algorithm(SDPA)

The SDPA[15] solves the following form of semidefinite programming and its dual,

$$\text{SDP}\begin{cases} \textit{primal}: & \text{minimize} & \displaystyle\sum_{i=1}^{m} c_i x_i \\ & \text{subject to} & \boldsymbol{X} = \displaystyle\sum_{i=1}^{m} \boldsymbol{F}_i x_i - \boldsymbol{F}_0, \ \ \boldsymbol{X} \succeq \boldsymbol{0} \\ \textit{dual}: & \text{maximize} & \boldsymbol{F}_0 \bullet \boldsymbol{Y} \\ & \text{subject to} & \boldsymbol{F}_i \bullet \boldsymbol{Y} = c_i \ \ (1 \leq i \leq m), \ \ \boldsymbol{Y} \succeq \boldsymbol{0} \end{cases} \tag{3.24}$$

where $\boldsymbol{X}$ and $\boldsymbol{Y}$ are $n \times n$ real symmetric matrices, $\boldsymbol{F}_i, (1 \leq i \leq m)$ symmetric constraint matrices, c_i and x_i real constant and variable numbers, respectively, $\boldsymbol{U} \bullet \boldsymbol{V}$ denotes inner product of the matrices, $\boldsymbol{U} \bullet \boldsymbol{V} = \sum_{i,j} \boldsymbol{U}_{i,j} \boldsymbol{V}_{i,j}$, and $\boldsymbol{X} \succeq \boldsymbol{0}$ means $\boldsymbol{X}$ to be positive semidefinite. We assume all the constraint matrices are linearly independent.

Semidefinite programming is usually solved by primal-dual interior-point method[18, 19]. This method is based on the primal-dual theorem of SDP, which shows an existence of the optimal solution and gives a necessary and sufficient condition for the optimal solution (minimum in primal problem, and maximum in dual problem): if there exists $(\boldsymbol{X}, \boldsymbol{Y}, \boldsymbol{x})$ such that they satisfy all the constraints and $\boldsymbol{X} \succeq \boldsymbol{0}$ and $\boldsymbol{Y} \succeq \boldsymbol{0}$, then

1. SDP has optimal solution.

2. Necessary and sufficient condition for the optimal solution $(\boldsymbol{X}^*, \boldsymbol{Y}^*, \boldsymbol{x}^*)$ is

$$\boldsymbol{X}^* \bullet \boldsymbol{Y}^* = \boldsymbol{F}_0 \bullet \boldsymbol{Y}^* - \sum_{i=1}^{m} c_i x_i^* = 0. \tag{3.25}$$

3.3.3 Set up of DMVT in SDPA

Our object is to solve the DMVT problem(3.19). It is equivalent to solve the *dual* of the problem(3.24), taking $\boldsymbol{Y}$ as 2-RDM, $\boldsymbol{F}_0$ as Hamiltonian, $\boldsymbol{F}_1$ as the constraint for the number of electrons, $\boldsymbol{F}_2$ as the constraint for spin squared operator, etc. Maximization is altered to minimization by just changing the sign of $\boldsymbol{F}_0$. The

problem(3.19) is written as:

$$\begin{cases} \text{Minimize} & \mathrm{Tr}H\Gamma \\ \text{subjected to} & \mathrm{Tr}N\Gamma = N \\ & \mathrm{Tr}S^2\Gamma = S(S+1) \\ & \mathrm{Tr}N_\alpha\Gamma = N_\alpha \\ & \mathrm{Tr}N_\alpha^2\Gamma = N_\alpha^2 \\ & \text{and } \Gamma^{(2)} \succeq 0, \boldsymbol{Q} \succeq 0 \text{ and } \boldsymbol{G} \succeq 0. \end{cases} \tag{3.26}$$

Note that some of the matrices appeared below have four indices, however, we can reduce them to two indices by mapping indices (i, j) to the composite index k. Imposing linear constraints for N or S^2 etc. is straightforward. Constraining the expectation value of the two body operator A to be $c_a(\mathrm{Tr}A\Gamma = c_a)$ is done as follows,

1. Explicit expression of A is give by,

$$A = \sum_{i_1 i_2 j_1 j_2} a^{i_1 i_2}_{j_1 j_2} a^\dagger_{i_1} a^\dagger_{i_2} a_{j_2} a_{j_1}, \tag{3.27}$$

   where $a^{i_1 i_2}_{j_1 j_2}$ is constant.

2. Set up the constraint matrix $\boldsymbol{F}_A$ such that

$$(\boldsymbol{F}_A)^{i_1 i_2}_{j_1 j_2} = a^{i_1 i_2}_{j_1 j_2}. \tag{3.28}$$

3. Then, the constraint is given by the equality:

$$\begin{aligned} \boldsymbol{F}_A \bullet \Gamma &= \sum_{i_1 i_2 j_1 j_2} a^{i_1 i_2}_{j_1 j_2} Y^{i_1 i_2}_{j_1 j_2} \\ &= \mathrm{Tr}A\Gamma \\ &= c_a. \end{aligned} \tag{3.29}$$

For example, we set up the constraint matrix for the number of particles N. Explicit expression of N is,

$$\begin{aligned} N &= \sum_i a^\dagger_i a_i \\ &= \frac{N-1}{2} \sum_{ij} a^\dagger_i a^\dagger_j a_j a_i. \end{aligned} \tag{3.30}$$

Then, the constraint matrix $\boldsymbol{F}_N$ for the number of particle is represented by

$$(\boldsymbol{F}_N)^{ij}_{kl} = \frac{N-1}{2}\delta_{ik}\delta_{jl}, \tag{3.31}$$

and we confirm the following relation,

$$\begin{aligned}
\boldsymbol{F}_N \bullet \boldsymbol{Y} &= \sum_{ijkl}(\boldsymbol{F}_N)^{ij}_{kl}\Gamma^{ij}_{kl} \\
&= \sum_{ijkl}\frac{N-1}{2}\delta_{ik}\delta_{jl}\Gamma^{ij}_{kl} \\
&= \frac{N-1}{2}\sum_{ij}\Gamma^{ij}_{ij} \\
&= \frac{N-1}{2}\sum_{i}\frac{2}{N-1}\gamma^i_i \\
&= \sum_i \gamma^i_i \\
&= N.
\end{aligned} \tag{3.32}$$

Now we consider how to enforce the 2-RDM to satisfy the P, Q, and G conditions, simultaneously. We first explain the case where only P and Q conditions are enforced simultaneously.

We introduce the variable matrix $\boldsymbol{Y}$ in which P and Q matrices are diagonally arranged,

$$\boldsymbol{Y} = \begin{pmatrix} \boldsymbol{P} & \boldsymbol{0} \\ \boldsymbol{0} & \boldsymbol{Q} \end{pmatrix}. \tag{3.33}$$

It is obvious that

$$\boldsymbol{Y} \succeq \boldsymbol{0} \leftrightarrow \boldsymbol{P} \succeq \boldsymbol{0} \quad \text{and} \quad \boldsymbol{Q} \succeq \boldsymbol{0}. \tag{3.34}$$

There is a linear relation between Γ and Q matrices:

$$\begin{aligned}
Q^{i_1 i_2}_{j_1 j_2} &= (\delta^{i_1}_{j_1}\delta^{i_2}_{j_2} - \delta^{i_1}_{j_2}\delta^{i_2}_{j_1}) - \sum_k \frac{N-1}{2}(\delta^{i_1}_{j_1}\Gamma^{i_2 k}_{j_2 k} + \delta^{i_2}_{j_2}\Gamma^{i_1 k}_{j_1 k}) \\
&\quad + \sum_k \frac{N-1}{2}(\delta^{i_1}_{j_2}\Gamma^{i_2 k}_{j_1 k} + \delta^{i_2}_{j_1}\Gamma^{i_1 k}_{j_2 k}) - 2\Gamma^{i_1 i_2}_{j_1 j_2}.
\end{aligned} \tag{3.35}$$

Therefore, we can find a set of linear constraints for *each* element of the Q matrix as

$$\boldsymbol{E}^{i_1 i_2}_{j_1 j_2} \bullet \boldsymbol{Y} = c^{i_1 i_2}_{j_1 j_2}$$

$$
\begin{aligned}
&= 2\Gamma^{i_1 i_2}_{j_1 j_2} + (\delta^{i_1}_{j_1}\gamma^{i_2}_{j_2} + \delta^{i_2}_{j_2}\gamma^{i_1}_{j_1}) - (\delta^{i_1}_{j_2}\gamma^{i_2}_{j_1} + \delta^{i_2}_{j_1}\gamma^{i_1}_{j_2}) + Q^{i_1 i_2}_{j_1 j_2} \\
&= \delta^{i_1}_{j_1}\delta^{i_2}_{j_2} - \delta^{i_1}_{j_2}\delta^{i_2}_{j_1}. \qquad (3.36)
\end{aligned}
$$

Using these constraints, the SDP formalism is given by:

$$
\begin{cases}
\text{Minimize} & \boldsymbol{H} \bullet \boldsymbol{Y} \\
\text{subject to} & \boldsymbol{F}_i \bullet \boldsymbol{Y} = c_i \\
& \tilde{\boldsymbol{E}}^{i_1 i_2}_{j_1 j_2} \bullet \boldsymbol{Y} = \delta^{i_1}_{j_1}\delta^{i_2}_{j_2} - \delta^{i_1}_{j_2}\delta^{i_2}_{j_1}
\end{cases} \qquad (3.37)
$$

where $\tilde{\boldsymbol{E}}^{i_1 i_2}_{j_1 j_2}$ is a symmetric matrix defined by:

$$
\tilde{\boldsymbol{E}}^{i_1 i_2}_{j_1 j_2} = \frac{1}{2}\left(\boldsymbol{E}^{i_1 i_2}_{j_1 j_2} + \boldsymbol{E}^{j_1 j_2}_{i_1 i_2}\right), \qquad (3.38)
$$

and the explicit expression of the element of the constraint matrix, $(\boldsymbol{E}^{i_1 i_2}_{j_1 j_2})^{k_1 k_2}_{l_1 l_2}$ is given by

$$
\begin{aligned}
(\boldsymbol{E}^{i_1 i_2}_{j_1 j_2})^{k_1 k_2}_{l_1 l_2} &= 2\delta^{i_1}_{k_1}\delta^{i_2}_{k_2}\delta^{j_1}_{l_1}\delta^{j_2}_{l_2} + \delta^{i_1+n}_{k_1}\delta^{i_2+n}_{k_2}\delta^{j_1+n}_{l_1}\delta^{j_2+n}_{l_2} \\
&\quad + \frac{N-1}{2}\delta^{i_1}_{j_1}\delta^{i_2}_{k_1}\delta^{j_2}_{l_1}\delta^{k_2}_{l_2} + \frac{N-1}{2}\delta^{i_2}_{j_2}\delta^{i_1}_{k_1}\delta^{j_1}_{l_1}\delta^{k_2}_{l_2} \\
&\quad - \frac{N-1}{2}\delta^{i_1}_{j_2}\delta^{i_2}_{k_1}\delta^{j_1}_{l_1}\delta^{k_2}_{l_2} - \frac{N-1}{2}\delta^{i_2}_{j_1}\delta^{i_1}_{k_1}\delta^{j_2}_{l_1}\delta^{k_2}_{l_2} \qquad (3.39)
\end{aligned}
$$

and the constant $c^{i_1 i_2}_{j_1 j_2}$ in Eq.(3.36) is

$$
c^{i_1 i_2}_{j_1 j_2} = \delta^{i_1}_{j_1}\delta^{i_2}_{j_2} - \delta^{i_1}_{j_2}\delta^{i_2}_{j_1}, \qquad (3.40)
$$

We can confirm Eq.(3.41) holds

$$
\boldsymbol{E}^{i_1 i_2}_{j_1 j_2} \bullet \boldsymbol{Y} = \sum_{k_1 k_2 l_1 l_2} (\boldsymbol{E}^{i_1 i_2}_{j_1 j_2})^{k_1 k_2}_{l_1 l_2} (\boldsymbol{Y})^{k_1 k_2}_{l_1 l_2} = c^{i_1 i_2}_{j_1 j_2} \qquad (3.41)
$$

as follows. The first two terms of Eq.(3.41) are

$$
\begin{aligned}
\sum_{k_1 k_2 l_1 l_2} (2\delta^{i_1}_{k_1}\delta^{i_2}_{k_2}\delta^{j_1}_{l_1}\delta^{j_2}_{l_2} &+ \delta^{i_1+n}_{k_1}\delta^{i_2+n}_{k_2}\delta^{j_1+n}_{l_1}\delta^{j_2+n}_{l_2})(\boldsymbol{Y})^{k_1 k_2}_{l_1 l_2} \\
&= 2(\boldsymbol{Y})^{i_1 i_2}_{j_1 j_2} + (\boldsymbol{Y})^{i_1+n, i_2+n}_{j_1+n, j_2+n} \\
&= 2\Gamma^{i_1 i_2}_{j_1 j_2} + Q^{i_1 i_2}_{j_1 j_2}, \qquad (3.42)
\end{aligned}
$$

the second two terms of Eq.(3.41) give,

$$\begin{aligned}
&\sum_{k_1k_2l_1l_2}\left(\frac{N-1}{2}\delta^{i_1}_{j_1}\delta^{i_2}_{k_1}\delta^{j_2}_{l_1}\delta^{k_2}_{l_2}+\frac{N-1}{2}\delta^{i_2}_{j_2}\delta^{i_1}_{k_1}\delta^{j_1}_{l_1}\delta^{k_2}_{l_2}\right)(\boldsymbol{Y})^{k_1k_2}_{l_1l_2}\\
=\;&\frac{N-1}{2}\sum_k\delta^{i_1}_{j_1}\Gamma^{i_2k}_{j_2k}+\frac{N-1}{2}\sum_k\delta^{i_2}_{j_2}\Gamma^{i_1k}_{j_1k}\\
=\;&\delta^{i_1}_{j_1}\gamma^{i_2}_{j_2}+\delta^{i_2}_{j_2}\gamma^{i_1}_{j_1},
\end{aligned}\tag{3.43}$$

and the last term gives

$$\begin{aligned}
&\sum_{k_1k_2l_1l_2}\left(-\frac{N-1}{2}\delta^{j_2}_{i_1}\delta^{i_2}_{k_1}\delta^{j_1}_{l_1}\delta^{k_2}_{l_2}-\frac{N-1}{2}\delta^{j_1}_{i_2}\delta^{i_1}_{k_1}\delta^{j_2}_{l_1}\delta^{k_2}_{l_2}\right)(\boldsymbol{Y})^{k_1k_2}_{l_1l_2}\\
=\;&-\frac{N-1}{2}\sum_k\delta^{j_2}_{i_1}\Gamma^{i_2k}_{j_1k}-\frac{N-1}{2}\sum_k\delta^{j_1}_{i_2}\Gamma^{i_1k}_{j_2k}\\
=\;&-\delta^{i_1}_{j_2}\gamma^{i_2}_{j_1}-\delta^{i_2}_{j_1}\gamma^{i_1}_{j_2}.
\end{aligned}\tag{3.44}$$

Combining Eq.(3.42)$\sim$ Eq.(3.44), we get Eq.(3.36).

Constraining P, Q and G matrices to be positive semidefinite is done in essentially the same way as above. In this case, the variable matrix $\boldsymbol{Y}$ is defined as:

$$\boldsymbol{Y}=\begin{pmatrix}\boldsymbol{P}&\mathbf{0}&\mathbf{0}\\\mathbf{0}&\boldsymbol{Q}&\mathbf{0}\\\mathbf{0}&\mathbf{0}&\boldsymbol{G}\end{pmatrix}.\tag{3.45}$$

We have a linear relation between Γ and G:

$$G^{i_1i_2}_{j_1j_2}=\delta^{i_2}_{j_2}\sum_k\frac{N-1}{2}\Gamma^{i_1k}_{j_1k}-2\Gamma^{i_1j_2}_{j_1i_2},\tag{3.46}$$

which is described by a set of linear constraints $\boldsymbol{J}^{i_1i_2}_{j_1j_2}$ for each element of G matrix as

$$\begin{aligned}
\boldsymbol{J}^{i_1i_2}_{j_1j_2}\bullet Y&=0\\
&=-\delta^{i_2}_{j_2}\gamma^{i_1}_{j_1}+2\Gamma^{i_1j_2}_{j_1i_2}+G^{i_1j_2}_{j_1i_2},
\end{aligned}\tag{3.47}$$

and an explicit expression of the constraint matrix $(\boldsymbol{J}^{i_1i_2}_{j_1j_2})^{k_1k_2}_{l_1l_2}$ is given by

$$(\boldsymbol{J}^{i_1i_2}_{j_1j_2})^{k_1k_2}_{l_1l_2}=2\delta^{i_1}_{k_1}\delta^{i_2}_{k_2}\delta^{j_1}_{l_1}\delta^{j_2}_{l_2}+\delta^{i_1+2n}_{k_1}\delta^{i_2+2n}_{k_2}\delta^{j_1+2n}_{l_1}\delta^{j_2+2n}_{l_2}-\frac{N-1}{2}\delta^{i_2}_{j_2}\delta^{i_1}_{k_1}\delta^{i_2}_{l_1}\delta^{k_2}_{l_2},\tag{3.48}$$

which is further symmetrized as

$$\tilde{\boldsymbol{J}}^{i_1 i_2}_{j_1 j_2} = \frac{1}{2}\left(\boldsymbol{J}^{i_1 i_2}_{j_1 j_2} + \boldsymbol{J}^{j_1 j_2}_{i_1 i_2}\right). \tag{3.49}$$

Thus, the DMVT using the P, Q and G conditions is formulated into SDPA as

$$\begin{cases} \text{Minimize} & \boldsymbol{H} \bullet \boldsymbol{Y} \\ \text{subjected to} & \boldsymbol{F}_i \bullet \boldsymbol{Y} = c_i \\ & \tilde{\boldsymbol{E}}^{i_1 i_2}_{j_1 j_2} \bullet \boldsymbol{Y} = \delta^{i_1}_{j_1}\delta^{i_2}_{j_2} - \delta^{i_1}_{j_2}\delta^{i_2}_{j_1} \\ & \tilde{\boldsymbol{J}}^{i_1 i_2}_{j_1 j_2} \bullet \boldsymbol{Y} = 0. \end{cases} \tag{3.50}$$

It is convenient to fold our 2-RDM into a compact form,

$$P^{i_1 i_2}_{j_1 j_2} \to P^{i}_{j} \tag{3.51}$$

by renumbering $i = i_1 + \frac{i_2(i_2-1)}{2}$ if $i_1 > i_2$ and discarding P when $i_1 \leq i_2$. This helps to cut down unnecessary variables and to automatically assume that 2-RDM has antisymmetric property. Similarly, the Q matrix and other linear constraints are also folded. Note that the G matrix does not have such a symmetry property, so that we use all the elements.

The present method involves very large number of linear constraints and may not be efficient: a merit is that the SDPA program is used without any modification. However, if we make a problem-specific SDP solver, it would be much more efficient than the present one, and such study is now in progress.

The DMVT formulated above has been applied to the ground states of different space and spin symmetries of neutral and charged species of 16 different atoms and molecules. They are Be(^{1}S), Be(^{3}S), LiH($^1\Sigma^+$), LiH($^3\Sigma^+$), BeH^+ BH^+, BH, CH^+, CH, CH^-, NH^+, NH^-, NH, OH^+, OH^-, OH, HF^+, HF, $BH_2(^2A_1)$, $BH_2(^2B_1)$, $CH_2(^1A_1)$, $CH_2(^3B_1)$, linear $CH_2(^3\Sigma_u^-)$, $NH_2(^2A_1)$, $NH_2(^2B_1)$, H_2O, H_2O^+, FH_2^+, BH_3, CH_3, NH_3, NH_3(dis) ('dis' stands for distorted in the sense that one bond length shorten by 0.9 time, another one lengthen by 1.1 time) and H_3O^+.

We used three different basis sets, double and triple-ζ s-type GTOs and STO-6G, for Be, and double-ζ s-type GTOs by Huzinaga[20] and Dunning[21] and STO-6G for LiH. For all the other molecules, we used STO-6G basis set[22]. The geometries we used are the experimental ones[23, 24].

TABLE I: Total energy and correlation energy in % in parentheses calculated by DMVT with $P+Q$ and $P+Q+G$ conditions compared with those obatined by the wave function methods, full CI and Hartree-Fock. The basis set is STO-6G except for notice.

System	State	Active MO[a]	Ele[b] $(\alpha+\beta)$	DM$(P+Q)$	DM$(P+Q+G)$	Full CI	Hartree-Fock
Be[c]	^{1}S	4	4(2+2)	-14.5934(176)	-14.5827(100)	-14.5827(100)	-14.5685(0)
Be	^{1}S	5	4(2+2)	-14.5579(103)	-14.5561(100)	-14.5561(100)	-14.5034(0)
Be[d]	^{1}S	5	4(2+2)	-14.6064(200)	-14.5895(100)	-14.5895(100)	-14.5725(0)
Be[c]	^{3}S	4	4(3+1)	-13.3168(120)	-13.3146(100)	-13.3146(100)	-13.3036(0)
Be[d]	^{3}S	5	4(3+1)	-14.3346(177)	-14.3241(100)	-14.3241(100)	-14.3105(0)
LiH[c]	$^1\Sigma^+$	6	4(2+2)	-8.0034(139)	-7.9924(100)	-7.9922(100)	-7.9635(0)
LiH	$^1\Sigma^+$	6	4(2+2)	-7.9731(104)	-7.9724(100)	-7.9723(100)	-7.9519(0)
LiH[c]	$^3\Sigma^+$	6	4(3+1)	-7.8997(167)	-7.8939(98)	-7.8940(100)	-7.8854(0)
LiH	$^3\Sigma^+$	6	4(3+1)	-7.8554(191)	-7.8552(97)	-7.8552(100)	-7.8549(0)
BeH^+	$^1\Sigma^+$	6	4(2+2)	-14.8452(106)	-14.8439(100)	-14.8438(100)	-14.8226(0)
BH^+	$^2\Sigma^+$	6	5(3+2)	-24.8169(151)	-24.8015(100)	-24.8015(100)	-24.7712(0)
BH	$^1\Sigma^+$	6	6(3+3)	-25.1234(211)	-25.0630(106)	-25.0593(100)	-25.0015(0)
CH^+	$^1\Sigma^+$	6	6(3+3)	-37.9618(227)	-37.8896(107)	-37.8853(100)	-37.8251(0)
CH^-	$^3\Sigma^-$	6	8(5+3)	-37.9834(148)	-37.9714(99)	-37.9718(100)	-37.9477(0)
CH	$^2\Pi$	6	7(4+3)	-38.2472(240)	-38.1917(111)	-38.1871(100)	-38.1443(0)
NH^+	$^2\Pi$	6	7(4+3)	-54.4510(248)	-54.3957(111)	-54.3914(100)	-54.3510(0)
NH^-	$^2\Pi$	6	9(5+4)	-54.5292(161)	-54.5150(99)	-54.5151(100)	-54.4920(0)
NH	$^3\Sigma^-$	6	8(5+3)	-54.8280(144)	-54.8160(100)	-54.8161(100)	-54.7887(0)
OH^+	$^3\Sigma^-$	6	8(5+3)	-74.7805(138)	-74.7719(100)	-74.7720(100)	-74.7491(0)
OH^-	$^1\Sigma^+$	6	10(5+5)	-74.8127(100)	-74.8112(95)	-74.8127(100)	-74.7851(0)
OH	$^2\Pi$	6	9(5+4)	-75.1164(158)	-75.1013(99)	-75.1014(100)	-75.0756(0)

CONTINUE

CONTINUED

HF^+	$^2\Pi$	6	9(5+4)	-99.1376(153)	-99.1278(100)	-99.1279(100)	-99.1096(0)
HF	$^1\Sigma^+$	6	10(5+5)	-99.5258(100)	-99.5229(89)	-99.5258(100)	-99.4998(0)
BH_2	$^2A_1$	7	7(4+3)	-25.7549(235)	-25.7089(115)	-25.7031(100)	-25.6649(0)
BH_2	$^2B_1$	7	7(4+3)	-25.7317(233)	-25.6837(113)	-25.6783(100)	-25.6383(0)
CH_2	$^1A_1$	7	8(4+4)	-38.9301(294)	-38.8228(119)	-38.8110(100)	-38.7497(0)
CH_2	$^3B_1$	7	8(5+3)	-38.9043(214)	-38.8566(107)	-38.8534(100)	-38.8089(0)
CH_2	$^3\Sigma_u^-$	7	8(5+3)	-38.8836(187)	-38.8358(103)	-38.8342(100)	-38.7772(0)
NH_2	$^2A_1$	7	9(5+4)	-55.4134(244)	-55.3570(111)	-55.3525(100)	-55.3101(0)
NH_2	$^2B_1$	7	9(5+4)	-55.4856(243)	-55.4195(108)	-55.4157(100)	-55.3670(0)
H_2O	$^1A_1$	7	10(5+5)	-75.7953(232)	-75.7310(104)	-75.7290(100)	-75.6789(0)
H_2O^+	$^2A_1$	7	9(5+4)	-75.4912(262)	-75.4218(106)	-75.4192(100)	-75.3748(0)
FH_2^+	$^1A_1$	7	10(5+5)	-99.8894(244)	-99.8305(103)	-99.8294(100)	-99.7879(0)
BH_3	$^1A_1$	8	8(4+4)	-26.4681(258)	-26.3932(120)	-26.3827(100)	-26.3287(0)
CH_3	$^2A_2$	8	9(5+4)	-39.6375(290)	-39.5283(117)	-39.5178(100)	-39.4547(0)
NH_3	$^1A_1$	8	10(5+5)	-56.2061(334)	-56.0617(115)	-56.0516(100)	-55.9855(0)
NH_3 (dis)	^1A	8	10(5+5)	-56.1808(326)	-56.0394(115)	-56.0293(100)	-55.9622(0)
H_3O^+	$^1A_1$	8	10(5+5)	-75.9422(276)	-75.8636(103)	-75.8621(100)	-75.8166(0)

[a] Number of active MOs.

[b] Number of electrons with the number of α and β electrons in parentheses.

[c] Basis set is double-ζ.

[d] Basis set is triple-ζ.

3.4 Result and discussion

We show in Table I the total energy of the system calculated by the present method and in parentheses the calculated correlation energy in percentage relative to the Hartree-Fock (0%) and full-CI (100%) results. Two types of the SDP relaxation calculations are performed. One uses the P and Q conditions together with the seven conditions given by Eqs(2.3)-(2.10): it is referred to as DM($P+Q$). The other uses the G condition additionally and it is denoted as DM($P+Q+G$).

We first examine the results of DM($P+Q$) calculations. We see that the results for OH^- and HF are excellent, but this is not a good news but simply due to the too restrictive variational space: 10 electrons are distributed into six orbitals and therefore in this case P+Q condition gives the complete N-representability condition(2 hole system)[25]. Similarly, the extent of overshooting is relatively small because the variational space is too restrictive. When the variation is reasonably free, the DM($P+Q$) energy overshoots too much the full-CI energy up to 334% of the full-CI correlation energy for NH_3. This result shows that the $P+Q$ condition together with the above seven conditions is still too far from the complete N-representability condition.

When we impose further the G condition, we obtain the results shown under DM($P+Q+G$). They are much improved in comparison with the results of DM(P+Q). The calculated correlation energy percentages range within 100 to 110% for atoms and diatomic molecules, while they range in 110% $\sim$ 120% for triatomic molecules. This means that the G condition is a nice restrictive condition for the N-representability. We investigated distorted ammonia to examine whether the spatial symmetry affects the N-representability condition, however, this calculation shows that there is no effect by such a small distortion; the accuracies of the two calculations are almost the same.

The SDP variational method should give, in principle, a lower bound for energy, however, compared to the full-CI results, the breakdown where the calculated SDPA energy is *higher* than the full-CI energy occurs for LiH($^3\Sigma$, STO-6G), LiH($^3\Sigma$, double-ζ), CH^-, NH^-, OH, OH^- and HF, though the violations are within

1 mhartree. It seems that these breakdowns are related to the numerical errors in the SDPA procedure, which we discuss later.

In Table II, we show the (non-zero) dipole moments of the molecules calculated here. The dipole moment obtained at the level of DM($P+Q$) is not so good. In particular, those for CH, NH^+, CH_2, H_2O and H_2O^+ are worse than the Hartree-Fock results. At the DM($P+Q+G$) level, however, the dipole moments are drastically improved and all the results well reproduce the full-CI ones, except for NH_3 and NH_3(dis) for which even Hartree-Fock calculations give good results and the deviations are very small.

In Table III, we show the virial coefficient $\langle V\rangle/\langle T\rangle$, where $\langle V\rangle$ and $\langle T\rangle$ denote average potential and kinetic energies, respectively, which must be two for completely variational wave function. When we use DM($P+Q+G$) approximation, the calculated virial is almost completely identical with the full-CI result.

Next, we discuss the numerical accuracy of the SDP method. In Tables IV and V, we summarize the number of the constraints and the numerical errors of the DM($P+Q$) and DM($P+Q+G$) calculations. The primal feasible error is defined by

$$\max\left\{\left|[\boldsymbol{X}-\sum_{i=1}^{m}\boldsymbol{F}_i x_i+\boldsymbol{F}_0]_{pq}\right| \ : \ p,q=1,2,\ldots,n\right\} \tag{3.52}$$

and the dual feasible error is defined by:

$$\max\left\{|\boldsymbol{F}_i\bullet\boldsymbol{Y}-c_i| \ : i=1,2,\ldots,m\right\}. \tag{3.53}$$

The gap denotes the difference between the primal and dual functions defined by:

$$\left|\sum_{i=1}^{m}c_i x_i-\boldsymbol{F}_0\bullet\boldsymbol{Y}\right|. \tag{3.54}$$

These three quantities give criteria of the accuracy of the SDPA. In the SDPA, our object is the minimization of the dual form of the problem, so that the dual feasible error is an important quantity, indicating the numerical accuracy of the calculation.

For DM($P+Q$), the dual feasible error is in the range of $10^{-7}\sim 10^{-12}$, while for DM($P+Q+G$), it ranges $10^{-5}\sim 10^{-8}$. As the number of the constraints increases drastically in the $P+Q+G$ calculations, the numerical accuracy becomes much

TABLE II: Dipole moments calulated by the DMVT with $P+Q$ and $P+Q+G$ conditions compared with those obtained by the wave function method.The basis set is STO-6G except for notice.

Molecle	State	DM($P+Q$)	DM($P+Q+G$)	Full CI	Hartree-Fock
LiH[a]	$^1\Sigma^+$	1.6445	1.6164	1.6192	2.0764
LiH	$^1\Sigma^+$	1.7372	1.7523	1.7519	1.9339
LiH[a]	$^3\Sigma^+$	0.6225	0.6258	0.6258	0.6261
LiH	$^3\Sigma^+$	1.5897	1.5906	1.5907	1.5915
BeH^+	$^1\Sigma^+$	1.3203	1.3188	1.3196	1.2987
BH^+	$^2\Sigma^+$	0.0495	0.0223	0.0223	0.0197
BH	$^1\Sigma^+$	0.2833	0.2935	0.2994	0.3806
CH^+	$^1\Sigma^+$	0.6893	0.6764	0.6905	0.7253
CH^-	$^3\Sigma^-$	0.1826	0.1925	0.1929	0.1669
CH	$^2\Pi$	0.6016	0.4878	0.5044	0.4406
NH^+	$^2\Pi$	0.8937	0.8729	0.8804	0.8789
NH^-	$^2\Pi$	0.1359	0.1311	0.1321	0.1431
NH	$^3\Sigma^-$	0.4730	0.4995	0.4996	0.5233
OH^+	$^3\Sigma^-$	0.9988	0.9741	0.9742	0.9875
OH^-	$^1\Sigma^+$	0.0620	0.0637	0.0620	0.0725
OH	$^2\Pi$	0.4497	0.4738	0.4745	0.5166
HF^+	$^2\Pi$	0.9600	0.9993	0.9999	1.0786
HF	$^1\Sigma^+$	0.5420	0.5383	0.5420	0.5228
BH_2	$^2A_1$	0.0037	0.0328	0.0344	0.0466
CH_2	$^1A_1$	0.2435	0.5057	0.5293	0.6224
CH_2	$^3B_1$	0.0838	0.0857	0.0934	0.1006
NH_2	$^2A_1$	0.5170	0.5407	0.5509	0.5580
NH_2	$^2B_1$	0.6433	0.6816	0.6896	0.7200
H_2O	$^1A_1$	0.5993	0.6460	0.6487	0.6927
H_2O^+	$^2A_1$	0.8718	0.9857	0.9920	1.0724
FH_2^+	$^1A_1$	1.0368	1.0429	1.0437	1.0560
NH_3	$^1A_1$	0.6903	0.6901	0.6922	0.6935
NH_3 (dis)	^1A	0.6660	0.6634	0.6767	0.6937
H_3O^+	$^1A_1$	1.4162	1.4286	1.4289	1.4320

[a] Basis set is double-ζ.

TABLE III: Virial coefficients calulated by the DMVT with the $P+Q$ and $P+Q+G$ conditions compared with those obtained by the wave function methods.The basis set is STO-6G except for notice.

System	State	DM$(P+Q)$	DM$(P+Q+G)$	Full CI	Hartree-Fock
Be[a]	^{1}S	1.9975	1.9989	1.9989	1.9994
Be	^{1}S	1.9621	1.9614	1.9614	1.9558
Be[b]	^{1}S	2.0017	2.0006	2.0006	2.0000
Be[a]	^{3}S	1.7459	1.7461	1.7461	1.7464
Be[b]	^{3}S	1.9774	1.9766	1.9766	1.9759
LiH[a]	$^1\Sigma^+$	2.0038	1.9977	1.9977	1.9929
LiH	$^1\Sigma^+$	1.9832	1.9826	1.9826	1.9837
LiH[a]	$^3\Sigma^+$	1.9908	1.9875	1.9875	1.9826
LiH	$^3\Sigma^+$	1.9579	1.9577	1.9577	1.9574
BeH^+	$^1\Sigma^+$	2.0036	2.0031	2.0031	2.0041
BH^+	$^2\Sigma^+$	1.9918	1.9919	1.9918	1.9931
BH	$^1\Sigma^+$	1.9574	1.9565	1.9566	1.9550
CH^+	$^1\Sigma^+$	2.0044	2.0040	2.0039	2.0025
CH^-	$^3\Sigma^-$	1.9393	1.9392	1.9393	1.9396
CH	$^2\Pi$	1.9781	1.9778	1.9777	1.9773
NH^+	$^2\Pi$	2.0164	2.0156	2.0154	2.0144
NH^-	$^2\Pi$	1.9596	1.9597	1.9597	1.9601
NH	$^3\Sigma^-$	1.9941	1.9939	1.9938	1.9939
OH^+	$^3\Sigma^-$	2.0199	2.0194	2.0194	2.0183
OH^-	$^1\Sigma^+$	1.9672	1.9671	1.9672	1.9678
OH	$^2\Pi$	1.9967	1.9965	1.9965	1.9965

CONTINUE

CONTINUED

HF^+	$^2\Pi$	2.0218	2.0212	2.0212	2.0201
HF	$^1\Sigma^+$	2.0001	2.0001	2.0001	1.9999
BH_2	$^2A_1$	1.9722	1.9727	1.9731	1.9738
BH_2	$^2B_1$	1.9699	1.9702	1.9705	1.9712
CH_2	$^1A_1$	1.9849	1.9840	1.9840	1.9841
CH_2	$^3B_1$	1.9889	1.9884	1.9886	1.9886
CH_2	$^3\Sigma_u^-$	1.9882	1.9876	1.9878	1.9877
NH_2	$^2A_1$	1.9950	1.9943	1.9942	1.9940
NH_2	$^2B_1$	1.9956	1.9955	1.9955	1.9956
H_2O	$^1A_1$	1.9966	1.9968	1.9968	1.9967
H_2O^+	$^2A_1$	2.0176	2.0152	2.0151	2.0138
FH_2^+	$^1A_1$	2.0183	2.0159	2.0158	2.0143
BH_3	$^1A_1$	1.9835	1.9836	1.9843	1.9853
CH_3	$^2A_2$	1.9941	1.9939	1.9944	1.9948
NH_3	$^1A_1$	1.9981	1.9985	1.9984	1.9985
NH_3 (dis)	^1A	1.9973	1.9976	1.9974	1.9976
H_3O^+	$^1A_1$	1.9972	1.9941	1.9941	1.9934

[a] Basis set is double-ζ.

[b] Basis set is triple-ζ.

worse in the DM(P+Q+G) results. The gap value shows the same tendency. Worst five are HF(3.99×10^{-5}), OH^- (2.72×10^{-5}) LiH(double-ζ, $^3\Sigma$; 2.41×10^{-5}), CH^- (2.31×10^{-5}) and NH^- (1.37×10^{-5}). We notice that they have the DM($P+Q+G$) energies *higher* than the full-CI ones, though these values must be *lower* than the full-CI values. There seems to be some relation between the gap value and the numerical accuracy in the SDPA technique. Another reason is certainly the too small variational freedom in the calculations of HF and OH^-: actually in these cases P and Q conditions are already sufficient: the number of hole is 2, so, 2 hole system with Q condition is just like performing variational calculation for 2 electron system with P condition, therefore enforcing P, Q and G conditions is essentially the same as enforcing P and Q conditions.

The primal feasible values are very small ($10^{-12} \sim 10^{-14}$) for DM($P+Q$) calculations and also small ($10^{-10} \sim 10^{-12}$) for DM($P+Q+G$) calculations. We do not find any relationship between the accuracies of the present calculations and the primal feasible errors. So the accuracy of the present calculation seems to be related only to that of the primal problem.

In table VI, we show the occupation numbers (eigenvalues of 1-RDM) for Be(^{1}S, STO-6G), Be(^{1}S, triple-ζ), Be(^{3}S, triple-ζ), H_2O($^1A_1$, STO-6G), and CH_2($^1A_1$, STO-6G). For Be(^{1}S, STO-6G), the occupation numbers of the $2p$ orbitals should be 6-fold degenerate. Although we didn't impose such constraints, this degeneracy accurately holds in both DM($P+Q$) and DM($P+Q+G$) calculations. For singlet states, both DM($P+Q$) and DM($P+Q+G$) calculations reproduced the degeneracy of the two-fold occupation without constraints. Generally, the occupation numbers of the DM calculations are much more distributed over all the natural orbitals than those of the fullCI. Although such trend is reduced for DM($P+Q+G$) calculation, it contradicts our expectation: the occupation numbers are expected to be less distributed in the calculations with less sufficient N-representability conditions. An extreme case was CH_2, this tendency is very amplified and the accidental degeneracy of occupation are found in the DM($P+Q$) calculation.

In table VII, the rms (root-mean-square) deviation d of the 2-RDM from the

TABLE IV: Occupation number calculated by DMVT with $P+Q$ and $P+Q+G$ conditions compared with those obatined by the wave function methods, full CI and Hartree-Fock, for Be, H_2O, CH_2.

Systam, state, basis	DM(P+Q)	DM(P+Q+G)	FullCI	Hatree-Fock
Be, ^{1}S , STO-6G	0.036641×4	0.035909×6	0.035901×6	0×6
	0.036642×2			
	0.890243×2	0.892275×2	0.892298×2	1×4
	0.999832×2	0.999997×2	0.999998×2	
Be, ^{1}S, triple-ζ	0.000202×2	0.000064×2	0.000055×2	0×6
	0.001041×2	0.000595×2	0.000590×2	
	0.006149×2	0.004153×2	0.004119×2	
	0.993649×2	0.995837×2	0.995879×2	1×4
	0.998959×2	0.999352×2	0.999357×2	
Be, ^{3}S, triple-ζ	0.000004	0.000000	0.000000	0×6
	0.000187	0.000001	0.000000	
	0.000573	0.000011	0.000007	
	0.000645	0.000013	0.000009	
	0.000702	0.000707	0.000707	
	0.001511	0.000712	0.000711	
	0.998534	0.999280	0.999284	1×4
	0.999252	0.999286	0.999287	
	0.999293	0.999990	0.999995	
	0.999299	0.999998	1.000000	

CONTINUE

CONTINUED

H_2O, $^1A_1$, STO-6G	0.029795×2	0.013850×2	0.013304×2	0×4
	0.031585×2	0.014766×2	0.013509×2	
	0.970205×2	0.986433×2	0.986732×2	1×10
	0.970570×2	0.987475×2	0.988323×2	
	0.998733×2	0.998702×2	0.998973×2	
	0.999114×2	0.998776×2	0.999161×2	
	0.999998×2	0.999999×2	0.999999×2	
CH_2, $^1A_1$, STO-6G	0.037796×4	0.014336×2	0.010854×2	0×6
	0.314251×2	0.016294×2	0.012979×2	
	0.685804×2	0.069501×2	0.050589×2	
	0.962204×4	0.929480×2	0.947809×2	1×8
	0.999945×2	0.984098×2	0.987470×2	
		0.986297×2	0.990307×2	
		0.999993×2	0.999993×2	

fullCI,

$$d = \sqrt{\sum_{i_1 i_2 j_1 j_2} \{(\Gamma_{\text{calculated}})^{i_1 i_2}_{j_1 j_2} - (\Gamma_{\text{fullci}})^{i_1 i_2}_{j_1 j_2}\}^2} \tag{3.55}$$

is presented for the systems examined in table VI. The deviations of the 2-RDM are quite small in DM($P + Q + G$) calculation especially for small systems, where DM($P + Q + G$) give the identical total energy and virial coefficient to fullCI. However, DM($P + Q$) calculations gave worse results and even worse than Hartree-Fock for H_2O and CH_2.

In table VIII, we compare the largest eigenvalues of P, Q and G-matrices and smallest eigenvalues of G-matrix, for the same systems. Largest eigenvalues of P and Q-matrices become smaller as the calculation quality becomes better, while those of G-matrix become larger. In DM($P + Q$) calculations, smallest eigenvalues of G-matrix are negative. As we expected, smallest eigenvalue of G-matrix becomes smaller when electron correlation gets larger. We didn't show the smallest eigenvalues of P and Q-matrices since in any case, they are almost zero (absolute values are smaller than 10^{-6}). The deviation of these values are large for CH_2 (largest

TABLE V: RMS deviations of the 2-RDMs calculated by DMVT with $P+Q$ and $P+Q+G$ conditions from those by fullCI for Be, H_2O, CH_2

System, state, basis	DM(P+Q)	DM(P+Q+G)	FullCI	Hartree-Fock
Be, ^{1}S, STO-6G	0.049208	0.000162	0	0.526569
Be, ^{1}S, triple-ζ	0.049615	0.003567	0	0.100331
Be, ^{3}S, triple-ζ	0.029401	0.000715	0	0.039123
H_2O, $^1A_1$, STO-6G	0.467084	0.029694	0	0.266154
CH_2, $^1A_1$, STO-6G	1.604712	0.153503	0	0.484788

eigenvalue of G-matrix for DM($P+Q+G$)) calculation is 7.679238 compared to fullCI's one 7.746013), while the SDPA errors are small(primal and dual feasibilities are 4.14×10^{-12} and 3.54×10^{-6}, respectively, and gap is 2.69×10^{-7}). Therefore, we conclude that the error originates from the insufficiency of the N-representability conditions rather than that of the SDPA.

The trace of Q matrix is normalized to $(r-N)\times(r-N+1)$, where r is number of MO(or rank of 1-RDM) and N is the number of the electrons. This condition is satisfied when we impose the constraint for the number of the electrons.

Lastly we note that we find essentially no problem in finding the minimum and this should be the case for other systems. This is certainly a merit of the present method.

TABLE VI: Number of the constraints and the numerical errors of the DM($P+Q$) calculations.The basis set is STO-6G except for notice.

System	State	Active[a] set	Ele($\alpha+\beta$)[b] Constraints	No. of error	Primal feasible error	Dual feasible	Gap
Be[c]	^{1}S	4	4(2+2)	183	1.87×10^{-14}	9.24×10^{-11}	1.17×10^{-9}
Be	^{1}S	5	4(2+2)	440	7.87×10^{-14}	4.35×10^{-11}	8.03×10^{-13}
Be[d]	^{1}S	5	4(2+2)	440	5.49×10^{-14}	1.41×10^{-10}	1.89×10^{-11}
Be[c]	^{3}S	4	4(3+1)	183	4.12×10^{-11}	1.17×10^{-7}	3.87×10^{-8}
Be[d]	^{3}S	5	4(3+1)	440	7.86×10^{-12}	1.12×10^{-7}	9.58×10^{-9}
LiH[c]	$^1\Sigma^+$	6	4(2+2)	911	7.24×10^{-14}	9.24×10^{-9}	3.46×10^{-9}
LiH	$^1\Sigma^+$	6	4(2+2)	911	8.52×10^{-14}	1.08×10^{-9}	4.76×10^{-11}
LiH[c]	$^3\Sigma^+$	6	4(3+1)	911	3.80×10^{-12}	1.75×10^{-6}	3.64×10^{-7}
LiH	$^3\Sigma^+$	6	4(3+1)	911	3.41×10^{-11}	4.57×10^{-8}	1.89×10^{-8}
BeH^+	$^1\Sigma^+$	6	4(2+2)	911	1.16×10^{-13}	3.02×10^{-11}	5.73×10^{-13}
BH^+	$^2\Sigma^+$	6	5(3+2)	911	6.69×10^{-14}	1.86×10^{-10}	3.26×10^{-12}
BH	$^1\Sigma^+$	6	6(3+3)	911	4.43×10^{-14}	8.29×10^{-10}	2.41×10^{-11}
CH^+	$^1\Sigma^+$	6	6(3+3)	911	3.62×10^{-14}	1.30×10^{-9}	9.62×10^{-12}
CH^-	$^3\Sigma^-$	6	8(5+3)	911	5.49×10^{-12}	8.97×10^{-8}	6.05×10^{-9}
CH	$^2\Pi$	6	7(4+3)	911	5.91×10^{-14}	2.23×10^{-9}	2.80×10^{-11}
NH^+	$^2\Pi$	6	7(4+3)	911	3.15×10^{-14}	9.98×10^{-10}	1.49×10^{-11}
NH^-	$^2\Pi$	6	9(5+4)	911	8.57×10^{-12}	7.06×10^{-8}	3.70×10^{-9}
NH	$^3\Sigma^-$	6	8(5+3)	911	9.79×10^{-12}	4.97×10^{-7}	1.85×10^{-8}
OH^+	$^3\Sigma^-$	6	8(5+3)	911	6.77×10^{-12}	8.16×10^{-8}	2.49×10^{-9}
OH^-	$^1\Sigma^+$	6	10(5+5)	911	7.50×10^{-12}	5.25×10^{-7}	7.32×10^{-8}
OH	$^2\Pi$	6	9(5+4)	911	5.54×10^{-12}	1.35×10^{-7}	3.48×10^{-9}

CONTINUE

CONTINUED

HF^+	$^2\Pi$	6	9(5+4)	911	2.36×10^{-12}	8.42×10^{-8}	2.96×10^{-9}
HF	$^1\Sigma^+$	6	10(5+5)	911	6.82×10^{-12}	1.12×10^{-7}	6.65×10^{-9}
BH_2	$^2A_1$	7	7(4+3)	1692	6.43×10^{-14}	4.94×10^{-10}	4.65×10^{-11}
BH_2	$^2B_1$	7	7(4+3)	1692	5.66×10^{-14}	8.16×10^{-12}	3.20×10^{-12}
CH_2	$^1A_1$	7	8(4+4)	1692	3.25×10^{-14}	3.26×10^{-11}	3.19×10^{-10}
CH_2	$^3B_1$	7	8(5+3)	1692	3.98×10^{-14}	5.94×10^{-11}	5.75×10^{-10}
CH_2	$^3\Sigma_u^-$	7	8(5+3)	1692	4.12×10^{-14}	6.59×10^{-11}	5.88×10^{-11}
NH_2	$^2A_1$	7	9(5+4)	1692	3.63×10^{-14}	1.21×10^{-9}	1.22×10^{-10}
NH_2	$^2B_1$	7	9(5+4)	1692	3.99×10^{-14}	2.46×10^{-11}	3.91×10^{-10}
H_2O	$^1A_1$	7	10(5+5)	1692	3.33×10^{-14}	2.88×10^{-10}	1.29×10^{-10}
H_2O^+	$^2A_1$	7	9(5+4)	1692	3.31×10^{-14}	3.02×10^{-11}	2.64×10^{-10}
FH_2^+	$^1A_1$	7	10(5+5)	1692	3.46×10^{-14}	3.19×10^{-10}	1.12×10^{-10}
BH_3	$^1A_1$	8	8(4+4)	2897	6.57×10^{-14}	7.62×10^{-10}	3.37×10^{-11}
CH_3	$^2A_2$	8	9(5+4)	2897	3.87×10^{-14}	1.12×10^{-11}	8.68×10^{-10}
NH_3	$^1A_1$	8	10(5+5)	2897	4.07×10^{-14}	5.16×10^{-11}	1.02×10^{-10}
NH_3 (dis)	^1A	8	10(5+5)	2897	4.38×10^{-14}	5.87×10^{-10}	1.62×10^{-10}
H_3O^+	$^1A_1$	8	10(5+5)	2897	4.13×10^{-14}	5.29×10^{-10}	6.77×10^{-11}

[a] Number of active MOs.

[b] Number of electrons with the number of α and β electrons in parentheses.

[c] Basis set is double-ζ.

[d] Basis set is triple-ζ.

TABLE VII: Number of the constraints and the numerical errors of the DM($P+Q+G$) calculations.The basis set is STO-6G except for notice.

System	State	Active[a] MOs	Ele($\alpha+\beta$)[b]	No. of Constraints	Primal feasible error	Dual feasible error	Gap
Be[c]	^{1}S	4	4(2+2)	983	6.55×10^{-11}	1.87×10^{-7}	2.87×10^{-6}
Be	^{1}S	5	4(2+2)	2365	7.02×10^{-12}	4.93×10^{-7}	1.42×10^{-6}
Be[d]	^{1}S	5	4(2+2)	2365	7.92×10^{-11}	4.15×10^{-7}	2.48×10^{-6}
Be[c]	^{3}S	4	4(3+1)	983	1.12×10^{-10}	7.44×10^{-7}	3.08×10^{-6}
Be[d]	^{3}S	5	4(3+1)	2365	1.41×10^{-11}	1.65×10^{-7}	2.94×10^{-7}
LiH[c]	$^1\Sigma^+$	6	4(2+2)	4871	5.72×10^{-12}	2.33×10^{-5}	4.50×10^{-6}
LiH	$^1\Sigma^+$	6	4(2+2)	4871	5.77×10^{-12}	7.55×10^{-8}	1.69×10^{-6}
LiH[c]	$^3\Sigma^+$	6	4(3+1)	4871	3.53×10^{-11}	6.35×10^{-7}	2.41×10^{-5}
LiH	$^3\Sigma^+$	6	4(3+1)	4871	5.79×10^{-11}	6.56×10^{-7}	2.58×10^{-6}
BeH^+	$^1\Sigma^+$	6	4(2+2)	4871	2.42×10^{-11}	1.88×10^{-7}	1.93×10^{-6}
BH^+	$^2\Sigma^+$	6	5(3+2)	4871	7.84×10^{-12}	7.50×10^{-8}	7.82×10^{-7}
BH	$^1\Sigma^+$	6	6(3+3)	4871	2.80×10^{-11}	1.43×10^{-5}	1.61×10^{-8}
CH^+	$^1\Sigma^+$	6	6(3+3)	4871	3.75×10^{-12}	2.41×10^{-7}	9.68×10^{-7}
CH^-	$^3\Sigma^-$	6	8(5+3)	4871	1.43×10^{-11}	3.73×10^{-7}	2.13×10^{-5}
CH	$^2\Pi$	6	7(4+3)	4871	6.06×10^{-12}	8.54×10^{-6}	1.91×10^{-7}
NH^+	$^2\Pi$	6	7(4+3)	4871	4.15×10^{-12}	3.64×10^{-6}	4.98×10^{-7}
NH^-	$^2\Pi$	6	9(5+4)	4871	6.89×10^{-12}	3.39×10^{-6}	1.37×10^{-5}
NH	$^3\Sigma^-$	6	8(5+3)	4871	8.69×10^{-11}	1.88×10^{-5}	2.90×10^{-6}
OH^+	$^3\Sigma^-$	6	8(5+3)	4871	7.98×10^{-12}	4.05×10^{-7}	1.90×10^{-6}
OH^-	$^1\Sigma^+$	6	10(5+5)	4871	2.54×10^{-11}	5.65×10^{-6}	2.72×10^{-5}
OH	$^2\Pi$	6	9(5+4)	4871	1.01×10^{-11}	2.78×10^{-6}	6.15×10^{-6}

CONTINUE

CONTINUED

HF^+	$^2\Pi$	6	9(5+4)	4871	1.09×10^{-11}	1.40×10^{-6}	6.07×10^{-6}
HF	$^1\Sigma^+$	6	10(5+5)	4871	1.39×10^{-11}	7.37×10^{-6}	3.99×10^{-5}
BH_2	$^2A_1$	7	7(4+3)	8993	2.50×10^{-12}	8.84×10^{-8}	8.00×10^{-7}
BH_2	$^2B_1$	7	7(4+3)	8993	9.48×10^{-12}	1.23×10^{-6}	1.59×10^{-6}
CH_2	$^1A_1$	7	8(4+4)	8993	4.14×10^{-12}	3.54×10^{-6}	2.69×10^{-7}
CH_2	$^3B_1$	7	8(5+3)	8993	1.57×10^{-10}	4.05×10^{-5}	1.28×10^{-7}
CH_2	$^3\Sigma_u^-$	7	8(5+3)	8993	4.72×10^{-12}	3.98×10^{-7}	1.58×10^{-6}
NH_2	$^2A_1$	7	9(5+4)	8993	7.65×10^{-12}	4.30×10^{-6}	1.30×10^{-6}
NH_2	$^2B_1$	7	9(5+4)	8993	2.36×10^{-12}	3.22×10^{-8}	2.16×10^{-6}
H_2O	$^1A_1$	7	10(5+5)	8993	1.54×10^{-12}	1.05×10^{-7}	3.63×10^{-7}
H_2O^+	$^2A_1$	7	9(5+4)	8993	1.12×10^{-11}	6.86×10^{-6}	7.63×10^{-7}
FH_2^+	$^1A_1$	7	10(5+5)	8993	3.78×10^{-12}	5.14×10^{-7}	6.07×10^{-7}
BH_3	$^1A_1$	8	8(4+4)	15313	5.02×10^{-11}	5.34×10^{-7}	2.88×10^{-7}
CH_3	$^2A_2$	8	9(5+4)	15313	4.26×10^{-12}	6.16×10^{-7}	9.01×10^{-8}
NH_3	$^1A_1$	8	10(5+5)	15313	1.65×10^{-12}	4.62×10^{-7}	4.39×10^{-7}
NH_3 (dis)	^1A	8	10(5+5)	15313	3.29×10^{-12}	1.42×10^{-6}	4.14×10^{-6}
H_3O^+	$^1A_1$	8	10(5+5)	15313	1.59×10^{-12}	2.30×10^{-7}	2.24×10^{-6}

[a] Number of active MOs.

[b] Number of electrons with the number of α and β electrons in parentheses.

[c] Basis set is double-ζ.

[d] Basis set is triple-ζ.

TABLE VIII: Comparison of largest eigenvalues P, Q, G-matrices and smallest G-matrix calculated by DMVT with $P+Q$ and $P+Q+G$ conditions compared with those obatined by the wave function methods, full CI and Hartree-Fock for Be, H_2O, CH_2.

System, state, basis	DM(P+Q)	DM(P+Q+G)	FullCI	Hartree-Fock
Be, ^{1}S, STO-6G				
Largest P	1.005284	1.000907	1.000874	1
Largest Q	2.264502	2.259861	2.259834	2
Largest G	3.675970	3.682340	3.682407	4
Smallest G	-0.007288	0.000000	0.000000	0
Be, ^{1}S, triple-ζ				
Largest P	1.004751	1.000672	1.000612	1
Largest Q	2.008541	2.002209	2.002072	2
Largest G	3.978475	3.985686	3.985726	4
Smallest G	-0.002482	0.000000	0.000000	0
Be, ^{3}S, triple-ζ				
Largest P	1.002019	0.999991	0.999995	1
Largest Q	2.005387	2.000230	2.000233	2
Largest G	3.994883	3.997833	3.997849	4
Smallest G	-0.001439	0.000000	0.000000	0
H_2O, $^1A_1$, STO-6G				
Largest P	1.034378	1.010041	1.008652	1
Largest G	9.805708	9.900236	9.904312	10
Smallest G	-0.188367	0.000000	0.000000	0
CH_2, $^1A_1$, STO-6G				
Largest P	1.090030	1.024402	1.019529	1
Largest Q	2.227026	2.059546	2.042417	2
Largest G	6.942144	7.679238	7.746013	8
Smallest G	-0.208966	0.000001	0.000000	0

3.5 Conclusion

The DMVT is developed systematically by using SDPA as a problem solver. This technique is very stable and there were no example where we could not get a convergence. In addition to several trivial conditions, the $P + Q$ condition is insufficient, while the $P + Q + G$ condition gives satisfactory results, the extent of overshooting the full-CI energy being small for the systems presently examined. The dipole moment and the virial coefficient calculated by the DM($P + Q + G$) method are also very close to the full-CI values. This method is applicable to the ground state of any spin- and space symmetry of closed and open-shell systems.

In this DMVT approach, the calculated energy is a lower bound of the exact energy. The errors of the present DM($P + Q + G$) method are permissible in both energy and properties. Though most quantum chemical method available give the ground-state energy higher than the full-CI one, the present method giving lower energy is equally permissible as an approximate quantum chemical method, if it is stable and feasible in cost performance. For the second requirement, the present stage of the theory is an infant stage, but much progress is expected in future.

3.6 Acknowledgment

This study has been supported by the Grand-in-Aid for Scientific Research from the Japanese Ministry of Education, Science, Culture, and Sports.

BIBLIOGRAPHY

[1] K. Husimi, Proc. Phys. Math. Soc. Jap. **22**, 264(1940).

[2] P.-O, Löwdin, Phys. Rev. **99**, 1474(1955).

[3] H. Nakatsuji, in *Many-Electron Densities and Reduced Density Matrices* , ed by J. Cioslowski, Kluwer Academic, New York, 2000.

[4] H. Nakatsuji, Phys. Rev. A **14**, 41(1976).

[5] H. Nakatsuji, Theor. Chem. Acc. **102**, 97(1999).

[6] H. Nakatsuji and K. Yasuda, Phys. Rev. Lett. **76**, 1039(1996).

[7] K. Yasuda and H. Nakatsuji, Phys. Rev. A **56**, 2648(1997).

[8] M. Ehara, M. Nakata, H. Kou, K. Yasuda, and H. Nakatsuji, Chem. Phys. Lett. **305**, 483(1999).

[9] M. Nakata, M. Ehara, K. Yasuda and H. Nakatsuji, J. Chem. Phys., **112**, 8772(2000).

[10] A. J. Coleman, Rev. Mod. Phys. **35**, 668 (1963).

[11] C. Garrod and J. Percus, J. Math. Phys. **5**, 1756, (1964).

[12] C. Garrod and M. A. Fusco, Int. J. Quantum Chem. **x**, 495(1976).

[13] C. Garrod, M. V. Mihailović, and M. Rosina, J. Math. Phys. **16**, 868 (1975).

[14] M. V. Mihailović, and M. Rosina, Nuclear Physics, **A237**, 229(1975).

[15] K. Fujisawa, M. Kojima, K. Nakata, SDPA (SemiDefinite Programming Algorithm) User's Manual Version 5.00, August 1999.
`ftp://ftp.is.titech.ac.jp/pub/OpRes/software/SDPA/5.00/`.

[16] R. M. Erdahl and C. Garrod, Proc. Conf. on density matrices, Kingston, June 1974, ed. A. J. Coleman and R.M. Erdahl.

[17] H. Kummer, J. Math. Phys. **8**, 2063, (1967).

[18] Yu. Nesterov and A. S. Nemirovskii, *Interior Point Polynomial Method in Convex Programming: Theory and Applications* SIAM, Philadelphia, 1993.

[19] M. Kojima, *Semidefinite Programming and Interior-Point Methods*, `http://www.is.titech.ac.jp/~kojima/wabun.html`, 1996(in Japanese).

[20] S. Huzinaga, J. Chem. Phys. **42**, 1293 (1965).

[21] T.H. Dunning, JR., J. Chem. Phys. **53**, 2823 (1970).
T.H. Dunning, JR. and P.J. Hay, *In method of electronic structure theory*, vol. 2, H.F. Schaefer III, ed., Plenum press (1977).
Actually, basis sets are taken from EMSL Gaussian Basis Set Order Form, `http://www.emsl.pnl.gov:2080/forms/basisform.html`.

[22] W.J. Hehre, R.F. Stweart, and J.A. Pople, J. Chem. Phys. **51**, 2657(1969).

[23] K. P. Huber and G. Herzberg, *Molecular Spectra and Molecular Structure IV.*, Electronic Constants of Diatomic Molecules, Van Nostrand Reinhold, New York, 1979.

[24] J.H. Callomon, E. Horita, K. Kuchitsu, W.J. Lafferty, A.G. Maki and C.S. Pote, Landolt-Börnstein, Springer-Verlag, Berlin, 1976.

[25] A. J. Coleman, Rep. Math. Phys. **4**, 113(1973).

Chapter 4.

Density matrix variational theory: application to the potential energy surfaces and strongly correlated systems

Abstract

The density matrix variational theory(DMVT) algorithm developed previously [J. Chem. Phys., **114**, 8282 (2001)] was utilized for calculations of the potential energy surfaces of molecules, H_4, H_2O, NH_3, BH_3, CO, N_2, C_2 and Be_2. The DMVT(PQG), using the P, Q and G conditions as subsidiary condition, reproduced the full-CI curves very accurately even up to the dissociation limit. The method described well the quasi-degenerate states and the strongly correlated systems. On the other hand, the DMVT(PQ) was not satisfactory especially in the dissociation limit and its potential curves were always repulsive. The size-consistency of the method was discussed and the G-condition was found to be essential for the correct behavior of the potential curve. Further, we also examined the Weinhold-Wilson inequalities for the resultant 2-RDM of DMVT(PQG) calculations. Two linear inequalities were violated when the results were less accurate, suggesting that this inequality may provide a useful N-representability condition for the DMVT.

4.1 Introduction

The second-order reduced density matrix(2-RDM) completely describes the N-body fermion system since any observable properties of the system can be calculated from the 2-RDM[1, 2]. This fact has motivated us to use 2-RDM as a basic variable of quantum mechanics instead of the wave function Ψ. If we can determine 2-RDM without using Ψ, we have a closed form of quantum mechanics where the basic variable is 2-RDM. We refer to such formalism of quantum mechanics as density matrix theory(DMT). There are two categories in the DMT with respect to the determination of the RDM. One is based on the density equation[3], which is equivalent to the Schrödinger equation in the necessary and sufficient sence. This approach is called density equation theory(DET). Recently, DET is extensively studied and developed[4, 5, 6]. They have been summarized in a recent review article[7]. The other is based on the Ritz variational principle expressed in terms of 2-RDM. This latter approach is called density matrix variational theory(DMVT). The key in this approach is how well we can restrict our variable 2-RDM to be N-representable[8].

Garrod and Percus[9] first formulated the DMVT. Kijewski applied the DMVT to C^{2+} and found that the G-condition was rather strong condition[10]. Garrod *et al.*[11, 12] also implemented their method and calculated the ground state of Be atom very accurately. Erdahl proposed to use the convex program for solving the DMVT and performed accurate calculation for He_2 molecule[13]. Afterwards, the interest for solving 2-RDM using the DMVT has almost disappeared for about 20 years. The reasons were probably that there was no rigorous mathematical and computational algorithm for the DMVT calculation, and the computer facilities were not so powerful at that time, so that their methods were applicable only to extremely small systems from the limitation in the number of variational parameters.

Recently, Erdahl and Jin[19] developed the DMVT based on the 3-RDM, and applied it to the model system of one-dimensional periodic lattice of electron pairs. They generalized the work of Garrod and Percus for higher order RDMs, and gave

some insights for using 3-RDM as a basic variable.

In our previous study[14], we could efficiently implement the DMVT using the semidefinite programming algorithm(SDPA)[15, 16, 17, 18] and succeeded to calculate the 2-RDM of the ground state of different symmetry for many atoms and molecules. We transformed the DMVT to the standard type problem of SDP. We showed that the positive semidefiniteness conditions of the P, Q[8] and G[9] matrices were very strong for atoms and molecules, though they are only necessary conditions of the N-representability.

In the recent work of Mazziotti and Erdahl[20], positive semidefinite condition of 3- and 4- RDMs were examined for solving the DMVT coupled with DET. They demonstrated its performance for a boson model of two-energy-level system with $N = 10 \sim 75$. Valdemoro *et al.* also considered the functional reconstruction with respect to the ensemble representability conditions[21].

Another promising approach was initiated by one of the authors[22, 23, 24, 25]. Since the exact Ψ is an eigen function of the Hamiltonian that has so simple structure composed of only one- and two-body operators, the Ψ itself should also have a simple structure reflecting the simple structure of the Hamiltonian. Some explicit expressions of the structure of the exact wave function were given and the theories for the ground and excited states was formulated and applied to a simple model system.

In this paper, we extensively apply our DMVT to calculations of the potential energy surfaces of molecules. Previously, we applied our DET to calculations of the potential energy curves of small molecules[26]. Though the results were encouraging around the equilibrium and elongated geometry, the calculation failed to converge at large internuclear distances. Here, special attentions are paid to the performance of DMVT for describing the electronic state of strongly correlated systems and the multi-configurational systems. We also discuss the size-consistency property of the method in connection with the N-representability condition. We will also examine the Weinhold-Wilson inequalities[27, 28, 29] for the obtained 2-RDM and consider their possibilities as another N-representability conditions in our method.

4.2 Theory

4.2.1 Definitions and basic algorithm

First and second order reduced density matrices (1-, 2-RDMs), γ and Γ, are defined by:

$$\gamma_j^i = \langle \Psi | a_i^\dagger a_j | \Psi \rangle \tag{4.1}$$

$$\Gamma_{j_1 j_2}^{i_1 i_2} = \frac{1}{2} \langle \Psi | a_{i_1}^\dagger a_{i_2}^\dagger a_{j_2} a_{j_1} | \Psi \rangle \tag{4.2}$$

where $a^\dagger$ and a are creation and annihilation operators, respectively. Practical complete N-representability condition is not known for 2-RDM: we know only some necessary conditions. In the present DMVT, we use P, Q, and G conditions. The P, Q, and G-matrices are defined by,

$$P_{j_1 j_2}^{i_1 i_2} = \langle \Psi | a_{i_1}^\dagger a_{i_2}^\dagger a_{j_2} a_{j_1} | \Psi \rangle \tag{4.3}$$

$$Q_{j_1 j_2}^{i_1 i_2} = \langle \Psi | a_{i_1} a_{i_2} a_{j_2}^\dagger a_{j_1}^\dagger | \Psi \rangle \tag{4.4}$$

$$G_{j_1 j_2}^{i_1 i_2} = \langle \Psi | a_{i_1}^\dagger a_{i_2} a_{j_2}^\dagger a_{j_1} | \Psi \rangle \tag{4.5}$$

respectively. We enforce all of these matrices to be positive semidefinite. We also use seven trivial conditions of 2-RDM, which are antisymmetric condition, hermiticity, trace condition, number of electrons, number of spins, and expectation values of S_z and S^2.

In the DMVT, we take 2-RDM as a variational variable, and minimize the energy within N-representability conditions, namely,

$$E_{\min} = \underset{\Gamma \in \mathcal{P}^{(2)}}{\mathrm{Min}} \ \mathrm{Tr} H\Gamma, \tag{4.6}$$

where H is the Hamiltonian of the system, $\mathcal{P}^{(2)}$ is a set of 2-RDM that satisfy approximate or nearly complete N-representability condition. We did two types of calculations using the approximate N-representability conditions: one is with the trivial representability condition plus P and Q condition, denoted as DMVT(PQ), and the other is with the trivial condition plus P, Q and G conditions, denoted as DMVT(PQG).

For implementing the minimization problem with these linear and semidefiniteness conditions, we casted this problem into the SDP[15, 16, 17], and we employ SDPA[18] as a standard SDP solver. Details were described in ref.[14].

4.2.2 Additional linear inequalities for the density matrices

Weinhold and Wilson[27], Davidson[28] and McRae and Davidson[29] derived some other N-representability conditions that were expressed as linear inequalities using only the diagonal elements of 2-RDM. Among them, the conditions independent from those already used in our present method are,

Condition VI:

$$\gamma_i^i - 2\Gamma_{ij}^{ij} - 2\Gamma_{ik}^{ik} + 2\Gamma_{jk}^{jk} \geq 0 \tag{4.7}$$

Condition VII:

$$1 - \gamma_i^i - \gamma_j^j - \gamma_k^k + 2\Gamma_{ij}^{ij} + 2\Gamma_{ik}^{ik} + 2\Gamma_{jk}^{jk} \geq 0 \tag{4.8}$$

Condition VIII: Positive semidefiniteness of the Ω matrix

$$\Omega = \begin{pmatrix} \gamma_1^1 & 2\Gamma_{12}^{12} & 2\Gamma_{13}^{13} & \cdots & 2\Gamma_{1t}^{1t} & \gamma_1^1 \\ 2\Gamma_{12}^{12} & \gamma_2^2 & 2\Gamma_{23}^{23} & \cdots & 2\Gamma_{2t}^{2t} & \gamma_2^2 \\ 2\Gamma_{13}^{13} & 2\Gamma_{23}^{23} & \gamma_3^3 & \cdots & 2\Gamma_{3t}^{3t} & \gamma_3^3 \\ \vdots & \vdots & \vdots & & \vdots & \vdots \\ 2\Gamma_{1t}^{1t} & 2\Gamma_{2t}^{2t} & 2\Gamma_{3t}^{3t} & \cdots & \gamma_t^t & \gamma_t^t \\ \gamma_1^1 & \gamma_2^2 & \gamma_3^3 & \cdots & \gamma_t^t & 1 \end{pmatrix}. \tag{4.9}$$

These are the representability conditions that may be *stronger* than and/or may reinforce the P, Q and G conditions. Since these conditions are given as *linear* inequalities, it is easy to include them into the present DMVT formalism within the SDP formalism, since SDP is an extension of the linear programming. In this study, we examine the resultant 2-RDM against these two inequalities, the condition VI, VII and VIII, and discuss the possibility of using these conditions as the additional constraints in our DMVT formalism.

4.2.3 Size-consistency

The positive semidefiniteness of the G-matrix includes a necessary condition for size-consistency. In the original nonlinear form, the position representation of the G-matrix is given by,

$$\begin{aligned} G(12|1'2') &= \langle(\psi^\dagger(2)\psi(1) - \langle\psi^\dagger(2)\psi(1)\rangle)^\dagger(\psi^\dagger(2')\psi(1') - \langle\psi^\dagger(2')\psi(1')\rangle)\rangle \\ &= \langle(\psi^\dagger(1)\psi(2) - \langle\psi^\dagger(2)\psi(1)\rangle^*)(\psi^\dagger(2')\psi(1') - \langle\psi^\dagger(2')\psi(1')\rangle)\rangle \\ &= \langle\psi^\dagger(1)\psi(2)\psi^\dagger(2')\psi(1')\rangle - \langle\psi^\dagger(2)\psi(1)\rangle^*\langle\psi^\dagger(2')\psi(1')\rangle \\ &\quad -\langle\psi^\dagger(1)\psi(2)\rangle\langle\psi^\dagger(2')\psi(1')\rangle + \langle\psi^\dagger(2)\psi(1)\rangle^*\langle\psi^\dagger(2')\psi(1')\rangle \\ &= \langle\psi^\dagger(1)\psi(2)\psi^\dagger(2')\psi(1')\rangle - \langle\psi^\dagger(1)\psi(2)\rangle\langle\psi^\dagger(2')\psi(1')\rangle, \end{aligned} \tag{4.10}$$

where $\psi(i)$ is a field operator defined by using one-particle complete basis set $\{\psi_j\}$,

$$\psi(i) = \sum_j \psi_j(i)a_j. \tag{4.11}$$

A static density-density autocorrelation function $F(1|1')$ [30] corresponds to the G-matrix as,

$$\begin{aligned} F(1|1') &= \langle n(1)n(1')\rangle - \langle n(1)\rangle\langle n(1')\rangle, \\ &= \langle\psi^\dagger(1)\psi(1)\psi^\dagger(1')\psi(1')\rangle - \langle\psi^\dagger(1)\psi(1)\rangle\langle\psi^\dagger(1')\psi(1')\rangle \\ &= G(11|1'1') \end{aligned} \tag{4.12}$$

where $n(i)$ is the density operator defined by,

$$n(i) = \psi^\dagger(i)\psi(i). \tag{4.13}$$

Using the positive semidefiniteness of $G(12|1'2')$,

$$\int x(12)G(12|1'2')x(1'2')^* d\tau_1 d\tau_2 d\tau_{1'} d\tau_{2'} \geq 0, \tag{4.14}$$

where $x(12)$ is an arbitrary two particle function, $F(1|1')$ is shown to be also positive semidefinite by integrating the G-matrix with respect to the two particle function $x(12)$ given by $x(12) = x(1)\delta(1-2)$, as

$$0 \leq \int x(12)G(12|1'2')x(1'2')^* d\tau_1 d\tau_2 d\tau_{1'} d\tau_{2'}$$

$$= \int x(1)\delta(1-2)G(12|1'2')x(1')^*\delta(1'-2')^* d\tau_1 d\tau_2 d\tau_{1'} d\tau_{2'}$$
$$= \int x(1)G(11|1'1')x(1')^* d\tau_1 d\tau_{1'}$$
$$= \int x(1)F(1|1')x(1')^* d\tau_1 d\tau_{1'} \tag{4.15}$$

where $x(1)$ is an arbitrary one-particle function. From the positive semidefiniteness of $F(1|1')$, it is shown that $F(1|1')$ is everywhere non-negative.

The size-consistency requires more strict condition; when $|1-1'| \to \infty$, $F(1|1')$ should asymptotically goes to zero, namely,

$$\lim_{|1-1'|\to\infty} F(1|1') = 0. \tag{4.16}$$

The positive semidefiniteness of the G-matrix guarantees only the non-negativity of $F(1|1')$, but does not this asymptotical condition. Thus, the DMVT(PQG) includes a necessary condition for the size-consistency, while in the DMVT(PQ), even $F(1|1')$ is not necessarily non-negative.

4.3 Results and discussions

4.3.1 H_4 system

First, we applied our DMVT to the potential energy surface of H_4. This system has been frequently used as a benchmark molecule of many methods for the quasi-degenerate situation:[31] the $a_g b_{2u}$ and $a_g b_{3u}$ configurations become equivalent for a square geometry and therefore, become degenerate. We used the DZ basis set[33, 34] for H and defined the potential energy surface with the coordinates (θ, R) depicted in Fig. 1. R gives the size of the molecule and θ defines the asymmetry of the structure. We calculated three different cuts of the potential energy surface that were also tested in ref.[31].

First, we examined the cut of stretching R with $\theta = 90^\circ$ fixed, namely, the square structure as a function of R. The results are summarized in table I. The

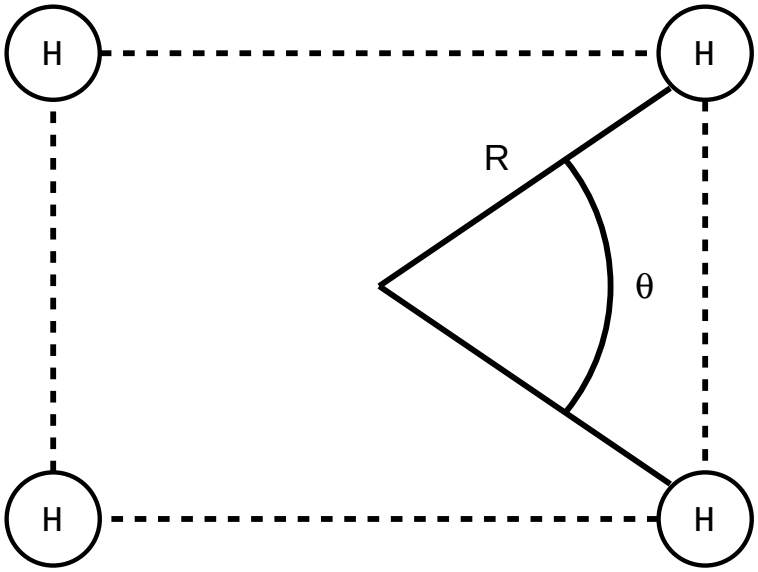

Figure I: Coordinate for H_4.

TABLE I: Total energy and correlation energy in (%) for H_4 as a function of R with θ fixed at 90 degree.

R(Å)	DMVT(PQ)	DMVT(PQG)	Full-CI	Hartree-Fock
0.6	-2.0405(186)	-1.9553(104)	-1.9511(100)	-1.8474(0)
0.8	-2.1485(168)	-2.0629(101)	-2.0610(100)	-1.9330(0)
1.0	-2.1881(177)	-2.0693(101)	-2.0684(100)	-1.9122(0)
1.2	-2.2210(191)	-2.0480(100)	-2.0474(100)	-1.8568(0)
1.4	-2.2407(194)	-2.0251(100)	-2.0246(100)	-1.7939(0)
1.6	-2.2367(183)	-2.0087(100)	-2.0085(100)	-1.7340(0)
1.8	-2.2226(141)	-1.9993(100)	-1.9992(100)	-1.4551(0)
2.0	-2.2055(141)	-1.9945(100)	-1.9945(100)	-1.4818(0)

TABLE II: Total energy and correlation energy in (%) for H_4 as a function of θ with R fixed at the equilibrium value of 0.869Å.

θ(degrees)	DMVT(PQ)	DMVT(PQG)	Full-CI	Hartree-Fock
90.0	-2.1656(170)	-2.0711(101)	-2.0697(100)	-1.9326(0)
89.9	-2.1656(170)	-2.0711(101)	-2.0697(100)	-1.9335(0)
89.5	-2.1656(172)	-2.0713(101)	-2.0698(100)	-1.9372(0)
89.0	-2.1655(174)	-2.0718(101)	-2.0703(100)	-1.9418(0)
88.0	-2.1654(177)	-2.0738(101)	-2.0721(100)	-1.9509(0)
85.0	-2.1673(180)	-2.0849(102)	-2.0830(100)	-1.9777(0)
80.0	-2.1869(185)	-2.1120(101)	-2.1106(100)	-2.0205(0)
70.0	-2.2337(185)	-2.1727(101)	-2.1721(100)	-2.0992(0)

DMVT(PQG) reproduced the full-CI curve quite accurately. For large R, it gave almost identical total energy and the errors were within 1 mhartree for $R > 1.0$Å, though the total correlation energies were large, for example, 0.51 au for $R = 2.0$Å. The method was found to give good description for the quasi-degenerate system. On the other hand, the DMVT(PQ) gave $40 \sim 90\%$ errors of the correlation energies.

Second, the cut of θ ranging from 70.0° to 90.0° with $R = 0.869$Å, which is near equilibrium distance is examined in table II. At $\theta = 90^\circ$, electronic state becomes quasi-degenerate. The DMVT(PQG) gave very smooth potential curve parallel to the full-CI without artificial cusp at $\theta = 90^\circ$[31]. The deviations were within 2 mhartree and 2% of the total correlation energy through out the geometries. For this system, the errors were constant regardless of the quasi-degeneracy.

Lastly, the cut of $\theta = 70^\circ \sim 90^\circ$ with R elongated to 1.738Å, namely, $2 \times R_e$, is examined in table III. Surprisingly, the DMVT(PQG) gave almost identical results with the full-CI ones: the deviations were less than 1 mhartree for all the geometries. Though the present calculations did not include polarization functions, the DMVT(PQG) gave very accurate potential energy surface of H_4.

TABLE III: Total energy and correlation energy in (%) for H_4 as a function of θ with R fixed at 1.738Å.

θ(degrees)	DMVT(PQ)	DMVT(PQG)	Full-CI	Hartree-Fock
90.0	-2.2275(174)	-2.0016(100)	-2.0015(100)	-1.6962(0)
89.9	-2.2275(174)	-2.0015(100)	-2.0015(100)	-1.6967(0)
89.5	-2.2276(175)	-2.0017(100)	-2.0015(100)	-1.6988(0)
89.0	-2.2276(175)	-2.0019(100)	-2.0015(100)	-1.7014(0)
88.0	-2.2278(177)	-2.0023(100)	-2.0018(100)	-1.7067(0)
85.0	-2.2289(181)	-2.0041(100)	-2.0033(100)	-1.7231(0)
80.0	-2.2327(188)	-2.0087(100)	-2.0080(100)	-1.7523(0)
70.0	-2.2465(207)	-2.0258(100)	-2.0255(100)	-1.8198(0)

For this system all the Weinhold-Wilson inequalities were satisfied for all the potential energy surfaces examined here. This also support the high quality of 2-RDM calculated by the DMVT(PQG).

4.3.2 Ne and the equilibrium geometry of N_2, CO, C_2, LiF and CH_4

Next, the DMVT is applied to the ground state of Ne, N_2, CO, C_2, LiF and CH_4, which were not calculated in the previous study[14]. In table IV, we summarized the total energy for these systems. In all calculations, we adopted STO-6G minimal basis[35] and experimental geometries[36, 37] except for Ne. For Ne, [3s2p] basis set was used. The 1s orbitals of the second raw atoms were fixed as cores.

Generally, the results of DMVT(PQG) calculations were satisfactory except for C_2 and CH_4. The DMVT(PQ) calculations overshoot the energy of these molecules, especially for C_2, by 802%. The DMVT(PQG) recovered it up to 117%. The deviation is still not small, however, the convergence to the exact value is encouraging since the ground state of C_2 is known to be quasi-degenerate even at the equilibrium

TABLE IV: Total energy and correlation energy in (%) Ne, CO, N_2, LiF, C_2, and CH_4 at equilibrium geometry.

System	State	MO[a]	Act. Ele[b]	DMVT(PQ)	DMVT(PQG)	Full-CI	Hartree-Fock
Ne	^1S	8(9)	8	-129.2430(705)	-128.6292(105)	-128.6245(100)	-128.5224(0)
CO	$^1\Sigma$	8(10)	12	-113.1163(584)	-112.4544(108)	-112.4426(100)	-112.3033(0)
N_2	$^1\Sigma_g^+$	8(10)	12	-109.4466(571)	-108.7123(108)	-108.7002(100)	-108.5418(0)
LiF	$^1\Sigma$	8(10)	10	-106.7727(568)	-106.4448(102)	-106.4435(100)	-106.3731(0)
C_2	$^1\Sigma_g^+$	8(10)	10	-77.3387(802)	-75.4793(117)	-75.4340(100)	-75.1626(0)
CH_4	$^1A_1$	8(10)	8	-40.4335(403)	-40.2100(124)	-40.1905(100)	-40.1102(0)

[a] Number of active MOs, with the number of total MOs in parentheses.

[b] Number of active electrons.

geometry. We also obtained remarkable improvement for other systems by requiring the G-condition.

The Weinhold-Wilson inequalities VI, VII and VIII were examined for these systems. For CO, LiF, and Ne, all of the inequalities were satisfied. For CH_4 and C_2, the inequality type VI and VII were violated, and for N_2, the inequality type VI was violated but others were satisfied, though the violations were very small as -0.000297∼-0.002063(CH_4, type VI), -0.000127∼-0.001803(CH_4, type VII), -0.004169∼-0.019446(C_2, type VI), -0.000169∼-0.030852(C_2, type VII) and -0.00283 ∼-0.00551(N_2, type VI), respectively. These violations were parallel to the errors of the DMVT(PQG) calculations: the deviations CH_4(124%), C_2(117%), and N_2(108%) were larger than those of the other systems. This implies that the inequalities VI and VII may be adopted as one of the additional N-representability conditions for the DMVT.

4.3.3 Potential curves of H_2O, NH_3 and BH_3

Double dissociation of H_2O and triple dissociation of NH_3 and BH_3 are interesting examples, since four and six electrons are correlated in the bond dissociation pro-

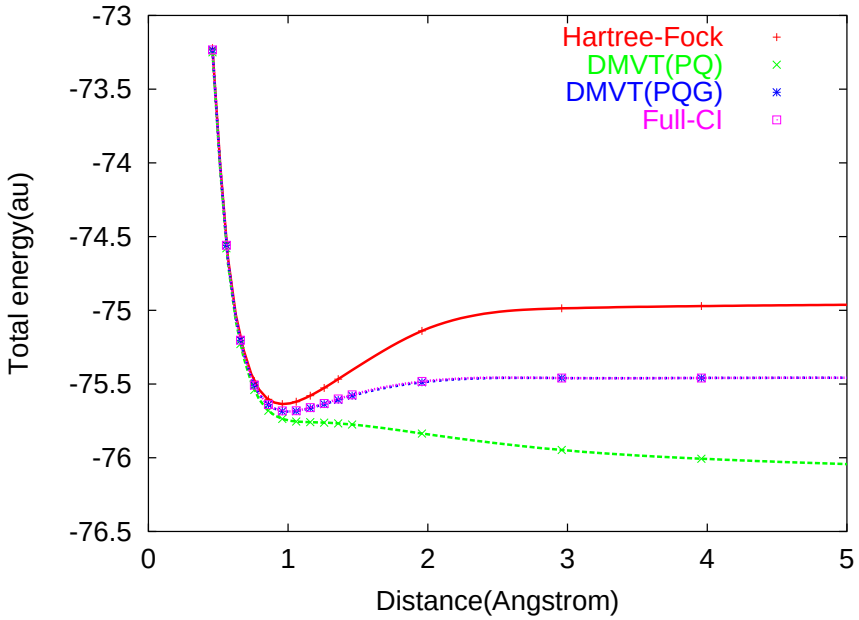

Figure II: Potential curve for the double dissociation of H_2O.

cesses. We calculated the potential curves for the symmetric stretching mode of these systems at several points within $R = 0.5 \sim 5.0$Å, and the results were shown in Figs. 2-4. We used STO-6G basis set and kept 1s orbitals of O, N and B to be frozen. Spectroscopic constants of equilibrium distance (r_e), harmonic frequency (ω_e), and dissociation energy (D_e) were summarized in table V. The potential energy curve was fit with the 6-th extended Rydberg function for some points near the equilibrium geometry and the ω_e was calculated by the Dunhum method[38]. The H-O-H and H-N-H angles were fixed at the experimental values and only the H-O and H-N bonds were symmetrically stretched: ω_e was defined for this coordinate and therefore different from that of the normal mode analysis.

For H_2O and NH_3, DMVT(PQG) simulated the full-CI curves very accurately even up to the dissociation limit and the two curves almost overlapped. H_2O and NH_3 dissociate into $O(^3P) + H(^1S) + H(^1S)$ and $N(^4S) + H(^1S) + H(^1S) + H(^1S)$, respectively, and at the dissociation limit, the electronic state becomes multi-configurational state. DMVT(PQG) accurately described these multi-configurational

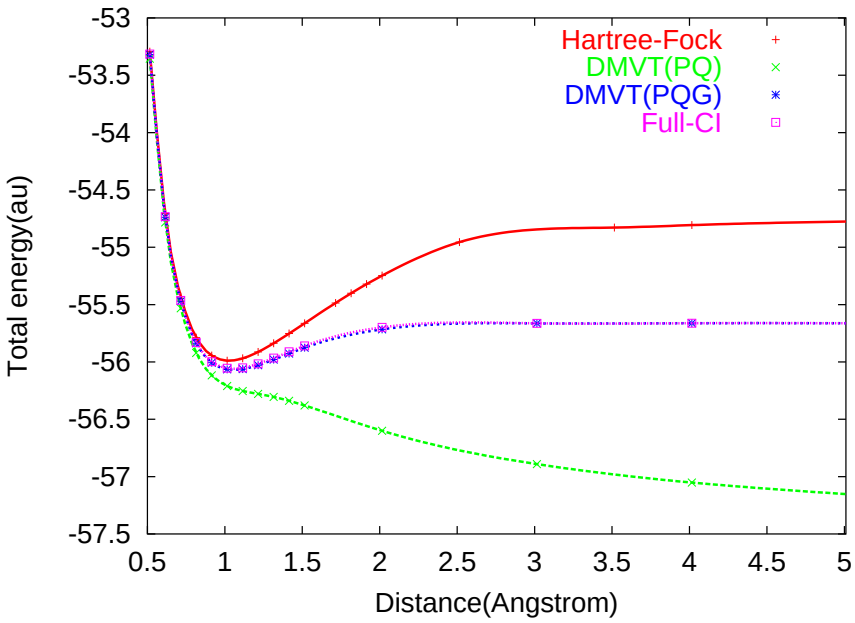

Figure III: Potential curve for the triple dissociation of NH_3.

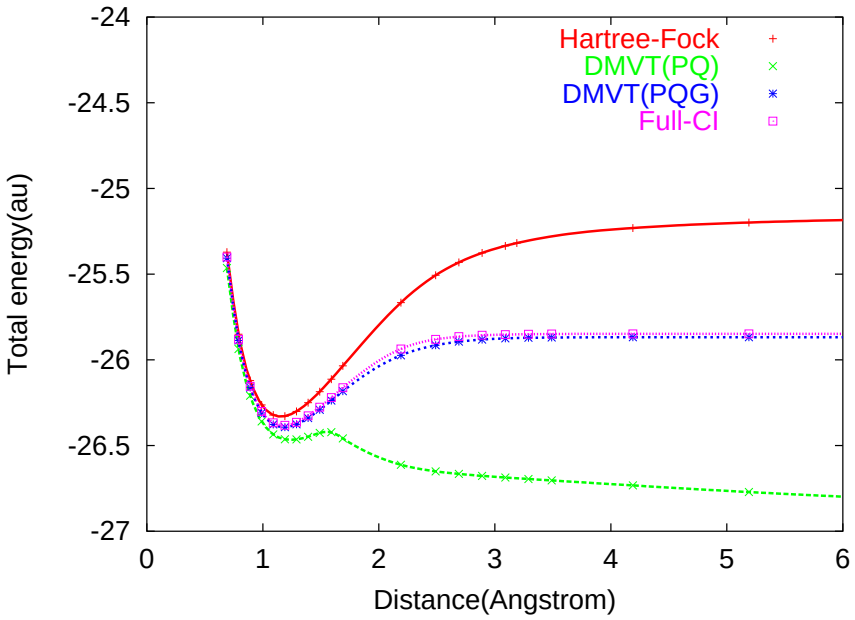

Figure IV: Potential curve for the triple dissociation of BH_3.

TABLE V: Spectroscopic constants of H_2O, NH_3, BH_3, C_2, N_2 and CO.

System	Method	r_e(Å)	ω_e(cm^{-1})	D_e(eV)
H_2O	Hartree-Fock	1.824	3952	18.471
	Full-CI	1.895	3253	6.162
	DMVT(PQG)	1.894	3276	6.227
NH_3	Hartree-Fock	1.025	3750	33.008
	Full-CI	1.057	3324	10.686
	DMVT(PQG)	1.057	3291	10.956
BH_3	Hartree-Fock	1.154	3115	31.284
	Full-CI	1.178	2883	14.280
	DMVT(PQG)	1.181	2854	14.537
C_2	Hartree-Fock	1.233	2207	16.876
	Full-CI	1.257	2035	6.790
	DMVT(PQG)	1.299	1679	7.212
N_2	Hartree-Fock	1.129	2715	31.211
	Full-CI	1.210	2061	6.220
	DMVT(PQG)	1.199	1980	6.622
CO	Hartree-Fock	1.146	2461	12.692
	Full-CI	1.193	2063	9.328
	DMVT(PQG)	1.201	1990	9.540

states, namely, static electron correlations: the deviations from the full-CI were less than 0.5 mhartree in the dissociation limit. On the other hand, while DMVT(PQ) reproduced the curves in the short bond region, it failed at the large internuclear distances. DMVT(PQ) curve did not bound. For BH_3, even the DMVT(PQG) curve slightly deviates from the full-CI curve for $R_{B-H} > 2.0$Å. The dissociation limit of BH_3 is heavily quasi-degenerate: the electronic state is represented by several configurations including quadruple excitations. DMVT(PQ) curve for BH_3 has a hump at around 1.5Å, and, the potential curve is repulsive in nature.

Since DMVT(PQG) calculations gave accurate potential curves, their spectroscopic constants were also accurate. For these systems, the deviations from the full-CI were within 0.003Å and 30 cm^{-1}, for r_e and ω_e, respectively. The dissociation energies (D_e) were estimated slightly larger by 0.06, 0.27 and 0.26 eV, for H_2O, NH_3 and BH_3, respectively. This is because DMVT(PQG) calculations overshoot the full-CI energy around the equilibrium geometries rather than they deviate in the dissociation limit. Since the dissociations of these systems are homolytic and include multiple bonds, the Hartree-Fock description of the dissociation limit was of course very crude.

We examined the Weinhold-Wilson inequalities for BH_3, since the deviation from the full-CI was large for this molecule. Actually, the violations of the conditions VI and VII at the equilibrium distance ranged $-0.000019 \sim -0.003018$ and $-0.000391 \sim -0.002608$, respectively, and those of the conditions VI and VII were $-0.004804 \sim -0.013975$, and $-0.001448 \sim -0.001956$ at the dissociation limit($R = 5$Å).

4.3.4 Potential curves of CO, C_2, N_2, and Be_2.

Next, we apply the DMVT to the potential energy curves of CO, C_2, N_2 and Be_2, since their electronic states are very characteristic. In the potential curve of CO, the Hartree-Fock configuration is dominant at around the equilibrium distance, but its weight decreases as the distance increases and finally becomes zero at the dissociation limit. C_2 has unoccupied $p\sigma$ MO, therefore, the ground state is always quasi-degenerate even in the equilibrium geometry. N_2 includes triple-bond dissoci-

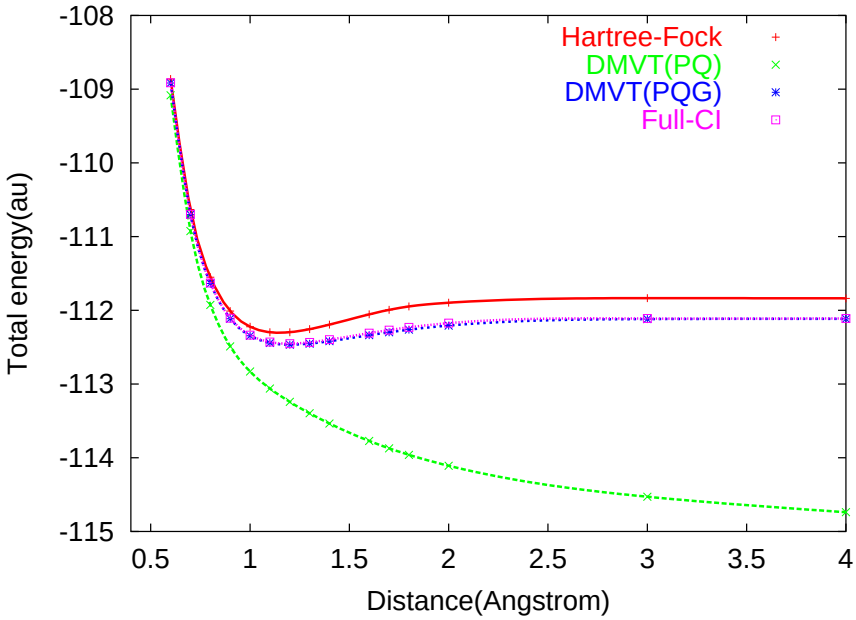

Figure V: Potential curve of CO.

ation, therefore its potential curve is highly quasi-degenerate at large internuclear distance. Be_2 has no bonding interaction. Potential curves of these molecules were calculated for $R = 0.5 \sim 5.0$Å. Minimal STO-6G basis set was used and the 1s orbitals were kept as frozen. The potential curves were shown in Figs. 5-8 and the spectroscopic constants were given in table V.

As in other systems, DMVT(PQG) curves almost overlapped with the full-CI curves, while DMVT(PQ) curves were calculated as repulsive. The deviations of DMVT(PQG) from the full-CI increases in the order of N_2, CO and C_2. Though it is true that the description of the quasi-degeneracy of C_2 is difficult, there is another factor in the accuracy. Since we used minimal basis set, the calculations of N_2 and CO were for 16 spin orbitals with 12 electrons, namely, 4 hole spin orbitals, while those of C_2 are for 16 spin orbitals with 10 electrons; 6 hole spin orbitals. We think this also affected the accuracy of the results. The potential curve of Be_2 was repulsive, since van der Waals interaction was not described by the present basis set. The DMVT(PQ) gave better description than other systems.

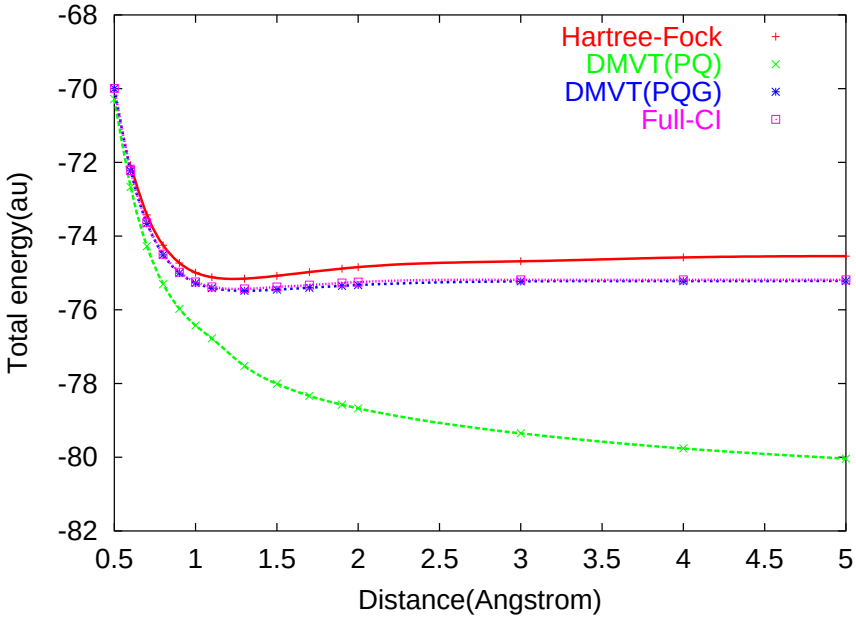

Figure VI: Potential curve of C_2.

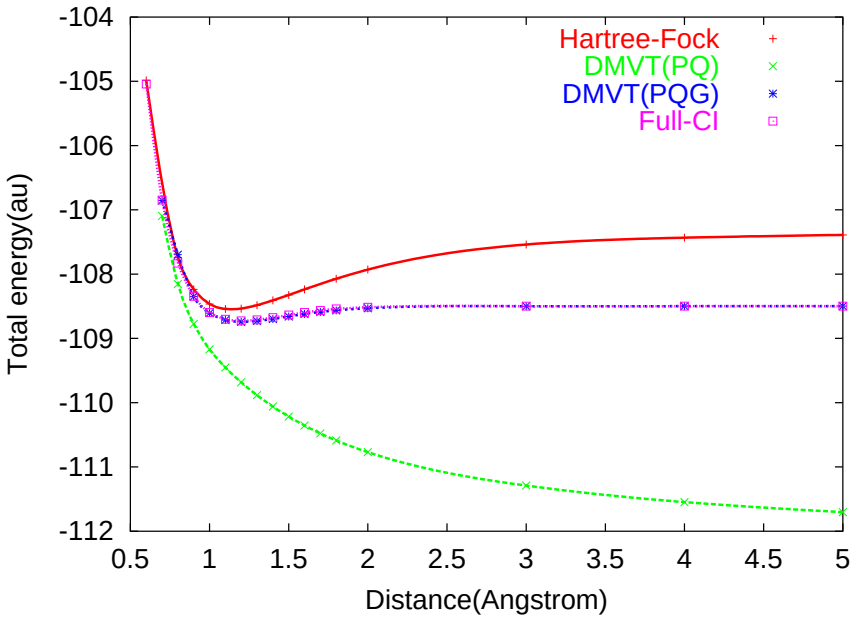

Figure VII: Potential curve of N_2.

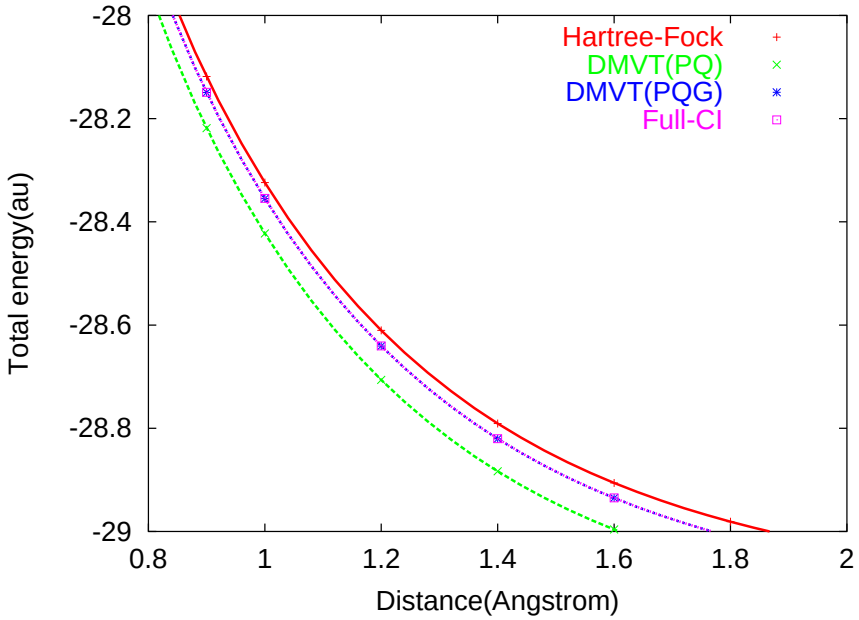

Figure VIII: Potential curve of Be_2.

The DMVT(PQG) results for the spectroscopic constants of these diatomic molecules were less accurate than those for H_2O and NH_3. The deviations were $\sim$ 0.01Å and $\sim$ 80 cm^{-1} for r_e and ω_e, respectively, for CO and N_2. For C_2, the errors were as large as 0.04Å and 350cm^{-1}. These results reflect the quality of the DMVT around the equilibrium geometry.

We also calculated the Weinhold-Wilson inequalities for C_2 and CO. As expected, large violations occurred for the inequalities VI and VII. For C_2, the violations were calculated as $-0.001810 \sim -0.027667$ and $-0.000900 \sim -0.011494$ for conditions VI and VII, respectively, at $R = 1.5$Å, and $-0.003047 \sim -0.002500$ only for condition VI at $R = 5.0$Å: the violations at $R = 1.5$Å were larger than those at $R = 5.0$Å. The ground state of C_2 is quasi-degenerate even at the equilibrium geometry and this is the reason of the crude spectroscopic constants for C_2 by the DMVT(PQG). For CO, the violations ranged $-0.008185 \sim -0.008434$ for condition VI at the dissociation limit and -0.000546 for condition VI at $R = 1.3$Å. There were no errors of conditions VII and VIII for CO.

TABLE VI: Examination of size-consistency for Ne and H_2O, NH_3, BH_3, Be_2, CO, and C_2.

System	Method	$E^a_{\rm mol}$	$E^b_{\rm atom}$	ΔE
H_2O	DMVT(PQG)	-75.4589	-75.4589	0.0000
	Full-CI	-75.4588	-75.4588	0.0000
NH_3	DMVT(PQG)	-55.6622	-55.6622	0.0000
	Full-CI	-55.6622	-55.6622	0.0000
BH_3	DMVT(PQG)	-25.8680	-25.8482	0.0198
	Full-CI	-25.8482	-25.8482	0.0000
Be_2	DMVT(PQG)	-29.1655	-29.1654	0.0001
	Full-CI	-29.1654	-29.1654	0.0000
CO	DMVT(PQG)	-112.1153	-112.1095	0.0058
	Full-CI	-112.1095	-112.1095	0.0000
C_2	DMVT(PQG)	-75.2187	-75.1854	0.0333
	Full-CI	-75.1854	-75.1854	0.0000
N_2	DMVT(PQG)	-108.4982	-108.4982	0.0000
	Full-CI	-108.4982	-108.4982	0.0000

[a] Energy of molecule at the dissociation limit.

[b] Sum of the energies of the isolated atoms.

4.3.5 Size-consistency

As we discussed in Sec II.C, the G-condition is very important for the size-consistent property of the method. Here, we examine the size-consistency of the results. In table VI, the total energy of the molecule in the dissociation limit and the sum of the total energies of the isolated atoms are compared for H_2O, NH_3, BH_3, N_2, C_2, CO and Be_2. For H_2O, NH_3 and N_2, the total energies calculated by DMVT(PQG) agree within numerical accuracy, which shows the size-consistency holds for these systems. In these system, Weinhold-Wilson inequalities were also satisfied and the

TABLE VII: Total energy for the model Hamiltonian, $H = F + \lambda V$ of Be and the correlation energy in (%).

λ	DMVT(PQ)	DMVT(PQG)	Full-CI	Hartree-Fock
0.10	-10.5324(249)	-10.5322(100)	-10.5322(100)	-10.5321(0)
0.50	-12.3365(226)	-12.3317(100)	-12.3317(100)	-12.3278(0)
1.00	-14.6064(200)	-14.5895(100)	-14.5895(100)	-14.5725(0)
2.00	-19.2097(151)	-19.1600(100)	-19.1596(100)	-19.0619(0)
3.00	-24.1197(115)	-24.0491(100)	-24.0469(100)	-23.5513(0)
4.00	-29.6662(139)	-29.2180(101)	-29.2115(100)	-28.0407(0)
5.00	-37.1084(212)	-34.7026(100)	-34.6922(100)	-32.5301(0)
10.00	-76.5823(165)	-68.0991(100)	-68.0414(100)	-54.9771(0)
10000.0	-81838.44(102)	-81294.14(100)	-81290.74(100)	-44904.03(0)

calculations were quite accurate. As seen from the potential curves, DMVT(PQ) calculations gave miserable results from the standpoint of the size-consistency. The G-condition is apparently indispensable for the size-consistent property. For other systems, BH_3, C_2, CO and Be_2, the size-consistency of DMVT(PQG) was not satisfactory. This is because the G-condition is not a sufficient condition for the size-consistency. Note that the Weinhold-Wilson inequalities VI and VII was not satisfied for these systems.

4.3.6 Artificially correlation enhanced system

It is interesting to see the performance of the present method for the strongly correlated system. We here introduced the model Hamiltonian in which the electron correlations are controlled by a parameter. The Hamiltonian is partitioned into F, Fock operator and the rest, V:

$$H = F + \lambda V \tag{4.17}$$

TABLE VIII: Total energy for the model Hamiltonian, $H = F + \lambda V$ of H_2O and the correlation energy in (%).

λ	DMVT(PQ)	DMVT(PQG)	Full-CI	Hartree-Fock
0.10	-41.1669(234)	-41.1664(100)	-41.1664(100)	-41.1661(0)
0.50	-56.5293(233)	-56.5158(102)	-56.5155(100)	-56.5051(0)
1.00	-75.7953(232)	-75.7310(104)	-75.7290(100)	-75.6789(0)
1.50	-95.1938(235)	-95.0064(106)	-94.9978(100)	-94.8526(0)
2.00	-115.0471(222)	-114.5560(115)	-114.4863(100)	-114.0264(0)
3.00	-155.4737(137)	-154.6553(101)	-154.6348(100)	-152.3740(0)
4.00	-196.0891(124)	-195.0768(101)	-195.0347(100)	-190.7215(0)
5.00	-236.8429(120)	-235.6115(101)	-235.5285(100)	-229.0690(0)
10.00	-441.1663(116)	-438.6811(102)	-438.3447(100)	-420.8068(0)
10000.0	-417093.18(124)	-411089.69(102)	-410645.30(100)	-383512.82(0)

where λ is a real parameter that controls the strength of the electron correlations and $\lambda = 1$ corresponds to the original Hamiltonian. We adopted Be and H_2O and changed λ form $0.1 \sim 10000$ and the results were shown in tables VII and VIII, respectively.

For Be system, the DMVT(PQG) reproduced the exact correlation energy quite accurately and the deviations were even-tempered for the variation of λ within 1%. On the other hand, the DMVT(PQ) gave random errors for the variation of λ. For H_2O, the errors of the DMVT(PQG) became large, but, were within 15% relative to the total electron correlations. The DMVT(PQG) calculations converged even for the heavily correlated systems ($\lambda = 10000$), though the absolute errors were not small.

We did not see the Weinhold-Wilson violations in the Be system for all λ. The violations for H_2O were not so simple. For $\lambda = 1.0$, the violations of the condition VI occurred as $-0.00054 \sim -0.00368$, but no violations occurred for $\lambda = 2.0$, which has the largest correlation energy error in %. For $\lambda = 10000$, we got large violations

as $-0.00871 \sim -0.001036$.

4.4 Conclusion

The DMVT was applied to the calculations of the potential energy surfaces of the atoms and small molecules, Ne, H_4, H_2O, NH_3, BH_3, CO, N_2, C_2 and Be_2. This is the first study in which the bond dissociation was properly described by the DMVT. In the previous DET study of potential curves[26], the results were good up to $R \sim 2R_e$, but at large distances, the calculations failed to converge. Generally, the DMVT(PQG) calculation reproduced the full-CI curves very accurately and they sometimes overlapped even in the dissociation limit, though the potential curves for BH_3 and C_2 were less accurate than others. The quasi-degenerate states were well described by the DMVT(PQG) calculations. On the other hand, the curves by DMVT(PQ) were always repulsive, which showed the potential importance of the G-condition.

We examined the size-consistency of the present method. The G-condition is found to be related to the size-consistency of the method and shown to be essential to the behavior of the potential curves of DMVT(PQG), especially in the dissociation limit.

We also examined the Weinhold-Wilson inequalities for the 2-RDM of DMVT(PQG) calculations where the results were less accurate, and found that the inequalities VI and VII were violated. We think these inequalities may be new candidates for the N-representability condition of the DMVT. Since these are linear conditions, it would be easily included in the conditions of the DMVT relaxed with the SDP. Such study is now in progress.

4.5 Acknowledgment

This study has been supported by the Special Grand for Scientific Research from the Japanese Ministry of Education, Science, Culture, and Sports. The authors give warm thanks to Mr. Mitsuhiro Fukuda, Dr. Katsuki Fujisawa, Dr. Kazuhide Nakata, and Prof. Masakazu Kojima, for useful discussions and encouragements.

BIBLIOGRAPHY

[1] K. Husimi, Proc. Phys. Math. Soc. Jap. **22**, 264 (1940).

[2] P.-O, Löwdin, Phys. Rev., **99**, 1474 (1955).

[3] H. Nakatsuji, Phys. Rev. A **14**, 41 (1976).

[4] C. Valdemoro, Phys. Rev. A **45**, 4462 (1992); F. Colmenero C. Pérez del Valle, and C. Valdemoro, Phys. Rev. A **47**, 971 (1993), F. Colmenero and C. Valdemoro Phys. Rev. A **47**, 979 (1993).

[5] H. Nakatsuji and K. Yasuda, Phys. Rev. Lett. **76**, 1039(1996), K. Yasuda and H. Nakatsuji, Phys. Rev. A **56**, 2648(1997).

[6] D. A. Mazziotti, Phys, Rev. A **57**, 4219(1998); Chem. Phys. Lett. **289**, 419(1998).

[7] H. Nakatsuji, in *Many-Electron Densities and Reduced Density Matrices*, ed by J. Cioslowski, Kluwer Academic, New York, 2000.

[8] A. J. Coleman, Rev. Mod. Phys., **35**, 668 (1963).

[9] C. Garrod, and J. K. Percus, J. Math. Phys., **5**, 1756 (1964).

[10] L. J. Kijewski and J. K. Percus, Phys. Rev. A **2**, 1659 (1970), L. J. Kijewski, Phys. Rev. A **6**, 1659 (1972), L. J. Kijewski, Phys. Rev. A **9**, 2263 (1974),

[11] C. Garrod, M. V. Mihailović, and M. Rosina, J. Math. Phys., **16**, 868 (1975).

[12] C. Garrod and M. A. Fusco, Int. J. Quantum Chem. **x**, 495 (1976).

[13] R. M. Erdahl, Rep. Math. Phys., **15** 147 (1979).

[14] M. Nakata, H. Nakatsuji, M. Ehara, M. Fukuda, K. Nakata, K. Fujisawa, J. Chem. Phys., **114**, 8282 (2001).

[15] Y. Nesterov and A. S. Nemirovskii, *Interior Point Polynomial Method in Convex Programming: Theory and Applications* SIAM, Philadelphia, 1993.

[16] L. Vandenberghe and S. Boyd, SIAM Review, **38**, 4 9(1996).

[17] M. Kojima, *Semidefinite Programming and Interior-Point Methods*, URL is `http://www.is.titech.ac.jp/~kojima/wabun.html`, 1996(in Japanese).

[18] K. Fujisawa, M. Kojima, K. Nakata, SDPA (SemiDefinite Programming Algorithm) User's Manual Version 5.00, August 1999.
URL is `http://is-mj.archi.kyoto-u.ac.jp/~fujisawa/software.html`.

[19] R. M. Erdahl and B. Jin, J. Mol. Struct.: THEOCHEM, **527**, 207 (2000); R. M. Erdahl and B. Jin, in *Many-Electron Densities and Reduced Density Matrices*, ed by J. Cioslowski, Kluwer Academic, New York, 2000.

[20] D. A. Mazziotti and R. M. Erdahl, Phys. Rev A, **63**, 042113 (2001).

[21] C. Valdemoro, L. M. Tel, E. Perez-Romero, Phys. Rev A, **61**, 032507 (2000).

[22] H. Nakatsuji, J. Chem. Phys., **113**, 2949 (2000).

[23] H. Nakatsuji and E. R. Davidson, J. Chem. Phys., **115**, 2000 (2001).

[24] H. Nakatsuji, J. Chem. Phys., **115**, 2465 (2001).

[25] H. Nakatsuji, submitted.

[26] M. Ehara, M. Nakata, H. Kou, K. Yasuda, and H. Nakatsuji, Chem. Phys. Lett. **305**, 483(1999).

[27] F. Weinhold and E. B. Wilson Jr, J. Chem. Phys., **47**, 2298 (1967).

[28] E. R. Davidson, J. Math. Phys., **10**, 725 (1969).

[29] W. B. McRae and E. R. Davidson, J. Math. Phys., **13**, 1527 (1972).

[30] J.-P. Hansen and I.R. McDonald, *Theory of simple liquids*, Academic Press, Harcourt Brace & company, Publishers, 1990.

[31] T. V. Voorhis and Martin Head-Gordon, J. Chem. Phys., **113**, 8873 (2001).

[32] K. Fujisawa, M. Kojima and K. Nakata, "Exploiting Sparsity in Primal-Dual Interior-Point Methods for Semidefinite Programming", Mathematical Programming, **79**. 235 (1977).

[33] S. Huzinaga, J. Chem. Phys., **42**, 1293 (1970).
T.H. Dunning, JR., J. Chem. Phys., **53**, 2823 (1970).
T.H. Dunning, JR. and P.J. Hay, In method of electronic structure theory, vol. 2, H.F. Schaefer III, ed., Plenum press, 1977.

[34] Basis sets were obtained from the Extensible Computational Chemistry Environment Basis Set Database, Version 4/22/01, as developed and distributed by the Molecular Science Computing Facility, Environmental and Molecular Sciences Laboratory, the Pacific Northwest Laboratory, P.O. Box 999, Richland, Washington 99352, USA. URL is `http://www.emsl.pnl.gov:2080/forms/basisform.html`.

[35] W. J. Hehre, R. F. Stweart, and J. A. Pople, J. Chem. Phys. **51**, 2657 (1969).

[36] J. H. Callomon, E. Horita, K. Kuchitsu, W. J. Lafferty, A. G. Maki and C. S. Pote, Landolt-Börnstein, Springer-Verlag, Berlin, 1976.

[37] K. P. Huber and G. Herzberg, *Molecular Spectra and Molecular Structure IV.*, Electronic Constants of Diatomic Molecules, Van Nostrand Reinhold, New York, 1979.

[38] J. L. Dunhum, Phys. Rev. **41**, 713, 721 (1932), H. M. Hulburt, J. O. Hirschfelder J. Chem. Phys. **9**, 61 (1941).

Chapter 5.

Density Matrix variational theory: Strength of Weinhold-Wilson inequalities

Abstract

We examine the strength of the Weinhold-Wilson (WW) inequalities for calculating the second-order density matrix(2-RDM) by the density matrix variational theory (DMVT) using the P, Q and G conditions as subsidiary conditions. We calculated the 2-RDM of various molecular electronic states and found that some violations of WW inequalities occur especially for the systems for which the DMVT(PQG) calculations were less accurate. We then developed the DMVT method including further the WW inequalities as the restrictive conditions, DMVT(PQG+WW), and applied it to CH_4, C_2, $CH_2(^1A_1)$ and H_2O. The WW inequalities certainly improved the results, but the improvement was not so remarkable.

5.1 Introduction

As far as our world involves only up-to-two body elementary operators, this world should be described solely by the second-order reduced density matrix (2-RDM). Professor Löwdin not only did a lot of great works in this and related field[1, 2], but also encouraged many young researchers. HN is one of such researchers and would like to thank Professor Per-Olov Löwdin for his great contributions in the field of quantum molecular science and his encouragement warmly given to him.

Recently, special attentions have been paid to the direct determination of the reduced density matrix (RDM), which is called as density matrix theory(DMT). This approach adopts the 2-RDM as the basic variable of quantum mechanics and there are two formalisms in the DMT. One is based on the density equation[3], which is equivalent to the Schrödinger equation in the necessary and sufficient sense. This approach is called density equation theory (DET). Recent development of the DET[4, 5, 6] has been remarkable and they have been summarized in the review article [7]. The other is based on the Ritz variational principle expressed in terms of the 2-RDM and is referred to as the density matrix variational theory (DMVT). The quality of the calculated 2-RDM in the DMVT is dependent on how well we can restrict our variable 2-RDM to be N-representable[8].

The DMVT method was first introduced by Garrod and Percus. They proposed the variational method using P, Q and G conditions and some trivial N-representability conditions[9], and applied it to the ground state of Be[10]. Erdahl proposed to use convex programming for the DMVT and applied it to He_2[11]. The applications in these early studies were limited to very small systems. Recently, Erdahl and Jin[12] developed the DMVT using 3-RDM as variable and applied it to the model system of one-dimensional periodic lattice of electron pairs. Mazziotti and Erdahl[13] examined the positive semidefinite condition of 3- and 4-RDMs for solving the DMVT combined with the DET and calculated Lipkin model, namely, a boson model of two-energy-level system.

In this series of our DMVT studies[14, 15], we could efficiently implement the DMVT using the semidefinite programming algorithm (SDPA)[16], and successfully

calculate the 2-RDMs of the ground states of many different spin-space symmetries for *many atoms and molecules*. We also applied this method to the potential energy surfaces of molecules and reproduced the full-CI curves in good approximation up to the dissociation limit[15]; the G condition was found to be very important for describing the dissociation limit.

Another promising approach was initiated by one of the authors[17]. Since the exact Ψ is an eigen function of the Hamiltonian that has so simple structure composed of only one- and two-body operators, the Ψ itself should also have a simple structure reflecting this simplicity of the Hamiltonian. Some explicit expressions of the structure of the exact wave function were given and the theories for the ground and excited states was formulated. Applications were given to a simple model system and to atoms and molecules.

For improving the DMVT(PQG) method developed previously[14, 15], we may use some additional N-representability conditions. Some inequalities for the 2-RDM were proposed by Weinhold and Wilson[18], Davidson[19] and McRae and Davidson[20]. Since all of these inequalities can be written as linear conditions, it is easy to include these conditions in our formalism. In our previous work[15], we actually examined these inequalities for the resultant 2-RDM of the DMVT(PQG) calculations and found that two linear inequalities were violated in some cases.

In this paper, we examine the Weinhold-Wilson (WW) inequalities for calculating the 2-RDM by the DMVT(PQG) method. Examinations have been done for all the systems that were calculated in the previous studies[14, 15]. Then, we propose an efficient formalism for including these conditions as the subsidiary conditions.

5.2 Theory and calculation

5.2.1 Definitions and basic algorithm

First and second order reduced density matrices (1-, 2-RDMs), γ and Γ, are defined by:

$$\gamma^i_j = \langle \Psi | a^\dagger_i a_j | \Psi \rangle \tag{5.1}$$

$$\Gamma^{i_1 i_2}_{j_1 j_2} = \frac{1}{2}\langle\Psi|a^\dagger_{i_1} a^\dagger_{i_2} a_{j_2} a_{j_1}|\Psi\rangle \tag{5.2}$$

where $a^\dagger$ and a are creation and annihilation operators, respectively. Practical complete N-representability condition is not known for the 2-RDM: we know only some necessary conditions. In the present DMVT, we use P, Q, and G conditions. The P, Q, and G-matrices are defined by,

$$P^{i_1 i_2}_{j_1 j_2} = \langle\Psi|a^\dagger_{i_1} a^\dagger_{i_2} a_{j_2} a_{j_1}|\Psi\rangle \tag{5.3}$$

$$Q^{i_1 i_2}_{j_1 j_2} = \langle\Psi|a_{i_1} a_{i_2} a^\dagger_{j_2} a^\dagger_{j_1}|\Psi\rangle \tag{5.4}$$

$$G^{i_1 i_2}_{j_1 j_2} = \langle\Psi|a^\dagger_{i_1} a_{i_2} a^\dagger_{j_2} a_{j_1}|\Psi\rangle \tag{5.5}$$

respectively. We enforce all of these matrices to be positive semidefinite. We also use seven trivial conditions of 2-RDM, which are antisymmetric condition, hermiticity, trace condition, number of electrons, number of spins, and expectation values of S_z and S^2.

In the DMVT, we take 2-RDM as a variational variable, and minimize the energy within N-representability conditions, namely,

$$E_{\min} = \underset{\Gamma\in\mathcal{P}^{(2)}}{\mathrm{Min}} \ \mathrm{Tr}H\Gamma, \tag{5.6}$$

where H is the Hamiltonian of the system, $\mathcal{P}^{(2)}$ is a set of 2-RDM that satisfy approximate or nearly complete N-representability condition. In the previous papers [14, 15], we performed two types of calculations using the approximate N-representability conditions: the DMVT(PQ) adopts the trivial representability conditions plus P and Q conditions as the approximate conditions, and the DMVT(PQG) further includes G condition. In this work, we also include the Weinhold-Wilson inequalities, and we call the method as the DMVT(PQG+WW) method.

5.2.2 Weinhold-Wilson inequalities

The Weinhold-Wilson inequalities which are independent from P, Q, G, and 7 trivial conditions are:

Condition IV:

$$1 - \gamma_i^i - \gamma_j^j + 2\Gamma_{ij}^{ij} \geq 0 \tag{5.7}$$

Condition V:

$$\gamma_i^i - 2\Gamma_{ij}^{ij} \geq 0 \tag{5.8}$$

Condition VI:

$$\gamma_i^i - 2\Gamma_{ij}^{ij} - 2\Gamma_{ik}^{ik} + 2\Gamma_{jk}^{jk} \geq 0 \tag{5.9}$$

Condition VII:

$$1 - \gamma_i^i - \gamma_j^j - \gamma_k^k + 2\Gamma_{ij}^{ij} + 2\Gamma_{ik}^{ik} + 2\Gamma_{jk}^{jk} \geq 0 \tag{5.10}$$

Condition VIII: Positive semidefiniteness of the Ω matrix

$$\Omega = \begin{pmatrix} \gamma_1^1 & 2\Gamma_{12}^{12} & 2\Gamma_{13}^{13} & \cdots & 2\Gamma_{1t}^{1t} & \gamma_1^1 \\ 2\Gamma_{12}^{12} & \gamma_2^2 & 2\Gamma_{23}^{23} & \cdots & 2\Gamma_{2t}^{2t} & \gamma_2^2 \\ 2\Gamma_{13}^{13} & 2\Gamma_{23}^{23} & \gamma_3^3 & \cdots & 2\Gamma_{3t}^{3t} & \gamma_3^3 \\ \vdots & \vdots & \vdots & & \vdots & \vdots \\ 2\Gamma_{1t}^{1t} & 2\Gamma_{2t}^{2t} & 2\Gamma_{3t}^{3t} & \cdots & \gamma_t^t & \gamma_t^t \\ \gamma_1^1 & \gamma_2^2 & \gamma_3^3 & \cdots & \gamma_t^t & 1 \end{pmatrix}. \tag{5.11}$$

Note that different definition is employed for Γ by factor 2. In this study, we examined the 2-RDM by the DMVT(PQG) method with respect to these five inequalities, and we found that two types of conditions VI and VII were violated for some systems. Therefore, we develop the DMVT method including these conditions.

5.2.3 DMVT method including Weinhold-Wilson inequalities

Since all the Weinhold-Wilson inequalities are linear conditions, it is possible to include all of these inequalities in the SDP formalism simultaneously. However, the number of conditions becomes large since it scales as N^3, and therefore we enforce the inequalities only for those molecules for which the WW inequalities were violated in the preceding DMVT(PQG) calculation. Then, the algorithm of the DMVT (PQG+WW) is as follows:

1. Standard DMVT(PQG) is executed.

2. Weinhold-Wilson inequalities of type IV$\sim$ VIII are examined.

3. DMVT(PQG+WW) is performed with additional WW conditions if some of the WW inequalities are violated.

The procedure of 2 and 3 is repeated until all the inequalities are satisfied. Note that the inequality holds after it is included in the condition. Actually, this iteration is necessary only for one or two times. As noted in section 2.2., the conditions VI and VII were violated for the resultant 2-RDM calculated by the DMVT(PQG), and therefore we developed the method of including only these two WW conditions. In the DMVT method using SDPA, the conditions should be reduced to the standard form and we introduce two types of constraint matrices $\boldsymbol{C}^{\mathrm{VI}}_{ijk}$ and $\boldsymbol{C}^{\mathrm{VII}}_{ijk}$. In the following, we employ the same notations as those in the previous paper[14]. In the DMVT(PQG+WW) calculations, we extend the variable matrix $\boldsymbol{Y}$ given by Eq. (3.25) of Ref.[14] as $\boldsymbol{Y}'$,

$$\boldsymbol{Y}' = \begin{pmatrix} \boldsymbol{P} & \boldsymbol{0} & \boldsymbol{0} & \boldsymbol{0} & \boldsymbol{0} \\ \boldsymbol{0} & \boldsymbol{Q} & \boldsymbol{0} & \boldsymbol{0} & \boldsymbol{0} \\ \boldsymbol{0} & \boldsymbol{0} & \boldsymbol{G} & \boldsymbol{0} & \boldsymbol{0} \\ \boldsymbol{0} & \boldsymbol{0} & \boldsymbol{0} & \boldsymbol{W}^{\mathrm{VI}} & \boldsymbol{0} \\ \boldsymbol{0} & \boldsymbol{0} & \boldsymbol{0} & \boldsymbol{0} & \boldsymbol{W}^{\mathrm{VII}} \end{pmatrix} = \begin{pmatrix} \boldsymbol{Y} & \boldsymbol{0} & \boldsymbol{0} \\ \boldsymbol{0} & \boldsymbol{W}^{\mathrm{VI}} & \boldsymbol{0} \\ \boldsymbol{0} & \boldsymbol{0} & \boldsymbol{W}^{\mathrm{VII}} \end{pmatrix} \tag{5.12}$$

where $\boldsymbol{W}^{\mathrm{VI}}$, and $\boldsymbol{W}^{\mathrm{VII}}$ are the diagonal matrices and their diagonal elements are given in the right hand sides of Eqs.(5.9) and (5.10), respectively.

We define the constraint matrix $\boldsymbol{C}^{\mathrm{VI}}_{ijk}$ by

$$(\boldsymbol{C}^{\mathrm{VI}}_{ijk})_{p_1,p_2,q_1,q_2} = \begin{cases} -\frac{2}{N-1}\delta^i_{p_1}\delta^i_{q_1}\delta^{p_2}_{q_2} + 2\delta^i_{p_1}\delta^j_{p_2}\delta^i_{q_1}\delta^j_{q_2} + 2\delta^i_{p_1}\delta^k_{p_2}\delta^i_{q_1}\delta^k_{q_2} \\ \qquad\qquad - 2\delta^j_{p_1}\delta^k_{p_2}\delta^j_{q_1}\delta^k_{q_2}, \\ \qquad\qquad \text{for } 1 \le p_1, p_2, q_1, q_2 \le 3n, \\ 1 \qquad\qquad \text{for } 3n{+}1 \le p_1, p_2, q_1, q_2 \le 3n{+}n^{\mathrm{VI}}, \\ 0 \qquad\qquad \text{otherwise} \end{cases} \tag{5.13}$$

and C^{VII}_{ijk} by

$$(\boldsymbol{C}^{\mathrm{VII}}_{ijk})_{p_1,p_2,q_1,q_2} = \begin{cases} \frac{2}{N-1}\left(\delta^i_{p_1}\delta^i_{q_1}\delta^{p_2}_{q_2} + \delta^j_{p_1}\delta^j_{q_1}\delta^{p_2}_{q_2} + \delta^k_{p_1}\delta^k_{q_1}\delta^{p_2}_{q_2}\right) \\ \qquad\qquad - 2\delta^i_{p_1}\delta^j_{p_2}\delta^i_{q_1}\delta^j_{q_2} + 2\delta^j_{p_1}\delta^k_{p_2}\delta^j_{q_1}\delta^k_{q_2}, \\ \qquad \text{for } 1 \le p_1, p_2, q_1, q_2 \le 3n, \\ 1 \qquad \text{for } 3n{+}n^{\mathrm{VI}}{+}1 \le p_1, p_2, q_1, q_2 \le 3n{+}n^{\mathrm{VI}}{+}n^{\mathrm{VII}}, \\ 0 \qquad \text{otherwise}, \end{cases} \tag{5.14}$$

where n^{VI} and n^{VII} are the numbers of the Weinhold-Wilson inequality conditions, which were not satisfied in the previous iteration. The constants for constraints $\boldsymbol{C}^{\mathrm{VI}}$ and $\boldsymbol{C}^{\mathrm{VII}}$ are all 0 and 1, respectively.

Then, these constraints work as

$$\begin{aligned} \boldsymbol{C}^{\mathrm{VI}}_{ijk} \bullet \boldsymbol{Y}' &= \sum_{p_1p_2q_1q_2} (-\frac{2}{N-1}\delta^i_{p_1}\delta^i_{q_1}\delta^{p_2}_{q_2} + 2\delta^i_{p_1}\delta^j_{p_2}\delta^i_{q_1}\delta^j_{q_2} \\ &\quad +2\delta^i_{p_1}\delta^k_{p_2}\delta^i_{q_1}\delta^k_{q_2} - 2\delta^j_{p_1}\delta^k_{p_2}\delta^j_{q_1}\delta^k_{q_2})Y^{p_1p_2}_{q_1q_2} + (\boldsymbol{W}^{\mathrm{VI}})_{ijk} \\ &= -\sum_{p_2}\frac{2}{N-1}\Gamma^{ip_2}_{ip_2} + 2\Gamma^{ij}_{ij} + 2\Gamma^{ik}_{ik} - 2\Gamma^{kj}_{kj} + (\boldsymbol{W}^{\mathrm{VI}})_{ijk} \\ &= -\gamma^i_i + 2\Gamma^{ij}_{ij} + 2\Gamma^{ik}_{ik} - 2\Gamma^{kj}_{kj} + (\boldsymbol{W}^{\mathrm{VI}})_{ijk} \\ &= 0 \end{aligned} \tag{5.15}$$

and

$$\begin{aligned} \boldsymbol{C}^{\mathrm{VII}}_{ijk} \bullet \boldsymbol{Y}' &= \sum_{p_1p_2q_1q_2} (\frac{2}{N-1}\left(\delta^i_{p_1}\delta^i_{q_1}\delta^{p_2}_{q_2} + \delta^j_{p_1}\delta^j_{q_1}\delta^{p_2}_{q_2} + \delta^k_{p_1}\delta^k_{q_1}\delta^{p_2}_{q_2}\right) \\ &\quad - 2\delta^i_{p_1}\delta^j_{p_2}\delta^i_{q_1}\delta^j_{q_2} - 2\delta^i_{p_1}\delta^k_{p_2}\delta^i_{q_1}\delta^k_{q_2} \\ &\quad - 2\delta^j_{p_1}\delta^k_{p_2}\delta^j_{q_1}\delta^k_{q_2})Y^{p_1p_2}_{q_1q_2} + (\boldsymbol{W}^{\mathrm{VII}})_{ijk} \\ &= \gamma^i_i + \gamma^j_j + \gamma^k_k - 2\Gamma^{ij}_{ij} - 2\Gamma^{ik}_{ik} - 2\Gamma^{kj}_{kj} + (\boldsymbol{W}^{\mathrm{VII}})_{ijk} \\ &= 1, \end{aligned} \tag{5.16}$$

since $(\boldsymbol{W}^{\mathrm{VI}})_{ijk}$ and $(\boldsymbol{W}^{\mathrm{VII}})_{ijk}$ are

$$\begin{aligned} (\boldsymbol{W}^{\mathrm{VI}})_{ijk} &= \gamma^i_i - 2\Gamma^{ij}_{ij} - 2\Gamma^{ik}_{ik} + 2\Gamma^{jk}_{jk} \\ (\boldsymbol{W}^{\mathrm{VII}})_{ijk} &= 1 - \gamma^i_i - \gamma^j_j - \gamma^k_k + 2\Gamma^{ij}_{ij} + 2\Gamma^{ik}_{ik} + 2\Gamma^{jk}_{jk}. \end{aligned} \tag{5.17}$$

We further antisymmetrize the indices $i_1 \leftrightarrow i_2$ and $j_1 \leftrightarrow j_2$, hermitize the indices $(i_1, i_2) \leftrightarrow (j_1, j_2)$ to be suitable for the SDPA formalism, and pack the elements to remove unnecessary variables.

The resultant SDP formalism of the DMVT(PQG+WW) method is now given by,

$$\begin{cases} \text{Minimize} & \boldsymbol{H} \bullet \boldsymbol{Y'} \\ \text{subjected to} & \boldsymbol{F}_i \bullet \boldsymbol{Y'} = c_i \\ & \tilde{\boldsymbol{E}}^{i_1 i_2}_{j_1 j_2} \bullet \boldsymbol{Y'} = \delta^{i_1}_{j_1}\delta^{i_2}_{j_2} - \delta^{i_1}_{j_2}\delta^{i_2}_{j_1} \\ & \tilde{\boldsymbol{J}}^{i_1 i_2}_{j_1 j_2} \bullet \boldsymbol{Y} = 0, \\ & \boldsymbol{C}^{\mathrm{VI}}_{ijk} \bullet \boldsymbol{Y'} = 0, \\ & \boldsymbol{C}^{\mathrm{VII}}_{ijk} \bullet \boldsymbol{Y'} = 1. \end{cases} \tag{5.18}$$

where the matrices of $\boldsymbol{F}_i$, $\tilde{\boldsymbol{E}}$, and $\tilde{\boldsymbol{J}}$ are defined in ref.[14].

5.3 Results

First we examined the Weinhold-Wilson inequalities for the 2-RDM obtained by the DMVT(PQG) calculations. We calculated the various electronic states of molecules, which were studied in the previous works[14, 15]. For N_2, CO, BH_3 and H_2O, the examinations were performed at both the equilibrium geometry and dissociation limit. In table I, we presented the results of the number of the violated conditions whose absolute errors were lager than 1×10^{-5} together with the DMVT(PQG) and full-CI energies. The violation occurred for the conditions VI and VII in some cases, while the conditions IV and V and VIII held for all the electronic states. For all the other atoms and molecules which were calculated in the previous paper and were not included in table I, all of these inequalities were correctly held. As seen in table I, when the DMVT(PQG) calculations are less accurate, the violation of the inequalities becomes large: the number of violations are large for BH_3, $CH_2(^1A_1)$, C_2 and CH_4.

We also calculated the artificially correlation enhanced system, introduced in the previous study[15]: namely, the Hamiltonian is partitioned into F, Fock operator

TABLE I: Number of violated Weinhold-Wilson inequalities for the 2-RDM determined by DMVT(PQG), whose absolute errors are larger than 1×10^{-5}.

System	State	Violation	DMVT(PQG)	FullCI
BH_3 [a]	$^1A_1$	VI: 12, VII: 12	-26.3926(120)	-26.3822(100)
BH_3 [b]	$^1A_1$	VI: 14, VII: 6	-25.8678(103)	-25.8482(100)
C_2 [a]	$^1\Sigma$	VI: 16, VII: 32	-75.4793(117)	-75.4340(100)
C_2 [b]	$^1\Sigma$	VII: 4	-75.2187(105)	-75.1855(100)
CO [a]	$^1\Sigma$	No	-112.4544(108)	-112.4426(100)
CO [b]	$^1\Sigma$	VI: 12	-112.1156(102)	-112.1096(100)
N_2 [a]	$^1\Sigma_g^+$	VI: 4	-108.7123(108)	-108.7002(100)
N_2 [b]	$^1\Sigma_g^+$	No	-108.4982(100)	-108.4982(100)
H_2O [a]	$^1A_1$	VI: 6	-75.7310(104)	-75.7290(100)
H_2O [b]	$^1A_1$	No	-75.4589(100)	-75.4589(100)
BH_2	$^2A_1$	VII: 6	-25.7089(115)	-25.7032(100)
CH^+	$^1\Sigma^+$	VI: 8	-37.8896(107)	-37.8853(100)
CH^-	$^3\Sigma^-$	VII: 2	-37.9714(99)	-37.9718(100)
CH	$^2\Pi$	VI: 2	-38.1916(111)	-38.1871(100)
CH_2	$^1A_1$	VI: 14, VII: 17	-38.8228(119)	-38.8110(100)
CH_2	$^3B_1$	VI: 2, VII: 4	-38.8556(107)	-38.8534(100)
CH_2(linear)	$^3\Sigma_u^-$	VI: 10, VII: 8	-38.8358(103)	-38.8342(100)
FH_2^+	$^1A_1$	VI: 8	-99.8305(103)	-99.8294(100)
H_2O^+	$^2A_1$	VI: 5	-75.4218(106)	-75.4192(100)
NH_2	$^2A_1$	VI: 4, VII: 8	-55.3570(111)	-55.3525(100)
NH_2	$^2B_1$	VI: 1, VII: 3	-55.4195(108)	-55.4157(100)
CH_4	$^1A_1$	VI: 30, VII:24	-40.2030(124)	-40.1905(100)

[a] At equilibrium geometry

[b] At dissociation limit

TABLE II: Number of violated Weinhold-Wilson inequalities for the 2-RDM of H_2O determined by DMVT(PQG), whose absolute errors are larger than 1×10^{-5}.

λ	Violation	DMVT(PQG)	FullCI
0.5	VI: 8	-56.5158(102)	-56.5155(100)
1.0	VI: 6	-75.7310(104)	-75.7290(100)
1.5	VI: 8	-95.0064(106)	-94.9978(100)
$\lambda > 1.5$	No	-	-

and the rest, V as:

$$H = F + \lambda V, \tag{5.19}$$

where λ is a real parameter that controls the strength of the electron correlation. Using this Hamiltonian, the DMVT(PQG) calculations were performed for H_2O and the results for some λ were summarized in table II. The violations have occurred for the condition VI and they were large for $\lambda = 1.5$. Note that no violation has occurred for large λ.

We examined the violations in details for C_2, $CH_2(^1A_1)$ and CH_4 and artificially correlation enhanced system with $\lambda = 1.5$ of H_2O.

TABLE III: Violation of Weinhold-Wilson inequalities for C_2

Condition VI

(i,j,k)	violation	(i,j,k)	violation	(i,j,k)	violation	(i,j,k)	violation
$(5,\overline{4},\overline{7})$	-1.95×10^{-2}	$(\overline{5},4,7)$	-1.94×10^{-2}	$(\overline{5},3,6)$	-1.94×10^{-2}	$(5,\overline{3},\overline{6})$	-1.941×10^{-2}
$(6,4,7)$	-9.29×10^{-3}	$(\overline{6},\overline{4},\overline{7})$	-9.29×10^{-3}	$(\overline{7},\overline{3},\overline{6})$	-9.29×10^{-3}	$(7,3,6)$	-9.28×10^{-3}
$(7,\overline{5},\overline{7})$	-8.01×10^{-3}	$(\overline{7},5,7)$	-8.00×10^{-3}	$(\overline{6},5,6)$	-7.99×10^{-3}	$(6,\overline{5},\overline{6})$	-7.98×10^{-3}
$(\overline{7},\overline{3},6)$	-4.19×10^{-3}	$(7,3,\overline{6})$	-4.17×10^{-3}	$(6,4,\overline{7})$	-4.17×10^{-3}	$(\overline{6},\overline{4},7)$	-4.17×10^{-3}

Condition VII

(i,j,k)	violation	(i,j,k)	violation	(i,j,k)	violation	(i,j,k)	violation
$(2,5,\overline{5})$	-3.09×10^{-2}	$(\overline{2},5,\overline{5})$	-3.09×10^{-2}	$(3,4,\overline{6})$	-1.37×10^{-2}	$(\overline{3},\overline{4},6)$	-1.37×10^{-2}
$(3,4,\overline{7})$	-1.36×10^{-2}	$(\overline{3},\overline{4},7)$	-1.36×10^{-2}	$(3,\overline{3},6)$	-9.03×10^{-3}	$(3,\overline{3},\overline{6})$	-9.02×10^{-3}
$(4,\overline{4},7)$	-9.01×10^{-3}	$(4,\overline{4},\overline{7})$	-9.00×10^{-3}	$(\overline{3},\overline{4},\overline{6})$	-6.50×10^{-3}	$(3,4,6)$	-6.49×10^{-3}
$(3,4,7)$	-6.50×10^{-3}	$(\overline{3},\overline{4},\overline{7})$	-6.50×10^{-3}	$(2,\overline{5},\overline{6})$	-6.40×10^{-3}	$(\overline{2},5,6)$	-6.38×10^{-3}
$(\overline{2},5,7)$	-6.45×10^{-3}	$(2,\overline{5},\overline{7})$	-6.43×10^{-3}	$(2,5,7)$	-2.67×10^{-3}	$(\overline{2},\overline{5},\overline{7})$	-2.67×10^{-3}
$(2,5,6)$	-2.67×10^{-3}	$(\overline{2},\overline{5},\overline{6})$	-2.67×10^{-3}	$(2,4,7)$	-1.49×10^{-3}	$(\overline{2},\overline{4},\overline{7})$	-1.49×10^{-3}
$(2,3,6)$	-1.48×10^{-3}	$(\overline{2},\overline{3},\overline{6})$	-1.47×10^{-3}	$(\overline{3},\overline{5},\overline{6})$	-1.26×10^{-3}	$(3,5,6)$	-1.26×10^{-3}
$(\overline{4},\overline{5},\overline{7})$	-1.25×10^{-3}	$(4,5,7)$	-1.24×10^{-3}	$(1,5,8)$	-1.76×10^{-4}	$(\overline{1},\overline{5},\overline{8})$	-1.69×10^{-4}

TABLE IV: Violation of Weinhold-Wilson inequalities for $CH_2(^1A_1)$

Condition VI

(i,j,k)	violation	(i,j,k)	violation	(i,j,k)	violation	(i,j,k)	violation
$(5,\overline{4},\overline{5})$	-1.07×10^{-3}	$(\overline{5},4,5)$	-1.07×10^{-3}	$(7,\overline{4},\overline{6})$	-6.48×10^{-4}	$(\overline{7},4,6)$	-6.46×10^{-4}
$(2,\overline{3},\overline{6})$	-3.56×10^{-4}	$(\overline{2},3,6)$	-3.57×10^{-4}	$(6,\overline{6},\overline{7})$	-2.16×10^{-4}	$(\overline{6},6,7)$	-2.17×10^{-4}
$(\overline{6},\overline{2},7)$	-6.98×10^{-5}	$(6,2,\overline{7})$	-6.90×10^{-5}	$(\overline{2},3,\overline{6})$	-4.02×10^{-5}	$(2,\overline{3},6)$	-3.89×10^{-5}
$(2,3,6)$	-3.66×10^{-5}	$(\overline{2},\overline{3},\overline{6})$	-3.61×10^{-5}				

Condition VII

(i,j,k)	violation	(i,j,k)	violation	(i,j,k)	violation	(i,j,k)	violation
$(\overline{2},5,\overline{7})$	-2.39×10^{-3}	$(2,\overline{5},7)$	-2.39×10^{-3}	$(\overline{2},\overline{5},7)$	-1.60×10^{-3}	$(2,5,\overline{7})$	-1.59×10^{-3}
$(2,5,7)$	-1.54×10^{-3}	$(\overline{2},\overline{5},\overline{7})$	-1.54×10^{-3}	$(3,4,6)$	-1.54×10^{-3}	$(\overline{3},\overline{4},\overline{6})$	-1.54×10^{-3}
$(\overline{2},5,7)$	-1.21×10^{-3}	$(2,\overline{5},\overline{7})$	-1.20×10^{-3}	$(3,4,\overline{6})$	-1.14×10^{-3}	$(\overline{3},\overline{4},6)$	-1.14×10^{-3}
$(2,4,5)$	-4.47×10^{-4}	$(\overline{2},\overline{4},\overline{5})$	-4.47×10^{-4}	$(3,6,7)$	-4.46×10^{-4}	$(\overline{3},\overline{6},\overline{7})$	-4.47×10^{-4}
$(\overline{3},6,7)$	-1.87×10^{-4}	$(3,\overline{6},\overline{7})$	-1.86×10^{-4}				

TABLE V: Violation of Weinhold-Wilson inequalities for CH_4

Condition VI							
(i,j,k)	violation	(i,j,k)	violation	(i,j,k)	violation	(i,j,k)	violation
$(3,\overline{1},5)$	-2.06×10^{-3}	$(\overline{3},1,\overline{5})$	-2.06×10^{-3}	$(4,\overline{1},6)$	-2.06×10^{-3}	$(\overline{4},1,\overline{6})$	-2.06×10^{-3}
$(5,3,\overline{8})$	-1.21×10^{-3}	$(\overline{5},\overline{3},8)$	-1.21×10^{-3}	$(6,4,\overline{8})$	-1.21×10^{-3}	$(\overline{6},\overline{4},8)$	-1.21×10^{-3}
$(4,\overline{1},\overline{6})$	-9.15×10^{-4}	$(\overline{4},1,6)$	-9.15×10^{-4}	$(3,\overline{1},\overline{5})$	-9.15×10^{-4}	$(\overline{3},1,5)$	-9.15×10^{-4}
$(4,1,\overline{6})$	-5.49×10^{-4}	$(\overline{4},\overline{1},6)$	-5.49×10^{-4}	$(3,1,\overline{5})$	-5.49×10^{-4}	$(\overline{3},\overline{1},5)$	-5.49×10^{-4}
$(1,3,\overline{4})$	-4.87×10^{-4}	$(1,\overline{3},4)$	-4.87×10^{-4}	$(\overline{1},\overline{3},4)$	-4.87×10^{-4}	$(\overline{1},3,\overline{4})$	-4.86×10^{-4}
$(1,\overline{2},\overline{3})$	-4.76×10^{-4}	$(\overline{1},2,3)$	-4.75×10^{-4}	$(\overline{1},2,4)$	-4.76×10^{-4}	$(1,\overline{2},\overline{4})$	-4.76×10^{-4}
$(1,\overline{3},\overline{4})$	-4.75×10^{-4}	$(\overline{1},3,4)$	-4.75×10^{-4}	$(\overline{5},3,8)$	-2.97×10^{-4}	$(5,\overline{3},\overline{8})$	-2.97×10^{-4}
$(6,\overline{4},\overline{8})$	-2.97×10^{-4}	$(\overline{6},4,8)$	-2.97×10^{-4}				
Condition VII							
(i,j,k)	violation	(i,j,k)	violation	(i,j,k)	violation	(i,j,k)	violation
$(1,5,\overline{6})$	-1.80×10^{-3}	$(1,\overline{5},6)$	-1.80×10^{-3}	$(\overline{1},5,\overline{6})$	-1.80×10^{-3}	$(\overline{1},\overline{5},6)$	-1.80×10^{-3}
$(1,\overline{5},\overline{6})$	-1.15×10^{-3}	$(\overline{1},5,6)$	-1.15×10^{-3}	$(1,\overline{5},\overline{7})$	-1.15×10^{-3}	$(\overline{1},5,7)$	-1.15×10^{-3}
$(1,\overline{6},\overline{7})$	-1.15×10^{-3}	$(\overline{1},6,7)$	-1.15×10^{-3}	$(3,\overline{4},8)$	-7.38×10^{-4}	$(3,\overline{4},\overline{8})$	-7.38×10^{-4}
$(\overline{3},4,8)$	-7.38×10^{-4}	$(\overline{3},4,\overline{8})$	-7.38×10^{-4}	$(2,4,5)$	-5.50×10^{-4}	$(\overline{2},\overline{4},\overline{5})$	-5.50×10^{-4}
$(2,3,6)$	-5.50×10^{-4}	$(\overline{2},\overline{3},\overline{6})$	-5.50×10^{-4}	$(2,4,\overline{8})$	-1.27×10^{-4}	$(\overline{2},\overline{4},8)$	-1.27×10^{-4}
$(2,3,\overline{8})$	-1.27×10^{-4}	$(\overline{2},\overline{3},8)$	-1.27×10^{-4}	$(3,4,\overline{8})$	-1.27×10^{-4}	$(\overline{3},\overline{4},8)$	-1.27×10^{-4}

In tables III$\sim$ VI, we listed the violations with the indices and values, whose absolute value is larger than 1×10^{-5} for C_2, CH_4 and H_2O at the equilibrium geometry. As seen in table III, large violations occurred for both conditions VI and VII for C_2: the largest values were in the order of 1×10^{-2}. The violations mainly occurred for the valence orbitals, which are $p\sigma$, $p\pi$ and $p\pi^*$ orbitals, except for some violations with respect to the 1s orbital for condition VI. The violation of conditions VI and VII was also found for the $^1A_1$ state of CH_2. In this case, the violation occurred for the variable for the valence orbitals and not for the 1s core orbitals. In the case of CH_4, the order of the violations was smaller and the absolute errors were within 2.1×10^{-3} as shown in table V. In this case, the violations were also found for the 1s orbital of C. For H_2O with artificially correlation enhanced Hamiltonian of $\lambda = 1.5$, the violations occur only for the condition VI. The errors are calculated to be very small: the order is 1×10^{-4}. As shown in these examples, the absolute values of the violations are related to the accuracy of the DMVT(PQG), which indicates that these conditions may be effective as the necessary conditions for the DMVT method.

We performed, therefore, the DMVT(PQG+WW) calculations including these two WW conditions. The results were presented in table VII. The largest improvement was obtained for C_2 as expected, but it was not so drastic as 7.2×10^{-4} au in total energy. The deviation from the full-CI value is still large. For other systems, $CH_2(^1A_1)$, CH_4 and H_2O, the effect of these conditions was not so prominent and the improved energies were 1.7×10^{-4}, 9.0×10^{-5} and 1.0×10^{-5} au, respectively. These N-representability conditions actually improved the results, however, did not effectively work at least in the combination with the DMVT(PQG) calculation.

TABLE VI: Violation of condition VI for H_2O with various λ

$\lambda = 0.50$			
(i,j,k)	violation	(i,j,k)	violation
$(5,\overline{4},\overline{5})$	-1.05×10^{-5}	$(\overline{5},4,5)$	-9.78×10^{-6}
$(5,\overline{5},7)$	-6.82×10^{-6}	$(\overline{5},5,\overline{7})$	-6.43×10^{-6}
$(5,2,\overline{5})$	-4.94×10^{-6}	$(\overline{5},\overline{2},5)$	-4.79×10^{-6}
$(5,\overline{5},\overline{6})$	-4.47×10^{-6}	$(\overline{5},5,6)$	-4.12×10^{-6}
$\lambda = 1.00$			
(i,j,k)	violation	(i,j,k)	violation
$(5,\overline{4},\overline{5})$	-7.52×10^{-5}	$(\overline{5},4,5)$	-7.46×10^{-5}
$(\overline{5},\overline{2},5)$	-4.25×10^{-5}	$(5,2,\overline{5})$	-4.15×10^{-5}
$(5,\overline{5},6)$	-3.40×10^{-6}	$(\overline{5},5,\overline{6})$	-2.53×10^{-6}
$\lambda = 1.50$			
(i,j,k)	violation	(i,j,k)	violation
$(\overline{5},\overline{2},5)$	-3.69×10^{-4}	$(5,2,\overline{5})$	-3.68×10^{-4}
$(\overline{5},3,5)$	-3.00×10^{-4}	$(5,\overline{3},\overline{5})$	-2.99×10^{-4}
$(\overline{5},4,5)$	-1.83×10^{-4}	$(5,\overline{4},\overline{5})$	-1.81×10^{-4}
$(5,\overline{5},6)$	-5.63×10^{-5}	$(\overline{5},5,\overline{6})$	-5.44×10^{-5}

TABLE VII: Total energy by DMVT(PQG), DMVT(PQG+WW), and FullCI.

	DMVT(PQG)	DMVT(PQG+WW)	ΔE^a	FullCI
CH_4, STO-6G, 1s core	-40.20999	-40.20990	9.0×10^{-5}	-40.19049
C_2, STO-6G, 1s core	-75.47932	-75.47860	7.2×10^{-4}	-75.43398
$H_2O(\lambda = 1.50)$, STO-6G	-95.00638	-95.00637	1.0×10^{-5}	-94.99780
$CH_2(^1A_1)$, STO-6G	-38.82261	-38.82278	1.7×10^{-4}	-38.81099

[a] Improvement by including Weinhold-Wilson conditions.

5.4 Conclusion

We examined the Weinhold-Wilson inequalities for the 2-RDM determined by the DMVT(PQG) method. The violations of the conditions VI and VII were found for some electronic states of several molecules, though they were not so large; the largest error was in the order of 1×10^{-2}. We therefore developed the formalism of the DMVT including these inequalities for the SDPA, which is denoted as DMVT(PQG+WW). These conditions certainly improved the results, however, they were not so drastic; the largest improvement was in the order of mhartree. These conditions were not so effective at least for the DMVT method including P, Q and G conditions.

5.5 Acknowledgment

This research was supported by a Grant-in-Aid for Scientific Research from the Ministry of Education, Science, Culture and Sports.

BIBLIOGRAPHY

[1] 1. P.-O. Löwdin, Phys. Rev. **97**, 1474 (1955); **97**, 1490 (1955); **97**, 1512 (1955).

[2] 2. P.-O. Löwdin, Adv. Quantum Chem. **2**, 213 (1965); **3**, 323 (1967); **5**, 185 (1970); **12**, 263 (1980); **17**, 285 (1985); **19**, 87 (1988).

[3] 3. H. Nakatsuji, Phys. Rev. A **14**, 41(1976).

[4] 4. C. Valdemoro, Phys. Rev. A **45**, 4462 (1992); F. Colmenero C. Pérez del Valle, and C. Valdemoro, Phys. Rev. A **47**, 971 (1993), F. Colmenero and C. Valdemoro Phys. Rev. A **47**, 979 (1993).

[5] 5. H. Nakatsuji and K. Yasuda, Phys. Rev. Lett. **76**, 1039(1996), K. Yasuda and H. Nakatsuji, Phys. Rev. A **56**, 2648(1997).

[6] 6. D. A. Mazziotti, Phys, Rev. A **57**, 4219(1998); Chem. Phys. Lett. **289**, 419(1998).

[7] 7. H. Nakatsuji, in *Many-Electron Densities and Reduced Density Matrices*, ed by J. Cioslowski, Kluwer Academic, New York, 2000.

[8] 8. A. J. Coleman, Rev. Mod. Phys. **35**, 668 (1963).

[9] 9. C. Garrod, and J. K. Percus, J. Math. Phys., **5**, 1756 (1964).

[10] 10. C. Garrod, M. V. Mihailović, and M. Rosina, J. Math. Phys. **16**, 868 (1975), C. Garrod and M. A. Fusco, Int. J. Quantum Chem. **x**, 495 (1976).

[11] 11. R. M. Erdahl, Rep. Math. Phys., **15** 147 (1979).

[12] 12. R. M. Erdahl and B. Jin, J. Mol. Struct.: THEOCHEM, **527**, 207 (2000); R. M. Erdahl and B. Jin, in *Many-Electron Densities and Reduced Density Matrices*, ed by J. Cioslowski, Kluwer Academic, New York, 2000.

[13] 13. D. A. Mazziotti and R. M. Erdahl, Phys. Rev A, **63**, 042113 (2001).

[14] 14. M. Nakata, H. Nakatsuji, M. Ehara, M. Fukuda, K. Nakata, K. Fujisawa, J. Chem. Phys., **114**, 8282 (2001).

[15] 15. M. Nakata, M. Ehara, and H. Nakatsuji, J. Chem. Phys., **116**, 5432, (2002).

[16] 16. K. Fujisawa, M. Kojima, K. Nakata, SDPA (SemiDefinite Programming Algorithm) User's Manual Version 5.00, August 1999.
URL is `http://is-mj.archi.kyoto-u.ac.jp/~fujisawa/software.html`.

[17] 17. H. Nakatsuji, J. Chem. Phys., **113**, 2949 (2000); H. Nakatsuji and E. R. Davidson,*ibid*, **115**, 2000 (2001); H. Nakatsuji, *ibid*, **115**, 2465 (2001); *ibid*, **116**, 1811 (2002); H. Nakatsuji, Phys. Rev. A, in press; H. Nakatsuji and M. Ehara, J. Chem. Phys., submitted.

[18] 18. F. Weinhold and E. B. Wilson Jr, J. Chem. Phys., **47**, 2298 (1967).

[19] 19. E. R. Davidson, J. Math. Phys., **10**, 725 (1969).

[20] 20. W. B. McRae and E. R. Davidson, J. Math. Phys., **13**, 1527 (1972).

Part III.

Accurate theoretical spectroscopy on ionization spectra

Chapter 6.

Outer-valence ionization spectra of azines: pyrazine, pyridazine, pyrimidine, and *s*-triazine studied by the SAC-CI SD-R method

Abstract

The valence ionization spectra of pyrazine, pyridazine, pyrimidine, and *s*-triazine have been studied by the SAC-CI (symmetry-adapted-cluster configuration-interaction) method. Experimental photoelectron spectra of these molecules were accurately reproduced and the detailed characterization of both the main peaks and satellites was performed. The ordering of the main peaks, some of which were contradictory proposed in the previous works, was examined by the SAC-CI method. Low-lying satellite peaks in the energy region of 18 $\sim$ 20 eV were analyzed in detail. In this region, some satellites with considerable intensity were calculated for pyrazine and pyridazine, while no remarkable satellite peaks were obtained for pyrimidine and *s*-triazine in agreement with the recent experimental work by the Penning ionization electron spectrum (PIES) and He I ultraviolet photoelectron spectrum (UPS). In the higher-energy region above 20 eV, the remarkable breakdown of the Koopmans' picture was seen for all the azines and numerous shake-up states were obtained as the continuous band. And systematic explanation for a correlation peak at 24$\sim$30eV for position and the number of nitrogen atom. We also analyzed the breakdown of Koopmans' theorem, why ionized from n orbitals gets much more correlation energy than ionized from π orbitals.

6.1 Introduction

Recently, valence ionization spectrum of molecules has been extensively studied in both the experimental and theoretical works and the detailed assignment has become possible not only for the main peaks but satellite peaks. The accurate characterization of the spectrum has been achieved by the cooperative interplay of these works; since the correlation peaks are described by the more-than-two electron processes, theoretical information is indispensable for the detailed assignments of these peaks.

Azabenzenes are important parent molecules for the biological compounds such as nicotinic acid and the nucleotides cytosine, uracil, and thymine, and therefore have been the subject of extensive experimental and theoretical studies[1-28] Azabenzenes are also of interest since they are isoelectronic compounds of benzene. The nitrogen atoms introduce perturbations to the benzene energy levels and give rise to characteristic valence electronic structure due to their lone pair electrons. In particular, their lower excitation $n \rightarrow \pi^*$ and $\pi \rightarrow \pi^*$ may contribute the satellites in the ionization spectra. In this sense, their valence electronic structure has been extensively investigated, however, there are still contradictory assignments even for the main peaks. In the early studies, the valence ionization spectra of pyrazine, pyridazine, pyrimidine, and *s*-triazine were measured by He II photoelectron spectra[13-16]up to $\sim$ 25eV. Recently, the Penning ionization electron spectroscopy (PIES) and the He I ultraviolet photoelectron spectroscopy (UPS)[17] were applied to these spectra and the assignment of the main peaks were proposed by the collision energy dependence of the partial ionization cross sections (CEDPICS) with the help of *ab initio* interaction potential and trajectory calculations. In that study, some satellite peaks were identified in the energy region of 18 $\sim$ 20 eV, though the energy region was limited up to $\sim$20 eV.

Theoretically, the valence ionized states of these molecules have been investigated by the Green's function method of the 2ph-TDA [1], and the 2h-1p CI[3] calculations for *s*-triazine and pyrazine. In those studies, satellite peaks were also calculated, however, the shape of the theoretical spectra was different from the ex-

periment in some points, and therefore the detailed assignment of them was still not definitive. Outer-valence Green's function (OVGF) method[2] and the P3 method [9] were also applied to the outer-valence region to determine the order of the main peaks. However, there are still different assignment between theoretical and experimental works even for the main peaks.

In the series of the studies, we have investigated the valence ionization spectra of various molecules using the SAC-CI (symmetry-adapted-cluster configuration- interaction) method. The SAC/SAC-CI method[29-31] has been successfully applied to a number of molecular spectroscopies[32-37] including the ionization spectrum. In this study, we apply the SAC-CI method to the valence ionization spectra of three diazines; pyrazine, pyridazine, pyrimidine, and *s*-triazine to give the accurate assignments not only for the main peaks but for the satellites, and systematic explanation of satellite peak at 24∼30eV by position and number of nitrogen atoms. We also analyzed ionized from n orbital tend to include more correlation energy than neutral molecule as usually observed by breakdown of the Koopmans' theorem: inversion of ionization order from n and π orbital.

6.2 Computational details

The ionization process studied in this work is vertical in nature. The geometries of the molecules were due to the experimental ones from literature for *s*-triazine [38], pyrazine [39], pyrimidine [40] and pyridazine[41]. The molecular structure of *s*-triazine belongs to D_{3h}, those of pyrazine and pyridazine to C_{2v} and that of pyrazine to D_{2h}. The DZ1P basis set was adopted for all the molecules; [4s2p1d/2s1p] of Huzinaga-Dunning [42]. The resultant SCF dimensions were 110 for diazine and 105 for *s*-triazine.

The valence ionization spectra of these molecules were calculated by the SAC-CI method in the outer-valence region to interpret the spectra measured by the He I UPS, He II UPS, and PIES. In the SAC-CI calculation, single and double R-operators were adopted, namely SAC-CI SD-R method was used. The 1s orbitals of C, N and O were kept as frozen core and all the other MOs were included in

the active space; the active space of the SAC-CI consisted of 15 occupied and 89 unoccupied MOs for diazine and 15 occupied and 85 unoccupied MOs for *s*-triazine. The SAC-CI calculations were performed in the linear point group; C_{2v} was adopted for *s*-triazine.

To reduce the computational effort, perturbation selection [34] was performed in the state-selection scheme and the thresholds of the normal accuracy were adopted. In the SAC ground-state calculation, the energy threshold for selecting doubles was $\lambda_e = 1 \times 10^{-6}$. For unlinked terms, we include only the products of the double-excitation operators when the SDCI coefficients were larger than 0.005. In the SAC-CI calculations for the ionized states, Koopmans states were adopted as the reference states and the energy threshold for R-operators was of $\lambda_e = 1 \times 10^{-7}$. The thresholds of the CI coefficients for calculating the unlinked operators in the SAC-CI method are 0.05 and 1×10^{-3} for the R and S operators, respectively.

Ionization cross-sections were calculated using the monopole approximation [44, 45] to estimate the relative intensities of the peaks. Both initial- and final-state correlation effects are included.

The SAC/SAC-CI calculations were executed using the SAC96 program system [46], which has been incorporated into the development version of the Gaussian suite of programs [47].

6.3 Results and discussions

The SCF energies of these molecules were calculated to be −262.7279, −262.6943, −262.7374 and −278.7416 au for pyrazine, pyridazine, pyrimidine, and *s*-triazine, respectively, with the present basis set of DZ1P. The Hartree-Fock orbital sequences of the valence MOs were summarized for these diazines and *s*-triazine in Table I.

TABLE I: Ground-state valence electronic configurations

System	Hartree-Fock valence configuration
pyrazine	$(3a_g)^2(3b_{1u})^2(2b_{2u})^2(4a_g)^2(2b_{3g})^2(5a_g)^2(3b_{2u})^2(4b_{1u})^2(4b_{2u})^2(1b_{3u})^2(3b_{3g})^2(5b_{1u})^2(1b_{2g})^2(6a_g)^2(1b_{1g})^2$
pyridazine	$(4a_1)^2(4b_2)^2(5a_1)^2(5b_2)^2(6a_1)^2(7a_1)^2(8a_1)^2(6b_2)^2(7b_2)^2(9a_1)^2(1b_1)^2(10a_1)^2(8b_2)^2(2b_1)^2(1a_2)^2$
pyrimidine	$(5a_1)^2(3b_2)^2(6a_1)^2(4b_2)^2(7a_1)^2(8a_1)^2(5b_2)^2(9a_1)^2(6b_2)^2(10a_1)^2(1b_1)^2(11a_1)^2(1a_2)^2(7b_2)^2(2b_1)^2$
s-triazine	$(3a_1')^2(3e')^4(4e')^4(4a_1')^2(1a_2')^2(5e')^4(1a_2'')^2(5a_1')^2(6e')^4(1e'')^4$

Figure I: Structure and coordinate

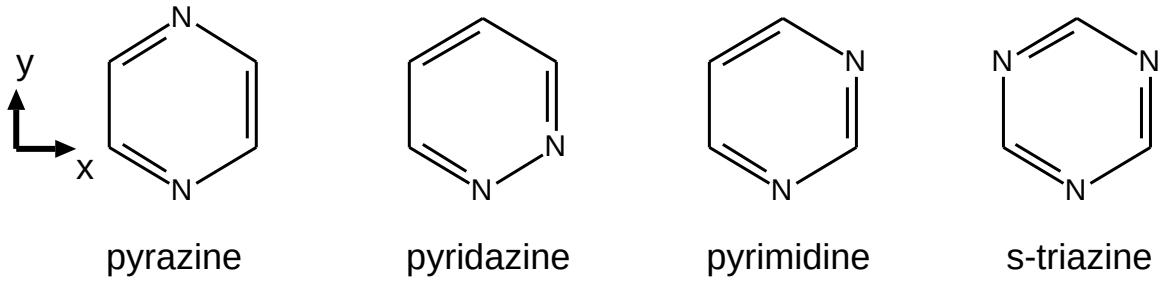

The valence ionization spectra of these molecules were intensively studied by the PIES and He I UPS by Kishimoto *et al.*[17] In that work, the observed peaks were assigned in terms of the behavior of the CEDPICS measured by the PIES , the ab initio potential energy surfaces and the trajectory calculations. In Figs. II-V, we compared our theoretical ionization spectra of these molecules with the He I UPS spectra: the resolution of the peaks of the He I UPS seems to be better than the PIES and the intensity of the PIES is characteristic for the nature of the peaks and the interaction between the ionizing MOs and He* atom determines the intensity. The theoretical spectrum was convoluted with Gaussian envelope for describing the Frank-Condon width and the resolution of spectrometer; the fwhm() of Gaussian was taken to $0.05 \times \Delta E$ (in eV). In Figs. VI-XI, we show valence MO with its pictures and orbital energy for azabenzens.

Figure II: Outer-valence ionization spectra of pyrazine by (a) He I PES and (b) SAC-CI SD-R

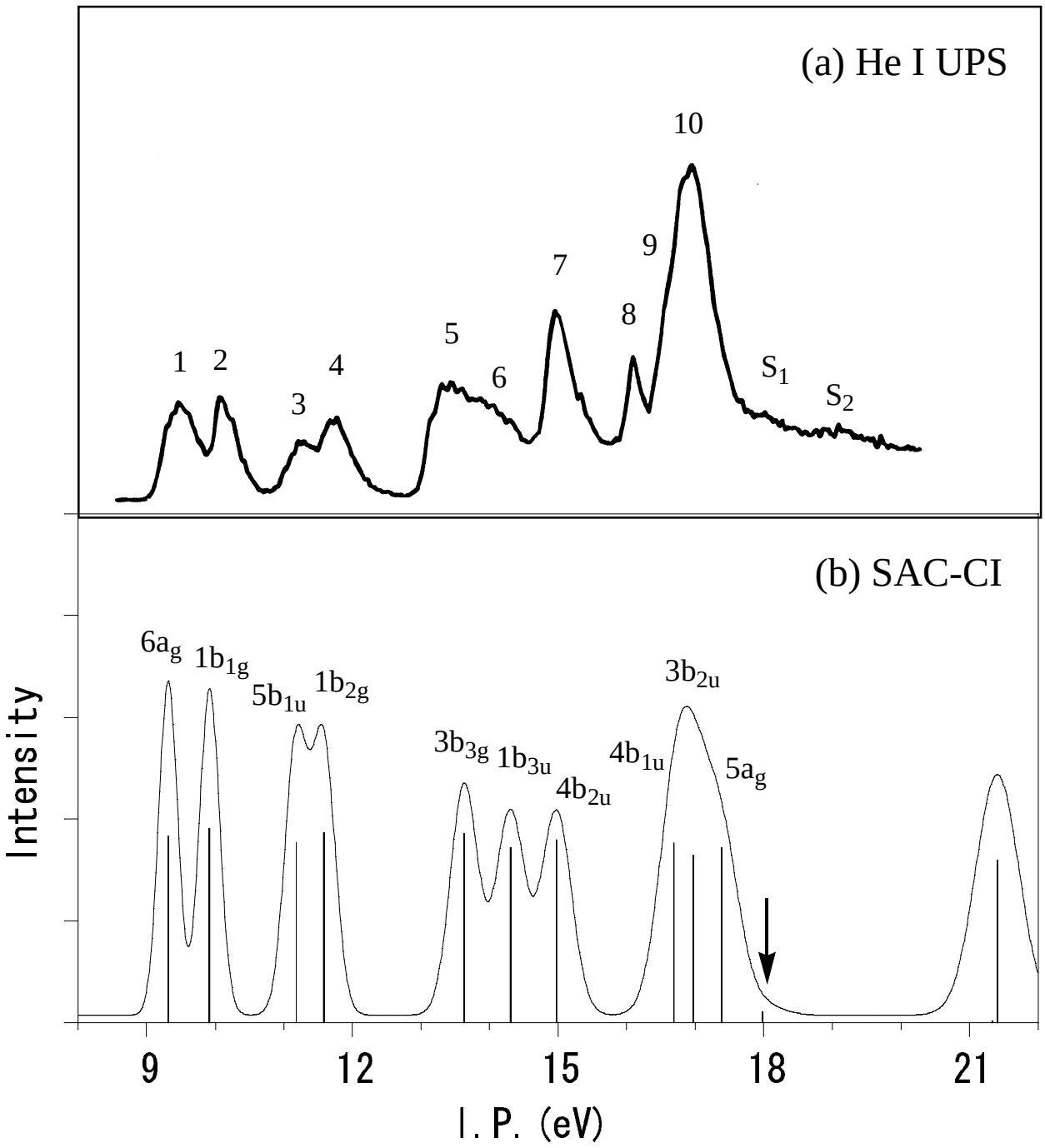

Figure III: Outer-valence ionization spectra of pyridazine by (a) He I PES and (b) SAC-CI SD-R

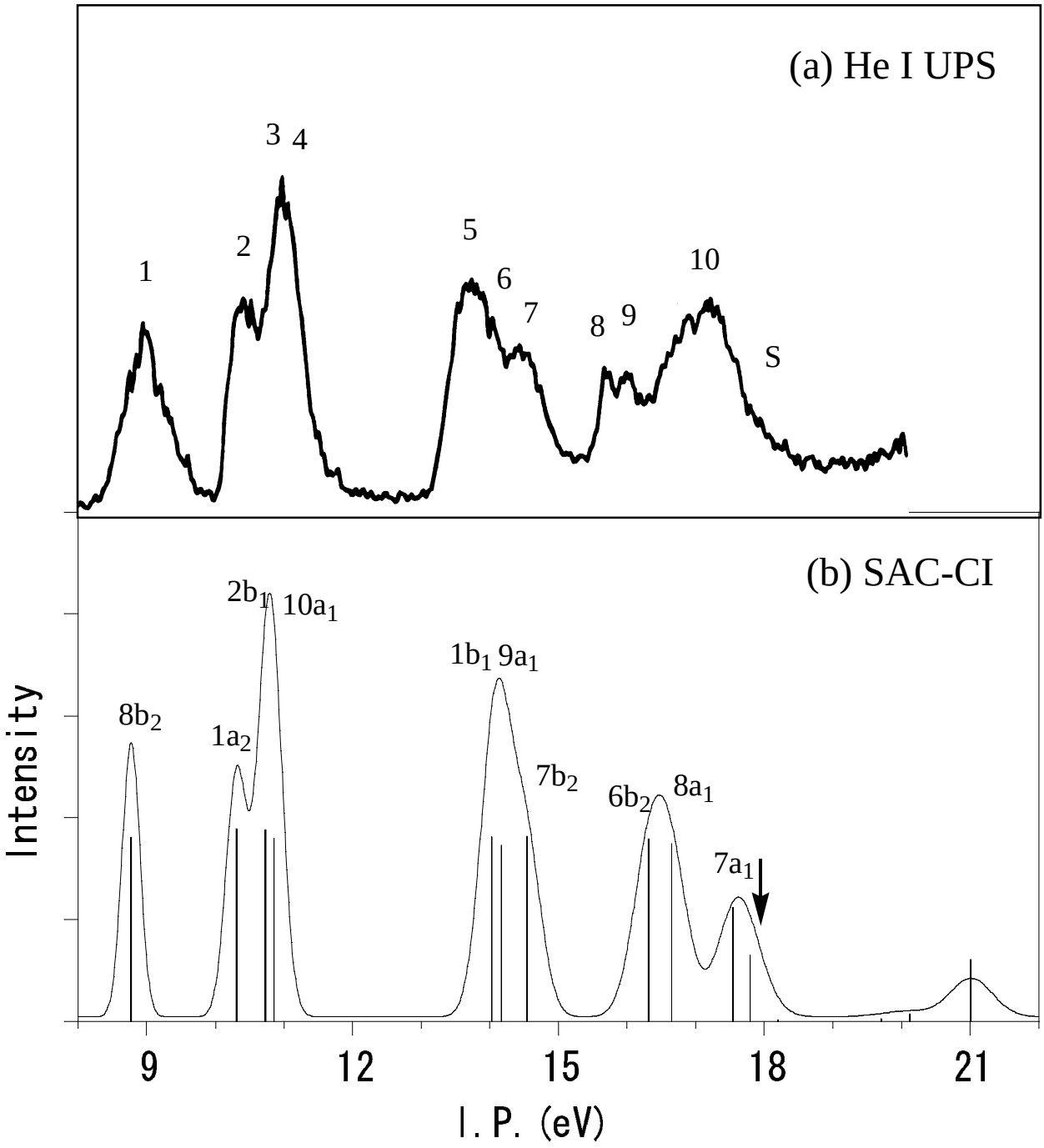

Figure IV: Outer-valence ionization spectra of pyrimidine by (a) He I PES and (b) SAC-CI SD-R

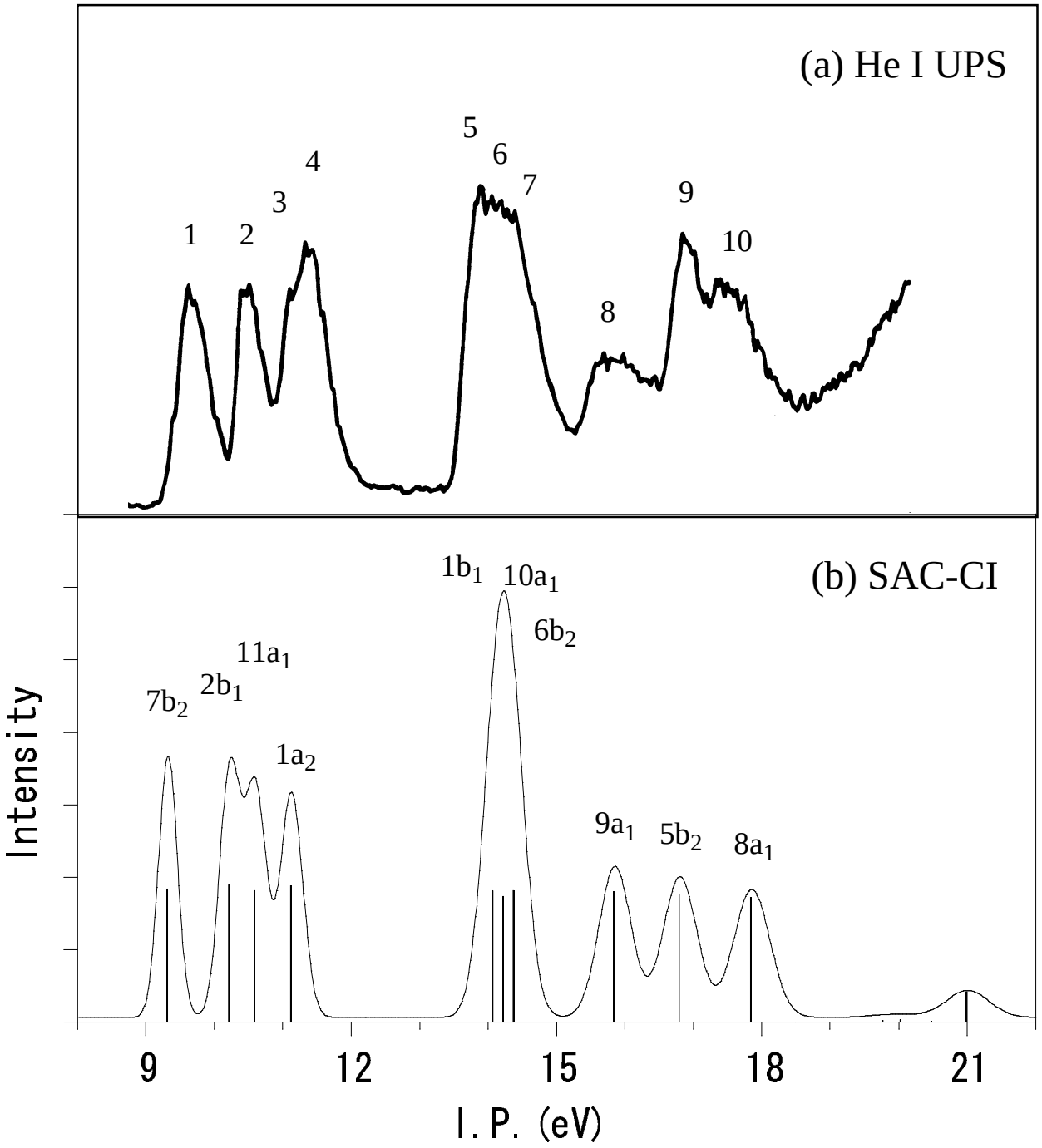

Figure V: Outer-valence ionization spectra of *s*-triazine by (a) He I PES and (b) SAC-CI SD-R

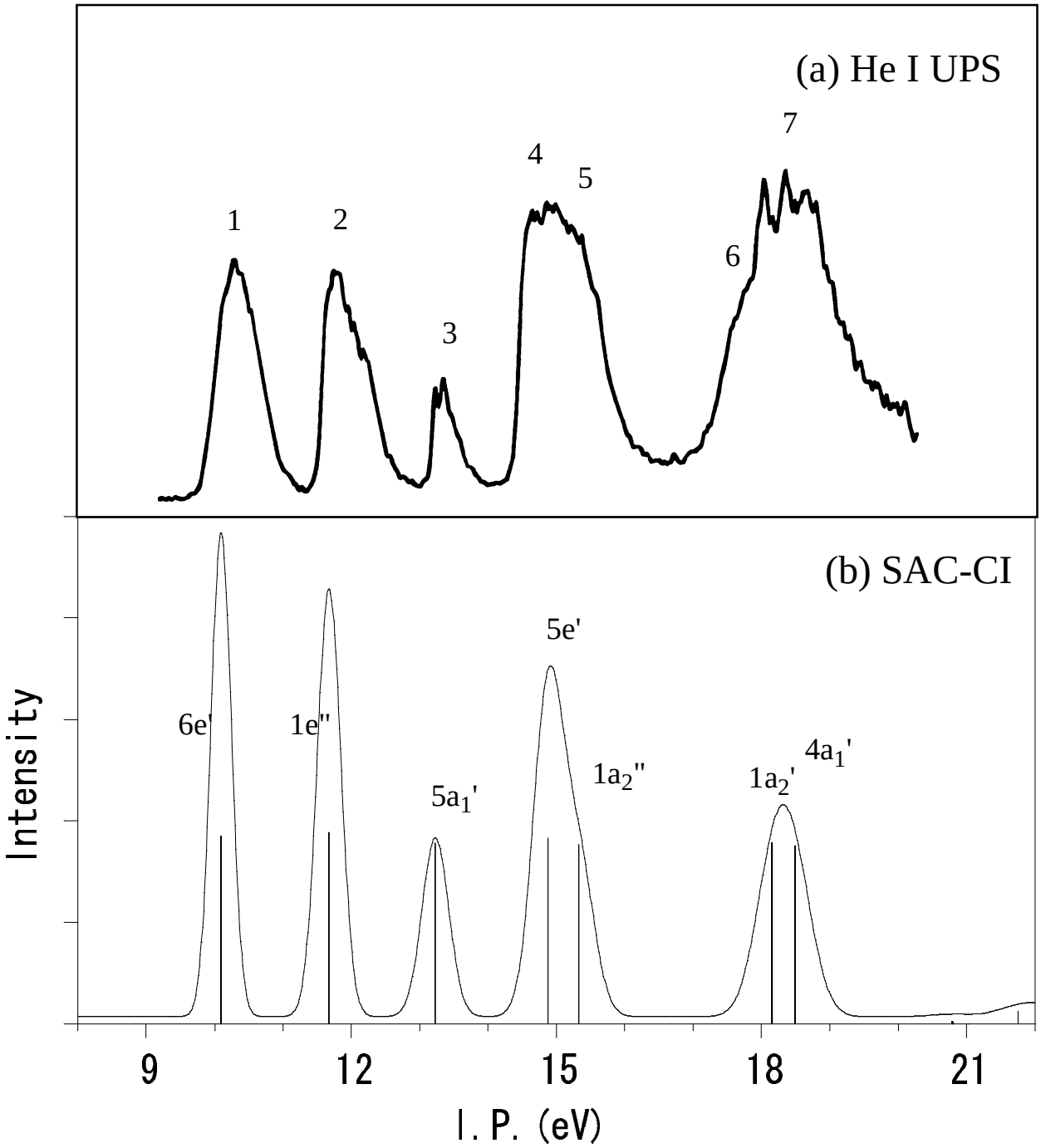

Figure VI: Valence MO plotting and its nature with orbital energy pyrazine

21st, $\pi(\mathrm{C}-\mathrm{C})$, $1b_{1g}$, -9.825

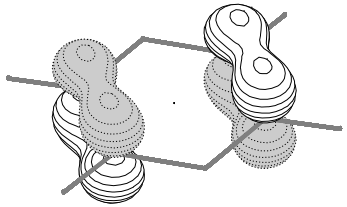

20th, $n(\mathrm{N})$, $6a_g$, -11.217

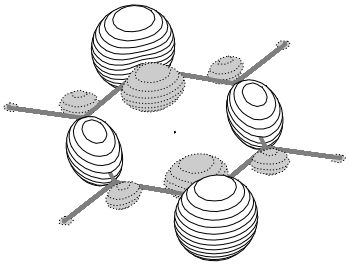

19th, $\pi(\mathrm{N}-\mathrm{N})$, $1b_{2g}$, -11.888

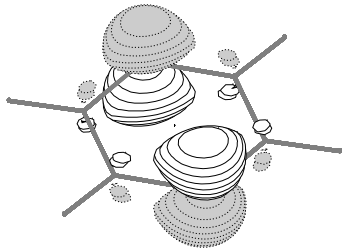

18th, $n(\mathrm{N})$ $5b_{1u}$, -13.656

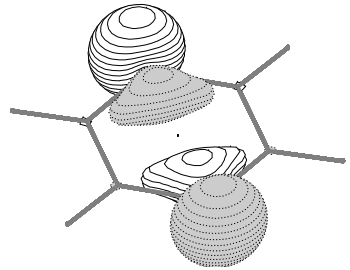

17th, $\sigma(\mathrm{C}-\mathrm{H})$, $3b_{3g}$, -15.104

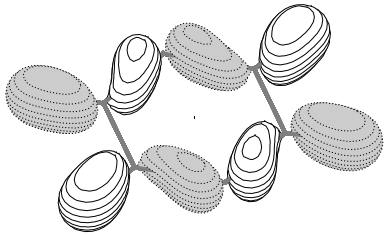

16th, $\pi(\mathrm{N}-\mathrm{N})$, $1b_{3u}$, -15.634

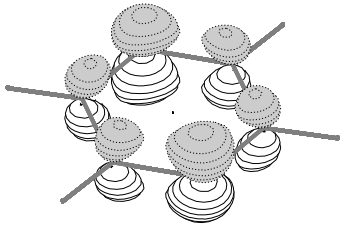

15th, $\sigma(\mathrm{C}-\mathrm{H})$, $4b_{2u}$, -16.675

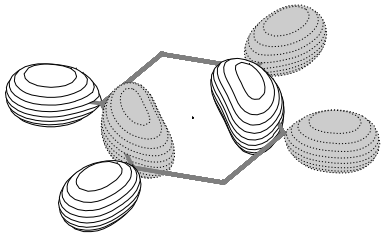

14th, $\sigma(\mathrm{C}-\mathrm{H})$, $4b_{1u}$, -18.508

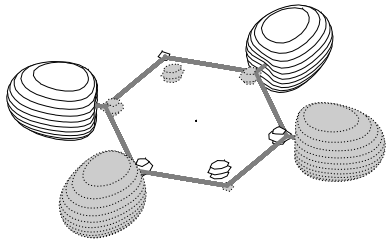

13th, $\sigma(\mathrm{C}-\mathrm{N})$, $3b_{2u}$, -19.201

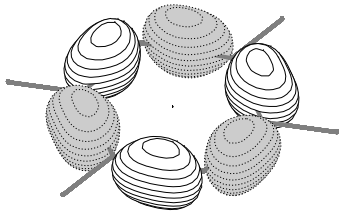

12th, $\sigma(\mathrm{C}-\mathrm{H})$, $5a_g$, -19.838

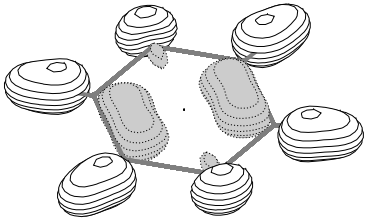

11th, $\sigma(\mathrm{C}-\mathrm{N})$, $2b_{3g}$, -24.232

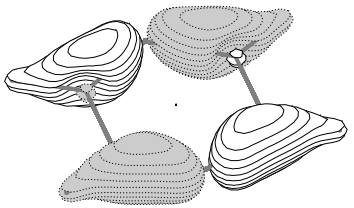

10th, $\sigma(\mathrm{C}-\mathrm{C})$, $4a_g$, -24.631

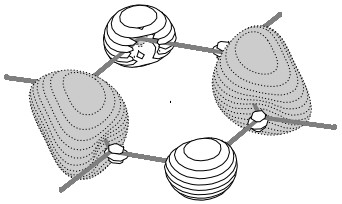

9th, $\sigma(\mathrm{C}-\mathrm{C})$, $2b_{2u}$, -28.759

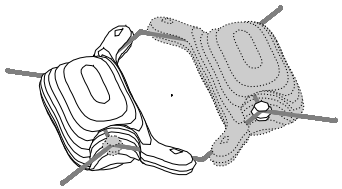

8th $\sigma(\mathrm{C}-\mathrm{N})$, $3b_{1u}$, -33.258

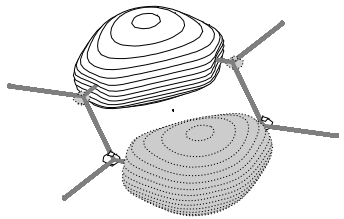

7th, $\sigma(\mathrm{C}-\mathrm{N})$, $3a_g$, -35.649

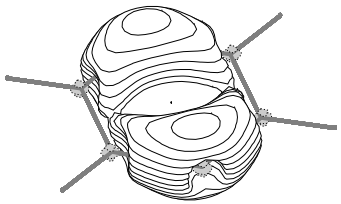

structure

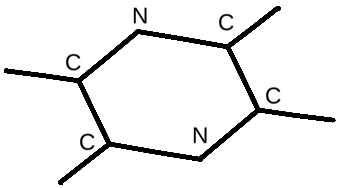

Figure VII: Valence MO plotting and its nature with orbital energy pyridazine

21st, $\pi(\mathrm{C}-\mathrm{N})$, $1a_2$, -10.459

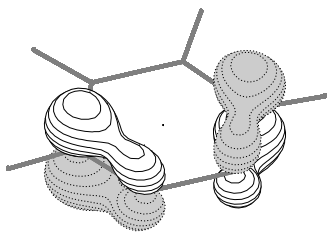

20th, $\pi(\mathrm{C}-\mathrm{C})$, $2b_1$, -11.003

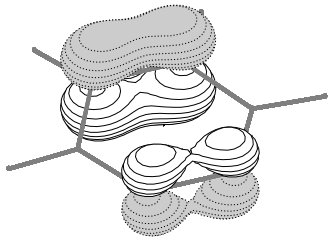

19th, $n(\mathrm{N})$, $8b_2$, -11.069

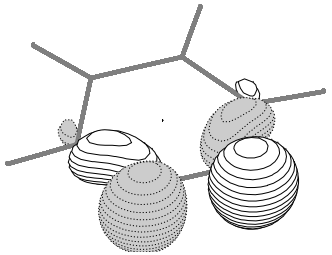

18th, $n(\mathrm{N})$, $10a_1$, -13.093

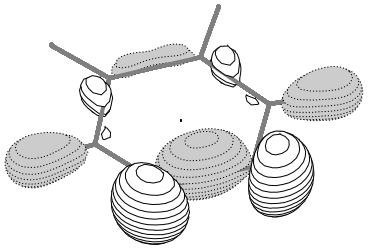

17th, $\pi(\mathrm{N}-\mathrm{N})$, $1b_1$, -15.637

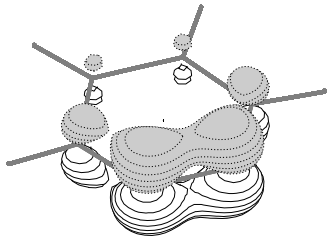

16th, $\sigma(\mathrm{C}-\mathrm{H})$, $9a_1$, -16.108

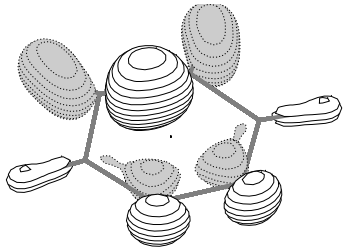

15th, $\sigma(\mathrm{C}-\mathrm{H})$, $7b_2$, -16.466

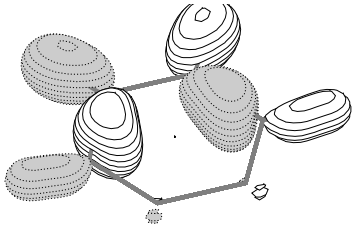

14th, $\sigma(\mathrm{C}-\mathrm{H})$, $6b_2$, -18.292

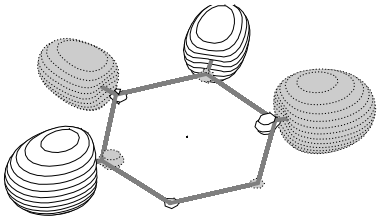

13th, $\sigma(\mathrm{C}-\mathrm{C})$, $8a_1$, -19.001

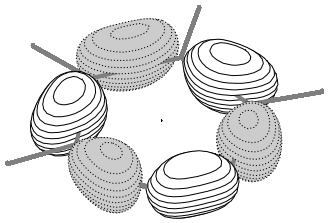

12th, $\sigma(\mathrm{C}-\mathrm{H})$, $7a_1$, -19.970

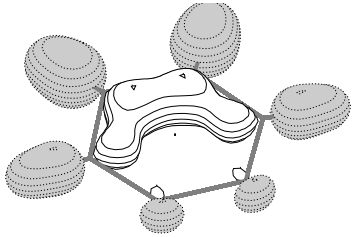

11th, $\sigma(\mathrm{C}-\mathrm{N})$, $6a_1$, -24.202

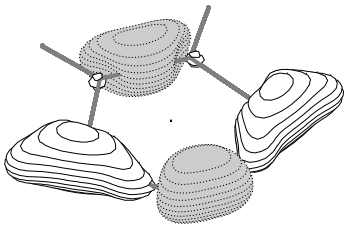

10th, $\sigma(\mathrm{C}-\mathrm{C})$, $5b_2$, -24.605

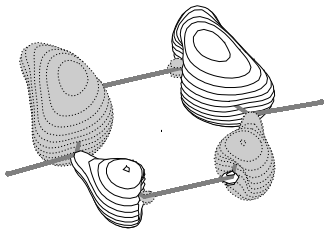

9th, $\sigma(\mathrm{C}-\mathrm{C})$, $5a_1$, -30.329

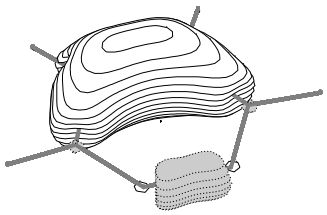

8th, $\sigma(\mathrm{C}-\mathrm{N})$, $4b_2$, -30.385

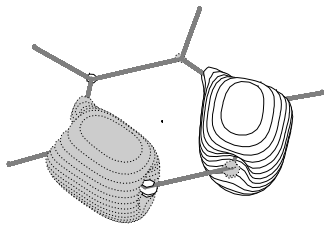

7th, $\sigma(\mathrm{N}-\mathrm{N})$, $4a_1$, -36.592

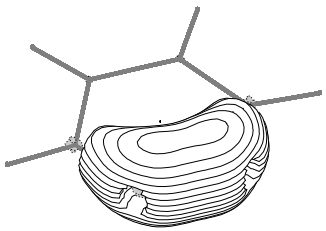

structure

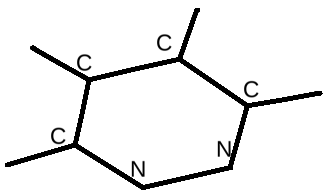

Figure VIII: Valence MO plotting and its nature with orbital energy pyrimidine

21nd, $\pi(\mathrm{C}-\mathrm{C})$, $2b_1$, -10.368

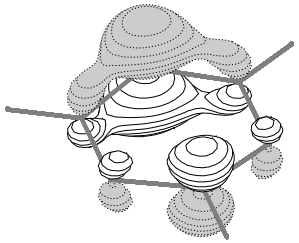

20th, $n(\mathrm{N})$, $7b_2$, -11.426

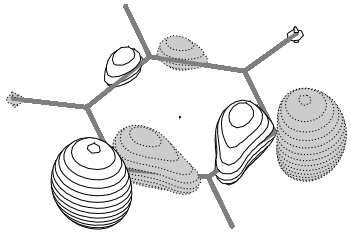

19th, $\pi(\mathrm{C}-\mathrm{N})$, $1a_2$, -11.434

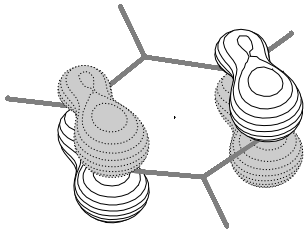

18th, $n(\mathrm{N})$, $11a_1$, -12.802

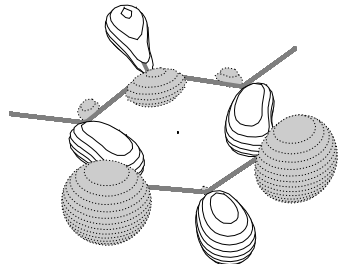

17th, $\pi(\mathrm{C}-\mathrm{N})$, $1b_1$, -15.667

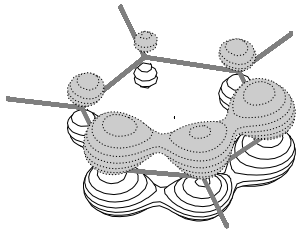

16th, $\sigma(\mathrm{C}-\mathrm{H})$, $10a_1$, -16.089

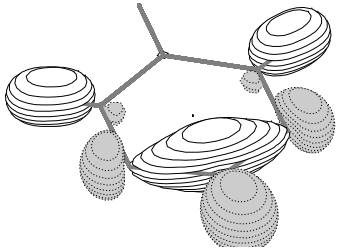

15th, $\sigma(\mathrm{C}-\mathrm{H})$, $6b_2$, -16.358

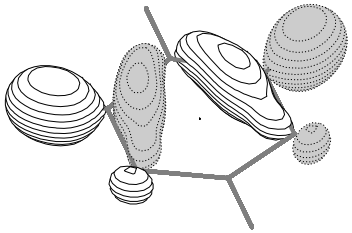

14th, $\sigma(\mathrm{C}-\mathrm{H})$, $9a_1$, -17.700

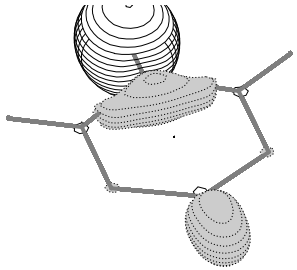

13th, $\sigma(\mathrm{C}-\mathrm{N})$, $5b_2$, -19.116

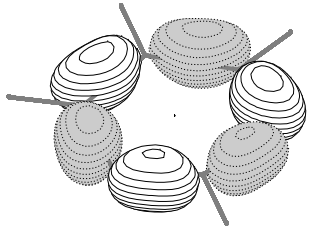

12th, $\sigma(\mathrm{C}-\mathrm{H})$, $8a_1$, -20.205

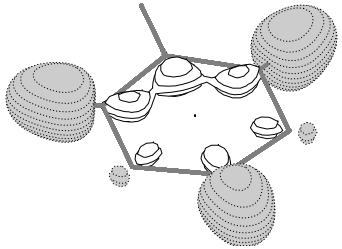

11th, $\sigma(\mathrm{C}-\mathrm{N})$, $7a_1$, -24.198

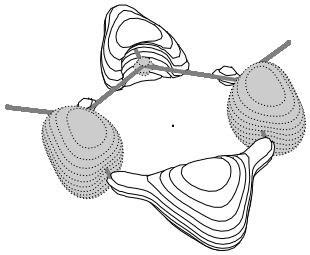

10th, $\sigma(\mathrm{C}-\mathrm{C})$, $4b_2$, -24.549

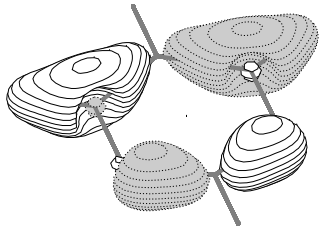

9th, $\sigma(\mathrm{C}-\mathrm{C})$, $6a_1$, -29.364

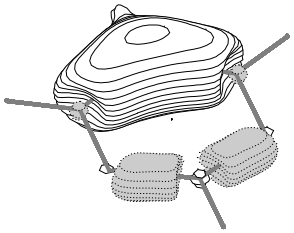

8th, $\sigma(\mathrm{C}-\mathrm{N})$, $3b_2$, -32.546

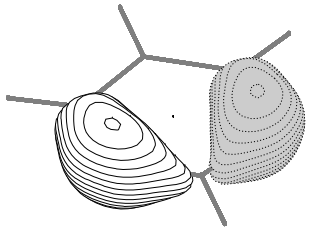

7th, $\sigma(\mathrm{C}-\mathrm{N})$, $5a_1$, -35.771

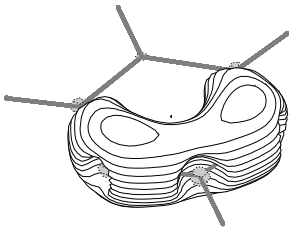

structure

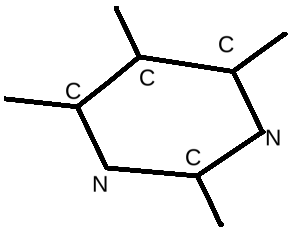

Figure IX: Valence MO plotting and its nature with orbital energy s-triazine

21st, $\pi(\mathrm{C}-\mathrm{N})$, $1e''$, -12.023

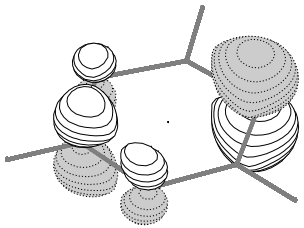

20th, $\pi(\mathrm{C}-\mathrm{N})$, $1e''$, -12.023

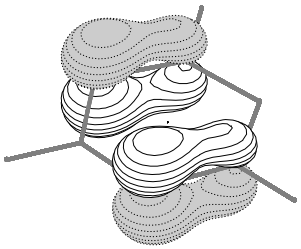

19th, $n(\mathrm{N})$, $6e'$, -12.067

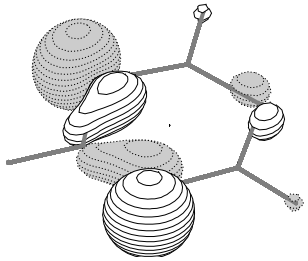

18th, $n(\mathrm{N})$, $6e'$, -12.067

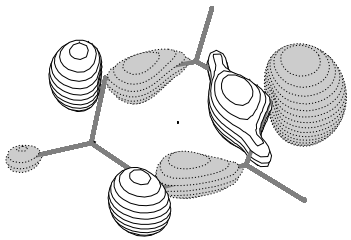

17th, $n(\mathrm{N})$, $5a_1'$, -15.713

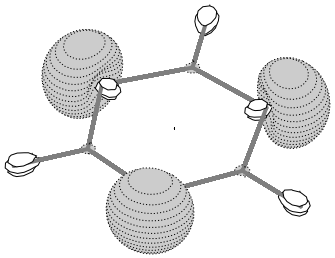

16th, $\pi(\mathrm{C}-\mathrm{N})$, $1a_2''$,-16.663

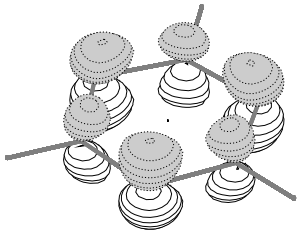

15th, $\sigma(\mathrm{C}-\mathrm{H})$, $5e'$, -16.681

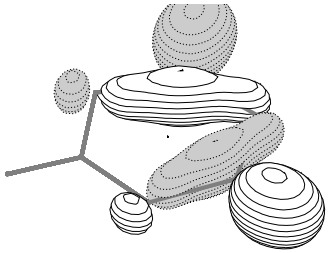

14th, $\sigma(\mathrm{C}-\mathrm{H})$, $5e'$, -16.681

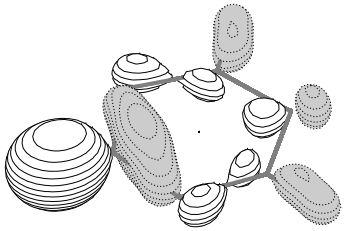

13th,$\sigma(\mathrm{C}-\mathrm{N})$, $1a_2'$, -20.357

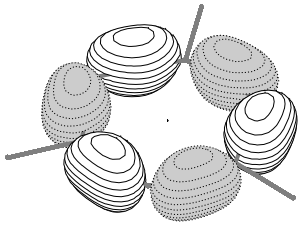

12th, $\sigma(\mathrm{C}-\mathrm{H})$, $4a_1'$, -20.617

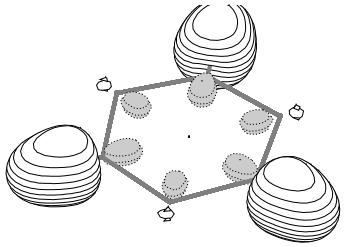

11th, $\sigma(\mathrm{C}-\mathrm{N})$, $4e'$, -25.364

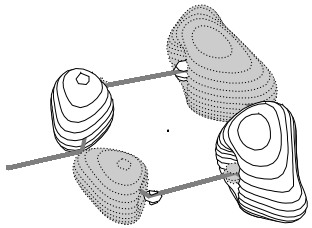

10th, $\sigma(\mathrm{C}-\mathrm{N})$, $4e'$, -25.364

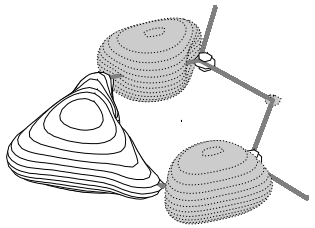

9th, $\sigma(\mathrm{C}-\mathrm{N})$, $3e'$, -33.191

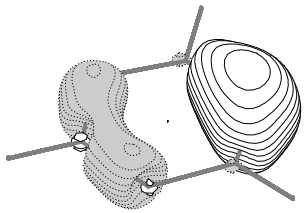

8th, $\sigma(\mathrm{C}-\mathrm{N})$, $3e'$, -33.191

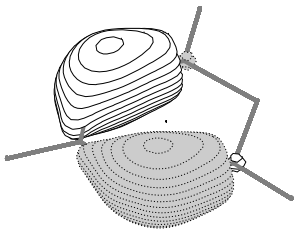

7th, $\sigma(\mathrm{C}-\mathrm{N})$, $3a_1'$, -37.208

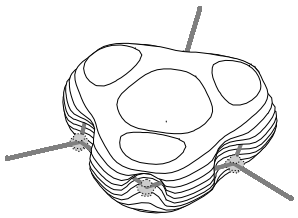

structure

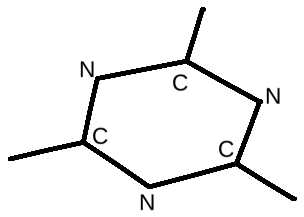

Figure X: Valence MO plotting and its nature with orbital energy benzene

21st, $\pi(\mathrm{C}-\mathrm{C})$, $1e_{1g}$, -9.113

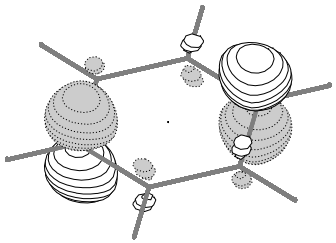

20th, $\pi(\mathrm{C}-\mathrm{C})$, $1e_{1g}$, -12.023

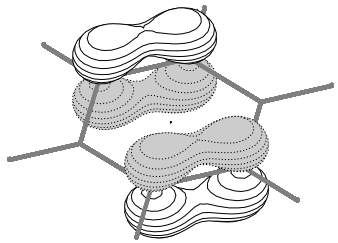

19th, $\sigma(\mathrm{C}-\mathrm{H})$, $3e_{2g}$, -13.425

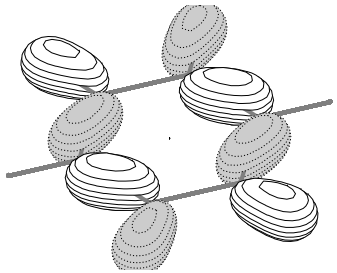

18th, $\sigma(\mathrm{C}-\mathrm{H})$, $3e_{2g}$, -13.425

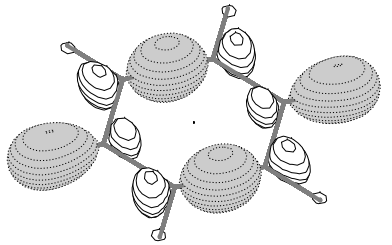

17th, $\pi(\mathrm{C}-\mathrm{C})$, $1a_{2u}$, -13.580

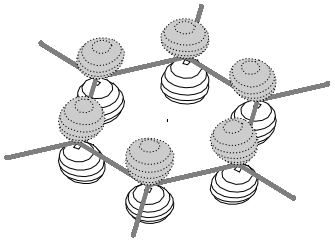

16th, $\sigma(\mathrm{C}-\mathrm{H})$, $3e_{1u}$, -15.952

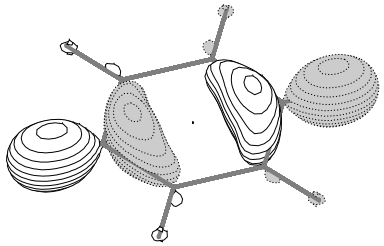

15th, $\sigma(\mathrm{C}-\mathrm{H})$, $3e_{1u}$, -15.952

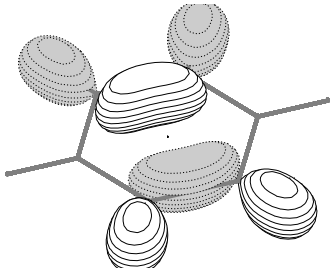

14th, $\sigma(\mathrm{C}-\mathrm{C})$, $1b_{2u}$, -16.784

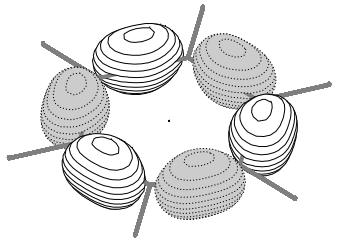

13th,$\sigma(\mathrm{C}-\mathrm{H})$, $2b_{1u}$, -17.463

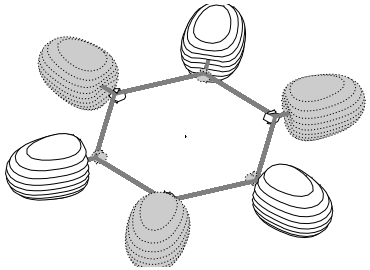

12th, $\sigma(\mathrm{C}-\mathrm{H})$, $3a_{1g}$, -19.249

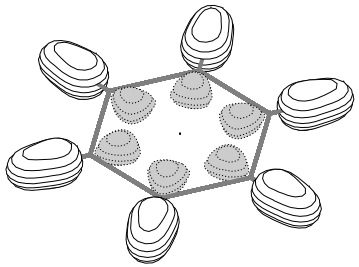

11th, $\sigma(\mathrm{C}-\mathrm{C})$, $2e_{2g}$, -22.379

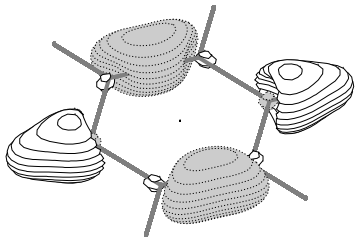

10th, $\sigma(\mathrm{C}-\mathrm{C})$, $2e_{2g}$, -22.379

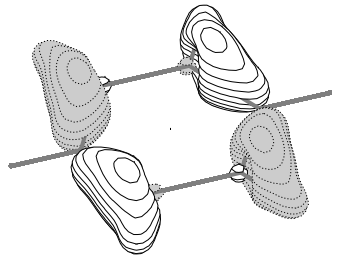

9th, $\sigma(\mathrm{C}-\mathrm{C})$, $2e_{1u}$, -27.591

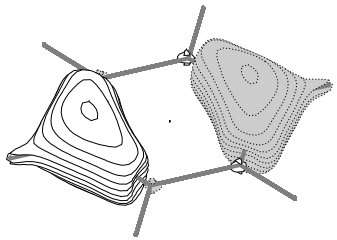

8th, $\sigma(\mathrm{C}-\mathrm{C})$, $2e_{1u}$, -27.591

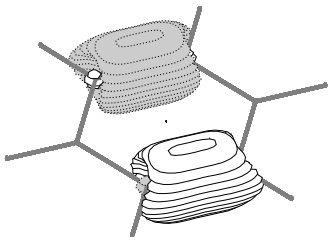

7th, $\sigma(\mathrm{C}-\mathrm{C})$, $2a_{1g}$, -31.268

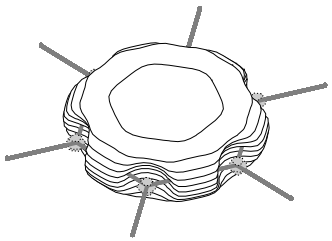

structure

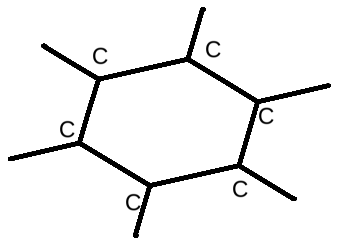

TABLE II: Calculated ionization potentials (IP, in eV), monopole intensities (M.I.), and main configurations with the basis set for pyrazine.

Sym.	Main Configuration($\|C\| > 0.3$)	M.I.	IP	Expt.[a,b]	Expt.[c]	P3[d,b]	CI[e]
A_g	$0.95(6a_g^{-1})$	0.7624	9.49	9.4	9.61	9.788	9.01
B_{1g}	$0.97(1b_{1g}^{-1})$	0.7906	10.06	10.2	10.20	10.290	10.08
B_{1u}	$0.94(5b_{1u}^{-1})$	0.7381	11.30	11.4	11.38	11.573	10.84
B_{2g}	$0.96(1b_{2g}^{-1})$	0.7710	11.64	11.7	11.80	12.013	11.65
B_{3g}	$0.96(3b_{3g}^{-1})$	0.7735	13.90	13.3	13.37	13.984	14.00
B_{3u}	$0.92(1b_{3u}^{-1})$	0.7168	14.43	14.0	13.93	14.441	13.87
B_{2u}	$0.95(4b_{2u}^{-1})$	0.7564	15.30	15.0	14.98	15.229	14.11
B_{1u}	$0.94(4b_{1u}^{-1})$	0.7413	17.02	16.2	16.10	16.791	16.32
B_{2u}	$0.91(3b_{2u}^{-1})+0.31(1b_{1g}^{-1}2b_{3u}6a_g^{-1})$	0.6950	17.25	~ 17	16.58	17.467	17.03
A_g	$0.92(5a_g^{-1})$	0.7179	17.67	~ 17	16.97	17.747	16.21
B_{2u}	$1.01(6a_g^{-1}2b_{3u}1b_{1g}^{-1})+0.71(1b_{1g}^{-1}2b_{3u}6a_g^{-1})$	0.0411	18.31	~ 18	~ 18.0		
B_{3g}	$0.91(5b_{1u}^{-1}2b_{3u}1b_{1g}^{-1})+0.81(1b_{1g}^{-1}2b_{3u}5b_{1u}^{-1})-0.41(6a_g^{-1}2b_{2g}1b_{1g}^{-1})$ $-0.38(1b_{1g}^{-1}2b_{2g}6a_g^{-1})$	0.0131	19.42				
B_{2u}	$0.68(1b_{1g}^{-1}2b_{3u}6a_g^{-1})-0.33(6a_g^{-1}2b_{3u}1b_{1g}^{-1})$	0.0212	19.82				
B_{3u}	$0.88(1b_{1g}^{-1}2b_{3u}1b_{1g}^{-1})+0.39(1b_{2g}^{-1}1a_u1b_{1g}^{-1})$	0.0226	20.29				
B_{3g}	$0.51(1b_{1g}^{-1}2b_{3u}5b_{1u}^{-1})-0.45(5b_{1u}^{-1}2b_{3u}1b_{1g}^{-1})$	0.0607	20.98				
A_g	$0.76(4a_g^{-1})+0.44(5b_{1u}^{-1}1a_u1b_{1g}^{-1})$	0.4956	21.62	20.6	~ 19.1		
B_{3g}	$0.86(2b_{3g}^{-1})$	0.6205	21.77	~ 21			
A_g	$0.70(5b_{1u}^{-1}1a_u1b_{1g}^{-1})-0.58(6a_g^{-1}2b_{3u}1b_{3u}^{-1})-0.44(1b_{3u}^{-1}2b_{3u}6a_g^{-1})$ $-0.42(4a_g^{-1})+0.30(1b_{1g}^{-1}1a_u5b_{1u}^{-1})$	0.1508	21.82				
A_g	$0.51(1b_{3u}^{-1}2b_{3u}6a_g^{-1})-0.51(1b_{2g}^{-1}2b_{3u}5b_{1u}^{-1})+0.35(1b_{1g}^{-1}1a_u5b_{1u}^{-1})$	0.0115	22.97				
B_{1u}	$0.58(1b_{1g}^{-1}1a_u6a_g^{-1})+0.47(1b_{2g}^{-1}2b_{3u}6a_g^{-1})-0.44(1b_{3u}^{-1}2b_{3u}5b_{1u}^{-1})$	0.0161	23.14				
B_{3u}	$0.68(1b_{2g}^{-1}1a_u1b_{1g}^{-1})+0.50(1b_{2g}^{-1}2b_{3u}1b_{2g}^{-1})$	0.0157	23.37				
A_g	$0.58(5b_{1u}^{-1}2b_{3u}1b_{2g}^{-1})-0.57(6a_g^{-1}2b_{2g}1b_{2g}^{-1})+0.48(6a_g^{-1}2b_{3u}1b_{3u}^{-1})$ $+0.34(4b_{2u}^{-1}2b_{3u}1b_{1g}^{-1})+0.30(5b_{1u}^{-1}1a_u1b_{1g}^{-1})$	0.0235	23.85				
B_{3u}	$0.85(1b_{1g}^{-1}1a_u1b_{2g}^{-1})+0.39(1b_{2g}^{-1}2b_{3u}1b_{2g}^{-1})-0.31(6a_g^{-1}1a_u3b_{3g}^{-1})$	0.0259	24.26				
B_{2u}	$0.77(1b_{2g}^{-1}1a_u6a_g^{-1})-0.32(1b_{3u}^{-1}1a_u5b_{1u}^{-1})+0.32(3b_{3g}^{-1}2b_{3u}1b_{2g}^{-1})$	0.0343	24.28				
B_{1u}	$0.78(1b_{1g}^{-1}2b_{3u}3b_{3g}^{-1})+0.46(1b_{2g}^{-1}1a_u3b_{3g}^{-1})$	0.0152	24.64				
B_{2u}	$0.59(2b_{2u}^{-1})-0.46(1b_{1g}^{-1}1a_u3b_{3g}^{-1})+0.36(1b_{2g}^{-1}2b_{3u}3b_{3g}^{-1})$	0.2913	24.95	~ 24			
B_{2u}	$0.46(1b_{1g}^{-1}1a_u3b_{3g}^{-1})+0.43(2b_{2u}^{-1})-0.38(5b_{1u}^{-1}2b_{2g}1b_{1g}^{-1})$ $+0.35(5a_g^{-1}2b_{3u}1b_{1g}^{-1})-0.31(4b_{2u}^{-1}2b_{3u}1b_{3u}^{-1})$	0.1584	25.75				
A_g	$0.63(1b_{2g}^{-1}1a_u4b_{2u}^{-1})+0.54(4b_{2u}^{-1}1a_u1b_{2g}^{-1})-0.37(4b_{2u}^{-1}2b_{3u}1b_{1g}^{-1})$ $-0.36(4b_{1u}^{-1}1a_u1b_{1g}^{-1})-0.31(1b_{1g}^{-1}1a_u4b_{1u}^{-1})$	0.0246	25.91				
B_{2u}	$0.46(5a_g^{-1}2b_{3u}1b_{1g}^{-1})-0.45(1b_{1g}^{-1}1a_u3b_{3g}^{-1})-0.43(2b_{2u}^{-1})$ $-0.39(5b_{1u}^{-1}2b_{2g}1b_{1g}^{-1})-0.38(4b_{2u}^{-1}2b_{3u}1b_{3u}^{-1})$	0.1569	26.06				
B_{3g}	$0.57(1b_{1g}^{-1}1a_u4b_{2u}^{-1})-0.30(1b_{1g}^{-1}2b_{2g}6a_g^{-1})+0.30(1b_{2g}^{-1}1a_u5b_{1u}^{-1})$	0.0135	26.38				
B_{2u}	$0.65(1b_{2g}^{-1}2b_{3u}3b_{3g}^{-1})$	0.0126	27.07				
A_g	$0.45(1b_{1g}^{-1}2b_{3u}3b_{2u}^{-1})-0.34(1b_{2g}^{-1}2b_{2g}6a_g^{-1})$	0.0267	27.18				
B_{1u}	$0.56(1b_{2g}^{-1}1a_u3b_{3g}^{-1})$	0.0231	27.19				
A_g	$0.73(1b_{1g}^{-1}8a_g1b_{1g}^{-1})$	0.0103	27.28				

CONTINUE

CONTINUED

B_{2u}	$0.69(1b_{1g}^{-1}6b_{2u}1b_{1g}^{-1})-0.49(1b_{1g}^{-1}5b_{2u}1b_{1g}^{-1})$	0.0176	27.38
B_{1u}	$0.40(1b_{3u}^{-1}2b_{2g}6a_{g}^{-1})-0.35(5b_{1u}^{-1}2b_{2g}1b_{2g}^{-1})-0.35(1b_{2g}^{-1}1a_{u}3b_{3g}^{-1})$	0.0159	27.47
B_{1u}	$0.48(1b_{1g}^{-1}6b_{1u}1b_{1g}^{-1})-0.31(1b_{1g}^{-1}7b_{1u}1b_{1g}^{-1})+0.30(1b_{3u}^{-1}2b_{3u}5b_{1u}^{-1})$	0.0501	27.73
A_{g}	$0.53(6a_{g}^{-1}8a_{g}6a_{g}^{-1})$	0.0108	27.77
B_{1u}	$0.47(6a_{g}^{-1}6b_{1u}6a_{g}^{-1})+0.31(6a_{g}^{-1}8a_{g}4b_{1u}^{-1})$	0.0130	28.10
A_{g}	$0.47(1b_{1g}^{-1}1a_{u}4b_{1u}^{-1})-0.40(1b_{2g}^{-1}1a_{u}4b_{2u}^{-1})+0.36(1b_{1g}^{-1}2b_{3u}4b_{2u}^{-1})$	0.0140	28.57
B_{1u}	$0.62(6a_{g}^{-1}7b_{1u}6a_{g}^{-1})+0.39(6a_{g}^{-1}6b_{1u}6a_{g}^{-1})$	0.0486	28.64
B_{1u}	$0.46(1b_{1g}^{-1}1a_{u}5a_{g}^{-1})+0.43(3b_{1u}^{-1})$	0.1600	28.87
B_{1u}	$0.50(4b_{2u}^{-1}1a_{u}1b_{3u}^{-1})+0.41(1b_{3u}^{-1}1a_{u}4b_{2u}^{-1})-0.37(4b_{1u}^{-1}2b_{3u}1b_{3u}^{-1})$ $+0.35(4b_{2u}^{-1}2b_{2g}1b_{1g}^{-1})$	0.0501	29.15
A_{g}	$0.53(1b_{2g}^{-1}2b_{2g}6a_{g}^{-1})+0.47(1b_{1g}^{-1}2b_{3u}4b_{2u}^{-1})+0.35(1b_{1g}^{-1}2b_{3u}3b_{2u}^{-1})$	0.0188	29.17
B_{1u}	$0.38(1b_{1g}^{-1}7b_{1u}1b_{1g}^{-1})-0.35(1b_{2g}^{-1}6b_{2u}1b_{1g}^{-1})+0.33(1b_{1g}^{-1}1a_{u}5a_{g}^{-1})$ $+0.30(1b_{1g}^{-1}6b_{1u}1b_{1g}^{-1})$	0.0472	29.33
B_{1u}	$0.46(4b_{2u}^{-1}1a_{u}1b_{3u}^{-1})+0.35(4b_{2u}^{-1}2b_{2g}1b_{1g}^{-1})-0.34(1b_{1g}^{-1}7b_{1u}1b_{1g}^{-1})$ $+0.32(6a_{g}^{-1}2b_{2g}1b_{3u}^{-1})+0.30(4b_{1u}^{-1}2b_{3u}1b_{3u}^{-1})$	0.0223	29.53
B_{1u}	$0.55(5a_{g}^{-1}2b_{3u}1b_{2g}^{-1})-0.39(6a_{g}^{-1}2b_{2g}1b_{3u}^{-1})+0.31(1b_{2g}^{-1}2b_{2g}5b_{1u}^{-1})$	0.0609	29.61
A_{g}	$0.70(1b_{2g}^{-1}7a_{g}1b_{2g}^{-1})+0.33(1b_{2g}^{-1}4b_{3g}1b_{1g}^{-1})$	0.0140	29.62
B_{1u}	$0.50(1b_{1g}^{-1}7b_{1u}1b_{1g}^{-1})-0.47(1b_{2g}^{-1}5b_{2u}1b_{1g}^{-1})+0.32(4b_{1u}^{-1}2b_{3u}1b_{3u}^{-1})$	0.0250	29.73
B_{1u}	$0.45(1b_{2g}^{-1}5b_{2u}1b_{1g}^{-1})-0.34(2b_{3g}^{-1}2b_{3u}1b_{1g}^{-1})+0.34(4b_{1u}^{-1}2b_{3u}1b_{3u}^{-1})$	0.0290	29.94

[a] Ref. [14], [b] Principal axis is different from original ones, so that two character b_{1g}, and b_{1u} are changed to b_{3g}, and b_{3u}, respectively., [c] Ref. [17], [d] Ref. [9], [e] Ref. [6]

In Tables II-IV, the results of IPs, monopole intensities, and detailed ionization characters for the valence ionized states, which have large intensity greater than 0.005 were presented with the IPs of the He I UPS [17], He II UPS [13, 14, 15, 16] and other theoretical results [5, 6, 7, 8, 9]

6.3.1 pyrazine

Ten main peaks were observed in the outer-valence region of pyrazine by the He I UPS. Our assignment is consistent with that of the PIES experiment [17]. First four peaks observed at 9.61, 10.20, 11.38 and 11.80 eV[17] were assigned to the ionizations from the outer three MOs, $6a_g$, $1b_{1g}$, $5b_{1u}$ and $1b_{2g}$, respectively. The present calculation computed the IPs of these states at 9.49, 10.06, 11.30 and 11.64 eV. The next continuous three peaks observed at 13.37, 13.93, and 14.98 eV [17] were attributed to the $(3b_{3g}^{-1})$, $(1b_{3u}^{-1})$, and $(4b_{2u}^{-1})$ states and were calculated at 13.90, 14.43, and 15.30 eV, respectively. These seven ionized states were dominantly described by the one-electron process and their monopole intensities were large.

TABLE III: Calculated ionization potentials (IP, in eV), monopole intensities (M.I.), and main configurations with the basis set for pyridazine.

Sym.	Main Configuration($\|C\| > 0.3$)	M.I.	IP	Expt.[a]	Expt.[b]	P3[c]	CI[d]
B_2	$0.95(8b_2^{-1})$	0.7621	9.14	9.3	9.27	9.284	8.523
A_2	$0.97(1a_2^{-1})$	0.7943	10.57	10.5	10.61	10.853	10.697
B_1	$0.97(2b_1^{-1})$	0.7905	11.02	11.3	11.2	11.287	10.872
A_1	$0.93(10a_1^{-1})$	0.7593	11.29	11.3	11.3	11.656	10.679
B_1	$0.93(1b_1^{-1})$	0.7257	14.44	13.8	13.97	14.554	13.776
A_1	$0.93(9a_1^{-1})$	0.7675	14.48	14.2	14.27	14.519	13.367
B_2	$0.95(7b_2^{-1})$	0.7674	14.95	14.8	14.66	14.880	14.239
	$0.94(6b_2^{-1})$	0.7555	16.76	15.9	15.90	16.517	16.502
A_1	$0.93(8a_1^{-1})$	0.7360	17.13	17.0	16.8	17.390	16.888
	$0.73(7a_1^{-1})-0.57(8b_2^{-1}2a_2 2b_1^{-1})-0.38(2b_1^{-1}2a_2 8b_2^{-1})$	0.4802	17.99	17.4	17.43	17.959	17.300
	$0.81(8b_2^{-1}2a_2 2b_1^{-1})+0.56(7a_1^{-1})+0.43(2b_1^{-1}2a_2 8b_2^{-1})$ $-0.32(8b_2^{-1}3b_1 1a_2^{-1})$	0.2650	18.24				
A_1	$0.88(8b_2^{-1}3b_1 1a_2^{-1})+0.46(1a_2^{-1}3b_1 8b_2^{-1})+0.37(2b_1^{-1}2a_2 8b_2^{-1})$	0.0165	19.51				
	$0.51(1a_2^{-1}2a_2 8b_2^{-1})+0.37(2b_1^{-1}3b_1 8b_2^{-1})$	0.0104	20.11				
A_1	$0.57(2b_1^{-1}2a_2 8b_2^{-1})-0.42(10a_1^{-1}2a_2 1a_2^{-1})+0.37(1b_1^{-1}2a_2 8b_2^{-1})$ $-0.32(1a_2^{-1}3b_1 8b_2^{-1})$	0.0207	20.36				
A_1	$0.64(10a_1^{-1}2a_2 1a_2^{-1})+0.49(1a_2^{-1}2a_2 10a_1^{-1})-0.47(8b_2^{-1}2a_2 1b_1^{-1})$ $-0.39(8b_2^{-1}3b_1 1a_2^{-1})$	0.0309	20.56				
A_1	$0.61(6a_1^{-1})-0.40(1a_2^{-1}3b_1 8b_2^{-1})+0.36(10a_1^{-1}2a_2 1a_2^{-1})$	0.3169	21.44	20.7			
B_2	$0.61(5b_2^{-1})-0.33(2b_1^{-1}2a_2 10a_1^{-1})$	0.3351	21.62	20.7			
B_2	$0.75(10a_1^{-1}3b_1 1a_2^{-1})+0.52(10a_1^{-1}2a_2 2b_1^{-1})+0.37(1a_2^{-1}3b_1 10a_1^{-1})$ $+0.34(10a_1^{-1}2a_2 1b_1^{-1})$	0.0654	21.77				
A_1	$0.64(6a_1^{-1})+0.39(1a_2^{-1}3b_1 8b_2^{-1})+0.33(1a_2^{-1}2a_2 10a_1^{-1})$	0.3553	21.93				
B_2	$0.58(5b_2^{-1})+0.31(2b_1^{-1}2a_2 10a_1^{-1})-0.31(1a_2^{-1}3b_1 10a_1^{-1})$	0.2880	22.09				
B_1	$0.90(2b_1^{-1}2a_2 1a_2^{-1})+0.48(1a_2^{-1}2a_2 2b_1^{-1})+0.41(1a_2^{-1}3b_1 1a_2^{-1})$	0.0466	22.60				
B_2	$0.63(2b_1^{-1}2a_2 10a_1^{-1})-0.53(2b_1^{-1}3b_1 8b_2^{-1})$	0.0137	23.33				
A_1	$0.59(2b_1^{-1}3b_1 10a_1^{-1})$	0.0110	24.40				
B_2	$0.72(1a_2^{-1}3b_1 10a_1^{-1})$	0.0121	24.41				
A_1	$0.74(6b_2^{-1}3b_1 1a_2^{-1})-0.60(6b_2^{-1}2a_2 2b_1^{-1})+0.42(1a_2^{-1}3b_1 6b_2^{-1})$ $-0.34(2b_1^{-1}2a_2 6b_2^{-1})$	0.0276	25.07				
A_1	$0.58(1a_2^{-1}2a_2 9a_1^{-1})$	0.0148	25.10				
B_1	$0.72(2b_1^{-1}3a_2 1a_2^{-1})+0.70(1a_2^{-1}3a_2 2b_1^{-1})+0.44(1a_2^{-1}2a_2 1b_1^{-1})$ $-0.39(2b_1^{-1}3b_1 1b_1^{-1})+0.31(1b_1^{-1}2a_2 1a_2^{-1})-0.31(1b_1^{-1}3b_1 2b_1^{-1})$	0.0217	25.42				
B_2	$0.52(6b_2^{-1}3b_1 2b_1^{-1})+0.44(2b_1^{-1}3b_1 6b_2^{-1})+0.34(8b_2^{-1}3b_1 1b_1^{-1})$ $-0.31(8a_1^{-1}2a_2 2b_1^{-1})-0.30(7b_2^{-1}3b_1 2b_1^{-1})$	0.0125	25.68				
B_2	$0.53(8a_1^{-1}3b_1 1a_2^{-1})-0.44(8a_1^{-1}2a_2 2b_1^{-1})+0.38(4b_2^{-1})$ $+0.31(1a_2^{-1}3b_1 8a_1^{-1})$	0.1276	26.12				
A_1	$0.35(1a_2^{-1}3b_1 7b_2^{-1})-0.34(2b_1^{-1}2a_2 7b_2^{-1})$	0.0128	26.14				
A_1	$0.48(6b_2^{-1}2a_2 2b_1^{-1})-0.38(2b_1^{-1}2a_2 7b_2^{-1})+0.30(9a_1^{-1}3b_1 1b_1^{-1})$	0.0136	26.34				
A_1	$0.55(5a_1^{-1})+0.37(2b_1^{-1}3a_2 8b_2^{-1})$	0.2643	26.40				

CONTINUE

CONTINUED

B_2	$0.36(1a_2^{-1}2a_26b_2^{-1})+0.35(2b_1^{-1}3b_16b_2^{-1})-0.34(2b_1^{-1}3b_17b_2^{-1})$	0.0332	26.55
A_1	$0.41(7a_1^{-1}2a_21a_2^{-1})+0.36(7b_2^{-1}2a_21b_1^{-1})+0.33(9a_1^{-1}3a_21a_2^{-1})$ $+0.31(1a_2^{-1}2a_27a_1^{-1})$	0.0145	26.63
A_1	$0.44(7b_2^{-1}2a_21b_1^{-1})+0.41(7a_1^{-1}2a_21a_2^{-1})-0.39(1a_2^{-1}3b_17b_2^{-1})$ $+0.31(1a_2^{-1}2a_28a_1^{-1})-0.30(1b_1^{-1}2a_28b_2^{-1})$	0.0197	26.69
B_2	$0.61(4b_2^{-1})$	0.3201	26.79
A_1	$0.53(8a_1^{-1}2a_21a_2^{-1})+0.32(9a_1^{-1}3b_11b_1^{-1})+0.32(1a_2^{-1}2a_28a_1^{-1})$ $+0.31(8b_2^{-1}3a_22b_1^{-1})$	0.0520	26.83
B_2	$0.41(1a_2^{-1}12a_12b_1^{-1})-0.32(2b_1^{-1}12a_11a_2^{-1})-0.32(2b_1^{-1}11a_11a_2^{-1})$ $+0.30(1a_2^{-1}11a_12b_1^{-1})$	0.0382	26.97
A_1	$0.40(1a_2^{-1}3b_16b_2^{-1})+0.38(6b_2^{-1}2a_22b_1^{-1})+0.31(2b_1^{-1}3a_28b_2^{-1})$ $+0.30(8b_2^{-1}3a_22b_1^{-1})$	0.0795	27.01
B_2	$0.42(1b_1^{-1}2a_210a_1^{-1})+0.36(1a_2^{-1}3b_19a_1^{-1})-0.31(1a_2^{-1}2a_26b_2^{-1})$	0.0143	27.15
A_1	$0.38(6b_2^{-1}3b_11a_2^{-1})+0.31(6b_2^{-1}2a_22b_1^{-1})$	0.0351	27.16
A_1	$0.42(1a_2^{-1}9b_22b_1^{-1})$	0.0261	27.38
B_2	$0.49(6b_2^{-1}2a_21a_2^{-1})-0.37(7a_1^{-1}3b_11a_2^{-1})$	0.0134	27.41
A_1	$0.33(1a_2^{-1}9b_22b_1^{-1})$	0.0279	27.44

[a] Ref. [15], [b] Ref. [17], [c] Ref. [9], [d] Ref. [7]

Other theoretical studies also explained these peaks in the same way.

The peaks 8-10 observed at 16.10, 16.58 and 16.97 eV were also characterized as one-electron process. For these peaks, theoretical studies gave different picture: the 2ph-TDA calculation [1] proposed that these line split into several peaks, while other theoretical studies gave single peak for each state. In our SAC-CI results, these peaks did not split, though the contribution of doubles was relatively large, especially for B_{2u} state.

In the energy region higher than 18 eV, two satellite peaks were observed at about $\sim$ 18.0 and $\sim$ 19.1 eV [17]. For these peaks, the assignments were not proposed in detail by both experimental and theoretical works. We calculated a B_{2u} state at 18.31 eV for the former peak, and three states, B_{3g}, B_{2u}, and B_{3u} states at 19.42, 19.82 and 20.98 eV, respectively, for the latter peak. These states were dominantly represented by the two electron process such as $(6a_g^{-1}2b_{3u}1b_{1g}^{-1})$ and $(1b_{1g}^{-1}2b_{3u}5b_{1u}^{-1})$. Above this energy region, He II UPS measured the composite peaks at about $\sim$ 20.6 and $\sim$ 21 eV [14]. B_{2g} and A_{1g} states were attributed for these peaks by 2ph-TDA and 2h1p calculations [1]. We also calculated $(4a_1^{-1})$ and $(2b_{3g}^{-1})$ states with large intensity at 21.62 and 21.77 eV, respectively. These states

TABLE IV: Calculated ionization potentials (IP, in eV), monopole intensities (M.I.), and main configurations with the basis set for pyrimidine.

Sym.	Main Configuration($\|C\| > 0.3$)	M.I.	IP	Expt.[a]	Expt.[b]	P3[c]	CI[d]
B_2	$0.95(7b_2^{-1})$	0.7742	9.73	9.7	9.69	9.863	9.351
B_1	$0.97(2b_1^{-1})$	0.7982	10.46	10.5	10.50	10.647	10.412
A_1	$0.94(11a_1^{-1})$	0.7677	11.05	11.2	11.22	11.334	10.713
A_2	$0.96(1a_2^{-1})$	0.7883	11.30	11.5	11.40	11.576	11.292
B_1	$0.93(1b_1^{-1})$	0.7341	14.51	13.6	13.9	14.558	14.015
A_1	$0.94(10a_1^{-1})$	0.7722	14.55	14.5	14.1	14.557	14.916
B_2	$0.95(6b_2^{-1})$	0.7720	14.84	14.5	14.4	14.726	15.007
A_1	$0.94(9a_1^{-1})$	0.7641	16.30	15.8	15.8	16.612	16.303
B_2	$0.94(5b_2^{-1})$	0.7508	17.24	16.9	16.88	17.450	18.049
A_1	$0.92(8a_1^{-1})$	0.7362	18.34	17.4	17.4	18.228	17.663
B_2	$0.83(11a_1^{-1}2a_2 2b_1^{-1})+0.64(2b_1^{-1}2a_2 11a_1^{-1})+0.37(7b_2^{-1}4b_1 2b_1^{-1})$	0.0133	20.15				
	$+0.34(2b_1^{-1}4b_1 7b_2^{-1})-0.31(7b_2^{-1}2a_2 1a_2^{-1})$						
A_1	$0.86(11a_1^{-1}3b_1 2b_1^{-1})-0.51(11a_1^{-1}2a_2 1a_2^{-1})+0.49(2b_1^{-1}3b_1 11a_1^{-1})$	0.0111	20.24				
A_1	$0.62(2b_1^{-1}2a_2 7b_2^{-1})+0.31(1a_2^{-1}3b_1 7b_2^{-1})-0.31(11a_1^{-1}2a_2 1a_2^{-1})$	0.0171	20.47				
A_1	$0.59(7b_2^{-1}3b_1 1a_2^{-1})+0.47(7a_1^{-1})-0.46(11a_1^{-1}2a_2 1a_2^{-1})$	0.1911	21.42				
B_2	$0.38(2b_1^{-1}3b_1 7b_2^{-1})+0.38(11a_1^{-1}2a_2 2b_1^{-1})-0.37(2b_1^{-1}2a_2 11a_1^{-1})$	0.0528	21.46				
A_1	$0.75(7a_1^{-1})-0.48(7b_2^{-1}3b_1 1a_2^{-1})$	0.4750	21.72	20.5	~ 20.5		
B_2	$0.63(4b_2^{-1})+0.58(2b_1^{-1}3b_1 7b_2^{-1})-0.32(1a_2^{-1}2a_2 7b_2^{-1})$	0.3421	21.81	20.5			
B_1	$0.74(2b_1^{-1}2a_2 1a_2^{-1})+0.42(2b_1^{-1}3b_1 2b_1^{-1})+0.34(1a_2^{-1}3b_1 1a_2^{-1})$	0.0118	21.98				
B_2	$0.47(4b_2^{-1})-0.44(11a_1^{-1}3b_1 1a_2^{-1})-0.44(1a_2^{-1}3b_1 11a_1^{-1})$	0.1908	21.99				
	$-0.38(7b_2^{-1}3b_1 1b_1^{-1})-0.31(1b_1^{-1}3b_1 7b_2^{-1})-0.30(2b_1^{-1}3b_1 7b_2^{-1})$						
B_2	$0.57(11a_1^{-1}3b_1 1a_2^{-1})+0.51(7b_2^{-1}3b_1 1b_1^{-1})-0.37(2b_1^{-1}2a_2 11a_1^{-1})$	0.0785	22.23				
	$+0.30(4b_2^{-1})+0.30(1a_2^{-1}2a_2 7b_2^{-1})$						
B_1	$0.90(1a_2^{-1}2a_2 2b_1^{-1})+0.34(2b_1^{-1}3b_1 2b_1^{-1})$	0.0329	22.61				
A_1	$0.60(2b_1^{-1}3b_1 11a_1^{-1})-0.45(1a_2^{-1}2a_2 11a_1^{-1})-0.36(1b_1^{-1}2a_2 7b_2^{-1})$	0.0120	22.88				
B_2	$0.64(6b_2^{-1}3b_1 2b_1^{-1})-0.59(6b_2^{-1}2a_2 1a_2^{-1})-0.44(10a_1^{-1}2a_2 2b_1^{-1})$	0.0170	23.42				
	$+0.33(2b_1^{-1}3b_1 6b_2^{-1})$						
B_2	$0.54(1a_2^{-1}2a_2 7b_2^{-1})+0.43(2b_1^{-1}3b_1 7b_2^{-1})+0.40(1b_1^{-1}2a_2 11a_1^{-1})$	0.0167	23.48				
	$+0.37(2b_1^{-1}2a_2 11a_1^{-1})$						
B_2	$0.68(10a_1^{-1}2a_2 2b_1^{-1})-0.57(6b_2^{-1}2a_2 1a_2^{-1})+0.39(2b_1^{-1}2a_2 10a_1^{-1})$	0.0111	23.63				
	$-0.33(1a_2^{-1}2a_2 6b_2^{-1})$						
A_1	$0.49(6b_2^{-1}2a_2 2b_1^{-1})-0.44(2b_1^{-1}3b_1 11a_1^{-1})+0.32(1a_2^{-1}3b_1 7b_2^{-1})$	0.0283	23.80				
	$0.49(1a_2^{-1}3b_1 7b_2^{-1})+0.47(1a_2^{-1}2a_2 11a_1^{-1})+0.32(1b_1^{-1}3b_1 11a_1^{-1})$	0.0291	24.35				
	$+0.30(2b_1^{-1}3b_1 11a_1^{-1})$						
B_2	$0.50(1a_2^{-1}3b_1 11a_1^{-1})+0.50(1b_1^{-1}3b_1 7b_2^{-1})$	0.0111	24.38				
	$0.58(10a_1^{-1}3b_1 1a_2^{-1})-0.44(1a_2^{-1}3b_1 11a_1^{-1})+0.42(7b_2^{-1}3b_1 1b_1^{-1})$	0.0146	24.46				
	$+0.38(1a_2^{-1}3b_1 10a_1^{-1})-0.35(11a_1^{-1}3b_1 1a_2^{-1})+0.31(6b_2^{-1}2a_2 1a_2^{-1})$						
A_1	$0.50(2b_1^{-1}2a_2 6b_2^{-1})-0.39(2b_1^{-1}3b_1 10a_1^{-1})$	0.0254	25.10				
A_1	$0.54(9a_1^{-1}3b_1 2b_1^{-1})-0.53(9a_1^{-1}2a_2 1a_2^{-1})-0.38(10a_1^{-1}2a_2 1a_2^{-1})$	0.0231	25.24				
	$-0.34(2b_1^{-1}2a_2 6b_2^{-1})-0.31(10a_1^{-1}3b_1 2b_1^{-1})$						
A_1	$0.54(11a_1^{-1}3b_1 1b_1^{-1})+0.50(6b_2^{-1}3b_1 1a_2^{-1})+0.40(11a_1^{-1}4b_1 2b_1^{-1})$	0.0256	25.41				
	$+0.31(1a_2^{-1}3b_1 6b_2^{-1})-0.30(7b_2^{-1}3b_1 1a_2^{-1})$						

CONTINUE

CONTINUED

B_2	$0.43(11a_1^{-1}2a_21b_1^{-1})-0.40(11a_1^{-1}4b_11a_2^{-1})-0.38(6b_2^{-1}2a_21a_2^{-1})$ $+0.35(10a_1^{-1}3b_11a_2^{-1})-0.35(6b_2^{-1}3b_12b_1^{-1})$	0.0116	25.56	
A_1	$0.54(6a_1^{-1})+0.39(1a_2^{-1}2a_210a_1^{-1})$	0.2551	25.72	24.4
B_2	$0.50(1a_2^{-1}2a_26b_2^{-1})-0.46(2b_1^{-1}3b_16b_2^{-1})$	0.0170	26.30	
A_1	$0.48(9a_1^{-1}2a_21a_2^{-1})+0.40(2b_1^{-1}3b_110a_1^{-1})+0.36(6a_1^{-1})$	0.1226	26.30	
A_1	$0.46(9a_1^{-1}2a_21a_2^{-1})-0.41(2b_1^{-1}3b_110a_1^{-1})+0.40(9a_1^{-1}3b_12b_1^{-1})$ $-0.35(6a_1^{-1})$	0.1069	26.40	
A_1	$0.34(1a_2^{-1}2a_211a_1^{-1})-0.34(1b_1^{-1}2a_27b_2^{-1})-0.33(1a_2^{-1}2a_210a_1^{-1})$	0.0454	26.55	
A_1	$0.75(2b_1^{-1}13a_12b_1^{-1})$	0.0511	27.07	
A_1	$0.43(2b_1^{-1}2a_25b_2^{-1})+0.30(1a_2^{-1}4b_17b_2^{-1})$	0.0264	27.31	
B_2	$0.35(2b_1^{-1}3b_16b_2^{-1})+0.35(2b_1^{-1}8b_22b_1^{-1})$	0.0323	27.39	
A_1	$0.40(5b_2^{-1}2a_22b_1^{-1})-0.36(2b_1^{-1}8b_21a_2^{-1})+0.35(8a_1^{-1}3b_12b_1^{-1})$	0.0132	27.51	

[a] Ref. [16], [b] Ref. [17], [c] Ref. [9], [d] Ref. [5]

have large intensities, however, Koopmans' picture was violated and the intensities were distributed through the final-state correlation interaction. Many shake-up states of two-electron processes continue from this energy region. Broad peak at $\sim$ 24 eV also reported by the He II UPS work [14]. We calculated prominent peaks originating $(2b_{2u}^{-1})$ state at 24.95 and 25.75, and 26.06 eV, which were attributed to the observed broad peak. Two electron processes, which interact with $(3b_{1u}^{-1})$ state and are centered at 28.9 eV, were also obtained.

6.3.2 pyridazine

First four peaks observed at 9.27, 10.61, 11.2, and 11.3 eV [17] were firmly assigned as $(8b_2^{-1})$, $(1a_2^{-1})$, $(2b_1^{-1})$, and $(10a_1^{-1})$ states calculated at 9.14, 10.57, 11.02, and 11.29 eV, respectively. The B_1 and A_1 states lie very close in energy and there were different assignments for these two states; our calculation support the assignments of the PIES by Kishimoto *et al*[17]. The order of next B_1 and A_1 states has also not been definitive since they lie very close in energy. In our SAC-CI result, they were calculated to be very close in energy as 14.44 and 14.48 eV; the order of these states accords with experimental analysis, however, this is not conclusive from our results since the energy separation is very small. Other theoretical studies of the P3 and CI predicted the different order of these states.

TABLE V: Calculated ionization potentials (IP, in eV), monopole intensities (M.I.), and main configurations with the basis set for s-triazine.

Sym.	Main Configuration($\|C\| > 0.3$)	M.I.	IP	Expt.[a]	Expt.[b]	P3[c]	CI[d]
E'	$0.95(6e'^{-1})$	0.7726	10.44	10.4	10.40	10.550	9.877
E''	$0.97(1e''^{-1})$	0.7890	11.94	12.0	11.79	12.104	11.731
A'_1	$0.94(5a'_1{}^{-1})$	0.7455	13.59	13.3	13.37	13.521	12.589
E'	$0.95(5e'^{-1})$	0.7739	15.32	14.7	14.99	15.429	15.294
A''_2	$0.93(1a''_2{}^{-1})$	0.7375	15.58	15.6	14.64	15.593	14.958
A'_2	$0.94(1a'_2{}^{-1})$	0.7494	18.55	17.6	17.6	18.714	16.639
A'_1	$0.93(4a'_1{}^{-1})$	0.7416	18.92	18.2	18.31	18.919	
E'	$0.47(1e''^{-1}2e''6e'^{-1})-0.46(1e''^{-1}2e''6e'^{-1})-0.33(6e'^{-1}2e''1e''^{-1})$ $-0.31(6e'^{-1}2e''1e''^{-1})$	0.0401	22.20				
E'	$0.66(6e'^{-1}2e''1e''^{-1})+0.40(6e'^{-1}2e''1e''^{-1})-0.30(5a'_1{}^{-1}2e''1a''_2{}^{-1})$	0.0621	22.53				
E'	$0.79(4e'^{-1})$	0.5242	22.83	22.0			
E'	$0.71(1e''^{-1}2e''6e'^{-1})+0.52(1e''^{-1}2e''6e'^{-1})$	0.0286	23.37				
E'	$0.56(5e'^{-1}2e''1e''^{-1})-0.43(6e'^{-1}2e''1a''_2{}^{-1})+0.43(6e'^{-1}2e''1a''_2{}^{-1})$ $+0.34(5e'^{-1}2e''1e''^{-1})+0.33(5a'_1{}^{-1}2e''1e''^{-1})-0.33(5a'_1{}^{-1}2e''1e''^{-1})$ $+0.30(1e''^{-1}2e''5e'^{-1})$	0.0198	24.06				
A''_2	$0.57(1e''^{-1}2e''1e''^{-1})+0.57(1e''^{-1}2e''1e''^{-1})-0.40(1e''^{-1}2e''1e''^{-1})$ $+0.39(1e''^{-1}2e''1e''^{-1})+0.34(1a''_2{}^{-1}2e''1e''^{-1})+0.33(1a''_2{}^{-1}2e''1e''^{-1})$	0.0490	24.15				
A'_1	$0.35(1a''_2{}^{-1}2e''6e'^{-1})-0.35(1e''^{-1}2e''6e'^{-1})+0.35(1a''_2{}^{-1}2e''6e'^{-1})$ $+0.35(1e''^{-1}2e''6e'^{-1})+0.34(1e''^{-1}2e''6e'^{-1})+0.34(1e''^{-1}2e''6e'^{-1})$	0.0199	24.46				
A'_1	$0.63(5e'^{-1}2e''1e''^{-1})+0.44(1e''^{-1}2e''5e'^{-1})+0.33(5a'_1{}^{-1}2e''1e''^{-1})$ $-0.33(5a'_1{}^{-1}2e''1e''^{-1})$	0.0273	24.94				
A'_2	$0.40(1e''^{-1}2e''6e'^{-1})+0.34(1e''^{-1}2e''6e'^{-1})-0.34(5e'^{-1}2e''1e''^{-1})$	0.0239	24.94				
A'_2	$0.50(5e'^{-1}2e''1e''^{-1})+0.41(5a'_1{}^{-1}2e''1e''^{-1})+0.41(1e''^{-1}2e''5e'^{-1})$ $+0.40(1e''^{-1}2e''6e'^{-1})+0.39(5a'_1{}^{-1}2e''1e''^{-1})$	0.0155	24.96				
A'_1	$0.58(1e''^{-1}2e''6e'^{-1})+0.43(1e''^{-1}2e''6e'^{-1})-0.35(1a''_2{}^{-1}2e''5a'_1{}^{-1})$	0.0120	24.98				
E'	$0.38(1e''^{-1}2e''5e'^{-1})+0.36(1a''_2{}^{-1}2e''6e'^{-1})+0.36(1a''_2{}^{-1}2e''6e'^{-1})$ $+0.34(1e''^{-1}2e''5e'^{-1})$	0.0137	25.98				
E'	$0.50(1e''^{-1}2e''5e'^{-1})$	0.0144	26.07				
A''_2	$0.53(1a''_2{}^{-1}2e''1e''^{-1})+0.53(1a''_2{}^{-1}2e''1e''^{-1})+0.38(1e''^{-1}2e''1a''_2{}^{-1})$ $-0.36(1e''^{-1}2a''_2 1e''^{-1})+0.36(1e''^{-1}2e''1a''_2{}^{-1})-0.34(1e''^{-1}2a''_2 1e''^{-1})$	0.0134	27.39				
A''_2	$0.45(1e''^{-1}2a''_2 1e''^{-1})-0.43(1e''^{-1}2a''_2 1e''^{-1})-0.42(1e''^{-1}2e''1a''_2{}^{-1})$ $+0.40(1e''^{-1}2e''1a''_2{}^{-1})$	0.0100	27.41				
E'	$0.59(1e''^{-1}2e''5e'^{-1})+0.41(1e''^{-1}2e''5e'^{-1})$	0.0135	27.56				
A'_1	$0.45(5a'_1{}^{-1}2e''1a''_2{}^{-1})-0.38(5e'^{-1}2e''1e''^{-1})-0.34(1a''_2{}^{-1}2e''5e'^{-1})$	0.0481	28.01				
A'_1	$0.39(1a''_2{}^{-1}2e''5e'^{-1})+0.31(5a'_1{}^{-1}2e''1a''_2{}^{-1})$	0.0273	28.01				
A'_2	$0.54(5a'_1{}^{-1}2e''1a''_2{}^{-1})-0.41(5e'^{-1}2e''1e''^{-1})+0.31(1a''_2{}^{-1}2e''5a'_1{}^{-1})$	0.0767	28.04				
A'_1	$0.48(4a'_1{}^{-1}2e''1e''^{-1})+0.47(4a'_1{}^{-1}2e''1e''^{-1})+0.40(5e'^{-1}2e''1a''_2{}^{-1})$ $+0.39(5e'^{-1}2e''1a''_2{}^{-1})$	0.0107	28.24				
A'_1		0.0123	28.33				
E'	$0.48(5e'^{-1}2e''1e''^{-1})+0.33(6e'^{-1}2a''_2 1e''^{-1})-0.33(6e'^{-1}2a''_2 1e''^{-1})$ $-0.33(6e'^{-1}2a''_2 1a''_2{}^{-1})$	0.0251	28.51				
E'	$0.35(3e'^{-1})$	0.1059	28.69				

[a] Ref. [13], [b] Ref. [17], [c] Ref. [9], [d] Ref. [8]

Next two peaks of $(6b_2^{-1})$ and $(8a_1^{-1})$ states also have the character of one electron processes, while the $(7a_1^{-1})$ state considerably interacts with shake-up states; twinning states were calculated at 17.99 and 18.24 eV: this is characteristic feature for pyridazine different from other azines. Actually, satellite peak was observed in the higher-energy region of peak 10 as the shoulder[17]. Above these states, many two-electron processes of A_1 symmetry were calculated, though the monopole intensities of these states were very small. Åsbrink *et al.* observed two broad peaks near ∼20.7 eV by the He II UPS [15]. In this energy region, many split peaks originating $(6a_1^{-1})$ and $(5b_2^{-1})$ were predicted; prominent peaks were calculated at 21.44, 21.62, 21.93, and 22.09 eV. These peaks correspond to $(2b_{3g}^{-1})$ and $(4a_g^{-1})$ states of pyridazine and the breakdown of the Koopmans' picture is also similar. The shake-up states originating from $(5a_1^{-1})$ state were calculated in higher energy region than other azines and they were located around $26 \sim 27$ eV, which is also characteristic to pyridazine.

6.3.3 pyrimidine

The assignment of the first four peaks was confirmed by the SAC-CI method: the B_2, B_1, A_1, and A_2 states observed at 9.69, 10.50, 11.22, and 11.40 eV [17] were calculated at 9.73, 10.46, 11.05, and 11.30 eV, respectively. Other theoretical works also gave same assignment for these peaks. Next three peaks are very close in energy, which is characteristic to pyrimidine. Two peaks measured at 13.9 and 14.1 eV were attributed to the B_1 and A_1 states, respectively, by the PIES work [17]. Our calculation reproduced the order of these states, though the energy separation was very small as 0.04 eV. The P3 calculation also gave almost the same IPs for these states [9]. Next three peaks at 15.8, 16.88, and 17.4 eV, which were assigned as the $(9a_1^{-1})$, $(5b_2^{-1})$, and $(8a_1^{-1})$ states, respectively, were also confirmed by the present calculation, though the IPs were calculated to be larger than the experimental values, especially for the $(8a_1^{-1})$ state.

No prominent shake-up states were calculated until $\sim$ 21.5 eV. The He II UPS measured the peak at around $\sim$ 20.5 eV [16]. For this peak, many correlation peaks

were obtained in the present calculation and the representative peaks were calculated at 21.42, 21.72, 21.81, and 21.99 eV, which are of either A_1 or B_1 symmetry. Broad peak was also observed at $\sim$ 24.4 eV by the He II UPS [16]. Accordingly, many A_1 states split through the final-state correlation interaction with $(6a_1^{-1})$ state were calculated for this peak. There are still discrepancies between the theoretical and experimental IPs. By including higher-order terms of R-operators, these values are to be improved, however, the feature of the spectrum and the present assignments are valid.

6.3.4 *s*-triazine

First three peaks were calculated at 10.44(E'), 11.94(E''), and 13.59(A_1') eV in agreement with the experimental assignment and IPs of 10.40, 11.79, and 13.37 eV [17]. The assignments of the next two peaks have been controversial. The SAC-CI method gave these peaks at 15.32 and 15.58 eV for E' and A_2'' states, respectively. Our assignment for these states accords with that of the P3 method [9], however, contradicts to that of the PIES experiment [17]. For the peaks 6 and 7, we calculated the $(1a_2'^{-1})$ and $(4a_1'^{-1})$, both of which are described by the one-electron process. In the energy region of 18 $\sim$ 20 eV, no satellite peaks were obtained, which was also indicated by the experimental work[13].

The He II PES observed the peak around $\sim$ 22.0 eV [13]. We assigned this peak as some E' states, one of which has large monopole intensity at 22.83 eV. Above this energy region, many shake-up states with small intensities were calculated up to $\sim$ 30 eV.

6.3.5 Correlation peaks of azabenzenes at 24$\sim$30eV

For pyrazine, pyridazine, pyrimidine, and *s*-triazine we have calculated (observed[17]) many correlation peaks centered at 24.95eV ($\sim$ 24eV), 26.40eV (not observed), 25.72eV (24.4eV) and 28.69eV (not observed), respectively.

These peaks are characterized as one electron process the nature of $2b_u^{-1}$, $5a_1^{-1}$, $6a_1^{-1}$ and $3e'^{-1}$ states, respectively, are important, which have largest coefficient.

The values of IP by Koopmans' are 28.76eV for pyrazine, 30.33eV for pyridazine, 29.36eV for pyrimidine, 33.19eV for *s*-triazine, respectively. Compare these values to calculated IPs, we find that the states which ionized from 9th orbital are stabilized about ∼4eV by taking into account the electron correlation, we would say that stabilization is due to the dynamic correlation. The difference of IP may be explained by the location of the nitrogen atoms and nature of the Hartree-Fock orbital; $\sigma(\mathrm{C}-\mathrm{N})$ and $\sigma(\mathrm{C}-\mathrm{C})$. For pyrazine, the nature of MO is $\sigma(\mathrm{C}-\mathrm{C})$, and delocalization of σ bond is separated by nitrogen(see figure VI); this orbital is most unstable among four compounds, so that this peak is observed as lowest IP. For pyridazine, this MO's nature is $\sigma(\mathrm{C}-\mathrm{C})$ and this orbital is delocalized, not splitted by nitrogen atoms. For pyrimidine, σ bond is more delocalized than pyrazine but not than pyridazine. For *s*-triazine, the nature of this orbital is $\sigma(\mathrm{C}-\mathrm{N})$ and degenerated, so that this most stabilized. We predict that there are correlation peaks which may be observed at ∼25eV, for pyridazine and ∼27eV for *s*-triazine. If this trend is true, this estimation can be compared to benzene, and pyridine. For pyridine, experimental IP is 24.3eV and Koopmans' value are 28.15eV, respectively, and for benzene(see Figure X), experimental IP is ∼23eV[56] and Koopmans' value is 27.59eV, so our estimation may not be so bad(calculation is performed with 6-31G*/B3LYP DFT optimized geometry).

6.4 The breakdown of Koopmans' theorem

Breakdown of Koopmans' theorem is the term introduced by Cederbaum *et al.*[48], a situation which Koopmans defect differs so much for some ionizations that sequence of the electronic states of the ion is altered in comparison to the equence of the occupied orbitals. Such situations are observed at ionization from outer valence electrons, especially, ionization from n orbital and π orbitals[1, 49, 50, 51, 52, 53, 54]. This effect is explained as many body effect by perturbative treatment for N_2 and F_2[48], and its simple explanation for them[49] was effect of mixing configurations of valence electron("static correlation"). Other explanation was based on "reorganization of orbital"[54]. In this section, we analyze this effect in detail.

Figure XI: Comparison of IP by Koopmans and SAC-CI calculation for pyrazine

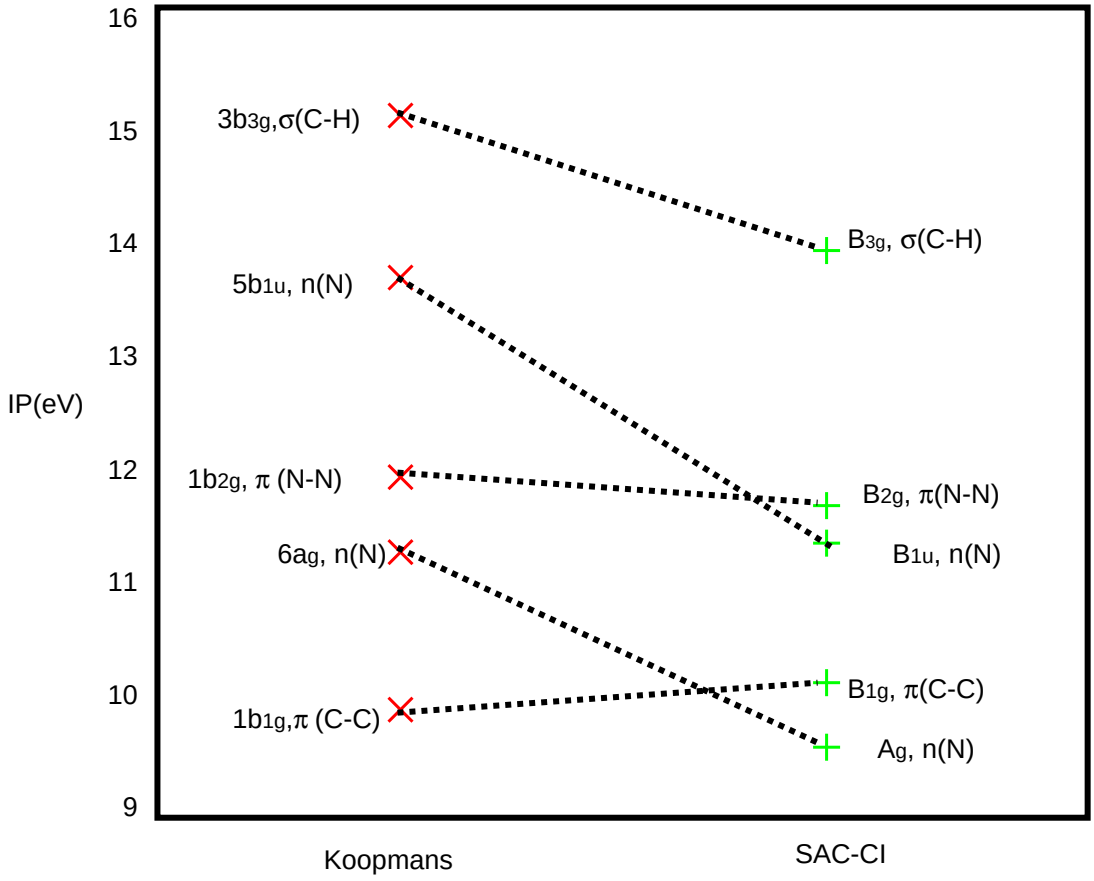

6.4.1 Calculation and experimental fact

We compared the SAC-CI result with the experimental and Koopmans' IPs of pyrazine, pyridazine, pyrimidine, *s*-triazine and trans-acrolein in table VI. We also dipicted the diagram of pyrazine in figure XI. The relative positions of the ionizations from n- and π- orbitals are not reproduced by the Koompans' theorem. Such breakdown can be generally observed for many other molecules. When we compare the Koomans' IPs and the SAC-CI IPs, we find a rule:

- Electron correlation and the orbital reorganization energes of the ionized states of (π^{-1}) is almost same as those in the ground state.

TABLE VI: Comparison of ionization order of SAC-CI, experiment and Koopmans.

pyrazine			SAC-CI(SD-R)	Exp.		Koopmans	
Sym.	Nature	Main Config.	IP	IP	Sym.	Nature	IP
A_g	n(N)	$0.95(6a_g{}^{-1})$	9.49	9.61	$1b_{1g}$	π(C − C)	9.83
B_{1g}	π(C − C)	$0.97(1b_{1g}{}^{-1})$	10.06	10.20	$6a_g$	n(N)	11.22
B_{1u}	n(N)	$0.94(5b_{1u}{}^{-1})$	11.30	11.38	$1b_{2g}$	π(N − N)	11.89
B_{2g}	π(N − N)	$0.96(1b_{2g}{}^{-1})$	11.64	11.80	$5b_{1u}$	n(N)	13.66
pyridazine			SAC-CI(SD-R)	Exp.		Koopmans	
Sym.	Nature	Main Config.	IP	IP	Sym.	Nature	IP
B_2	n(N)	$0.95(8b_2{}^{-1})$	9.49	9.27	$1a_2$	π(C − N)	10.46
A_2	π(C − C)	$0.97(1a_2{}^{-1})$	10.57	10.61	$2b_1$	π(C − C)	11.00
B_1	π(C − C)	$0.97(2b_1{}^{-1})$	11.02	11.2	$8b_2$	n(N)	11.07
A_1	n(N)	$0.93(10a_1{}^{-1})$	11.29	11.3	$10a_1$	n(N)	13.09
pyridazine			SAC-CI(SD-R)	Exp.		Koopmans	
Sym.	Nature	Main Config.	IP	IP	Sym.	Nature	IP
B_2	n(N)	$0.95(7b_2{}^{-1})$	9.73	9.69	$2b_1$	π(C − C)	10.37
B_1	π(C − C)	$0.97(2b_1{}^{-1})$	10.46	10.50	$7b_2$	n(N)	11.00
A_1	n(N)	$0.94(11a_1{}^{-1})$	11.05	11.22	$1a_2$	π(C − N)	11.07
A_2	π(C − N)	$0.96(1a_2{}^{-1})$	11.30	11.40	$11a_1$	n(N)	13.09
s-triazine			SAC-CI(SD-R)	Exp.		Koopmans	
Sym.	Nature	Main Config.	IP	IP	Sym.	Nature	IP
E'	n(N)	$0.95(6e'{}^{-1})$	10.44	10.40	$1e''$	π(C − N)	12.02
E''	π(C − N)	$0.97(1e''{}^{-1})$	11.94	11.79	$6e'$	n(N)	12.07
A_1'	n(N)	$0.94(5a_1'{}^{-1})$	13.59	13.37	$5a_1'$	n(N)	15.71
E'	σ(C − H)	$0.95(5e'{}^{-1})$	15.32	14.64	$1a_2''$	π(C − N)	16.66
trans-acrolein			SAC-CI(General-R)	Exp.		Koopmans	
Sym.	Nature	Main Config.	IP	IP	Sym.	Nature	IP
A'	n(O)	$0.92(13a'{}^{-1})$	9.62	10.10	$2a''$	π	10.85
A''	π	$0.95(2a''{}^{-1})$	10.50	10.92	$13a'$	n(O)	11.74

- Ionized species which ionized from n orbital are stabilized than neutral but more than σ so IP gets lower and sometimes breaks Koopmans' theorem.
- Ionized species which ionized from σ orbital are stabilized than neutral but less than n.

Ionized states of (n^{-1}) are much stabilized than those of (π^{-1}) and consequently, makes the ordering of Koopmans is inverted. Stablization of the (n^{-1}) state is remarkable and essential. We approximately analyze this effect into three categories: orbital reorganization, static correlation or dynamic correlation. Here we define three effect as follows. Orbital relaxation is described within the SCF level, so we can evaluate this effect by ROHF for ionized state. Static correlations are calculated using the CI calculations within valence orbitals. Rest part of the electron correlations are due to the dynamic correlation, explained by dynamic motion of two electrons.

6.4.2 trans-acrolein

First, we studied simple system, trans-acrolein. We used 6-31G*/DFT(B3LYP) optimized geometry and double-ζ+polarized function(total basis function is 40 and number of electron is 30). We also analyzed ionization spectrum of this system in detail in the next chapter of this thesis.

1. Orbital relaxation effect

   We performed ΔSCF calculations for this system to see whether the reorganization of orbitals are essential or not. Figure XII shows orbital plot of HOMO$(2a''; n(\mathrm{O}))$ and next HOMO$(13a'; \pi)$ of ground state, HOMO$(2a''; n(\mathrm{O}))$ of $^2A'$ state by ROHF, HOMO$(13a'; \pi)$ of $^2A''$ state by ROHF with orbital energy. Apparently, reorganization of orbital is important in this case, and the ordering between n^{-1} and π^{-1} states is reproduced within ΔSCF, but the comparison of the calculated IPs with experiment is still poor, in agreement with the result of G. Granozzi *et al*[54].

2. Static correlation effect

   ionzae performed CAS calculation which includes n, π and π^* orbitals to see the static correlations. Table IX shows absolute value of CI coefficients larger than 0.05, its electronic configuration, and excitation or ionization nature of neutral and ionized states. Notably, ground and π state didn't have large CI coefficents for CI configuration including excitation from n orbital and this calculation gave the same ordering as the Koopmans'.

These results are compiled at table VII. In the case of acrolein, the breakdown of Koopmans' theorem is due to the dynamical correlation and partially reorganization of Hartree-Fock orbital.

Figure XII: MO plotting with symmetry, IP and nature for HOMO and next HOMO of trans-acrolein and HOMO of its cations

RHF, $2a''$, IP=10.85eV, n(O)

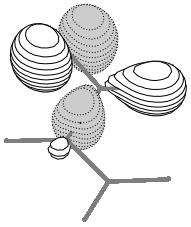

RHF, $13a'$, IP=11.74eV, π

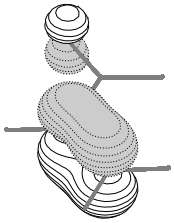

ROHF, $2a''$, IP=8.79eV, n(O)

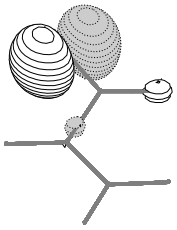

ROHF, $13a'$, IP=9.68eV, π

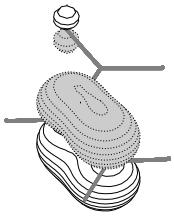

TABLE VII: The breakdown of Koopmans theorem for trans-acrolein.

	Nature	IP(Koopmans)	IP(ΔSCF)	IP(CI)	IP(SAC-CI/Gen-R)[a]	Exp.
$^2A'$	n(O)	11.74	8.789	11.07	9.62	10.10
$^2A''$	π	10.85	9.684	10.81	10.50	10.92

[a] Ref[57].

TABLE VIII: Small active space CI for trans-acrolein and its cations with coefficient, configuration and nature

ground state		
coeff. $\|C\| > 0.05$	configuration	nature
0.974322	–	–
−0.143017	$(2a'')^{-1}(2a'')^{-1}(3a'')(3a'')$	$\pi \to \pi^*, \pi \to \pi^*$
0.086639	$(1a'')^{-1}(2a'')^{-1}(3a'')(4a'')$	$\pi \to \pi^*, \pi \to \pi^*$
−0.073749	$(1a'')^{-1}(1a'')^{-1}(3a'')(4a'')$	$\pi \to \pi^*, \pi \to \pi^*$
−0.072494	$(1a'')^{-1}(1a'')^{-1}(3a'')(3a'')$	$\pi \to \pi^*, \pi \to \pi^*$
−0.055327	$(1a'')^{-1}(1a'')^{-1}(4a'')(4a'')$	$\pi \to \pi^*, \pi \to \pi^*$
0.058055	$(2a'')^{-1}(2a'')^{-1}(3a'')(4a'')$	$\pi \to \pi^*, \pi \to \pi^*$
	A' (n)	
0.945617	$(13a')^{-1}$	$n \to \infty$
−0.250830	$(13a')^{-1}(2a'')^{-1}(3a'')$	$n \to \infty, \pi \to \pi^*$
0.099352	$(13a')^{-1}(2a'')^{-1}(3a'')$	$n \to \infty, \pi \to \pi^*$
0.094282	$(13a')^{-1}(2a'')^{-1}(2a'')^{-1}(3a'')(3a'')$	$n \to \infty, \pi \to \pi^*, \pi \to \pi^*$
−0.075300	$(13a')^{-1}(2a'')^{-1}(4a'')$	$n \to \infty, \pi \to \pi^*$
0.061365	$(13a')^{-1}(1a'')^{-1}(4a'')$	$n \to \infty, \pi \to \pi^*$
	A'' (π)	
0.968055	$(2a'')^{-1}$	$\pi \to \infty$
−0.102828	$(2a'')^{-1}(1a'')^{-1}(1a'')^{-1}(3a'')(3a'')$	$\pi \to \infty, \pi \to \pi^*, \pi \to \pi^*$
0.100991	$(2a'')^{-1}(1a'')^{-1}(3a'')$	$\pi \to \infty, \pi \to \pi^*$
−0.095784	$(2a'')^{-1}(1a'')^{-1}(3a'')$	$\pi \to \infty, \pi \to \pi^*$
−0.084691	$(2a'')^{-1}(1a'')^{-1}(1a'')^{-1}(3a'')(4a'')$	$\pi \to \infty, \pi \to \pi^*, \pi \to \pi^*$
0.080244	$(2a'')^{-1}(1a'')^{-1}(4a'')$	$\pi \to \infty, \pi \to \pi^*$
−0.079420	$(2a'')^{-1}(1a'')^{-1}(1a'')^{-1}(2a'')(3a'')$	$\pi \to \infty, \pi \to \pi, \pi \to \pi^*$
−0.051979	$(2a'')^{-1}(1a'')^{-1}(2a'')$	$\pi \to \infty, \pi \to \pi$
−0.055090	$(2a'')^{-1}(1a'')^{-1}(1a'')^{-1}(4a'')(4a'')$	$\pi \to \infty, \pi \to \pi^*, \pi \to \pi^*$

TABLE IX: The breakdown of Koopmans theorem for pyrazine.

	Nature	IP(Koopmans)	IP(ΔSCF)	IP(CI)	IP(SAC-CI/SD-R)	Exp.[a]
A_g	n(N)	11.22	10.250	10.22	9.49	9.61
B_{1g}	π(C − C)	9.83	9.050	9.93	10.06	10.20
B_{1u}	n(N)	13.66	12.195	11.96	11.30	11.38
B_{2g}	π(N − N)	11.89	10.884	11.56	11.64	11.80

[a] Ref[17].

6.4.3 pyrazine

Next, we studied pyrazine. Results for these effects are compiled in table VIII.

1. Orbital relaxation effect

   Lower four ionized states have different spatial symmetry, so the ROHF is well-defined. Practically, we performed MCSCF calculation with higher four orbitals. In figure XIII, we show MOs of ground state: $6a_g$, $1b_{1g}$, $5b_{1u}$, $1b_{2g}$ and $6a_g$(HOMO) orbital of ROHF(A_g state), $1b_{1g}$(HOMO) of ROHF(B_{1g} state), $5b_{1u}$(HOMO) of ROHF(B_{1u} state) and $1b_{2g}$ of ROHF(B_{2g} state) calculation with orbital energy. Symmetric restriction of this system may prohibit to delocalize even for ROHF calculation, anyway, reorganization of MO was not drastic effect.

2. Static correlation effect

   In this system, we include n, π and π^* orbitals as active space and performed CI calculations up to 8 electron excitations(see table X). As shown before, ground and π state didn't have large CI coefficents for CI configuration including excitation from n orbital. Major improvement is observed for B_{1u} state, however $0.5 \sim 0.6$eV should be lower to be inverted, lacking taking into accout the dynamic correlation.

Figure XIII: MO plotting with symmetry, IP and nature for higher four orbitals form HOMO of pyrazine and HOMO of its cations

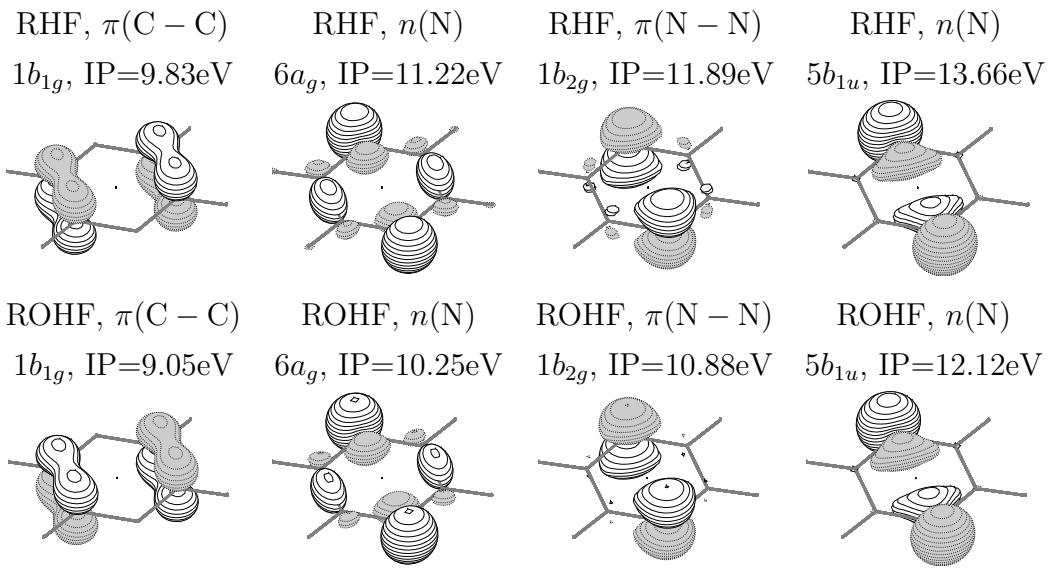

TABLE X: Small active space CI for pyrazine and its cations with coefficient, configuration and nature

coeff. $\lvert C\rvert > 0.05$	configuration	nature
	ground state	
0.956450	–	–
−0.133518	$(5b_{1u})^{-1}(5b_{1u})^{-1}(7a_g)(7a_g)$	$\pi \to \pi^*, \pi \to \pi^*$
−0.127366	$(1b_{2g})^{-1}(1b_{1g})^{-1}(2b_{3u})(1a_u)$	$\pi \to \pi^*, \pi \to \pi^*$
−0.124076	$(1b_{1g})^{-1}(1b_{1g})^{-1}(1a_u)(1a_u)$	$\pi \to \pi^*, \pi \to \pi^*$
0.095335	$(1b_{3u})^{-1}(1b_{2g})^{-1}(2b_{3u})(2b_{2g})$	$\pi \to \pi^*, \pi \to \pi^*$
0.076691	$(1b_{2g})^{-1}(1b_{1g})^{-1}(2b_{3u})(1a_u)$	$\pi \to \pi^*, \pi \to \pi^*$
−0.069815	$(1b_{3u})^{-1}(1b_{1g})^{-1}(1a_u)(2b_{2g})$	$\pi \to \pi^*, \pi \to \pi^*$
−0.054024	$(1b_{1g})^{-1}(1b_{1g})^{-1}(2b_{3u})(2b_{3u})$	$\pi \to \pi^*, \pi \to \pi^*$
	A_g (n)	
0.931961	$(6a_g)^{-1}$	$n \to \infty$
−0.207546	$(6a_g)^{-1}(5b_{1u})^{-1}(1b_{2g})^{-1}(6a_g)(2b_{3u})$	$n \to \infty, n \to \pi^*, \pi \to n$
0.103577	$(6a_g)^{-1}(1b_{1g})^{-1}(1b_{1g})^{-1}(1a_u)(1a_u)$	$n \to \infty, \pi \to \pi^*, \pi \to \pi^*$
−0.088880	$(6a_g)^{-1}(1b_{2g})^{-1}(2b_{2g})$	$n \to \infty, \pi \to \pi^*$
−0.084642	$(6a_g)^{-1}(1b_{2g})^{-1}(1b_{2g})^{-1}(2b_{3u})(2b_{3u})$	$n \to \infty, \pi \to \pi^*, \pi \to \pi^*$
0.081555	$(6a_g)^{-1}(5b_{1u})^{-1}(1b_{1g})^{-1}(6a_g)(1a_u)$	$n \to \infty, n \to \pi^*, n \to \pi$
−0.078792	$(6a_g)^{-1}(1b_{2g})^{-1}(1b_{1g})^{-1}(2b_{3u})(1a_u)$	$n \to \infty, \pi \to \pi^*, \pi \to \pi^*$
0.075114	$(6a_g)^{-1}(1b_{1g})^{-1}(1b_{1g})^{-1}(2b_{3u})(2b_{3u})$	$n \to \infty, \pi \to \pi^*, \pi \to \pi^*$
−0.067416	$(6a_g)^{-1}(1b_{3u})^{-1}(1b_{2g})^{-1}(2b_{3u})(2b_{2g})$	$n \to \infty, \pi \to \pi^*, \pi \to \pi^*$
−0.061705	$(6a_g)^{-1}(1b_{2g})^{-1}(1b_{1g})^{-1}(2b_{3u})(1a_u)$	$n \to \infty, \pi \to \pi^*, \pi \to \pi^*$
−0.056898	$(6a_g)^{-1}(1b_{3u})^{-1}(1b_{1g})^{-1}(1a_u)(2b_{2g})$	$n \to \infty, \pi \to \pi^*, \pi \to \pi^*$
−0.054627	$(6a_g)^{-1}(5b_{1u})^{-1}(1b_{1g})^{-1}(6a_g)(1a_u)$	$n \to \infty, n \to \pi, n \to \pi^*$
−0.050879	$(6a_g)^{-1}(1b_{3u})^{-1}(2b_{3u})$	$n \to \infty, \pi \to \pi^*$
	B_{1g} (π)	
0.960874	$(1b_{1g})^{-1}$	$\pi \to \infty$
0.136481	$(1b_{1g})^{-1}(1b_{3u})^{-1}(2b_{3u})$	$\pi \to \infty, \pi \to \pi^*$
−0.122533	$(1b_{1g})^{-1}(1b_{2g})^{-1}(1b_{2g})^{-1}(2b_{3u})(2b_{3u})$	$\pi \to \infty, \pi \to \pi^*, \pi \to \pi^*$
−0.089768	$(1b_{1g})^{-1}(1b_{3u})^{-1}(1b_{2g})^{-1}(2b_{3u})(2b_{2g})$	$\pi \to \infty, \pi \to \pi^*, \pi \to \pi^*$
−0.081438	$(1b_{1g})^{-1}(1b_{2g})^{-1}(1b_{1g})^{-1}(2b_{3u})(1a_u)$	$\pi \to \infty, \pi \to \pi^*, \pi \to \pi^*$
0.067593	$(1b_{1g})^{-1}(1b_{2g})^{-1}(2b_{2g})$	$\pi \to \infty, \pi \to \pi^*$
0.065952	$(1b_{1g})^{-1}(1b_{3u})^{-1}(1b_{2g})^{-1}(1b_{1g})(1a_u)$	$\pi \to \infty, \pi \to \pi^*, \pi \to \pi$
−0.056833	$(1b_{1g})^{-1}(1b_{3u})^{-1}(1b_{3u})^{-1}(2b_{3u})(2b_{3u})$	$\pi \to \infty, \pi \to \pi^*, \pi \to \pi^*$

CONTINUE

B_{1u} (n)

coeff. $\lvert C\rvert > 0.05$	configuration	nature
0.895097	$(5b_{1u})^{-1}$	$n \rightarrow \infty$
−0.290826	$(5b_{1u})^{-1}(1b_{2g})^{-1}(6a_g)^{-1}(5b_{1u})(2b_{3u})$	$n \rightarrow \infty, n \rightarrow \pi, n \rightarrow \pi^*$
−0.126430	$(5b_{1u})^{-1}(1b_{2g})^{-1}(2b_{2g})$	$n \rightarrow \infty, \pi \rightarrow \pi^*$
0.107622	$(5b_{1u})^{-1}(6a_g)^{-1}(1b_{1g})^{-1}(5b_{1u})(1a_u)$	$n \rightarrow \infty, n \rightarrow \pi, n \rightarrow \pi^*$
0.096936	$(5b_{1u})^{-1}(1b_{1g})^{-1}(1b_{1g})^{-1}(1a_u)(1a_u)$	$n \rightarrow \infty, \pi \rightarrow \pi^*, \pi \rightarrow \pi^*$
0.090525	$(5b_{1u})^{-1}(1b_{1g})^{-1}(1b_{1g})^{-1}(2b_{3u})(2b_{3u})$	$n \rightarrow \infty, \pi \rightarrow \pi^*, \pi \rightarrow \pi^*$
−0.088899	$(5b_{1u})^{-1}(1b_{3u})^{-1}(2b_{3u})$	$n \rightarrow \infty, \pi \rightarrow \pi^*$
−0.076040	$(5b_{1u})^{-1}(1b_{2g})^{-1}(6a_g)^{-1}(5b_{1u})(2b_{3u})$	$n \rightarrow \infty, n \rightarrow \pi, n \rightarrow \pi^*$
−0.075921	$(5b_{1u})^{-1}(6a_g)^{-1}(1b_{1g})^{-1}(5b_{1u})(1a_u)$	$n \rightarrow \infty, n \rightarrow \pi, n \rightarrow \pi^*$
0.067139	$(5b_{1u})^{-1}(1b_{3u})^{-1}(5b_{1u})(1b_{2g})^{-1}(6a_g)^{-1}(2b_{3u})(2b_{3u})$	$n \rightarrow \infty, \pi \rightarrow \pi^*, n \rightarrow \pi^*, \pi \rightarrow n$
−0.064184	$(5b_{1u})^{-1}(1b_{2g})^{-1}(1b_{1g})^{-1}(2b_{3u})(1a_u)$	$n \rightarrow \infty, \pi \rightarrow \pi^*, \pi \rightarrow \pi^*$
−0.059895	$(5b_{1u})^{-1}(1b_{2g})^{-1}(1b_{1g})^{-1}(2b_{3u})(1a_u)$	$n \rightarrow \infty, \pi \rightarrow \pi^*, \pi \rightarrow \pi^*$
−0.059485	$(5b_{1u})^{-1}(1b_{2g})^{-1}(1b_{2g})^{-1}(2b_{3u})(2b_{3u})$	$n \rightarrow \infty, \pi \rightarrow \pi^*, \pi \rightarrow \pi^*$
0.055060	$(5b_{1u})^{-1}(1b_{3u})^{-1}(1b_{1g})^{-1}(1a_u)(2b_{2g})$	$n \rightarrow \infty, \pi \rightarrow \pi^*, \pi \rightarrow \pi^*$

B_{2g} (π)

0.943009	$(1b_{2g})^{-1}$	$\pi \rightarrow \infty$
−0.115680	$(1b_{2g})^{-1}(1b_{3u})^{-1}(2b_{3u})$	$\pi \rightarrow \infty, \pi \rightarrow \pi^*$
0.133021	$(1b_{2g})^{-1}(1b_{3u})^{-1}(1b_{1g})^{-1}(1b_{2g})(1a_u)$	$\pi \rightarrow \infty, \pi \rightarrow \pi, \pi \rightarrow \pi^*$
−0.131040	$(1b_{2g})^{-1}(1b_{3u})^{-1}(2b_{3u})$	$\pi \rightarrow \infty, \pi \rightarrow \pi^*$
−0.100320	$(1b_{2g})^{-1}(1b_{2g})^{-1}(2b_{2g})$	$\pi \rightarrow \infty, \pi \rightarrow \pi^*$
0.099386	$(1b_{2g})^{-1}(1b_{1g})^{-1}(1b_{1g})^{-1}(1a_u)(1a_u)$	$\pi \rightarrow \infty, \pi \rightarrow \pi^*, \pi \rightarrow \pi^*$
0.086177	$(1b_{2g})^{-1}(1b_{1g})^{-1}(1b_{1g})^{-1}(2b_{3u})(2b_{3u})$	$\pi \rightarrow \infty, \pi \rightarrow \pi^*, \pi \rightarrow \pi^*$
0.075080	$(1b_{2g})^{-1}(1b_{1g})^{-1}(1b_{1g})^{-1}(1b_{2g})(2b_{2g})$	$\pi \rightarrow \infty, \pi \rightarrow \pi, \pi \rightarrow \pi^*$
0.068746	$(1b_{2g})^{-1}(1b_{3u})^{-1}(1b_{3u})^{-1}(2b_{3u})(2b_{3u})$	$\pi \rightarrow \infty, \pi \rightarrow \pi^*, \pi \rightarrow \pi^*$
−0.057473	$(1b_{2g})^{-1}(1b_{2g})^{-1}(1b_{1g})^{-1}(2b_{3u})(1a_u)$	$\pi \rightarrow \infty, \pi \rightarrow \pi^*, \pi \rightarrow \pi^*$
0.055556	$(1b_{2g})^{-1}(1b_{3u})^{-1}(1b_{1g})^{-1}(1a_u)(2b_{2g})$	$\pi \rightarrow \infty, \pi \rightarrow \pi^*, \pi \rightarrow \pi^*$
0.053723	$(1b_{2g})^{-1}(1b_{3u})^{-1}(1b_{2g})^{-1}(2b_{3u})(2b_{2g})$	$\pi \rightarrow \infty, \pi \rightarrow \pi^*, \pi \rightarrow \pi^*$

6.5 Conclusion

The SAC-CI SD-R method has been applied to the detailed assignment of the outer-valence ionization spectra of pyrazine, pyridazine, pyrimidine, and s-triazine. The peak positions of the photoelectron spectra of these molecules have successfully reproduced and the detailed characterization for both main peaks and satellite peaks has been proposed.

We examined the ordering of the main peaks, some of which were contradictory proposed in the previous works. We also analyzed the low-lying satellite peaks in the energy region of $18 \sim 20$ eV in detail. These satellite peaks of these molecules have not been well assigned so far. In this region, some satellites with considerable intensity were calculated for pyrazine and pyridazine, while no remarkable satellite peaks were obtained for pyrimidine and s-triazine. This accords with the recent experimental work by the PIES and He I UPS. In the higher-energy region above 20 eV, the remarkable breakdown of the Koopmans' picture was seen for all the azines and numerous shake-up states were obtained as the continuous band.

Positions of the correlation peaks at 24$\sim$30eV were accounted by the nature of the canonical orbital energy. Position of the nitrogen atom, which separates σ orbital and affects the orbital energy, was found to be important, and we predicted some peaks which have not been observed for pyridazine and s-triazine.

Finally, we proved that breakdown of Koopmans' theorem were due to dynamic correlation. However, it is still unclear why this is effective *only* for n orbitals. A simple explanation by Cederbaum[49] was that static correlation is important for N_2 and F_2, but does not seems to be true for generic systems, because the number of electrons is so small that they may also include quite large amount of dynamic correlation. In section 6.4, all calculation other than SAC-CI are calculated by gamess[58].

6.6 Acknowledgments

This study has been supported by the Grant for Creative Scientific Research from the Japanese Ministry of Education, Science, Culture, and Sports and a grand of Kyoto University VBL project. All MO plottings were done by MOLDEN[59].

BIBLIOGRAPHY

[1] W. von Niessen, W. P. Kraemer and G. H. F. Diercksen, Chem. Phys., **10**, 345 (1975); *ibid*, **41** 113 (1979).

[2] W. von Niessen, J. Schirmer and L. S. Cederbaum, Comput. Phys. Rep., **1**, 57 (1984).

[3] P. Decleva, G. Fronzoni, G. Dealti and A. Lisini, J. Mol. Spectrosc., **184**, 49 (1989).

[4] I. C. Walker, M. H. Palmer, and A. Hopkirk, Chem. Phys., **141**, 365 (1990).

[5] M. H. Palmer, I. C. Walker, M. F. Guest, and A. Hopkirk, Chem. Phys., **147**, 19 (1990).

[6] I. C. Walker and M. H. Palmer, Chem. Phys., **153**, 169 (1991).

[7] M. H. Palmer and I. C. Walker, Chem. Phys., **157**, 187 (1991).

[8] I. C. Walker, M. H. Palmer, and C. C. Ballard, Chem. Phys.,**167**, 61 (1992).

[9] J. V. Ortiz and V. G. Zakrzewski, J. Chem. Phys., **105**, 2762 (1996).

[10] O. Kitao and H. Nakatsuji, J. Chem. Phys., **88**, 4913 (1988).

[11] J. Wan, M. Hada, M. Ehara, H. Nakatsuji, J. Chem. Phys., **114**, 5117 (2001).

[12] M. S. Moghaddam, A. D. O. Bawagan, K. H. Tan, and W. von Niessen, Chem. Phys., **207**, 19 (1996).

[13] C. Fridh, L. Åsbrink, B. Ö. Jonsson, and E. Lindholm, Int. J. Mass Spec. and Ion Phys., **8**, (85) 1972.

[14] Fridh, L. Åsbrink, B. Ö. Jonsson, and E. Lindholm, Int. J. Mass Spec. and Ion Phys., **8**, 101 (1972).

[15] L. Åsbrink, C. Fridh, B. Ö. Jonsson, and E. Lindholm, Int. J. Mass Spec. and Ion Phys., **8**, (229) 1972.

[16] L. Åsbrink, C. Fridh, B. Ö. Jonsson, and E. Lindholm, Int. J. Mass Spec. and Ion Phys., **8**, (215) 1972.

[17] N. Kishimoto, K. Ohno, J. Phys. Chem. A, **104**, 6940 (2000).

[18] R. E. Turmer, V. Vaida, C. A. Mollini, J. O. Berg, and D. H. Parker, Chem. Phys., **28**, 47 (1978).

[19] K. K. Innes, I. G. Ross, and W. R. Moomaw, J. Mol. Spectrosc., **132**, 492 (1988).

[20] A. Bolovinos, P. Tsekeris, J. Philis, E. Pantos, and G. Andritsopoulus, J. Mol. Spectrosc., **103**, 240 (1984).

[21] R. A. MacRae, M. W. Williams, and E. T. Arakawa, J. Chem. Phys., **61**, 861 (1974).

[22] J. O. Berg, D. H. Parker, and M. A. El-Sayed, Chem. Phys. Lett., **56**, 411 (1978).

[23] B. O. Jonsson and E. Lindholm, Int. J. Mass Spectrom. Ion Phys., **3**, 385 (1969).

[24] E. H. van Veen, and F. L. Plantenga, Chem. Phys. Lett., **80**, 28 (1975).

[25] J. P. Doering and J. H. Moore, J. Chem. Phys., **56**, 2176 (1972).

[26] C. R. Brundle, M. B. Robin, and N. A. Kuebler, J. Am. Chem. Soc., **94**, 1466 (1974).

[27] I. Reineck, R. Maripuu, H. Veenhuizen, L. Karlsson, K. Siegbahn, M. S. Powar, W. N. Zu, J. M. Rong, and S. H. Alshamma, J. Electron Spectrosc., **27**, 15 (1982).

[28] M. P. Fülscher, K. Andersson, and B. O. Roos, J. Phys. Chem. **96**, 9204 (1992).

[29] H. Nakatsuji, and K. Hirao, J. Chem. Phys., **68**, 2053(1978).

[30] H. Nakatsuji, Chem. Phys. Lett., **59**, 362(1978).

[31] H. Nakatsuji, Chem. Phys. Lett., **67**, 329(1979).

[32] H. Nakatsuji, in *Computational Chemistry: Reviews of Current trends*, edited by J. Leszcznski (World Scientific, Singapore,1997), Vol. 2.

[33] K. Hirao and H. Nakatsuji, Chem. Phys. Lett., **79**, 292(1981).

[34] H. Nakatsuji, Chem. Phys., **75**, 425 (1983).

[35] H. Nakatsuji, Chem. Phys. Lett., **177**, 331 (1991).

[36] H. Nakatsuji, J. Chem. Phys., **83**, 5743 (1985).

[37] H. Nakatsuji, M. Hada, M. Ehara, J. Hasegawa, T. Nakajima, H. Nakai, O. Kitao, and K. Toyota, SAC/SAC-CI program system (SAC-CI96) for calculating ground, excited, and electron attached sates and singlet to septet spin multiplicites.

[38] W. Pyckout, I. Callaerts C. V. Alsenoy and H. J. Geise, J. Mol. Struct., **147**, 321 (1986).

[39] S. Cradock, P. B. Liescheski, D. W. H. Rankin, H. E. Robertson, J. Am. Chem. Soc., **110**, 2758 (1988).

[40] S. Cradock, C. Purves, D. W. H. Rankin, J. Mol. Struct., **220**, 193 (1990).

[41] B. Bak, L. Hansen, J. Rastrup-Andersen, J. Chem. Phys., **22**, 2013 (1954).

[42] S. Huzinaga, J. Chem. Phys. **42**, 1293 (1965), T.H. Dunning, Jr., J. Chem. Phys., **53**, 2823 (1970), T.H. Dunning, Jr. and P.J. Hay, In Methods Of Electronic Structure Theory, Vol. 2, H.F. Schaefer III, Ed., Plenum Press (1977).

[43] Basis sets were obtained from the Extensible Computational Chemistry Environment Basis Set Database, Version 4/22/01, as developed

and distributed by the Molecular Science Computing Facility, Environmental and Molecular Sciences Laboratory, the Pacific Northwest Laboratory, P.O. Box 999, Richland, Washington 99352, USA. URL is `http://www.emsl.pnl.gov:2080/forms/basisform.html`.

[44] S. Süzer, S. T. Lee, and D. A. Shirley, Phys. Rev. A, **13**, 1842 (1976).

[45] R. I. Martin and D. A. Shirley, J. Chem. Phys., **64**, 3685 (1976).

[46] H. Nakatsuji, M. Hada, M. Ehara, J. Hasegawa, T. Nakajima, H. Nakai, O. Kitao, and K. Toyota, SAC/SAC-CI program system (SAC-CI96) for calculating ground, excited, and electron attached sates and singlet to septet spin multiplicites

[47] Gaussian01, M. J. Frisch, G. W. Trucks, H. B. Schlegel *et al.* (Gaussian, Inc., Pittsburgh, PA, 1998)

[48] L.S. Cederbaum, G. Hohlneicher and W. von Niessen, Chem. Phys. Lett., **18**, 503(1973).

[49] L.S. Cederbaum, Chem. Phys. Lett., **25**, 562(1974).

[50] L.S. Cederbaum, W. Domcke, W. von Nissen, Chem. Phys., **10**, 459(1975).

[51] W. von Nissen, G.H.F. Diereksen, L.S. Cederbaum, J. Chem. Phys., **67**, 4124(1977).

[52] W. von Nissen, W. Kraemer, G. Diercksen, Chem. Phys., **41**, 113(1979).

[53] G. Bieri, E. Heilbronner, V. Hornung, E. Kloster-Jensen, J. P. Maier, F. Thommen, Chem. Phys., **36**, 1(1979).

[54] G. Granozzi,D. Ajo, I. Fragala, J. Electron Spectrosc. Relat. Phenom., **18** 267 (1980).

[55] W. von Nissen, G. Bieri, J. Schirmer, L.S. Cederbaum, Chem. Phys., **65**, 157(1982).

[56] J. Electron Spectrosc. Relat. Phenom., **5** 985 (1974).

[57] K. Kimura, S. Katsumata, Y. Achiba, T. Yamasaki, and S. Iwata, *Handbook of He I Photoelectron Spectra*, Halsted Press, New York 1980.

[58] "General Atomic and Molecular Electronic Structure System" M.W.Schmidt, K.K.Baldridge, J.A.Boatz, S.T.Elbert, M.S.Gordon, J.H.Jensen, S.Koseki, N.Matsunaga, K.A.Nguyen, S.Su, T.L.Windus, M.Dupuis, J.A.Montgomery J. Comput. Chem., 14, 1347-63(1993).

[59] G.Schaftenaar and J.H. Noordik, "Molden: a pre- and post-processing program for molecular and electronic structures", J. Comput.-Aided Mol. Design, 14 (2000) 123-134.

Chapter 7.

Outer-valence ionization spectra of methylenecyclopropane and trans-acrolein studied by the SAC-CI general-R method

Abstract

The outer-valence ionization spectra of methylenecyclopropane and trans-acrolein have been studied by the SAC-CI (symmetry-adapted-cluster configuration-interaction) general-R method. Experimental photoelectron spectra of these molecules were accurately reproduced and the detailed interpretation of the satellite peaks was performed. For methylenecyclopropane, three satellite peaks were calculated at around 17 eV and the remarkable breakdown of the Koopman's picture was seen for $(5a_1)^{-1}$ state, which were not addressed in the experimental work. For trans-acrolein, a CI state at 15.5 eV was confirmed and many satellite peaks were obtained from 17 eV interacting with $(8a')^{-1}$ and $(7a')^{-1}$ states.

7.1 Introduction

Recently, valence ionization spectrum of molecules has been extensively studied in both the experimental and theoretical works and the detailed assignment has become possible not only for the main peaks but satellite peaks. The accurate characterization of the spectrum has been achieved by the cooperative interplay of these works; since the correlation peaks are described by the more-than-two electron processes [1, 2, 3], theoretical information is indispensable for the detailed assignments of these peaks. There are also interesting spectroscopies like Penning ionization spectroscopy (PIES) and electron momentum spectroscopy (EMS) besides the high-resolution photoelectron spectroscopy (PES) using synchrotron radiation (SR-PES) or X-ray PES.

Ionization spectrum of the molecule with π conjugation are of special interest, since they have many satellite peaks in the low-energy region. They are usually attributed to the two-electron process accompanied with the excitation to π^* MOs. Outer-valence ionization spectra of the trans-acrolein was measured by He I [4] and He II [5] PES. The He II PES was interpreted by the Green's function calculation [6] and later, the 2h-1p CI calculation [7]. The PIES was also applied to the outer-valence region [8]. For the methylenecyclopropane, only the He I PES [4, 9, 10] have been applied by some group and there is no information for the higher-energy outer-valence region. CI calculation was performed for the assignments, however, the results were limited up to 17 eV. Both of these molecules have some interesting correlation peaks in the outer-valence region and therefore, accurate theoretical information is very useful.

In the series of the studies, we have investigated the valence ionization spectra of various molecules using the SAC-CI (symmetry-adapted-cluster configuration-interaction) method. The SAC/SAC-CI method [11, 12, 13, 14, 15] has been successfully applied to a number of molecular spectroscopies [16, 17, 18, 19, 20] including the ionization spectrum. Especially, SAC-CI general-R method [21, 22] has been proved to be a powerful tool for describing the multiple electron processes in high accuracy and studying the large numbers of states appearing in the ionization

spectrum[23, 24, 25, 26, 27, 28, 29].

Figure I: Structure and coordinate for methylenecyclopropane and trans-acrolein

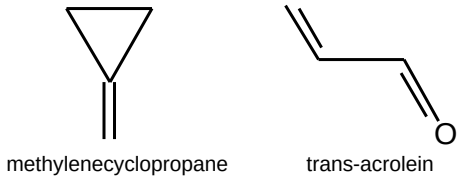

7.2 Computational details

The vertical ionization process was studied in this work and the optimized geometries were used for both methylenecyclopropane in C_{2v} and trans-acrolein in C_s. Optimizations were performed by B3LYP[30]/6-311G*[31]. The basis sets were due to the DZ1P quality; [4s2p1d/2s1p][32, 33] for both molecules. The resultant SCF dimensions were 90 and 60 for methylene cyclopropane and trans-acrolein, respectively.

The valence ionization spectra of these molecules were calculated by the SAC-CI general-R method in the outer-valence region to interpret the He I or He II PES. The 1s orbitals of C and O were kept as frozen core and all the other MOs were included in the active space; the active space of the SAC-CI consisted 11 occupied and 75 unoccupied MOs for methylenecyclopropane and 11 occupied and 65 unoccupied MOs for trans-acrolein. Valence MOs are plotted with orbital energy, and character by MOLDEN[34] are also shown in figure V and VI.

To reduce the computational effort, perturbation selection [15] was performed in the state-selection scheme [35]. In the SAC ground-state calculation, all single-excitation and selected S_I^+ were included in the linked term. The energy threshold λ_g for perturbation selection(PS) was 1.0×10^{-5} a.u. For the unlinked term, we included only the products of the double-excitation operators $S_I^+ S_J^+$ when the coefficients C_I and C_J, estimated by SD-CI in practice, were lager than 1.0×10^{-3}. In the SAC-CI

general-R calculations for the ionized states, a preliminary SDCI calculation was performed to select the higher-order operators required for a quantitative description of the multi-electron process. Since the shake-up states in the outer-valence region of these molecules are dominantly described by two-electron processes, the higher-order operators were limited up to triples and the energy thresholds of R-operators were of $\lambda_e = 1 \times 10^{-7}$ and 1×10^{-6} for doubles and triples, respectively. The thresholds of the CI coefficients for calculating the unlinked operators in the SAC-CI method are 0.05 and 1×10^{-8} for the R and S operators, respectively.

Ionization cross-sections were calculated using the monopole approximation [36, 37] to estimate the relative intensities of the peaks. Both initial- and final-state correlation effects are included.

The SAC/SAC-CI calculations were executed using the SAC96 program system [38], which has been incorporated into the development version of the Gaussian suite of programs [39].

7.3 Results and discussions

The Hartree-Fock orbital sequences of the methylenecyclopropane and trans-acrolein were summarized in Table I. The SCF energy of these molecules are calculated to be -154.9168 and -190.8027 au with the present conditions.

TABLE I: Ground-state valence electronic configurations

System	Hartree-Fock valence configuration
methylenecyclopropane	$(1a_1)(2a_1)(1b_2)(3a_1)(4a_1)(5a_1)(2b_2)(6a_1)(1b_1)(7a_1)(3b_2)(1a_2)(8a_1)(4b_2)(2b_1)$
trans-acrolein	$(1a')(2a')(3a')(4a')(5a')(6a')(7a')(8a')(9a')(10a')(11a')(12a')(1a'')(13a')(2a'')$

7.3.1 methylenecyclopropane

The He I PES of this molecule was measured by Kimura *et al.* and the theoretical assignment was done with the CI calculation up to 17.0 eV [4]. In the present

Figure II: Outer-valence ionization spectra of methylenecycloprpane by (a) He I PES and (b) SAC-CI general-R

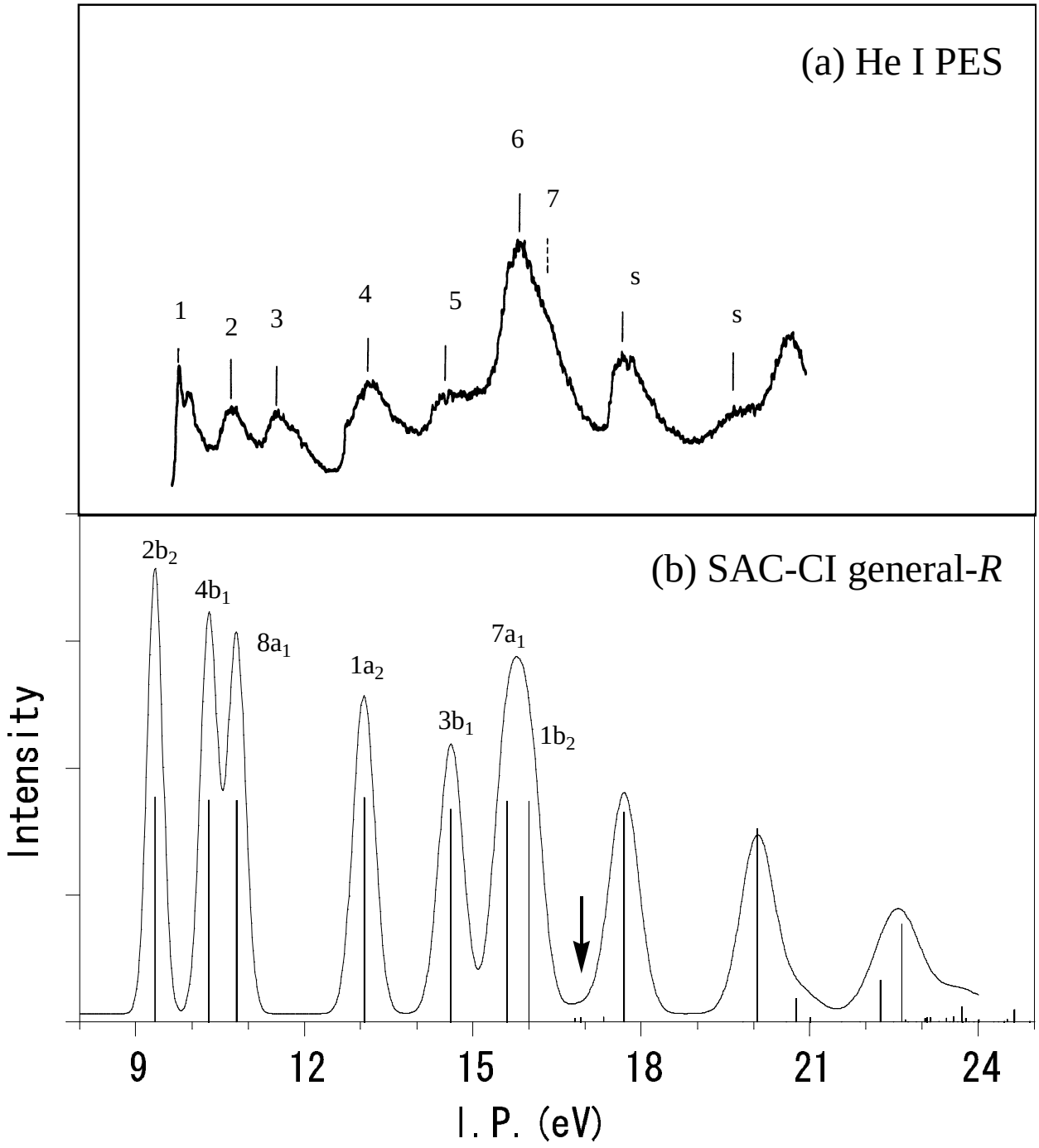

Figure III: Valence MO plotting and its nature with orbital energy methylenecyclopropane

15th, $\pi(\mathrm{C}-\mathrm{C})$, $2b_1$, -9.782

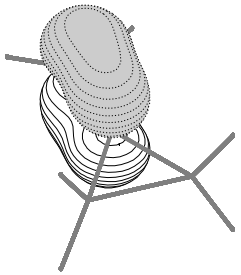

14th, $\sigma(\mathrm{C}-\mathrm{C})$, $4b_2$, -11.458

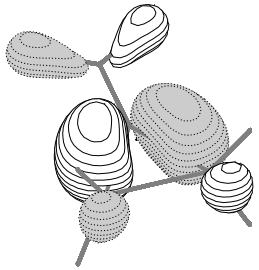

13th, $\sigma(\mathrm{C}-\mathrm{C})$, $8a_1$, -11.861

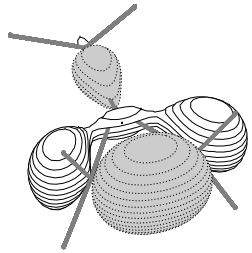

12th, $\sigma(\mathrm{C}-\mathrm{H})$, $1a_2$, -14.129

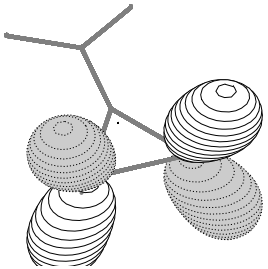

11th, $\sigma(\mathrm{C}-\mathrm{H})$, $3b_2$, -16.134

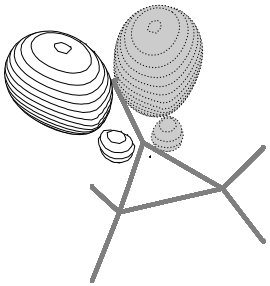

10th, $\sigma(\mathrm{C}-\mathrm{H})$, $7a_1$, -17.314

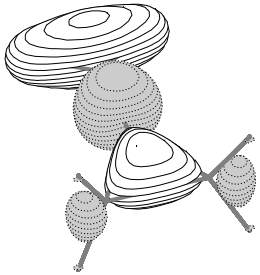

9th, $\sigma(\mathrm{C}-\mathrm{H})$, $1b_1$, -17.484

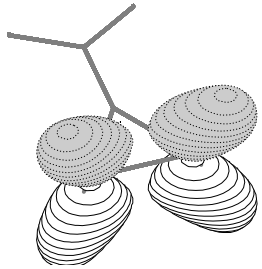

8th,$\sigma(\mathrm{C}-\mathrm{H})$, $6a_1$, -19.789

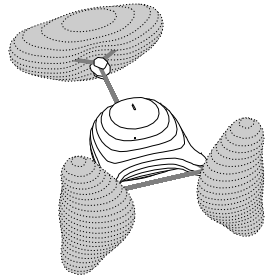

7th, $\sigma(\mathrm{C}-\mathrm{H})$, $2b_2$, -22.630

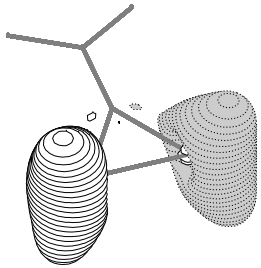

6th,$\sigma(\mathrm{C}-\mathrm{C})$, $5a_1$, -26.473

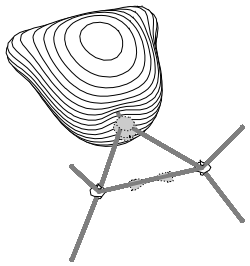

5th, $\sigma(\mathrm{C}-\mathrm{C})$, $4a_1$, -31.245

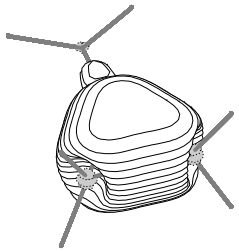

structure

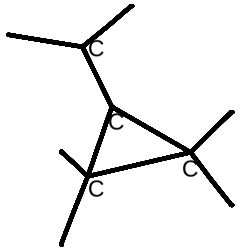

TABLE II: SAC-CI general-R dimensions

system	Single	Double	Triple	Quadruple	Quintuple	Sextuples
methylenecyclopropane(A_1)	5	2392	10824	6139	2753	33
methylenecyclopropane(A_2)	1	2034	11051	6886	2560	32
methylenecyclopropane(B_1)	2	2102	10246	6737	2675	39
methylenecyclopropane(B_2)	3	2340	11013	6082	2923	34
trans-acrolein(A')	9	4435	4389	1736	701	0
trans-acrolein(A'')	2	3120	5391	1980	805	9

work, the outer-valence ionization spectrum was studied up to around 22 eV. For obtaining the spectrum in this energy region, fifteen solutions were calculated for each symmetry of C_{2v} point group. The resultant SAC-CI general-R dimensions were summarized in Table II. In Fig. 1, the He I PES [4] and the SAC-CI spectra are compared. The theoretical spectrum was convoluted with Gaussian envelope for describing the Frank-Condon width and the resolution of spectrometer; the fwhm of Gaussian was taken to $0.05 \times \Delta E$ (in eV). In Table III, the results of IPs, monopole intensities, and detailed ionization characters for the valence ionized states, which have large intensity greater than 0.005 were presented with the IPs of He I PES and CI calculation. First three peaks observed at 9.76, 10.72 and 11.44 eV [4] were assigned to the ionizations from the outer three MOs, $2b_1$, $4b_2$ and $8a_1$, respectively. The present calculation computed the IPs of these states relatively lower in energy as 9.34, 10.30 and 10.79 eV. The next continuous four peaks at 13.1, 14.5, 15.8, and 16.3 eV in the He I PES [4] were attributed to the $^2A_2$, $^2B_2$, $^2A_1$ and $^2B_1$ states and they were calculated at 13.06, 14.61, 15.60 and 16.00 eV, respectively. These seven ionizations are dominantly described by the one-electron process and the monopole intensities are large. The Koopmans's ordering is valid for these states. Note that B_2 state at 14.61 eV is slightly contributed by two-electron process. In the higher-energy region of $(1b_1)^{-1}$, three shake-up states were predicted at 16.82, 16.92 and 17.34 eV. These peaks were not addressed in the He I PES work, however, the observed band around 16 eV has the asymmetric shape and

TABLE III: Calculated ionization potentials (IP, in eV), monopole intensities (M.I.), and main configurations with the basis set for methylenecyclopropane by SAC-CI general-R

Sym.	Main Configuration($\|C\| > 0.2$)	M.I.	IP	Expt.	CI
B_1	$0.94(2b_1^{-1})$	0.8873	9.34	9.76	9.35
B_2	$0.93(4b_2^{-1})$	0.8747	10.30	10.72	10.39
A_1	$0.93(8a_1^{-1})$	0.8734	10.79	11.44	10.87
A_2	$0.94(1a_2^{-1})$	0.8842	13.06	13.1	13.22
B_2	$0.91(3b_2^{-1})-0.25(2b_1^{-1}3b_14b_2^{-1})$	0.8393	14.61	14.5	14.79
A_1	$0.93(7a_1^{-1})$	0.8691	15.60	15.8	16.06
B_1	$0.93(1b_1^{-1})$	0.8702	16.00	16.3	16.37
B_2	$1.06(4b_2^{-1}3b_12b_1^{-1})+0.49(2b_1^{-1}3b_14b_2^{-1})+0.29(4b_2^{-1}7b_12b_1^{-1})$	0.0130	16.82		
A_1	$1.06(8a_1^{-1}3b_12b_1^{-1})+0.52(2b_1^{-1}3b_18a_1^{-1})+0.25(8a_1^{-1}7b_12b_1^{-1})$	0.0176	16.92		
B_1	$1.28(2b_1^{-1}3b_12b_1^{-1})+0.32(2b_1^{-1}7b_12b_1^{-1})$	0.0191	17.34		
A_1	$0.91(6a_1^{-1})$	0.8269	17.70	$\sim$17.7	
B_2	$0.87(2b_2^{-1})-0.26(2b_1^{-1}3b_14b_2^{-1})$	0.7589	20.07	$\sim$20.7	
B_2	$0.86(2b_1^{-1}3b_14b_2^{-1})+0.27(2b_2^{-1})$	0.0943	20.76		
A_1	$0.92(2b_1^{-1}3b_18a_1^{-1})$	0.0180	21.01		
A_1	$0.87(7a_1^{-1}3b_12b_1^{-1})+0.50(2b_1^{-1}3b_17a_1^{-1})+0.40(5a_1^{-1})$ $+0.28(4b_2^{-1}3b_11a_2^{-1})+0.25(1a_2^{-1}3b_14b_2^{-1})+0.23(7a_1^{-1}7b_12b_1^{-1})$	0.1632	22.26		
A_1	$0.62(5a_1^{-1})-0.38(7a_1^{-1}3b_12b_1^{-1})-0.36(6a_1^{-1}3b_12b_1^{-1})$ $-0.31(2b_1^{-1}3b_16a_1^{-1})+0.31(2b_1^{-1}12a_12b_1^{-1})-0.27(2b_1^{-1}10a_12b_1^{-1})$ $-0.25(2b_1^{-1}9a_12b_1^{-1})-0.21(4b_2^{-1}5b_28a_1^{-1})+0.20(2b_1^{-1}11a_12b_1^{-1})$	0.3845	22.64		
A_2	$0.85(2b_1^{-1}3b_11a_2^{-1})-0.22(8a_1^{-1}5b_22b_1^{-1})+0.20(2b_1^{-1}4b_11a_2^{-1})$	0.0093	22.71		
A_1	$0.82(1a_2^{-1}3b_14b_2^{-1})-0.42(4b_2^{-1}5b_28a_1^{-1})+0.41(4b_2^{-1}3b_11a_2^{-1})$ $-0.26(7a_1^{-1}3b_12b_1^{-1})-0.26(1a_2^{-1}3b_13b_2^{-1})-0.21(4b_2^{-1}6b_28a_1^{-1})$	0.0129	23.05		
A_1	$0.60(4b_2^{-1}3b_11a_2^{-1})-0.31(4b_2^{-1}5b_28a_1^{-1})-0.27(1a_2^{-1}3b_14b_2^{-1})$ $-0.21(8a_1^{-1}5b_24b_2^{-1})$	0.0181	23.09		
A_1	$0.61(4b_2^{-1}5b_28a_1^{-1})+0.59(4b_2^{-1}3b_11a_2^{-1})+0.37(4b_2^{-1}6b_28a_1^{-1})$ $+0.37(1a_2^{-1}3b_14b_2^{-1})+0.27(8a_1^{-1}6b_24b_2^{-1})+0.26(4b_2^{-1}10b_28a_1^{-1})$ $+0.25(8a_1^{-1}5b_24b_2^{-1})-0.20(7a_1^{-1}3b_12b_1^{-1})$	0.0157	23.16		
B_2	$0.90(4b_2^{-1}6b_24b_2^{-1})+0.67(4b_2^{-1}5b_24b_2^{-1})-0.34(8a_1^{-1}5b_28a_1^{-1})$ $+0.25(4b_2^{-1}10b_24b_2^{-1})-0.23(8a_1^{-1}6b_28a_1^{-1})+0.21(4b_2^{-1}8b_24b_2^{-1})$	0.0144	23.44		
A_1	$0.82(2b_1^{-1}5b_21a_2^{-1})+0.35(2b_1^{-1}6b_21a_2^{-1})-0.31(2b_1^{-1}9a_12b_1^{-1})$ $-0.30(2b_1^{-1}10a_12b_1^{-1})+0.23(1a_2^{-1}5b_22b_1^{-1})$	0.0212	23.56		
A_1	$0.50(2b_1^{-1}10a_12b_1^{-1})+0.49(2b_1^{-1}9a_12b_1^{-1})-0.41(2b_1^{-1}12a_12b_1^{-1})$ $-0.40(2b_1^{-1}11a_12b_1^{-1})-0.32(1a_2^{-1}5b_22b_1^{-1})-0.27(1a_2^{-1}6b_22b_1^{-1})$ $+0.24(2b_1^{-1}5b_21a_2^{-1})+0.24(5a_1^{-1})-0.23(6a_1^{-1}3b_12b_1^{-1})$	0.0584	23.71		
A_1	$0.66(2b_1^{-1}9a_12b_1^{-1})+0.60(1a_2^{-1}6b_22b_1^{-1})+0.51(2b_1^{-1}6b_21a_2^{-1})$ $+0.47(1a_2^{-1}5b_22b_1^{-1})-0.23(2b_1^{-1}12a_12b_1^{-1})-0.20(2b_1^{-1}9a_11b_1^{-1})$	0.0134	23.78		
A_1	$0.58(1a_2^{-1}5b_22b_1^{-1})-0.57(2b_1^{-1}11a_12b_1^{-1})+0.40(2b_1^{-1}5b_21a_2^{-1})$ $-0.35(2b_1^{-1}6b_21a_2^{-1})-0.24(2b_1^{-1}12a_12b_1^{-1})+0.22(2b_1^{-1}11a_11b_1^{-1})$ $+0.21(2b_1^{-1}7b_21a_2^{-1})+0.20(2b_1^{-1}9a_11b_1^{-1})$	0.0096	24.01		
	$0.76(2b_1^{-1}3b_13b_2^{-1})-0.28(8a_1^{-1}5b_28a_1^{-1})$	0.0111	24.52		
A_1	$0.76(8a_1^{-1}6b_24b_2^{-1})+0.21(4b_2^{-1}6b_28a_1^{-1})-0.20(8a_1^{-1}12b_24b_2^{-1})$ $-0.20(4a_1^{-1})$	0.0505	24.64		

shoulder in the high-energy region. We propose these states should correspond to this shoulder in the experimental spectrum. In the energy region higher than 17 eV, two prominent peaks were observed at about ∼17.7 and ∼19.6 eV. We assign these peaks to $(6a_1)^{-1}$ and $(2b_2)^{-1}$ states calculated at 17.70 and 20.07 eV, respectively, and the latter state has the character of two-electron process. These two peaks were not assigned in the He I PES work [4]. Above these two states, complete breakdown of Koopmans's picture was obtained in the present calculation: many correlation peaks continued in 21 ∼ 24 eV as shown in Table III. Two satellites were found as the shoulder of $(2b_2)^{-1}$ state at 20.76 and 21.01 eV, which are $^2B_2$ and $^2A_1$ states, respectively. The $(5a_1)^{-1}$ state split into twining peaks at 22.26 and 22.64 eV: for these state, many shake-up configurations contribute and their intensities are mainly due to the final-state correlation interactions. Many shake-up states of $^2A_1$ symmetry follow in the 23 ∼ 25 eV region with small intensities. These states have their intensities through the interaction with the $(5a_1)^{-1}$ state.

7.3.2 trans-acrolein

The outer-valence region of trans-acrolein has been intensively studied; the PES was measured using He I by Kimura *et al.* [4] and using He II [5] by von Niessen et al. Theoretical assignments were done by the Green's function [6] and the CI [7] calculations. The experimental assignment was also proposed using PIES by Ohno *et al*[8]. In the present work, the general-R method was applied to the spectrum up to ∼ 22 eV. For this energy region, fifteen solutions were obtained for each symmetry of C_s and therefore, the SAC-CI dimension were about 20,000 as shown in Table II. Table IV shows the results of binding energies, monopole intensities and characters of the valence-ionized states, whose intensities are larger than 0.005. Note that there are many other states with small intensities not listed in Table IV. In Fig. 2, we compare the spectrum by He II PES and the present theoretical spectrum with convolution using Gaussian of the fwhm of $0.05 \times \Delta E$ (in eV). For the first two peaks observed at 10.10 and 10.92 eV by He I PES [4], we assign A' and A'' states calculated at 9.62 and 10.54 eV, respectively. The ordering due to

Figure IV: Outer-valence ionization spectra of trans-acrolein by (a) He I PES and (b) SAC-CI general-R

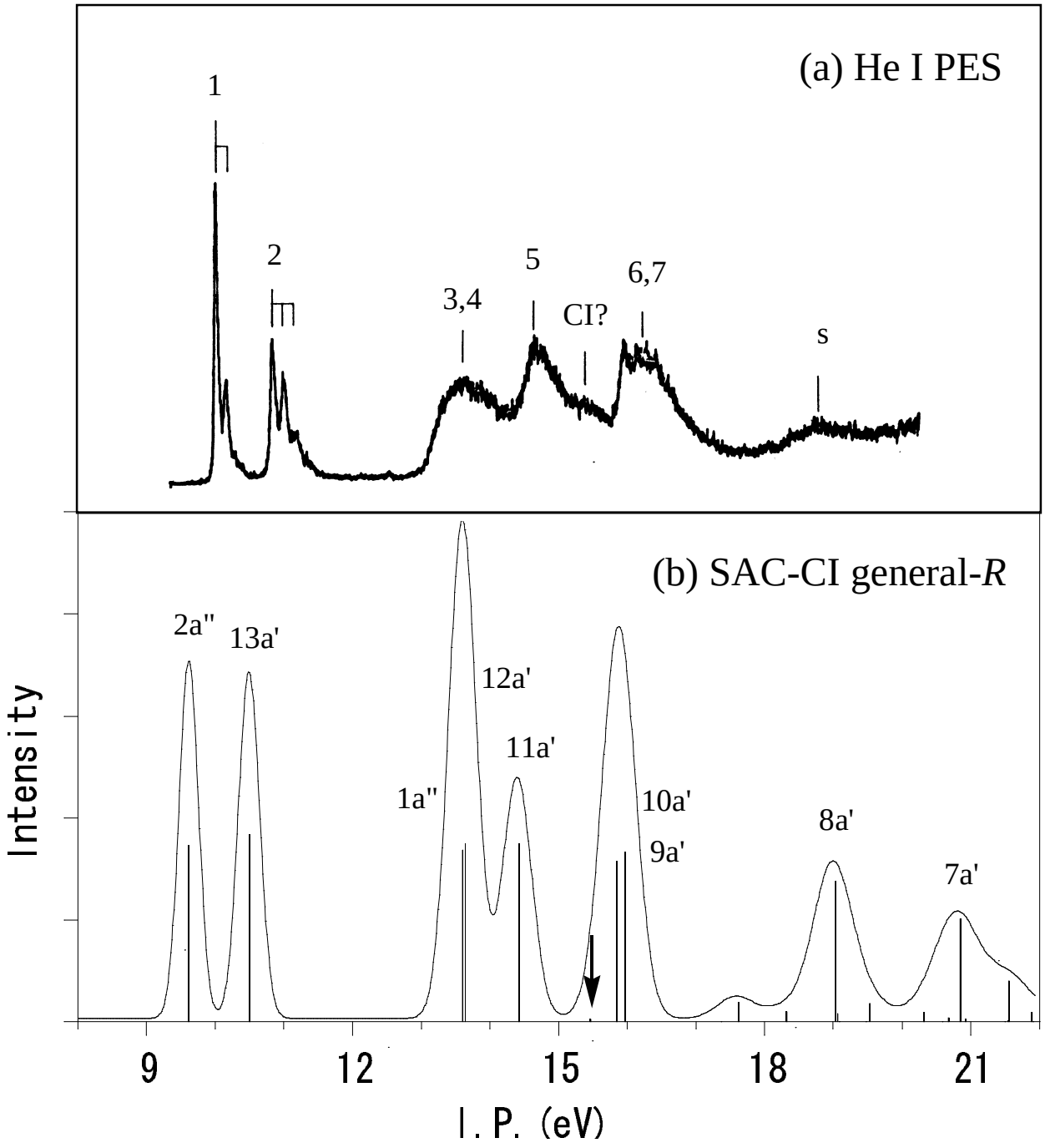

TABLE IV: Calculated ionization potentials (IP, in eV), monopole intensities (M.I.), and main configurations with the basis set for trans-acrolein by SAC-CI general-R.

Sym.	Main Configuration($\|C\| > 0.2$)	M.I.	IP	Expt.
A'	$0.92(13a'^{-1})-0.20(2a''^{-1}3a''13a'^{-1})$	0.8638	9.62	10.10
A''	$0.95(2a''^{-1})$	0.9143	10.50	10.92
	$0.91(1a''^{-1})-0.27(2a''^{-1}3a''1a''^{-1})+0.21(2a''^{-1}3a''2a''^{-1})$	0.8404	13.60	13.7
A'	$0.92(12a'^{-1})$	0.8738	13.64	13.7
	$0.91(11a'^{-1})$	0.8732	14.42	14.6
	$1.03(13a'^{-1}3a''2a''^{-1})+0.54(2a''^{-1}3a''13a'^{-1})+0.25(13a'^{-1}3a''1a''^{-1})$	0.0126	15.47	~ 15.5
	$0.70(10a'^{-1})+0.51(9a'^{-1})$	0.7856	15.85	16.3
	$0.71(9a'^{-1})-0.53(10a'^{-1})-0.21(2a''^{-1}3a''11a'^{-1})$	0.8327	15.97	16.3
	$-0.20(11a'^{-1})$			
A'	$0.70(2a''^{-1}3a''13a'^{-1})+0.38(2a''^{-1}4a''13a'^{-1})+0.28(1a''^{-1}3a''13a'^{-1})$	0.0958	17.62	
A''	$1.15(2a''^{-1}3a''2a''^{-1})-0.31(1a''^{-1}3a''1a''^{-1})-0.25(2a''^{-1}3a''1a''^{-1})$	0.0505	18.32	
	$-0.25(2a''^{-1}4a''1a''^{-1})+0.25(2a''^{-1}7a''2a''^{-1})-0.23(1a''^{-1}3a''2a''^{-1})$			
	$-0.21(2a''^{-1}4a''2a''^{-1})$			
A'	$0.82(8a'^{-1})-0.29(13a'^{-1}4a''2a''^{-1})+0.20(2a''^{-1}3a''12a'^{-1})$	0.6898	19.03	~ 18.8
	$0.94(13a'^{-1}4a''2a''^{-1})+0.46(2a''^{-1}4a''13a'^{-1})+0.28(12a'^{-1}3a''2a''^{-1})$	0.0411	19.06	
	$-0.25(13a'^{-1}7a''2a''^{-1})+0.25(13a'^{-1}4a''1a''^{-1})$			
A'	$0.59(12a'^{-1}3a''2a''^{-1})+0.56(13a'^{-1}3a''1a''^{-1})+0.31(13a'^{-1}4a''1a''^{-1})$	0.0902	19.53	
	$-0.29(8a'^{-1})+0.25(2a''^{-1}3a''12a'^{-1})-0.24(12a'^{-1}3a''1a''^{-1})$			
	$+0.21(10a'^{-1}3a''2a''^{-1})+0.21(1a''^{-1}3a''13a'^{-1})$			
A''	$0.75(2a''^{-1}4a''2a''^{-1})-0.67(2a''^{-1}3a''1a''^{-1})-0.36(2a''^{-1}4a''1a''^{-1})$	0.0437	20.32	
	$-0.29(2a''^{-1}3a''2a''^{-1})-0.28(2a''^{-1}7a''2a''^{-1})-0.26(1a''^{-1}3a''1a''^{-1})$			
	$-0.26(1a''^{-1}3a''2a''^{-1})-0.24(1a''^{-1}4a''1a''^{-1})$			
A'	$0.75(11a'^{-1}3a''2a''^{-1})-0.44(12a'^{-1}3a''2a''^{-1})+0.42(9a'^{-1}3a''2a''^{-1})$	0.0189	20.68	
	$+0.40(2a''^{-1}3a''11a'^{-1})+0.28(2a''^{-1}3a''9a'^{-1})+0.22(13a'^{-1}4a''1a''^{-1})$			
	$+0.22(13a'^{-1}3a''1a''^{-1})+0.20(12a'^{-1}4a''2a''^{-1})-0.20(2a''^{-1}3a''12a'^{-1})$			
A'	$0.71(7a'^{-1})-0.38(2a''^{-1}4a''13a'^{-1})+0.23(2a''^{-1}3a''13a'^{-1})$	0.5066	20.85	
	$0.56(11a'^{-1}3a''2a''^{-1})+0.55(12a'^{-1}3a''2a''^{-1})-0.37(13a'^{-1}3a''1a''^{-1})$	0.0127	20.93	
	$-0.36(13a'^{-1}4a''1a''^{-1})-0.33(12a'^{-1}4a''2a''^{-1})+0.30(2a''^{-1}3a''11a'^{-1})$			
	$+0.24(2a''^{-1}3a''12a'^{-1})$			
	$0.82(1a''^{-1}3a''2a''^{-1})+0.25(1a''^{-1}3a''1a''^{-1})-0.24(1a''^{-1}4a''2a''^{-1})$	0.0060	21.54	
A'	$0.56(2a''^{-1}4a''13a'^{-1})+0.44(7a'^{-1})-0.29(2a''^{-1}3a''13a'^{-1})$	0.2007	21.55	
	$-0.24(12a'^{-1}3a''1a''^{-1})-0.21(1a''^{-1}3a''12a'^{-1})$			
	$0.78(12a'^{-1}3a''1a''^{-1})+0.42(10a'^{-1}3a''2a''^{-1})+0.40(1a''^{-1}3a''12a'^{-1})$	0.0469	21.89	
	$+0.29(12a'^{-1}4a''1a''^{-1})-0.27(12a'^{-1}4a''2a''^{-1})+0.23(2a''^{-1}3a''10a'^{-1})$			
	$+0.21(7a'^{-1})-0.20(10a'^{-1}3a''1a''^{-1})$			

Figure V: Valence MO plotting and its nature with orbital energy trans-acrolein

15th, $\pi(\mathrm{C}-\mathrm{C})$, $2a''$, -10.859

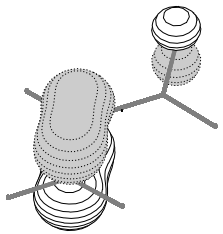

14th, $n(\mathrm{O})$, $13a'$, -11.741

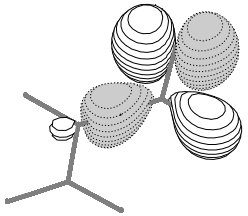

13th, $\pi(\mathrm{C}-\mathrm{O})$, $1a''$, -14.737

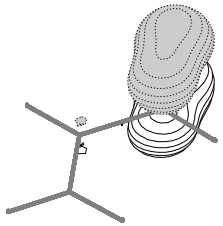

12th, $\sigma(\mathrm{C}-\mathrm{H})$, $12a'$, -15.193

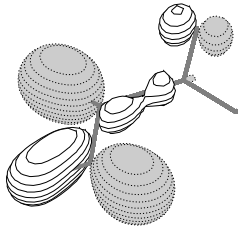

11th, $n(\mathrm{O})$, $11a'$, -16.463

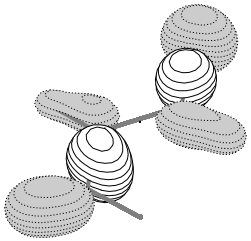

10th, $\sigma(\mathrm{C}-\mathrm{H})$, $10a'$, -18.125

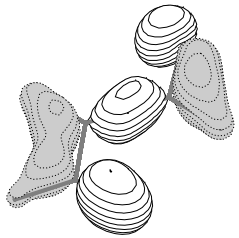

9th, $\sigma(\mathrm{C}-\mathrm{C})$, $9a'$, -18.282

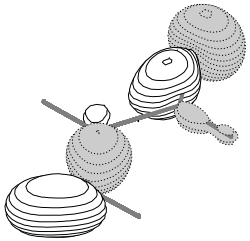

8th, $\sigma(\mathrm{C}-\mathrm{H})$, $8a'$, -21.408

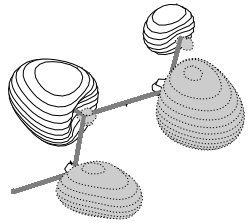

7th, $\sigma(\mathrm{C}-\mathrm{H})$, $7a'$, -24.157

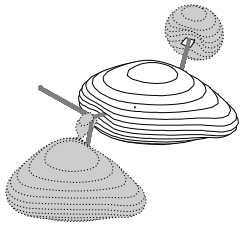

6, $\sigma(\mathrm{C}-\mathrm{C})$, $6a'$, -29.625

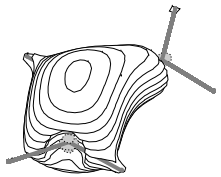

5th, $\sigma(\mathrm{C}-\mathrm{O})$, $5a'$, -37.850

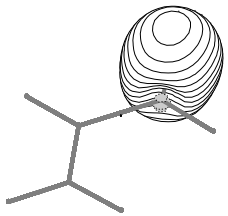

structure

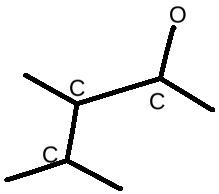

Koopman's theorem is wrong for these states. This assignment was also proposed by recent PIES [8]. For the next overlapping peaks at 13.7 eV, we calculated $(1a'')^{-1}$ and $(12a')^{-1}$ states at 13.60 and 13.64 eV, respectively. The effect of the electron correlations were found to be large for A' states. We calculated $(11a')^{-1}$ state at 14.42 eV in accordance with the peak observed at 14.6. In the higher-energy region of this peak, uncertain correlation peak ($\sim$15.5 eV) was measured by He I PES. Accordingly, we calculated shake-up state at 15.47 eV with small intensity of $\sim$ 0.01. Then, the overlapping band follows at 16.6 eV. We calculated two A' states for this band and these states are described by the linear combination of $(10a')^{-1}$ and $(9a')^{-1}$. In the higher energy region of the peak at 16.6 eV, many shake-up states were calculated. The $(8a')^{-1}$ and $(7a')^{-1}$ were obtained at 19.03, 20.85 and 21.55 eV with relatively small intensities: these intensities are distributed to the shake-up states through the final-state correlation interactions. Two satellites were obtained in between the $(9a_1)^{-1}$ and $(8a_1)^{-1}$ states and it seems that small structure exist in this energy region of He I PES. The $(7a_1)^{-1}$ peak split into twinning peaks with large energy separation. Two electron processes in this energy region accompanies the excitation to the $3a''$ or $4a''$ MOs, which are the π^* orbitals.

7.4 Conclusion

The SAC-CI general-R method has been applied to methylenecyclopropane and trans-acrolein to investigate their electronic structure in detail for assignment of the outer-valence ionization spectra. The method has successfully reproduced the spectrum shape of the PES of these molecules and the detailed characterization for both main peaks and satellite peaks has been proposed. For methylenecyclopropane, three shake-up states with considerable intensity were calculated at around 17 eV. Strong peaks at 17.7 and 19.7 eV were attributed to the $(6a_1)^{-1}$ and $(2b_2)^{-1}$ states, respectively. The remarkable breakdown of the Koopman's picture has been found for $(5a_1)^{-1}$ state at c.a. 22 eV and the twinning peaks were obtained. For trans-acrolein, a CI state was calculated in between the peaks 5 and 6 in agreement with the He I PES. Many shake-up states were also obtained in the energy region of

$17 \sim 22$ eV, whose intensities were originated in $(8a')^{-1}$ and $(7a')^{-1}$ states.

7.5 Acknowledgments

This research was supported by a Grant-in-Aid for Scientific Research from the Ministry of Education, Science, Culture and Sports.

BIBLIOGRAPHY

[1] L. S. Cederbaum, W. Domcke, J. Schirmer, and W. von Niessen, Adv. Chem. Phys., **65**, 115(1986).

[2] A.D.O. Bawagan and E.R. Davidson, Adv.in Chem. Phys., **110**, 215(1999).

[3] M. Ehara, M. Ishida, K. Toyota, and H. Nakatsuji, *Reviews in Modern Quantum Chemistry*, edited by K.D. Sen, (World Scientific, Singapore) submitted.

[4] K. Kimura, S. Katsumata, Y. Achiba, T. Yamasaki, and S. Iwata, *Handbook of He I Photoelectron Spectra*, Halsted Press, New York 1980.

[5] W. von Niessen, G. Bieri, L. Asbrink, J. Electron Spectrosc. Relat. Phenom., **21** 175 (1980).

[6] W. von Niessen, G. Bieri, J. Schirmer, L. S. Cederbaum, Chem. Phys., **65** 157 (1982).

[7] P. Decleva, G. Fronzoni, G. Dealti, A. Lisini, J. Molecular Structure (Theochem), **184** 49 (1989).

[8] K. Ohno, K. Okamura, H. Yamakado, S. Hoshino, T. Takami, and M. Yamauchi, J. Phys. Chem. **99** 14247 (1995).

[9] D. W. Turner, C. Baker, A. D. Baker, and C. R. Brundle, *Molecular Photoelectron Spectroscopy*, (Wiley-Interscience, London, 1970); D. W. Turner, Phil. Trans. Roy. Soc. London, A **268**, 7 (1970).

[10] G. Bieri, F. Burger, E. Heilbronner, and J. P. Maier, Helv. Chim. Acta. 60 (1977).

[11] H. Nakatsuji, and K. Hirao, J. Chem. Phys. **68**, 2053(1978).

[12] H. Nakatsuji, Chem. Phys. Lett., **59**, 362(1978).

[13] H. Nakatsuji, Chem. Phys. Lett., **67**, 329,334(1979).

[14] H. Nakatsuji, in *Computational Chemistry: Reviews of Current trends*, edited by J. Leszcznski (World Scientific, Singapore, 1997), Vol. 2.

[15] H. Nakatsuji, Acta. Chim. Acad. Sci. Hung., **129** , 719(1992).

[16] H. Nakatsuji, Chem. Phys., **75**, 425 (1983).

[17] H. Nakatsuji, M. Ehara, M.H. Palmer, M. F. Guest, J. Chem. Phys., **97**, 2561 (1992).

[18] H. Nakatsuji, M. Ehara, J. Chem. Phys., **101** 7658 (1994)

[19] H. Nakatsuji, J. Hasegawa, M. Hada, J. Chem. Phys., **104** 2321 (1996).

[20] H. Nakatsuji, J. Hasegawa, and K. Ohkawa, Chem. Phys. Lett., **296**, 499 (1998).

[21] H. Nakatsuji, Chem. Phys. Lett., **177** 331 (1991).

[22] H. Nakatsuji, J. Chem. Phys., **83**, 731, 5743 (1985), *ibid*, **94** 6716 (1991).

[23] M. Ehara, H. Nakatsuji, Chem. Phys. Lett., **282**, 347 (1998).

[24] M. Ehara, P. Tomasello, J. Hasegawa, H. Nakatsuji, Theor. Chem. Acc., **102** 161 (1999).

[25] M. Ehara, H. Nakatsuji, Spectrochim. Acta. A **55** 487 (1998).

[26] M. Ehara, P. Tomasello, J. Hasegawa, H. Nakatsuji, Theor. Chem. Acc. **102** 161 (1999).

[27] J. Wan, M. Ehara, M. Hada, and H. Nakatsuji, J. Chem. Phys. **113** 5245 (2000); ibid . 114 (2001).

[28] M. Ehara, M. Ishida, H. Nakatsuji, J. Chem. Phys. **114** 8990 (2001).

[29] M. Ishida, M. Ehara, H. Nakatsuji, J. Chem. Phys. in press.

[30] D. Becke, Phys. Rev. A **38**, 3098 (1988); J. Chem. Phys. **98**, 5648 (1993).

[31] R. Krishnan, J.S. Binkley, R. Seeger and J.A. Pople, J. Chem. Phys. **72**, 650 (1980).

[32] T.H. Dunning, Jr., J. Chem. Phys., **53**, 2823 (1970), T.H. Dunning, Jr. and P.J. Hay, In Methods Of Electronic Structure Theory, Vol. 2, H.F. Schaefer III, Ed., Plenum Press (1977).

[33] Basis sets were obtained from the Extensible Computational Chemistry Environment Basis Set Database, Version 4/22/01, as developed and distributed by the Molecular Science Computing Facility, Environmental and Molecular Sciences Laboratory, the Pacific Northwest Laboratory, P.O. Box 999, Richland, Washington 99352, USA. URL is `http://www.emsl.pnl.gov:2080/forms/basisform.html`.

[34] G.Schaftenaar and J.H. Noordik, "Molden: a pre- and post-processing program for molecular and electronic structures", J. Comput.-Aided Mol. Design, 14 (2000) 123-134.

[35] K. Toyota, H. Nakatsuji, submitted for publication.

[36] S. Süzer, S. T. Lee, and D. A. Shirley, Phys. Rev. A **13**, 1842 (1976).

[37] R. I. Martin and D. A. Shirley, J. Chem. Phys., **64**, 3685 (1976).

[38] H. Nakatsuji, M. Hada, M. Ehara, J. Hasegawa, T. Nakajima, H. Nakai, O. Kitao, and K. Toyota, SAC/SAC-CI program system (SAC-CI96) for calculating ground, excited, and electron attached sates and singlet to septet spin multiplicites.

[39] Gaussian98 (Revision A.1), M. J. Frisch, G. W. Trucks, H. B. Schlegel *et al.*(Gaussian, Inc., Pittsburgh, PA, 1998).